"When we long for life without difficulties,
remind us that oaks grow strong in contrary winds
and diamonds are made under pressure."- Peter Marshall

UNIVERSITY OF ALBERTA

HLA-DQ TRANSGENIC NOD MODELS OF AUTOIMMUNITY

BY

SARAH LOUISE HAYWARD

A thesis submitted to the Faculty of Graduate Studies and Research in partial fulfillment of the requirements for the degree of

DOCTOR OF PHILOSOPHY

in

IMMUNOLOGY

DEPARTMENT OF MEDICAL MICROBIOLOGY AND IMMUNOLOGY

EDMONTON, ALBERTA

SPRING 2006

Your file Votre référence
ISBN: 0-494-13984-6
Our file Notre référence
ISBN: 0-494-13984-6

ABSTRACT

Over 5% of North Americans suffer from autoimmune disorders. Although the initial trigger of this breakdown in self-tolerance is not understood, susceptibility is known to be influenced by genetic factors, particularly MHC class II genes. This thesis investigates two such MHC class II molecules, HLA-DQ8 (DQA1*0301, DQB1*0302) and HLA-DQ6 (DQA1*0102, DQB1*0602), which in humans have been linked, respectively, to susceptibility or resistance to type 1 diabetes (T1D). Nonobese Diabetic (NOD) mice express the mouse MHC class II gene IAg7 and spontaneously develop T1D; when DQ8 was expressed transgenically in the NOD background (NOD.DQ8), animals continued to develop T1D, whereas when DQ6 was expressed (NOD.DQ6), diabetes no longer occurred. However, removal of mouse MHC class II expression from these lines, by crossing onto the IAβ knockout (NOD/Ab^0), resulted in completely new and unexpected autoimmune phenotypes.

NOD.DQ8/Ab^0 animals develop spontaneous autoimmune myocarditis very similar to human idiopathic dilated cardiomyopathy. In this thesis the immune pathogenesis of the anti-cardiac autoimmunity was dissected using adoptive transfer of lymphocytes into syngeneic Rag1 knockout animals, as well as crosses into B lymphocyte and CD8 T cell deficient backgrounds. Autoimmune myocarditis required CD8 T cells for initiation, but was not dependent on B cells. Adoptive transfer of purified lymphocyte subsets revealed a final effector role for CD4 T cells, seemingly through the recruitment of macrophages.

Rather than anti-cardiac autoimmunity, the NOD.DQ6/Ab^0 line developed spontaneous autoimmune thyroiditis very similar to Hashimoto's disease in humans. All animals demonstrated circulating autoantibodies (against thyroglobulin and thyroid peroxidase) and infiltration of the thyroid gland by mononuclear cells and a subset of animals became overtly hypothyroid (decreased T4/elevated thyroid stimulating hormone). The anti-thyroid autoimmunity was demonstrated to be cell-mediated, with both CD4 and CD8 T cells playing a role in pathogenesis.

The two NOD.DQ/Ab^0 transgenic lines characterized in this thesis develop spontaneous autoimmune syndromes remarkably similar to those seen in humans; hence, they should be useful for identifying target autoantigens, defining immune-destructive mechanisms and testing new therapies. In addition, these lines may contribute to our understanding of why certain MHC class II variants lead to autoimmune diseases that target particular organs or tissues.

ACKNOWLEDGEMENTS

Firstly I would like to thank my supervisor, Dr. John Elliott for allowing me to join his lab and work on this project. My thesis has had its ups and downs, but if I had to do it all over again I would. This thesis would not have been possible without the support of the rest of the department: my committee members, Dr. Hanne Ostergaard and Dr. Colin Anderson; other faculty; the administration; my fellow students; and, of course, the members of the Elliott Lab, past and present. I also acknowledge Dr. Larry Guilbert and Dr. Noel Rose for their expertise and suggestions as my internal-external and external examiners, respectively.

This project was only possible with the technical support of Lynette Elder (histology), HSLAS (mouse care and maintenance) and Dr. David Rayner and Dr. Nick Nation (Pathology). I also thank Dr. Kavanagh's lab for their development of the mouse ECG, Dr. Sean McMurtry for his echocardiogram expertise, Dr. Weiping Liu for his expertise on bone marrow derived dendritic cells, Dr. Albert Parlow for coordinating the TSH radioimmunoassays and Dorothy Rutkowski for her assistance with the FACS sorting.

I would like to thank and acknowledge the unwavering support from my family, new and old, but especially my parents Denise and Barry Wallbank who taught me to be the person I am today. I hope I have done them proud.

Lastly I would like to thank my best friend and husband, Chad. His love and support throughout these last five years has been constant through both the ups and the downs. His interest in trying to understand what I have been doing every day has made it all worthwhile.

TABLE OF CONTENTS

CHAPTER ONE: GENERAL INTRODUCTION		1
1.1	Branches of the Immune System	2
1.2	The MHC Complex	3
1.3	MHC Class II	5
1.4	MHC Class II Antigen Processing and Presentation	6
1.5	The T cell Receptor	8
1.6	T cell Activation	10
1.7	Immune Tolerance and Autoimmunity	12
1.8	Type 1 Diabetes	13
1.9	MHC Class II Association with Type 1 Diabetes	15
1.10	NOD Mice	16
1.11	HLA-Transgenic Mouse Models of Type 1 Diabetes	18
1.12	DQ8 Transgenic NOD Mice	19
1.13	Autoimmune Myocarditis and IDCM	25
1.14	Autoimmune Thyroiditis	28
	1.14.1 The Thyroid Gland	28
	1.14.2 Autoimmune Thyroiditis in Humans	29
	1.14.3 HLA Associations	31
	1.14.4 Experimental Models	31
	1.14.5 Spontaneous Models	34
1.15	Experimental Design	36
1.16	References	38
CHAPTER TWO: IMMUNE MECHANISMS OF NOD.DQ8/Ab^0 MICE		55
2.1	Introduction	56
2.2	Materials and Methods	59
	2.2.1 Mice	59
	2.2.2 Establishment of DQ8 Transgenic NOD and DQ6 Transgenic IAb knockout NOD Lines	61
	2.2.3 Genotyping	63

2.2.4 Antibodies and FACS Analysis 64
2.2.5 Bone Marrow Derived Dendritic Cells 64
2.2.6 Superantigen Induced T cell Proliferation 65
2.2.7 Proliferation Blocking Assay 66
2.2.8 Lymphocyte Recall Response 66
2.2.9 Monitoring Mice for Myocarditis by ECG 67
2.2.10 ELISA for Cardiac Myosin Autoantibodies 68
2.2.11 Adoptive Transfers 68
2.2.12 Echocardiography 69
2.2.13 MACS Enrichment for CD4 T cells 69
2.2.14 Cell Enrichment by Fluorescent Cell Sorting 70
2.2.15 Histology/Immunohistochemistry 70
2.2.16 Preparation of RNA 71
2.2.17 Generation of Probe Templates 72
2.2.18 Generation of RNA Probes 74
2.2.19 RNAse Protection Assay 75
2.3 Results 76
2.4 Discussion 83
2.5 References 112
CHAPTER THREE: NOD.DQ6/Ab^0 MICE: AN ANIMAL MODEL OF SPONTANEOUS AUTOIMMUNE THYROIDITIS 119
3.1 Introduction 120
3.2 Materials and Methods 121
3.2.1 Mice 121
3.2.2 Histology/Immunohistochemistry 122
3.2.3 Indirect Immunofluorescence 123
3.2.4 Radioligand Binding Assay 123
3.2.5 Mouse Thyroid Lysates 124
3.2.6 FRTL-5 Cells 124
3.2.7 SDS-PAGE and Western Blots 125
3.2.8 Non-Rodent Thyroids 125

3.2.9 Preparation of Mouse Thyroglobulin 126
3.2.10 ELISA for Thyroglobulin Autoantibodies 126
3.2.11 TSH Radioimmunoassay 127
3.2.12 TSH ELISA 127
3.2.13 T4 ELISA 128
3.2.14 Adoptive Transfers 128
3.3 Results 129
3.3.1 Thyroid Infiltrates, Fibrosis, and Goiter 129
3.3.2 CD8 T cells Predominate in Goiter Infiltrates 130
3.3.3 Anti-Thyroid Autoantibodies Arise Spontaneously 130
3.3.4 Thyroid Hormone and TSH Levels are Altered 132
3.3.5 Thyroiditis Can Be Adoptively Transferred 133
3.4 Discussion 134
3.5 References 158
CHAPTER FOUR: A RADIOLIGAND BINDING ASSAY TO MEASURE ANTI-THYROID PEROXIDASE AUTOANTIBODIES IN MICE 165
4.1 Introduction 166
4.2 Materials and Methods 168
4.2.1 cDNA templates and other reagents 168
4.2.2 Mouse Serum 169
4.2.3 Preparation and Analysis of Radiolabeled Antigens 169
4.2.4 Detection of Anti-Thyroid Peroxidase Autoantibodies 171
4.2.5 Competitive RBA 172
4.2.6 Competitive ELISA 173
4.2.7 Indirect Immunofluorescence assay (iIFA) 173
4.3 Results 175
4.3.1 *In vitro* transcription/translation of muTPO, huGAD65, and huIA-2 175
4.3.2 Assessment of optimal serum-antigen ratios in RBA assay 176

4.3.3 Detection and quantification of anti- TPO autoantibodies in NOD.DQ6/Ab^0 mice 176
4.3.4 The anti-TPO autoantibodies in NOD.DQ6/Ab^0 mice do not cross-react with thyroglobulin 177
4.3.5 Anti-thyroid autoantibody titres can be semi-quantified by iIFA 177
4.3.6 Correlation of anti-TPO autoantibody titres by iIFA and RBA 178
4.4 Discussion 178
4.5 References 188
CHAPTER 5: GENERAL DISCUSSION AND FUTURE DIRECTIONS 191
5.1 General Discussion and Future Directions 192
5.2 References 207
APPENDIX I: SUPPLEMENTARY FIGURES AND TABLES 214
APPENDIX II: AUTOIMMUNITY OF NOD.DQ6$^{+/-}$DQ8$^{+/-}$/Ab^0 MICE 223
AII.1 Introduction 224
AII.2 Materials and Methods 225
AII.2.1 Mice 225
AII.2.2 Histology 226
AII.2.3 Monitoring Mice for Myocarditis by ECG 226
AII.2.4 TSH ELISA 226
AII.2.5 Protein Lysates 227
AII.2.6 SDS-PAGE and Western Blots 229
AII.3 Results 230
AII.4 Discussion 231
AII.5 References 237
APPENDIX III: NOD.DQ6/Ab^0 MOUSE ISLETS 238
AIII.1 Introduction 239
AIII.2 Materials and Methods 241
AIII.2.1 Mice 241
AIII.2.2 Diabetes Monitoring 241

AIII.2.3 Histology 242
AIII.2.4 Islet Measurement 242
AIII.2.5 Glucose Tolerance Test 242
AIII.2.6 Whole Pancreas Insulin Extraction 243
AIII.3 Results 243
AIII.4 Discussion 244
AIII.5 References 250

LIST OF TABLES

TABLE 2-1: Relative abundance of various lymphocyte subsets in progenitor strains and DQ transgenic IAb knockout lines 95

TABLE 2-2: Like NODs, NOD.DQ8/Ab^0 animals have reduced numbers of NKT cells 111

TABLE 3-1: NOD.DQ6/Ab^0 Rag1^0 recipients of total lymphocytes or CD4 T lymphocytes from NOD.DQ6/Ab^0 mice develop autoimmune thyroiditis 155

TABLE 3-2: Comparison of the thyroid autoimmunity in mouse EAT, NOD.DQ6/Ab^0 mice and humans. 157

TABLE 4-1: The RBA assay detects and quantifies anti-TPO autoantibodies in NOD.DQ6/Ab^0 mice 184

TABLE AI.1: MHC class II/Sfi I primers for cloning of RNA probes 222

LIST OF FIGURES

FIGURE 1-1	Adaptive immunity	4
FIGURE 1-2	The Major Histocompatibility Complex	4
FIGURE 1-3	Schematic of the structures of MHC class I and II	5
FIGURE 1-4	MHC class II antigen presentation	8
FIGURE 1-5	Schematic of the T cell Receptor Structure	9
FIGURE 1-6	NOD.DQ8/Ab^0 mice develop enlarged hearts and myocarditis	21
FIGURE 1-7	Myocardial infiltrate of NOD.DQ8/Ab^0 mice contains B cells, CD8 and CD4 T cells	22
FIGURE 1-8	NOD.DQ8/Ab^0 mice progress to complete heart block and heart failure	22
FIGURE 1-9	The autoimmune myocarditis of NOD.DQ8/Ab^0 mice can be adoptively transferred	23
FIGURE 1-10	Anti-heart autoantibodies in NOD.DQ8/Ab^0 mice can be detected by indirect immunofluorescence	24
FIGURE 1-11	NOD.DQ8/Ab^0 mice develop anti-heart autoantibodies as measured by ELISA and Western blot	25
FIGURE 2-1	DQ8 transgenic mice show tissue appropriate expression of the MHC class II transgene	93
FIGURE 2-2	DQ6 transgenic mice show tissue appropriate expression of the MHC class II transgene	94
FIGURE 2-3	Proliferative responses of splenocytes from NOD.DQ8/Ab^0, NOD.DQ6/Ab^0, NOD, and NOD.DQ8aDQ2b/Ab^0 mice to the superantigens SEB and TSST	96
FIGURE 2-4	An anti-DQ monoclonal antibody can block superantigen stimulation of DQ-transgenic splenocytes	97

FIGURE 2-5 NOD.DQ8/Ab^0 and NOD.DQ6/Ab^0 mice have similar recall responses to ovalbumin and hen egg lysozyme 98
FIGURE 2-6 NOD.DQ6/Ab^0 mice do not develop autoimmune myocarditis 99
FIGURE 2-7 NOD.DQ8/Ab^0 Rag1^0 mice do not develop autoimmune myocarditis 100
FIGURE 2-8 The autoimmune myocarditis of NOD.DQ8/Ab^0 mice can be adoptively transferred to NOD.DQ8/Ab^0 Rag1^0 mice 101
FIGURE 2-9 CD4 T cells alone can adoptively transfer myocarditis from NOD.DQ8/Ab^0 mice to NOD.DQ8/Ab^0 Rag1^0 mice 102
FIGURE 2-10 Adoptive transfer of CD4 T cells alone produces a more profound disease than adoptive transfer of total splenocytes 103
FIGURE 2-11 Analysis of cells separated by magnetic selection 104
FIGURE 2-12 Analysis of cells separated by fluorescent cell sorting 105
FIGURE 2-13 Macrophages predominate in the mononuclear cell infiltrate seen in the hearts of NOD.DQ8/Ab^0 Rag1^0 mice that received CD4 T cell transfers 106
FIGURE 2-14 CD8 T cells, but not B cells, are critical to the induction of autoimmune myocarditis in NOD.DQ8/Ab^0 mice 107
FIGURE 2-15 Histology results for NOD.DQ8/Ab^0 IgH^0 and NOD.DQ8/Ab^0 β2m^0 mice 108
FIGURE 2-16 DQ mRNA levels are not abnormally elevated in the hearts of NOD.DQ8$^{+/-}$/Ab$^{+/-}$ mice 109
FIGURE 2-17 Proposed immune mechanisms for autoimmunity in NOD.DQ8/Ab^0 mice 110

FIGURE 3-1 NOD.DQ6/Ab^0 mice show mononuclear cell infiltration of the thyroid and a subset of animals develop goiter 141

FIGURE 3-2 A variety of immune cells can be detected within the thyroids of NOD.DQ6/Ab^0 mice, but CD8 T cells predominate in end stage goitres 142
FIGURE 3-3 Anti-thyroid membrane autoantibodies can be detected in NOD.DQ6/Ab^0 serum by indirect immunofluorescence 143
FIGURE 3-4 NOD.DQ6/Ab^0 mice develop anti-thyroid peroxidase autoantibodies 144
FIGURE 3-5 NOD.DQ6/Ab^0 mice develop anti-thyroid autoantibodies as measured by Western blot 145
FIGURE 3-6 NOD.DQ6/Ab^0 mice develop anti-thyroglobulin autoantibodies 146
FIGURE 3-7 Serum titres of anti-thyroglobulin autoantibodies increase with age in NOD.DQ6/Ab^0 mice 147
FIGURE 3-8 A subset of NOD.DQ6/Ab^0 mice show elevated serum thyroid stimulating hormone (TSH) levels 148
FIGURE 3-9 NOD.DQ6/Ab^0 mice show reduced T4 hormone levels 149
FIGURE 3-10 The autoimmune thyroiditis of NOD.DQ6/Ab^0 mice can be adoptively transferred to syngeneic Rag1^0 recipients 150
FIGURE 3-11 Adoptive transfer of NOD.DQ6/Ab^0 lymphocytes into NOD.DQ6/Ab^0 Rag1^0 recipients induces anti-thyroglobulin Autoantibodies 151
FIGURE 3-12 NOD.DQ6/Ab^0 Rag1^0 recipients of NOD.DQ6/Ab^0 splenocytes develop elevated TSH levels 152
FIGURE 3-13 NOD.DQ6/Ab^0 Rag1^0 recipients of NOD.DQ6/Ab^0 splenocytes develop reduced T4 hormone levels 153
FIGURE 3-14 NOD.DQ6/Ab^0 splenocytes, but not serum can adoptively transfer autoimmune thyroiditis and hypothyroidism to NOD.DQ6/Ab^{0}Rag1^0 mice 154
FIGURE 3-15 NOD.DQ6/Ab^0 Rag1^0 recipients of total lymphocytes or CD4 T lymphocytes from NOD.DQ6/Ab^0 mice develop thyroid infiltrate 156

FIGURE 4-1 *In vitro* transcription/translation of muTPO, huGAD65, and hulA-2 182
FIGURE 4-2 The optimal serum dilution in a thyroid peroxidase RBA is 1/25 183
FIGURE 4-3 Thyroglobulin cannot inhibit the binding of NOD.DQ6/Ab0 serum autoantibodies to thyroid peroxidase 185
FIGURE 4-4 Example results demonstrating that iIFA can be used to semi-quantitatively measure titres of circulating anti-thyroid membrane autoantibodies in NOD.DQ6/Ab^0 mice 186
FIGURE 4-5 Indirect IFA titres of anti-thyroid membrane autoantibodies correlate with anti-thyroid peroxidase autoantibody levels determined by RBA 187

SUPPLEMENTARY FIGURE AI.1 ECG apparatus 215
SUPPLEMENTARY FIGURE AI.2 Determination of normal PR interval 216
SUPPLEMENTARY FIGURE AI.3 PCR confirms that NOD.DQ8/Ab^0 mice are DQA1*0301, DQB1*0302 217
SUPPLEMENTARY FIGURE AI.4 Preparation of RNA and probes for RNAse protection assay—Representative results 218
SUPPLEMENTARY FIGURE AI.5 DQ transgene mRNA levels are not abnormally elevated in thyroids of NOD.DQ6$^{+/-}$/Ab$^{+/-}$ mice 219
SUPPLEMENTARY FIGURE AI.6 Thyroid cell line and mouse thyroid glands used to prepare antigen lysates 220
SUPPLEMENTARY FIGURE AI.7 Anti-thyroid autoantibodies in NOD.DQ6/Ab^0 serum appear to specifically recognize rodent thyroid antigens 221

FIGURE AII.1 NOD.DQ6$^{+/-}$DQ8$^{+/-}$/Ab^{0} animals show both heart and thyroid pathology 233
FIGURE AII.2 NOD.DQ6$^{+/-}$DQ8$^{+/-}$/Ab^{0} mice can progress to heart failure 234
FIGURE AII.3 NOD.DQ6$^{+/-}$DQ8$^{+/-}$/Ab^{0} mice develop elevated serum TSH 235
FIGURE AII.4 NOD.DQ6$^{+/-}$DQ8$^{+/-}$/Ab^{0} mice develop both anti-heart and anti-thyroid autoantibodies 236

FIGURE AIII.1 Unlike NOD.DQ8 mice, NOD.DQ6 mice do not develop diabetes 246
FIGURE AIII.2 NOD.DQ6/Ab^{0} islets never show intraislet mononuclear cell infiltrates and they appear to be larger than islets of other strains (e.g. Balb/c, NOD.DQ8/Ab^{0}) 247
FIGURE AIII.3 NOD.DQ6/Ab^{0} mice have efficient glucose tolerance 248
FIGURE AII.4 NOD.DQ6/Ab^{0} pancreases contain normal levels of insulin 249

LIST OF ABBREVIATIONS

ABC	Avidin-Biotin-Enzyme Complex
ABTS	2,2'-azino-bis(3-ethylbenzthiazoline-6-sulfonic acid
APC	Antigen Presenting Cell
A ,C, G, or U TP	Adenosine (Cytidine, Guanosine, Uradine) Tri-phosphate
ATA	3-amino-1,2,4-triazole
AMP	Ampicillin
AV	Atrioventricular
β2m	β-2 microglobulin
BAC	Bacterial Artificial Chromosome
BB rats	Bio-breeding rats
βME	Beta-mercaptoethanol
BSA	Bovine Serum Albumin
CB3	Coxsackievirus B3
CD	Cluster Designation
CFA	Complete Freunds Adjuvant
CLIP	Class II Associated Invariant Chain Peptide
CPM	Counts Per Minute
CTL	Cytotoxic T lymphocyte
DAB	3,3'-diaminobenzidine
DAPI	4',6-diamidino-2-phenylindole, dihydrochloride
DC	Dendritic Cell
DEPC	Diethylpyrocarbonate
DTH	Delayed Type Hypersensitivity
DTT	Dithiothreitol
EAT	Experimental Autoimmune Thyroiditis
ECG	Electrocardiogram
ECL	Enhanced Chemiluminescent
ELISA	Enzyme-Linked Immunoorbent Assay
ER	Endoplasmic Reticulum

FACS	Fluorescent Activated Cell Sorting
FasL	Fas Ligand
FCS	Fetal Calf Serum
GAD	Glutamic Acid Decarboxylase
H-2	Mouse MHC
H & E	Hematoxylin and Eosin
HEL	Hen Egg Lysozyme
HLA	Human Leukocyte Antigen
HRP	Horseradish Peroxidase
IA-2	Tyrosine Phosphatase
IAA	Insulin Autoantibodies
ICA	Islet Cell Antigen
IDCM	Idiopathic Dilated Cardiomyopathy
IFN	Interferon
IgH	Immunoglobulin Heavychain
IGRP	Islet-specific G6Pase catalytic subunit-related protein
iIFA	Indirect Immunofluorescence
IL-	Interleukin
IDDM	Insulin Dependent Diabetes Mellitus
I.P.	Intraperitoneal
ITAM	Immunoreceptor Tyrosine-based Activation Motif
LPS	Lipopolysacharide
MΦ	Macrophage
MHC	Major Histocompatibility Complex
NOD	Nonobese Diabetic
NK	Natural Killer cell
NKT	Natural Killer T cell
OVA	Ovalbumin
PAGE	Polyacrylamide Gel Electrophoresis
PBL	Peripheral Blood Lymphocyte
PBS	Phosphate Buffered Saline

PBS-T	Phosphate Buffered Saline + 1% Tween-20
PCR	Polymerase Chain Reaction
Rag	Recombination Activating Gene
RBA	Radioligand Binding Assay
RPA	Ribonuclease Protection Assay
RR	Relative Risk
SAT	Spontaneous Autoimmune Thyroiditis
SCID	Severe Combined Immunodeficiency
SDS	Sodium Dodecyl Sulphate
SEB	*Staphylococcus aureus* Endotoxin B
SI	Stimulation Index
SPF	Specific Pathogen Free
STS	Sequence Tagged Site
T1D	Type 1 Diabetes
T3	Triiodothyroxine
T4	Thyroxine
TCA	Trichloroacetic Acid
TCR	T cell Receptor
TE	Tris-EDTA
Tg	Thyroglobulin
Th	T helper cell
TMB	3,3',5,5'-tetramethylbenzidine
TNF	Tumor Necrosis Factor
TPO	Thyroid Peroxidase
TRAIL	TNF-Related Apoptosis-Inducing Ligand
TRH	Thyroid Releasing Hormone
TSH	Thyroid Stimulating Hormone
TSST	Toxic Shock Syndrome Toxin
VAF	Virus Antibody Free
Vf	Final Volume

CHAPTER 1

GENERAL INTRODUCTION

Our most critical defense mechanism against foreign pathogens and cancer is our immune system. The numerous cells of the immune system work in concert to monitor, recognize and destroy the invading pathogens and abnormal cells. Unfortunately, in some individuals, the strict controls of the immune system fail, self tolerance breaks down and the immune system loses its ability to distinguish foreign antigen from self antigen. As a result the immune system attacks normal cells, tissues and/or organs within the body, causing a self-destructive process termed autoimmunity.

1.1 Branches of the Immune System

The immune system is divided into non-specific and specific branches. Innate immunity is the non-specific response, that is, it is not specific for any particular pathogen. The innate system includes anatomical and physiological barriers such as the skin and mucosa, as well as complement and certain immune cells such as natural killer cells (NKs), macrophages (MΦs), and dendritic cells (DCs) which recognize broad characteristics of infectious organisms such as double-stranded RNA and lipopolysaccaride (LPS) (1). In contrast, the antigen-specific defenses are accomplished by the adaptive immune system, which can recognize and selectively destroy particular invading pathogens. The exquisite specificity of adaptive immunity means that responses are inherently slower than those of the innate immune system; however, the adaptive immune system also possesses a strong immunological memory allowing it to rapidly and specifically block a repeat invasion (2-4).

The adaptive immune system makes use of co-operative interactions between humoral responses and cell-mediated responses. B cells are the key component of the humoral response and the interaction of B cells with antigen causes the proliferation and differentiation of B cells into antibody secreting plasma cells. The cell-mediated response involves the generation of effector T cells. These include both cytotoxic T lymphocytes (CTLs) that recognize and destroy target cells and T helper (Th) cells that secrete cytokines which in turn activate B cells, phagocytic cells, such as macrophages, and cytotoxic cells ((5-9); Figure 1-1).

1.2 The MHC Complex

The major histocompatibility complex (MHC) is a cluster of genes located on chromosome 6 in humans (10) and chromosome 17 in mice (11). The products of these genes are key components of the immune system and this MHC group is called the HLA (Human Leukocyte Antigen) complex in humans and the H-2 complex in mice. The H-2 complex consists of four major regions (K, I, S and D) which encode three classes of MHC molecules. The K and D regions encode class one MHC molecules, the I region encodes class II molecules and the S region encodes the class III MHC molecules. In humans, the class I MHC molecules are separated into three groups called HLA-A, -B and -C. Class III genes are located in the middle of the MHC region and the class II region is divided into HLA-DP, -DQ and –DR. ((11); Figure 1-2)

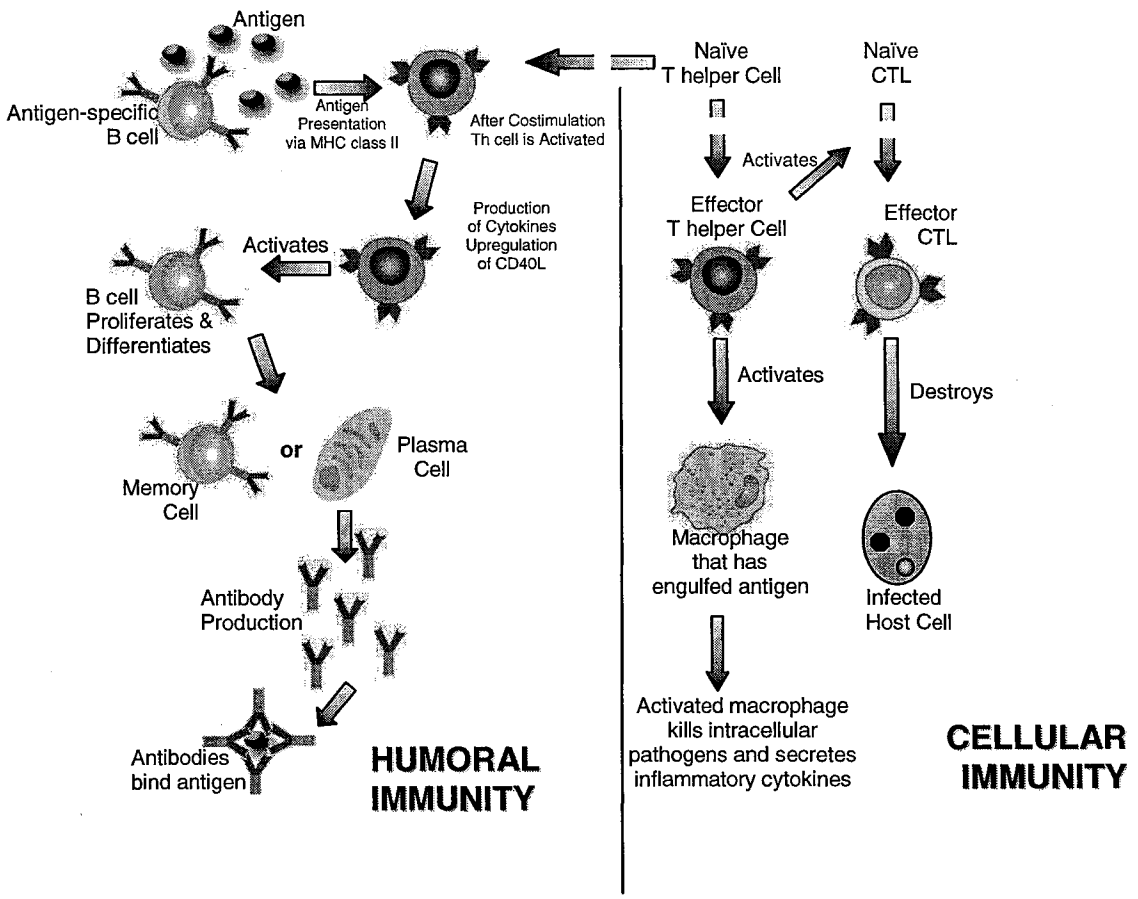

Figure 1-1: Adaptive Immunity

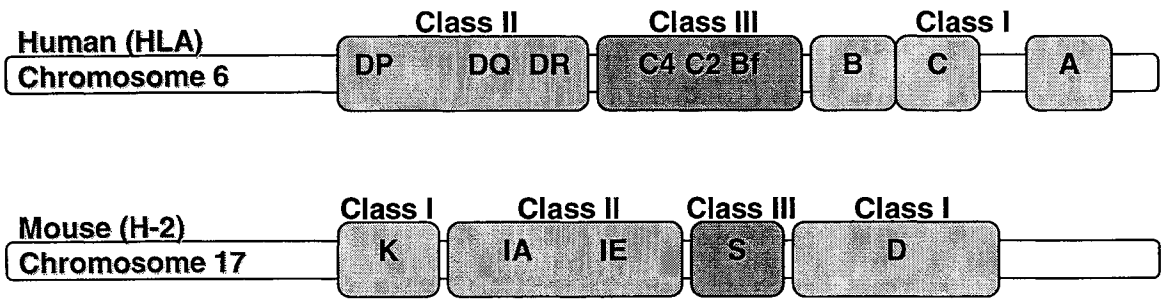

Figure 1-2: The Major Histocompatibility Complex.

Each class of MHC has a different function. Class I genes encode integral membrane glycoproteins that are found on almost all nucleated cell surfaces and they present antigen to CD8 T cells. Class II gene products are also integral membrane glycoproteins; however, they are expressed primarily on antigen presenting cells (APCs) such as B cells, macrophages and dendritic cells and these glycoproteins present antigen to CD4 T cells. Class III gene products provide a variety of functions in the immune system and include proteins such as complement and inflammatory cytokines (12-14). MHC class II is discussed further below as it is the primary focus of this thesis.

1.3 MHC Class II

MHC class II molecules are composed of a 34kDa α chain and a 29kD β chain (15). There are four domains in a class II molecule with the α1 and β1 domains forming a long, narrow peptide binding groove and the α2 and β2 domains forming the membrane proximal region which supports the floor of the peptide binding groove ((12, 16); Figure 1-3).

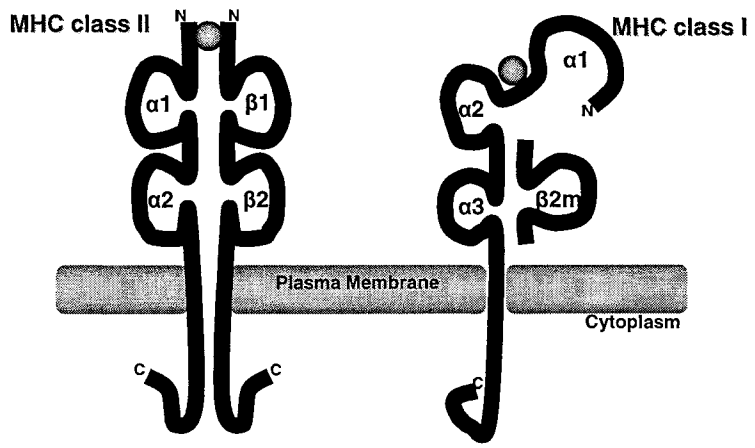

Figure 1-3: Schematic of the structures of MHC class I and II.

The peptide binding grove of an MHC class II molecule is open at both ends and displayed peptides are typically 13-25 amino acids in length, with only about 9-10 of the residues actually resting within the binding pocket (17). The bound region of the peptide typically has aromatic and hydrophobic residues towards the amino (N) terminus and three additional hydrophobic residues either in the middle or nearer the carboxy (C) terminus. By binding in appropriate pockets, these all act in concert to anchor the peptide into the binding groove (18).

Each individual inherits one set of MHC class II genes from his/her father and one set from his/her mother. However, MHC class II genes are co-dominantly expressed so that the individual will express both the maternal and the paternal alleles within each APC. Class II molecules have a high degree of polymorphism (12, 19); for example, both the α and β polypeptide chains of HLA-DQ and –DP molecules are polymorphic (across the human population there are at least 16 known variants of DQA1 and 25 of DQB1; (20)). The relatively large number of MHC class II combinations that can form in a given individual permits a vast repertoire of peptides to be bound and presented to CD4 T cells (21, 22). In this thesis, when referring to HLA molecules conventional nomenclature is used: e.g. DQA1*0102 refers to the alpha chain of DQ and specifically the 0102 allele.

1.4 MHC Class II Antigen Processing and Presentation

MHC class II molecules typically present fragments of exogenous antigens that have been internalized by APCs through either phagocytosis or endocytosis.

The exogenous antigens are degraded into peptides as they move through the endosomal compartments (12, 16, 23).

Assembly of MHC class II heterodimers begins in the endoplasmic reticulum (ER) where the newly synthesized α and β chain condense around a protein called the invariant chain which fits universally in all peptide binding grooves. Binding of the invariant chain allows stabilization of the MHC class II molecule and, in addition, prevents endogenous peptides from binding in the groove until the heterodimer reaches the secondary lysosomal compartment. From the ER, the signal sequence within the invariant chain transports the class II-invariant chain complex through the Golgi apparatus and on to the secondary lysosomal compartment (where primary lysosomes and phagosomes/endosomeshave already fused). Within the secondary lysosome compartment (sometimes called the "class II compartment in APCs) the invariant chain is degraded by acid proteases, but a small portion of the chain, called the CLIP (class II associated invariant chain peptide), initially remains associated with the peptide binding groove. However, if foreign or self peptides are present that have a higher affinity than CLIP for the peptide binding groove, they can displace CLIP and be loaded in its place. These peptide-MHC class II complexes are then transported to the cell surface by fusion of the secondary lysosome with the plasma membrane. Once on the surface the class II MHC-peptide complexes can be recognized by CD4 T cells. ((16, 23); Figure 1-4)

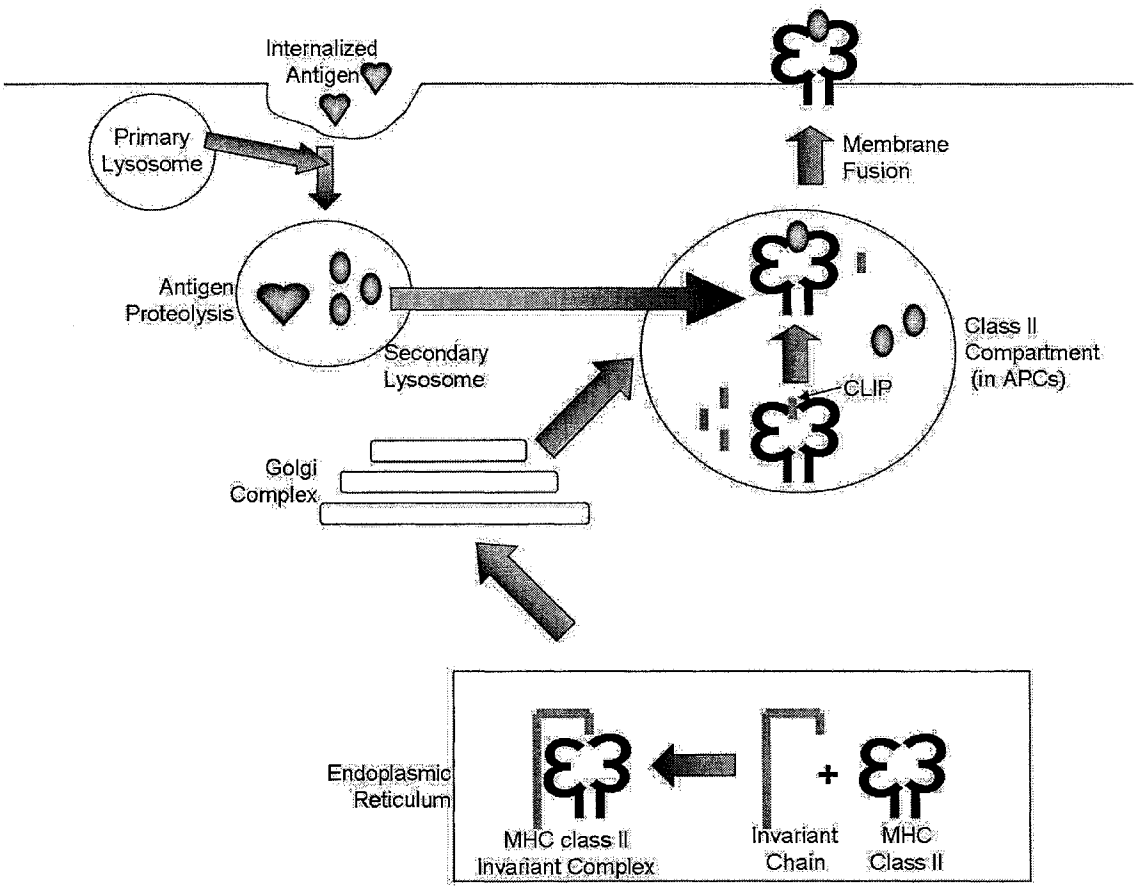

Figure 1-4: MHC Class II Antigen Presentation.

1.5 The T cell Receptor

The T cell receptor (TCR) is located on the surface of T cells and is capable of recognizing peptides that are presented on either class I MHC (in the case of CD8 T cells) or class II (in the case of CD4 T cells). On the majority of T cells, the TCR is an α/β heterodimer. Each chain in the TCR has two domains, an N terminal variable domain (having, in turn, three hypervariable regions (V)) and a constant domain (C). The carboxy-terminus of each TCR chain consists of a short hydrophobic cytoplasmic tail which anchors the TCR into the cell

membrane, with a single positively charged residue that enables the TCR to interact with the CD3 signal-transducing complex. The cytoplasmic tails of the CD3 chains contain immunoreceptor tyrosine-based activation motifs (ITAMs) that go on to interact with tyrosine kinases to initiate the signaling cascade for T cell activation. ((24, 25); Figure 1-5)

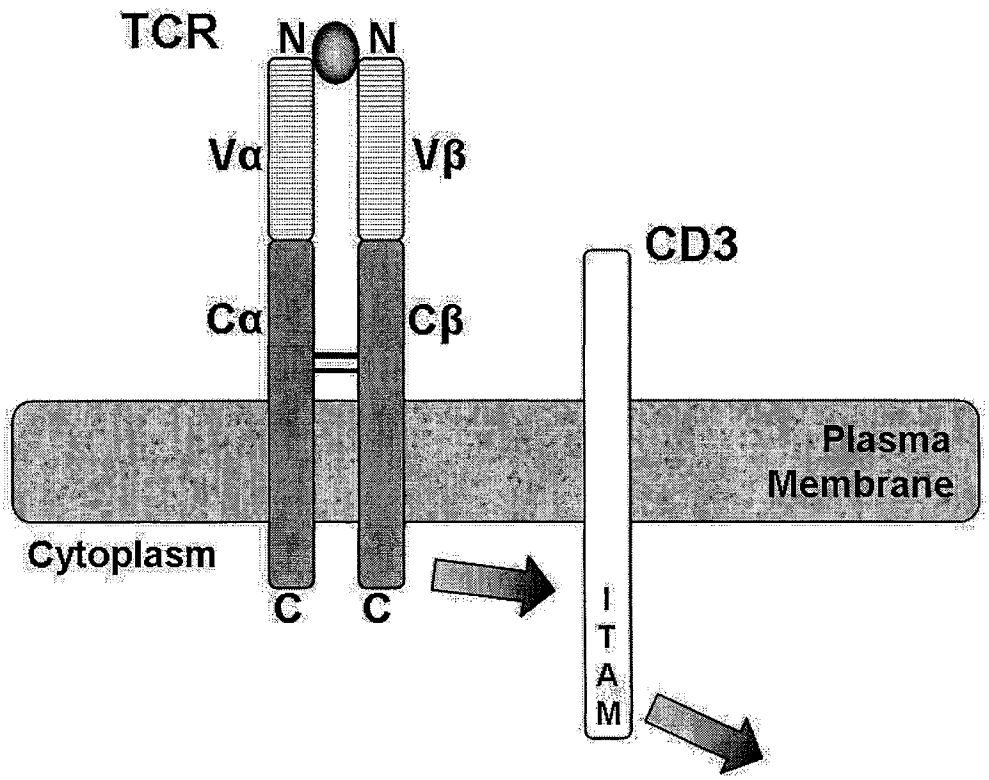

Figure 1-5: Schematic of the T cell receptor structure.

The T cell receptor is incapable of recognizing antigen directly, but instead recognizes processed antigenic peptides presented by self MHC molecules. The α chain of the TCR is encoded by the V, J and C gene segments and the β chain is encoded by the V, D, J and C gene segments. Rearrangements of these segments results in V and J joining for the α chain and V, D and J joining for the

β chain. The thousands of different combinations between V J and V D J is the basis for the diversity of the TCR which enables recognition of a vast number of different endogenous and exogenous antigens in the context of a much smaller number of self MHC molecules (26).

Gene rearrangement of the TCR occurs in the thymus during T cell maturation. During maturation, T cells are both positively and negatively selected—only those T cells expressing TCRs capable of binding to self MHCs are positively selected, and negative selection eliminates those immature T cells that have too strong an affinity for self MHC or self peptide-self MHC complexes (referred to as central tolerance to self antigen) (27).

In broad terms, T cells can be subdivided into two separate groups: CD4 T cells and CD8 T cells. CD4 and CD8 are both co-receptors that increase the affinity of a TCR-peptide-MHC complex, MHC class II in the case of CD4 and MHC class I in the case of CD8.

1.6 T cell Activation

The activation and subsequent expansion of CD4 T cells (Th cells) plays a critical role in the production of both humoral and cell-mediated immune responses. APCs, such as dendritic cells or B cells, present processed peptides in the context of MHC class II, allowing recognition of these peptides by helper T cells. An interaction between the peptide-MHC and the TCR will lead either to activation and expansion of the helper T cell or to the development of anergy leaving the T cell unresponsive (25, 28). One signal is sufficient to induce

anergy, but to fully activate naïve T cells a second signal is required: a co-stimulatory signal. This second signal comes from the interaction of a B7 molecule on the surface of an APC and CD28 expressed on the surface of the T cell (29-32). Signal 1 (MHC-peptide-TCR interaction) and signal 2 (co-stimulation) together upregulate the production of IL-2 and the expression of the high affinity IL-2 receptor allowing for the proliferation and differentiation of naïve T cells into CD4 effector T cells (29-33). When a naive CD4 T cell responds to antigen and co-stimulation in secondary lymphoid tissues, it is capable of differentiating into a Th1 cell or a Th2 cell, two different Th cell types which release distinctive patterns of cytokines and which functionally activate different types of effector cells. Pre-Th cells produce IL-2, then upon short term stimulation they become a Th0 cell which produces cytokines such as IFN-γ, IL-2, IL-4, IL-5 and IL-10. With further stimulation the Th0 cells differentiate into either Th1 cells (when stimulated in the presence of IL-12) or into Th2 cells (when stimulated under IL-4 positive conditions). Th1 cells, in general, produce IFN-γ and IL-2 and Th2 cells, in general, produce IL-4, IL-5, IL-6, and IL-10. Both cells can become memory Th cells which produce IL-2. Classically Th1 cells have been implicated in the cell-mediated pathway, e.g activating CTLs and macrophages, and on the other hand Th2 cells have classically been linked to the humoral mediated pathway because of their role in activating B cells and inducing the production of antibodies. However, these are not strict divisions of duty, for example cytokines from both subsets regulate particular types of antibody class switching from IgM. Th1 cytokines such as IFN-γ induce IgG2a

and IgG3 and inhibit IgG1, IgE and IgM, while Th2 cytokines such as IL-4 induce IgG1 and IgE, but inhibit IgG2a, IgG3 and IgM. In addition to determining various effector pathways by virtue of their lymphokine production, Th1 cells can inhibit the development of Th2 cells and vice versa (34, 35).

CTL are not fully mature when they exit the thymus; they have a functional TCR that recognizes antigenic peptide complexed with self-MHC class I, but they cannot yet lyse a target cell. To do this CTL cells must first differentiate in response to antigen. In order to differentiate into functional cytotoxic T lymphocytes, CD8+ pre-CTLs must receive three different signals. First, they must see antigenic peptide presented by self-MHC-I expressing cells, second they must receive a co-stimulatory signal (as discussed above), and third, they must be stimulated by cytokines, such as IL-2, IFN-γ and others made by nearby CD4 helper T cells activated as described above. As a result of these signals, the pre-CTL differentiates into an active CTL that can then lyse target cells that bear the appropriate peptide-MHC class I complex (36).

1.7 Immune Tolerance and Autoimmunity

Our immune system exists to protect our body from infection by a plethora of microorganisms, including bacteria, viruses and parasites. Although it is relatively easy for us to conceive that a protein fragment from a virus is foreign, it is not quite so apparent to our immune system. There is no inherent biochemical or structural difference between a protein fragment derived from a damaged cell within the body and a protein fragment from a virus. However, the immune

system must manage, reliably and consistently, to become activated only in response to the viral protein fragment and not the fragment from the host's own tissues. Hence the necessity of immune tolerance; that is, the ability of the immune system to be tolerant to antigens originating within the body, while at the same time being able to respond to antigens from environmental sources. When the immune system begins to attack its own tissues, we assume that immune tolerance has broken down and that autoimmunity has developed.

1.8 Type 1 Diabetes

Diabetes is a pancreatic endocrine disorder characterized by intermittent or persistent hyperglycemia (elevated blood sugar levels), especially after eating. Embedded throughout the pancreas are small clusters of cells called islets, which secrete insulin, glucagon and several other endocrine hormones. There are three major cell types within islets—alpha cells, beta cells and delta cells. Alpha cells produce glucagon, delta cells produce somatostatin and beta cells, the largest component of the islets, produce insulin (37).

Since insulin is the principal hormone that regulates the uptake of glucose into cells from the blood, deficiency of insulin or its action plays a central role in all forms of diabetes mellitus. In insulin-dependent (type 1) diabetes there is a breakdown in immune tolerance. Type 1 diabetes is most commonly diagnosed in children and adolescents, but can occur in adults as well. Most cases of type 1 diabetes are immune-mediated and characterized by autoimmune destruction of the β-cells in the islets of the pancreas, destroying them or damaging them

sufficiently to reduce insulin production beyond the critical threshold needed to maintain normoglycemia (37).

The two distinctive features of type 1 diabetes are the infiltration of pancreatic islets by macrophages and lymphocytes (termed insulitis) and the presence of autoantibodies in the serum. The initial trigger of the immune attack is unknown, though it is speculated to be viral in nature (37). Although the initial trigger has not been elucidated, the majority of the immune mechanism which occurs following the initial trigger has been deciphered. More than a dozen islet-cell proteins that elicit antibody responses in type 1 diabetics have been identified and the presence of autoantibodies against these autoantigens serves as an important diagnostic tool for the identification of pre-diabetic children (38). Insulin and glutamic acid decarboxylase (GAD) are the two autoantigens that have been most studied; presence of autoantibodies against these consistently indicates autoimmune activity in pancreatic islets (39). The characterization of autoantibodies has been valuable to identify proteins involved in β-cell autoimmunity; however, the precise role of these antibodies in the pathogenesis of type 1 diabetes remains unclear. In this respect, a greater emphasis has been placed on studying the cell-mediated (T cell) rather than the humoral (antibody) response. This shift in focus has led to the discovery that many of these autoantigens, including GAD (40) and insulin (41), are targeted not only by autoantibodies, but also very likely by T cells (42-44), although not all investigators have been able to reproduce these T cell results (J. Elliott, personal communication). Insulitis, during the prediabetic phase, occurs when

macrophages and activated T cells invade the islets and first begin destroying the insulin-secreting β-cells. Analysis of pancreatic islets during this stage has revealed the presence of both CD4 and CD8 T cells and immunological studies with experimental animals have indicated that both are necessary to induce β-cell autoimmunity (37). Several studies have also demonstrated an important role for many pro-apoptotic pathways, specifically the Fas/Fas Ligand (FasL), perforin and TNF-α pathways in the T cell-induced apoptosis of β-cells (45-47).

For most individuals, type 1 diabetes is treated with insulin injections, lifestyle adjustments and careful monitoring of blood glucose levels using blood test kits; the treatment must be continued throughout life.

1.9 MHC Class II Associations with Type 1 Diabetes

Type 1 diabetes is a complex disease influenced by both environmental and genetic factors. HLA has a strong association with susceptibility to type 1 diabetes (37). Studies analyzing twins have provided some of the strongest evidence for genetic predisposition to the disease. In identical twins, if one twin has diabetes the other twin has a 35-50% chance of developing the disease (48, 49). In HLA-identical siblings the concordance rate is 15-25%; however, in siblings that do not share any HLA alleles the concordance rate is only 1% (49, 50). In particular, the highly polymorphic HLA-DR and DQ genes influence both susceptibility and resistance to diabetes (49, 51).

A large percentage of people with type 1 diabetes have either the DR3 or DR4 alleles (49). DR1, DR8 or DR16 also increase susceptibility to type 1

diabetes, whereas DR11 and DR15 are found to be protective (37). The strongest association with susceptibility and resistance to diabetes is with particular HLA-DQ genotypes, which can be further influenced by the HLA-DR subtype. Susceptibility to type 1 diabetes in humans has been associated with DQ8 (DQA1*0301, DQB1*0302) with a relative risk of 8-12 and DQ2 (DQA1*0501, DQB1*0201) with a relative risk of 3-5 (relative risk is defined as the ratio of disease risk for a given genotype versus the risk for the general population, predisposing risk >1 and protection <1). The highest risk of diabetes is associated with the heterozygous combination of DQ8 and DQ2 with a relative risk of 5-35. In contrast, DQ6 (DQA1*0102, DQB1*0602) is associated with dominant protection from the disease (RR = 0.2). Even when a high risk allele, such as DQ8, is present, in combination with DQ6 the relative risk for disease development is much less than one (49, 51-53).

1.10 NOD Mice

The Nonobese Diabetic (NOD) mouse was originally established in 1980 by Makino et al (54). NOD mice spontaneously develop type 1 diabetes via a T cell-mediated pathway. Depletion of T cells by neonatal thymectomy or by administration of immunosuppressive agents such as anti-CD4, anti-CD8, anti-CD3 antibodies or cyclosporine can prevent diabetes in NOD mice (55-59). Furthermore, the disease can be induced by adoptively transferring T cells from diabetic NOD mice into immunodeficient syngeneic strains such as NOD-SCID or NOD-Rag$^{-/-}$ (56, 60, 61). The immune destruction appears to be via co-operation

between CD4 and CD8 T cells (60, 62, 63) and there is evidence for involvement by CD4 T cells (60, 64, 65) and CD8 T cells (56, 66-69). The three autoantigens that have been shown to be important in diabetes in humans (proinsulin, GAD and IA-2) are also associated with diabetes autoimmunity in the NOD mouse (70). More recently an additional autoantigen, IGRP (islet-specific glucose-6-phosphatase catalytic subunit-related protein), has been identified (71). Over 20% of CD8 T cells found infiltrating the NOD β-cell are IGRP responsive and NOD diabetes is blocked in the absence of these IGRP-reactive CD8 T cells (71).

The NOD mouse expresses the MHC class I molecules Kd and Db. NOD mice have a deletion in the Ea promoter which results in a lack of expression of IE molecules and, therefore, they express only a single MHC class II molecule, IAg7 (72). NOD mice that do not express IAg7 (NOD IAb knockout mice) do not develop diabetes (73); however, IAg7 by itself is not sufficient for diabetes development as shown by studies with MHC congenics (72).

There is evidence that both central and peripheral tolerance mechanisms may be defective in the NOD mouse. A number of studies have suggested that there is defect in the thymic negative selection process (74-77). For example, one set of studies compared a self-antigen specific TCR transgenic system in the NOD background versus the B10 genetic background and revealed that NOD has a decreased ability to negatively select the self-specific TCR (75). In another study (77) a defect in Aire expression in the NOD thymus was described (Aire controls the ectopic expression of many self proteins in the medullary epithelial cells of the thymus (76)); perhaps this is another mechanism by which central

tolerance is disrupted in this mouse strain. The association of certain MHC class II alleles with autoimmunity reflects the ability of these class II molecules to present peptides in a manner that fails to eliminate autoreactive CD4 T cells in the thymus and activates them in the periphery (70). It has been suggested that IAg7 forms weak, unstable interactions with peptides, thereby failing to negatively select eliminate or inactivate autoreactive T cells centrally (78, 79). Alternatively, the unusual structure of IAg7 (a non-Asp residue at position 57 of the beta chain (80) and a wider peptide binding groove) may allow it to bind and present certain peptides that cannot be presented by other MHC haplotypes (81). Within NOD mice it has been hypothesized that the maintenance of peripheral tolerance is impaired by alterations in T cell signaling (82, 83) and apoptosis (84), insufficient co-stimulation from accessory cells (85-88) and defects in regulatory T cells (89-93). All of these factors together appear to promote the production of autoreactive T cells.

The NOD mouse has contributed substantially to elucidating the pathogenesis of autoimmune diabetes. However, disease mechanisms in NOD mice do not necessarily mimic those in humans and many preventative therapies and treatments for autoimmune diabetes found to be effective in NOD mice have failed to be effective in humans.

1.11 HLA-Transgenic Mouse Models of Type 1 Diabetes

Every individual expresses a number of different MHC class I and II molecules, thus making it difficult to study the effects of individual MHC alleles in

humans without the influence of other MHC alleles. The creation of HLA-transgenics has allowed for the study of individual HLA molecules (94). A number of different transgenic mouse lines have been produced that express diabetes susceptible human MHC class II molecules including DQ8, DQ2, DR3 and DR4 on various backgrounds including NOD, C57BL/6 and C57/BL10. In one study, DQ8 and DR3 HLA transgenic mice created in the C57BL/6 background (in the absence of endogenous mouse class II and expressing the co-stimulatory molecule B7.1 on the β-cells) developed diabetes (95). These mice, and others (e.g. (96)), have provided valuable tools for mapping epitopes for diabetes-associated autoantigens restricted to these human HLA class II molecules. GAD65 and proinsulin epitopes have been identified for DQ8 and DR4 and IA-2 epitopes have been identified for DQ8 (94).

1.12 DQ8 Transgenic NOD Mice

Our lab formulated three hypotheses regarding HLA-DQ transgenic NOD mice.

1. NOD mice expressing both IAg7 and the diabetes susceptibility HLA DQ8 (DQA1*0301, DQB1*0302) will still be susceptible to diabetes.
2. Removal of the IAg7, leaving only the DQ8, will generate NOD mice that will still develop diabetes, but will be more relevant as a human model.
3. NOD mice expressing both IAg7 and the diabetes resistance HLA haplotype DQ6 (DQA1*0102, DQB1*0602) will be protected from diabetes.

NOD mice expressing both IAg7 and the human HLA DQ8 (designated NOD.DQ8) do indeed still develop diabetes and at the exact same incidence to NOD (L.Wicker (University of Cambridge, UK) unpublished results; Appendix III). However, data from L. Wicker revealed that the CD4 T cell responses of these NOD.DQ8 mice were predominantly restricted to IAg7. Analysis of 87 NOD.DQ8 CD4 T cell hybridomas, all made to OVA, revealed that 86 of them were restricted to IAg7 (L.Wicker personal communication with J.Elliott). This result suggested that in the presence of mouse MHC class II the human DQ8 MHC class II is ignored by the immune system. Therefore, NOD.DQ8 mice were crossed onto IAb knockout NOD mice to develop NOD mice with DQ8 as the only MHC class II, NOD.DQ8/Ab^0 mice. We hypothesized that the CD4 T cells of NOD.DQ8/Ab^0 animals would recognize antigen in the context of DQ8 and that these mice would still develop diabetes. However, NOD.DQ8/Ab^0 mice failed to develop diabetes and, instead, developed a fatal autoimmune myocarditis with disease characteristics resembling human idiopathic dilated cardiomyopathy (IDCM; (97, 98)).

NOD.DQ8/Ab^0 mice spontaneously develop progressive dilated cardiomyopathy (Figure1-6-A; (97, 98)) leading to early death from heart failure. The pathology in these animals results from a severe organ and cell specific autoimmune response against normal cardiomyocytes in the atrial and ventricular walls of the heart ((97, 98); Figure 1-6, B-E) with the infiltrate consisting primarily of B lymphocytes and plasma cells, with lesser numbers of CD4 and CD8 T cells ((97, 98); Figure 1-7). Progression of the autoimmune process in these animals

can be followed by serial ECG measurements with first degree heart block appearing as early as 7 weeks of age and by 18 weeks of age the majority of mice have complete heart block ((97); Figure 1-8-A). This heart block progresses to complete heart failure causing premature death in both females and males ((97); Figure 1-8-B).

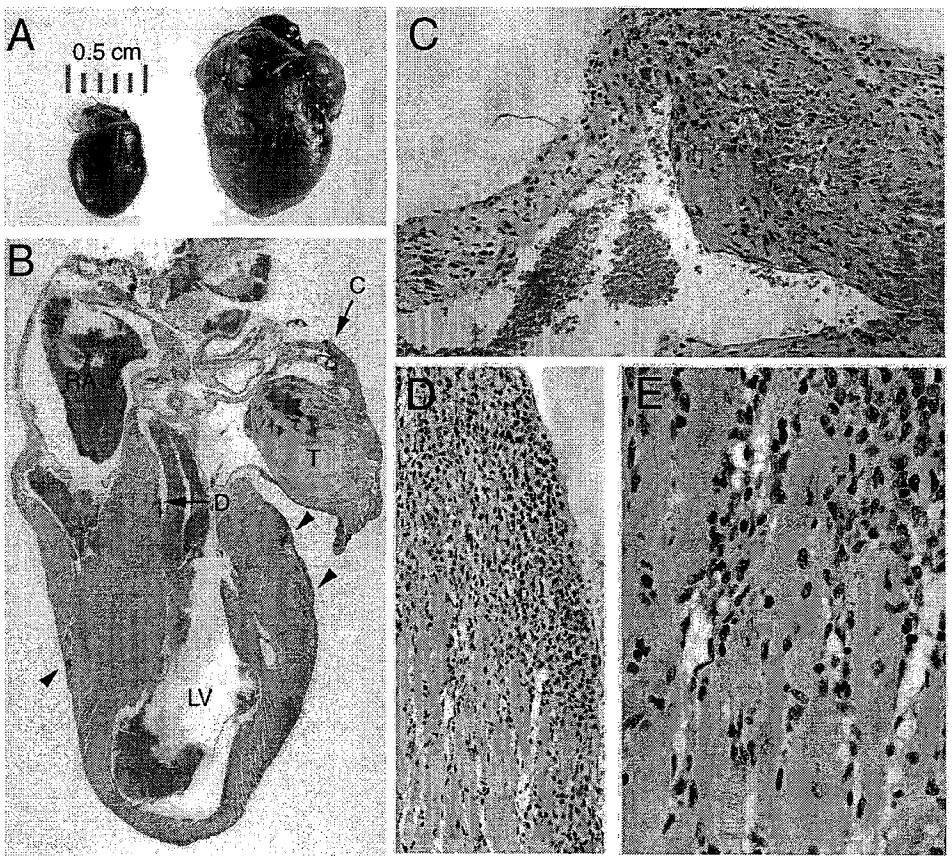

Figure 1-6: NOD.DQ8/Ab^0 mice develop enlarged hearts and myocarditis. (A) Photograph of a heart from a 22 week old NOD.DQ8/Ab^0 mouse (Right; 0.57g) compared with that of a healthy age- and sex-matched wild-type NOD mouse (Left; 0.14g). (B-E) H&E histology of an end-stage diseased heart. (B) Areas (3x) indicated by arrows are shown at higher power (100x) in (C) and (D). RA and LV indicate right atrium and left ventricle, respectively. A large thrombus (T) fills most of the left atrium. Atrial walls are extremely thin and the muscle is mostly fibrotic. Residual patches of dying atrial cardiomyocytes stain bright pink (C) and are associated with mononuclear cell infiltrates. Mononuclear cell infiltrates can be seen in the ventricular endocardium (D and at a higher magnification in E (400x)) and on the epicardial surface (arrow heads in B). *Adapted from Elliott et al. 2003 (97).*

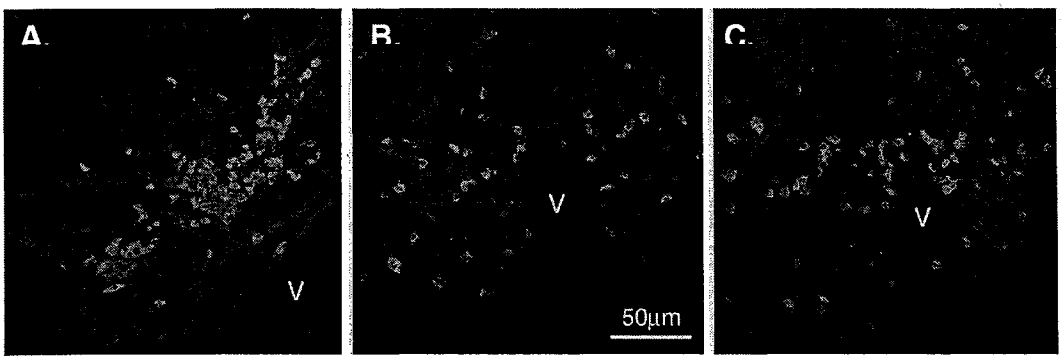

Figure 1-7: Myocardial infiltrate of NOD.DQ8/Ab^0 mice contains B cells, CD8 and CD4 T cells. Frozen sections of NOD.DQ8/Ab^0 hearts were stained via indirect immunofluorescence. Nuclei are counterstained in blue with DAPI. The majority of cells showed surface or cytoplasmic IgG expression consistent with B lymphocytes and plasma cells (A; light green staining). Smaller numbers of CD4 and CD8 T cells were also present (B and C, respectively). Magnification is 100x. *Adapted from Elliott et al. 2003 (97).*

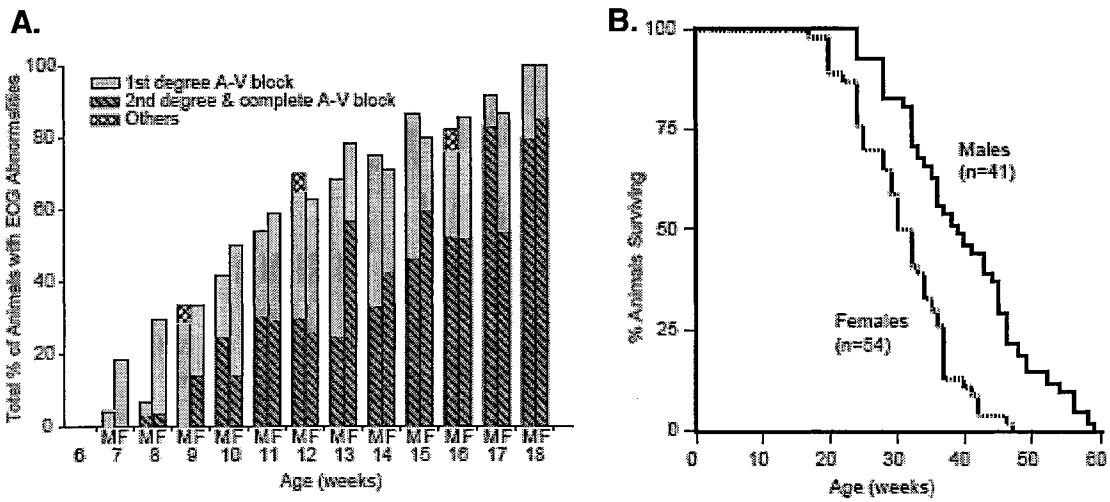

Figure 1-8: NOD.DQ8/Ab^0 mice progress to complete heart block and heart failure. (A) Summary of ECG findings for male, M, and female, F, NOD.DQ8/Ab^0 mice of various ages. Definitions of 1st degree, 2nd degree and complete heart block can be found in Supplementary Figure AI.1. (B) Survival curves for male and female NOD.DQ8/Ab^0 mice. Animals were monitored for 12 weeks of age and onward; severely ill animals were euthanized. *Adapted from Elliott et al. 2003 (97).*

Irradiation of young NOD.DQ8/Ab^0 animals significantly delays disease progression, which can be reversed by adoptive transfer of splenocytes taken from older animals with complete heart block ((97); Figure 1-9).

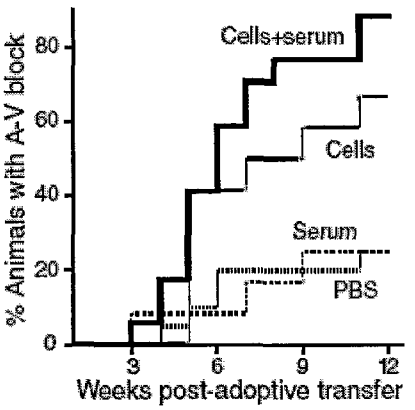

Figure 1-9: The autoimmune myocarditis of NOD.DQ8/Ab^0 mice can be adoptively transferred. Incidence of heart block (measured by ECG) in irradiated 5wk old NOD.DQ8/Ab^0 mice that received adoptive transfer of splenocytes (n=12), serum (n=12), both agents (n=17), or PBS alone (n=20). *Adapted from Elliott et al. 2003 (97).*

In addition to the destructive infiltrates within the myocardium, circulating anti-cardiac autoantibodies can also be detected (Figure 1-10) and these autoantibodies are against cardiac myosin ((97, 98); Figure 1-11-A) and the titres increase with age ((97, 98); Figure 1-11-B).

These symptoms of NOD.DQ8/Ab^0 animals are very similar to that of humans with idiopathic dilated cardiomyopathy. This transgenic strain provides a highly relevant animal model for human autoimmune myocarditis and dilated cardiomyopathy.

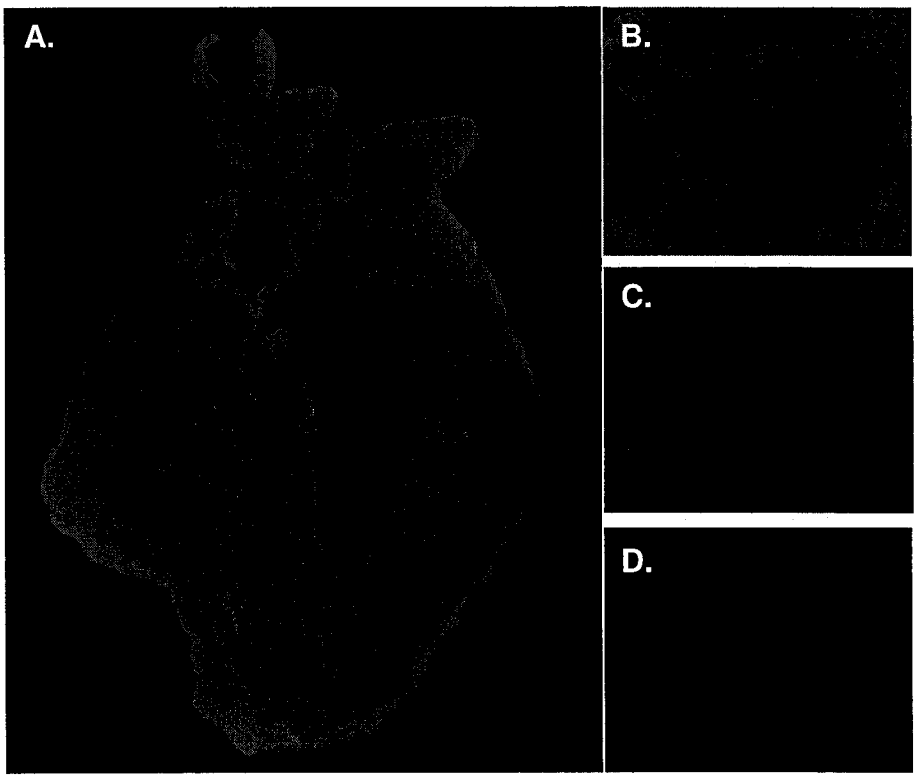

Figure 1-10: Anti-heart autoantibodies in NOD.DQ8/Ab^0 mice can be detected by indirect immunofluorescence. (A) A frozen section of a NOD.Rag1^0 heart was stained with serum from a NOD.DQ8/Ab^0 mouse and revealed the presence of anti-nuclear and anti-heart tissue autoantibodies in the serum of NOD.DQ8/Ab^0 mice. (B-D) Pre-treatment with 1%SDS/PBS revealed the binding of antibodies to the cardiomyocytes when NOD.DQ8/Ab^0 serum was used (B), but not when Balb/c serum (C) or the secondary antibody alone (D) was used. Serum was used at 1:200. *(S.Hayward, unpublished)*

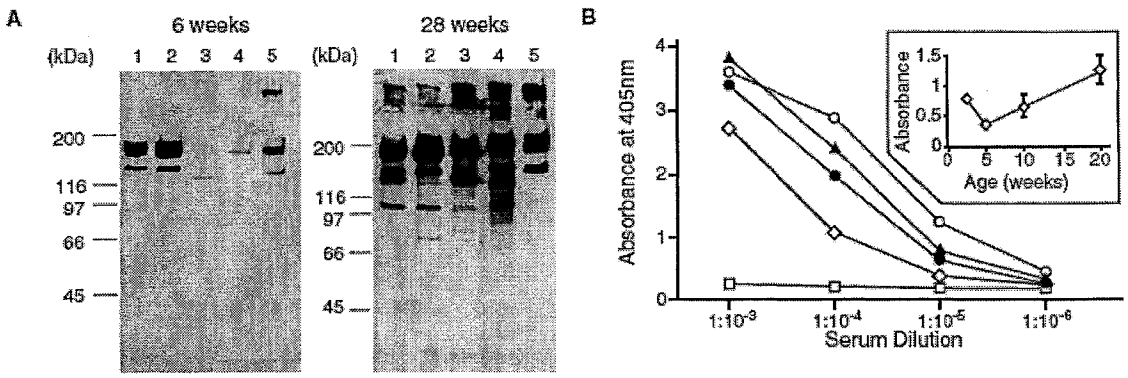

Figure 1-11: NOD.DQ8/Ab^0 mice develop anti-heart autoantibodies as measured by ELISA and Western blot. (A) Identical Western blots made with heart muscle proteins and probed with sera from two different NOD.DQ8/Ab^0 mice (6 week old animal without heart block, left and 28 week old animal with complete AV block, right). Lanes contain muscle proteins extracted from: 1, mouse atria; 2, mouse ventricles; 3, mouse skeletal muscle; 4, purified porcine skeletal myosin; and 5, purified porcine cardiac myosin. (B) Titration curves for anti-cardiac myosin antibodies present in pooled sera of NOD.DQ8/Ab^0 mice of various ages: 2.5wks (triangle), 5wks (diamond), 10wks (solid circle), and 20wks (open circle). Shown also is pooled NOD.DQ8 sera (square) as a negative control. (B, inset) Data re-plotted as absorbance versus age for pooled sera at the 1:100,000 dilution. *Adapted from Elliott et al. 2003 (97).*

1.13 Autoimmune Myocarditis and IDCM

Idiopathic dilated cardiomyopathy (IDCM) is a condition characterized by cardiac enlargement and impaired function of the ventricles with an estimated incidence rate greater than 1/20,000 (99, 100). Microscopic examination reveals myocyte hypertrophy, increased interstitial fibrosis, myocyte atrophy and myofilament loss (101, 102). In addition, areas of mononuclear cell infiltration can be seen (103) and in humans with IDCM a number of immune regulatory abnormalities have been identified including humoral (104) and cellular autoimmunity against myocytes (105), decreased NK cell activity (106) and

abnormal suppressor activity (107, 108). It has been suggested that IDCM may be triggered by subclinical viral myocarditis where the inflammation initiates a variety of autoimmune reactions against the myocardium, ultimately resulting in cardiac dilation and conduction defects. Presence of abnormalities in immune regulation and anti-cardiac autoantibodies in IDCM (109, 110) are consistent with this hypothesis. As with other autoimmune diseases, HLA associations have been identified in IDCM. The frequency of HLA-B27, HLA-A2, HLA-DR4 and HLA-DQ4 is increased compared to controls (111, 112); association of IDCM with specific HLAs reinforces the idea the disease is immunological in etiology.

Previous to NOD.DQ8/Ab^0 mice, there were two dominant experimental mouse models for autoimmune myocarditis: virus-induced and cardiac antigen-induced. Both models produce myocardial inflammation and heart reactive autoantibodies.

Viral myocarditis can be induced in mice using a cardio-tropic strain of Coxsackievirus B3 (CB3; (113)). This CB3-induced myocarditis generally begins about three days post infection and, in most strains, resolves at about three weeks. However, in some strains such as A/J mice, the disease has a second phase which may persist for two months (114). In all strains, the first phase of the disease is characterized by focal cardiomyocyte necrosis and mononuclear cell infiltrate. However, in mice genetically susceptible to the second phase heart reactive autoantibodies also occur. Indirect immunofluorescence reveals these antibodies are reactive to the surface of the cardiomyocytes and the interstitial

striations (115) and closer examination by Western blotting shows a predominance of anti-cardiac myosin heavy chain autoantibodies (116).

Myosin-induced myocarditis is the other major animal model of autoimmune myocarditis, typically studied in mice and less commonly in rats. Upon injection of cardiac myosin (but not skeletal myosin) emulsified in complete freunds adjuvant (CFA), autoimmune myocarditis can be induced in susceptible strains (117). Again, mononuclear cell infiltrate, cardiomyocyte damage and anti-cardiac autoantibodies can all be observed (117, 118). Adoptive transfer experiments with this model have shown that T cells (119), but not autoantibodies (120) can transfer the disease.

Based on these models, Rose and colleagues (121) have proposed an immune mechanism whereby CB3 infection causes damage to cardiomyocytes and the accumulation of inflammatory cells within the myocardium. During this inflammatory process, cardiac myosin is released and then taken up and presented by resident dendritic cells or invading macrophages to CD4 helper T cells. The cardiac myosin-specific CD4 T cells are then activated and induce even more widespread destruction of cardiomyocytes by activation of cytotoxic CD8 cells and by recruitment, through cytokines, of additional macrophages and lymphocytes. These macrophages and lymphocytes then go on to complete the destruction of the cardiac muscle (121).

1.14 Autoimmune Thyroiditis

As you will see later in this thesis we have also developed a DQ transgenic NOD line that develops autoimmune thyroiditis, and as such it seemed pertinent to provide some introduction to this disease as well.

1.14.1 The Thyroid Gland

In humans, the thyroid is a bowtie or butterfly shaped organ which wraps around the anterior-lateral trachea just below and extending behind the Adam's apple. The thyroid is a key organ in a signaling pathway that begins in the brain. The hypothalamus generates thyroid releasing hormone (TRH) which signals to the pituitary to release thyroid stimulating hormone (TSH) into the bloodstream, and this in turn signals the thyroid to produce and release thyroid hormones (122).

Thyroglobulin (Tg) is the dominant antigen of the thyroid. It is a ~660kDa glycoprotein with two identical subunits. Tg is expressed only in the thyroid gland where it functions as a matrix for the iodination of its tyrosines during the synthesis of thyroid hormones (123).

Another important antigen within the thyroid is thyroid peroxidase (TPO). It is ~105kDa in size and is found on the surface of and in the cytoplasm of thyroid follicular cells. TPO is the enzyme which generates the thyroid hormones by catalyzing two sequential reactions: the iodination of the tyrosines on thyroglobulin and the synthesis of the two thyroid hormones from two iodotyrosines (124).

The hormones generated by the thyroid are T3 (triiodothyroxine) and T4 (thyroxine), with the 3 and 4 indictating the number of iodines located within the molecule. The total thyroid hormone level is composed of approximately 80% T4 and 20% T3; however, T3 is the more biologically active hormone and most of the T3 is actually made from T4 outside the thyroid. Together T3 and T4 stimulate the synthesis of enzymes in the respiratory chain, thereby making the thyroid a critical player in the regulation of basal metabolic rate (122).

1.14.2 Autoimmune Thyroiditis in Humans

Autoimmune thyroiditis is the third most common autoimmune disease in the United States (125) and often occurs in individuals afflicted with other autoimmune conditions such as type 1 diabetes (126), lupus (127), rheumatoid arthritis (128) and multiple sclerosis (129).

About 5-10% of the female population of child-bearing age is afflicted with autoimmune thyroiditis and as such the condition can have serious consequences for pregnancy and fetal health (130). Women with autoimmune thyroiditis have an increased risk for miscarriage, and if the woman's autoimmune disease has progressed to hypothyroidism then she is at risk for obstetric complications such as premature labor and preeclampsia. Thyroid hormones have been shown to have direct effects on several different cell types within the ovary and, thus, thyroid abnormalities can directly interfere with normal ovarian function. In mild hypothyroidism ovulation and conception can occur, but such pregnancies frequently still end with miscarriage, fetal loss, or premature

birth. However, in severe hypothyroidism there is frequently ovulatory dysfunction which results in infertility (130).

Hashimoto's disease is one of the main forms of autoimmune thyroiditis and of most importance to the content of this thesis and thus will receive the most discussion.

Hashimoto's disease was first described by Dr. M. Hashimoto in 1912 (131). Symptoms include cold intolerance, apathy, mental slowing, dry skin and hair loss. In Hashimoto's disease a diffuse goiter is often, but not always visible. Further histological analysis of diseased thyroid glands reveals mononuclear cell infiltrates consisting primarily of lymphocytes, often aggregating to form lymphoid follicles with germinal centers (124). In addition, plasma cells and macrophages can be detected within the same glands. Destruction of the thyroid includes a reduced number of thyroid follicles, a variable degree of fibrosis and disruption of the normal architecture (124). The presence of circulating anti-thyroid peroxidase and anti-thyroglobulin autoantibodies can also be detected (132). Hasimoto's affects about 0.7% of the population, with the majority of afflicted individuals being over the age of 50 (133). Although Hashimoto's causes approximately 70% of hypothyroidism cases, only about 10% of Hashimoto's patients develop hypothyroidism. In hypothyroidism both T4 and T3 levels are lowered and TSH levels are elevated.

In Hashimoto's patients, the mononuclear cell infiltrates seen within the thyroid gland consist of CD4 and CD8 T lymphocytes, macrophages and plasma cells (134). The cytokine profiles suggest dominance towards a Th1 phenotype.

Apoptosis plays a key role in the destruction of the thyroid in Hashimoto's thyroiditis. In normal thyroid glands less than 1% of thyrocytes are apoptotic. However, in the thyroids of Hashimoto patients up to 20-30% of thyrocytes are apoptotic, especially at the periphery of infiltrated areas (124). Both Fas and TRAIL have been implicated in this apoptotic process and a decrease in the apoptotic proteins Bcl-2 and Bcl-xL has been reported in the thyrocytes of Hashimoto's patients (124, 135, 136).

1.14.3 HLA Associations

Various studies have looked at HLA associations with Hashimoto's disease. Studies by Shi and colleagues suggest that susceptibility in Caucasians is probably via DQA1*0301/DR4 and DQB1*0201/DR3 (137), whereas others have suggested an association of HLA-DR5 with goitrous thryoidits and HLA-DR3 with non-goitrous destructive thyroiditis (138).

1.14.4 Experimental Models

Much of our understanding of autoimmune thyroiditis comes from animal models. Experimental autoimmune thyroiditis (EAT) can be induced by injection of thyroid antigen into virtually all animal species including rabbit, guinea pig, mouse, rat, dog, monkey and chicken and thyroid lesions can be seen within all animals (124). Since thyroglobulin is an organ specific protein and it can be isolated quite easily from thyroids, the principle EAT induction antigen is thyroglobulin (Tg). Induction either includes the addition of adjuvant such as

CFA, LPS, or *Bordetella pertussis* or it involves the repeated injection of thyroglobulin (122).

Even when the disease is induced with Tg the autoantibodies that develop are not only against thyroglobulin; immune escalation occurs. Once an autoimmune process has begun in an organ, other antigens of the same organ are recruited into the autoimmune process and, in fact, virtually all human autoimmune diseases are characterized by the presence of multiple autoantibodies. Such is also the case in experimental models: in the experimental rhesus monkey model of EAT the disease is induced with thyroglobulin, but the monkeys generate autoantibodies not only to thyroglobulin, but also to thyroid peroxidase (139). However, although the appearance of anti-Tg autoantibodies is well documented in EAT, in contrast to humans, anti-TPO autoantibodies have not been observed to date except in the monkey model and those EAT models induced with TPO (124, 140).

EAT in various models has been shown to be T cell dependent (141, 142) and depleting anti-CD4 can prevent the induction and expression of EAT (143, 144). A role for T regulatory cells in EAT has also recently been established (145-147). For example, CD4+ CD25+ T cells have been shown to be suppressive for autoimmune thyroiditis both in naïve and mouse thyroglobulin tolerized mice (147).

The first evidence for the association of autoimmunity with the MHC complex actually came from EAT. In 1971 Vladutiu and Rose examined a large number of inbred mouse strains and they found differing susceptibility to EAT and

induction depended mainly upon class II genes whereas disease severity is modulated by class I MHC (148). For example, mice strains that are H-2k or H-2s are strongly susceptible to induction of EAT; they show high autoantibody titres and significant thyroid infiltrate. H-2b or H-2d mouse strains, on the other hand, are poor responders to EAT induction and exhibit low antibody titres and minimal thyroid infiltrate (123).

A number of humanized HLA transgenic models have been developed to investigate susceptibility to autoimmune thyroiditis including HLA-DRB1*0301 (DR3) mice which were found to be susceptible to EAT using mouse Tg while HLA-DRB1*0502 (DR2) transgenic mice were not (124, 149, 150). Both DQ8 (HLA-DQA1*0301, DQB1*0302) and DQ6 (HLA-DQA1*0103, DQB1*0601) transgenic mice are not susceptible to induction using mouse Tg; however, human Tg can induce moderate EAT in DQ8, but not DQ6 mice (151, 152). In double transgenic mice for DR3 and DQ8 the human Tg induced thyroiditis was less severe than in DR3 mice, but more severe than in DQ8 mice (153).

Some would suggest that experimental models have serious flaws as they are induced rather than spontaneous. A number of differences exist between EAT and Hashimoto's, including no female susceptibility dominance and no destruction of follicular cells and development of fibrosis and in most EAT models goiter and hypothyroidism do not develop (154). However, valuable information can still be obtained from experimental models and they have the added benefit that they are reliable and predictable.

1.14.5 Spontaneous Models

Spontaneous autoimmune thyroiditis (SAT) has been detected in a number of animals including chickens, rats, mice, dogs and monkeys; however, the incidence in the majority of these models is quite low. Perhaps the most well documented spontaneous model is an obese strain of chickens which develops symptoms very similar to humans, including high autoantibody titres, mononuclear cell infiltrate with complete destruction of the thyroid and hormonal changes. As with humans, the disease is under strict genetic control and is also affected by exogenous factors such as iodine (124, 155, 156).

BB rats and NOD mice are also models of SAT. However, like the spontaneous autoimmune diabetes that they both develop, the incidence within these strains varies considerably from colony to colony (124).

Rose and colleagues have investigated the spontaneous autoimmune thyroiditis of NOD.H2h4 mice. NOD.H2h4 mice were generated by the backcrossing of wild-type NOD mice (IAg7) with B10.A(4R)-H2h4 mice which creates an H-2k mouse on a NOD background. H-2k mice are good responders to EAT induction and NOD.H2h4 animals no longer develop diabetes; they develop thyroiditis (157). Although NOD.H2h4 mice show endogenous thyroiditis, the ingestion of iodine enhances the disease in a dose-dependent manner. 54% of females and 70% of males show thyroid lesions and anti-Tg autoantibodies after iodine treatment; however, they do not develop anti-TPO autoantibodies and their T4 level remains normal (157). The dependence on iodine in thyroid metabolism is well documented and it is not surprising that

dietary iodine might influence the incidence of autoimmune thyroiditis. Evidence suggests that iodine incorporation in thyroglobulin may enhance the antigenicity of Tg by increasing its affinity for the TCR or MHC molecule (132). In fact, in humans it has been shown that the peripheral blood lymphocytes (PBLs) from Hashimoto's patients are unable to recognize poorly iodinated Tg and that iodination of the Tg actually promotes the recognition by and proliferation of such human PBLs (132). Perhaps the addition of iodine creates new epitopes or exposes cryptic epitopes on thyroglobulin.

Rose and colleagues' work with NOD.H2h4 mice has also revealed evidence that CD4 and CD8 T cells are both required for initiation; however, only CD4 T cells are needed to maintain the chronicity of the disease. In fact if the disease is allowed to develop, and then CD4 T cells are depleted, the disease severity decreases, but if CD8 T cells are depleted instead, disease severity increases (132). NKT cells have been proposed to have a regulatory role in this autoimmune pathogenesis in NOD.H2h4 animals (158). NOD.H2h4 animals have increased numbers of NKT cells whose presence appears to enhance the thyroiditis within these animals (158).

Recently a new transgenic mouse model was developed that also develops SAT. A CD4 T cell clone was isolated from the thyroid of a patient with autoimmune thyroiditis and the TCR transgenic line, TAZ10 mice ($TCR^{+/+}$ $Rag1^{-/-}$ H-2k), was generated using the clone-specific TCR (159). The TAZ10 TCR is specific for two contiguous epitopes from the autoantigen TPO. These epitopes are differentially recognized; there is a naturally occurring antagonistic epitope

($TPO_{537-548}$) and an agonistic highly stimulatory epitope ($TPO_{536-547}$) (159, 160). The agonistic epitope is a cryptic epitope preferentially displayed after endogenous processing during inflammation and it is restricted to H-2k (or DQA1*0102, DQB1*0602 in humans) (159). TAZ10 animals show an increase in weight, a decrease in T4 levels, an increase in TSH levels and mononuclear cell infiltrate with follicular destruction. Within the interfollicular spaces are clusters of both CD4 and CD8 T lymphocytes and the thyrocytes (but not the lymphocytes) undergo apoptosis (159). Crossing of TAZ10 mice onto a $Rag1^{+/+}$ background still permits the development of SAT; although, the kinetics are slowed significantly compared to TAZ10 mice and studies reveal the importance of the suppression of regulatory cells in autoimmune thyroiditis (161).

1.15 Experimental Design

The main objective of this thesis was to characterize the autoimmunity and immune pathogenesis of HLA-transgenic NOD mice. As discussed, NOD.DQ8/Ab^0 mice develop spontaneous dilated cardiomyopathy leading to complete heart failure. Our initial hypothesis was: similarly to the spontaneous diabetes in NOD, the presence of CD4 T cells, CD8 T cells, and B cells are all critical to the autoimmune myocarditis of NOD.DQ8/Ab^0 animals. In Chapter 2 we begin to decipher the immune mechanism-of-action causing the destruction. We use adoptive transfer and knockout models to investigate the importance of B cells, CD4 T cells and CD8 T cells to the development of autoimmune myocarditis in NOD.DQ8/Ab^0 mice. NOD.DQ8 and NOD.DQ8/Ab^0 mice develop

diabetes and autoimmune myocarditis, respectively, and in Chapter 3 we investigate another diabetes-related HLA, DQ6 (DQA1*0102, DQB1*0602), by characterizing the phenotypes of NOD.DQ6 and NOD.DQ6/Ab^0 mice. Our initial hypothesis was that NOD.DQ6 would not develop diabetes and that NOD.DQ6/Ab^0 would not develop diabetes or myocarditis. Our secondary hypothesis became, NOD.DQ6/Ab^0 mice are a spontaneous model of autoimmune thyroiditis. Chapter 3 also begins to decipher the immune mechanism of action causing the autoimmunity in NOD.DQ6/Ab^0 mice using an adoptive transfer model. Autoantibodies are a key component of autoimmune diseases and in order to properly characterize the autoantibody response of NOD.DQ6/Ab^0 mice, a new autoantibody radioligand binding assay had to be developed—Chapter 4 explains this assay. Our base hypothesis for Chapter 4's radioligand binding assay was, the NOD.DQ6/Ab^0 serum staining of mouse thyroid follicles represents anti-thyroid peroxidase autoantibodies. The appendices, in addition to providing supplementary material (I), include the investigation of other areas of autoimmunity: II) The phenotype of NOD.$DQ6^{+/-}$ $DQ8^{+/-}$/Ab^0 mice and III) The lack of diabetes in NOD.DQ6/Ab^0 mice.

1.16 References

1. Tosi, M. F. 2005. Innate immune responses to infection. *J Allergy Clin Immunol 116:241.*

2. Lanzavecchia, A., and F. Sallusto. 2000. Dynamics of T lymphocyte responses: intermediates, effectors, and memory cells. *Science 290:92.*

3. Sallusto, F., J. Geginat, and A. Lanzavecchia. 2004. Central memory and effector memory T cell subsets: function, generation, and maintenance. *Annu Rev Immunol 22:745.*

4. McHeyzer-Williams, L. J., and M. G. McHeyzer-Williams. 2005. Antigen-specific memory B cell development. *Annu Rev Immunol 23:487.*

5. Foy, T. M., A. Aruffo, J. Bajorath, J. E. Buhlmann, and R. J. Noelle. 1996. Immune regulation by CD40 and its ligand GP39. *Annu Rev Immunol 14:591.*

6. DeFranco, A. L. 1987. Molecular aspects of B-lymphocyte activation. *Annu Rev Cell Biol 3:143.*

7. Paulnock, D. M. 1992. Macrophage activation by T cells. *Curr Opin Immunol 4:344.*

8. Stout, R. D., and K. Bottomly. 1989. Antigen-specific activation of effector macrophages by IFN-gamma producing (TH1) T cell clones. Failure of IL-4-producing (TH2) T cell clones to activate effector function in macrophages. *J Immunol 142:760.*

9. Berke, G. 1994. The binding and lysis of target cells by cytotoxic lymphocytes: molecular and cellular aspects. *Annu Rev Immunol 12:735.*

10. Beck, S., D. Geraghty, H. Inoko, and L. Rowen. 1999. Complete sequence and gene map of a human major histocompatibility complex. The MHC sequencing consortium. *Nature 401:921.*

11. Steinmetz, M., and L. Hood. 1983. Genes of the major histocompatibility complex in mouse and man. *Science 222:727.*

12. Germain, R. N. 1994. MHC-dependent antigen processing and peptide presentation: providing ligands for T lymphocyte activation. *Cell 76:287.*

13. Colten, H. R. 1984. Expression of the MHC class III genes. *Philos Trans R Soc Lond B Biol Sci 306:355.*

14. Whitehead, A. S., and R. Sackstein. 1985. Molecular biology of the human and mouse MHC class III genes: phylogenetic conservation, genetics and regulation of expression. *Immunol Rev 87:185.*

15. Springer, T. A., J. F. Kaufman, C. Terhorst, and J. L. Strominger. 1977. Purification and structural characterisation of human HLA-linked B-cell antigens. *Nature 268:213.*

16. Cresswell, P. 1994. Assembly, transport, and function of MHC class II molecules. *Annu Rev Immunol 12:259.*

17. Rudensky, A., P. Preston-Hurlburt, S. C. Hong, A. Barlow, and C. A. Janeway, Jr. 1991. Sequence analysis of peptides bound to MHC class II molecules. *Nature 353:622.*

18. Madden, D. R. 1995. The three-dimensional structure of peptide-MHC complexes. *Annu Rev Immunol 13:587.*

19. Andersen, L. C., J. S. Beaty, J. W. Nettles, C. E. Seyfried, G. T. Nepom, and B. S. Nepoom. 1991. Allelic polymorphism in transcriptional regulatory regions of HLA-DQB genes. *J Exp Med 173:181.*

20. Begovich, A. B., P. V. Moonsamy, S. J. Mack, L. F. Barcellos, L. L. Steiner, S. Grams, V. Suraj-Baker, J. Hollenbach, E. Trachtenberg, L. Louie, P. Zimmerman, A. V. Hill, M. Stoneking, T. Sasazuki, V. I. Konenkov, M. L. Sartakova, V. P. Titanji, O. Rickards, and W. Klitz. 2001. Genetic variability and linkage disequilibrium within the HLA-DP region: analysis of 15 different populations. *Tissue Antigens 57:424.*

21. Williams, T. M. 2001. Human leukocyte antigen gene polymorphism and the histocompatibility laboratory. *J Mol Diagn 3:98.*

22. Cullen, M., J. Noble, H. Erlich, K. Thorpe, S. Beck, W. Klitz, J. Trowsdale, and M. Carrington. 1997. Characterization of recombination in the HLA class II region. *Am J Hum Genet 60:397.*

23. Watts, C. 2004. The exogenous pathway for antigen presentation on major histocompatibility complex class II and CD1 molecules. *Nat Immunol 5:685.*

24. Kuhns, M. S., M. M. Davis, and K. C. Garcia. 2006. Deconstructing the form and function of the TCR/CD3 complex. *Immunity 24:133.*

25. Weiss, A., and D. R. Littman. 1994. Signal transduction by lymphocyte antigen receptors. *Cell 76:263.*

26. Davis, M. M., and P. J. Bjorkman. 1988. T-cell antigen receptor genes and T-cell recognition. *Nature 334:395.*

27. Hogquist, K. A., T. A. Baldwin, and S. C. Jameson. 2005. Central tolerance: learning self-control in the thymus. *Nat Rev Immunol 5:772.*

28. Powell, J. D. 2006. The induction and maintenance of T cell anergy. *Clin Immunol.*

29. Appleman, L. J., and V. A. Boussiotis. 2003. T cell anergy and costimulation. *Immunol Rev 192:161.*

30. Gimmi, C. D., G. J. Freeman, J. G. Gribben, K. Sugita, A. S. Freedman, C. Morimoto, and L. M. Nadler. 1991. B-cell surface antigen B7 provides a costimulatory signal that induces T cells to proliferate and secrete interleukin 2. *Proc Natl Acad Sci U S A 88:6575.*

31. Jenkins, M. K., P. S. Taylor, S. D. Norton, and K. B. Urdahl. 1991. CD28 delivers a costimulatory signal involved in antigen-specific IL-2 production by human T cells. *J Immunol 147:2461.*

32. Linsley, P. S., W. Brady, L. Grosmaire, A. Aruffo, N. K. Damle, and J. A. Ledbetter. 1991. Binding of the B cell activation antigen B7 to CD28 costimulates T cell proliferation and interleukin 2 mRNA accumulation. *J Exp Med 173:721.*

33. Liu, Y., and C. A. Janeway, Jr. 1992. Cells that present both specific ligand and costimulatory activity are the most efficient inducers of clonal expansion of normal CD4 T cells. *Proc Natl Acad Sci U S A 89:3845.*

34. Mosmann, T. R., and R. L. Coffman. 1989. TH1 and TH2 cells: different patterns of lymphokine secretion lead to different functional properties. *Annu Rev Immunol 7:145.*

35. Crane, I. J., and J. V. Forrester. 2005. Th1 and Th2 lymphocytes in autoimmune disease. *Crit Rev Immunol 25:75.*

36. Kuppers, R. C., and C. S. Henney. 1977. Studies on the mechanism of lymphocyte-mediated cytolysis. IX. Relationships between antigen recognition and lytic expression in killer T cells. *J Immunol 118:71.*

37. Atkinson, M. A., and N. K. Maclaren. 1994. The pathogenesis of insulin-dependent diabetes mellitus. *N Engl J Med 331:1428.*

38. Winter, W. E., N. Harris, and D. Schatz. 2002. Type 1 diabetes islet autoantibody markers. *Diabetes Technol Ther 4:817.*

39. Nepom, G. T. 1995. Glutamic acid decarboxylase and other autoantigens in IDDM. *Curr Opin Immunol 7:825.*

40. Kaufman, D. L., M. Clare-Salzler, J. Tian, T. Forsthuber, G. S. Ting, P. Robinson, M. A. Atkinson, E. E. Sercarz, A. J. Tobin, and P. V. Lehmann. 1993. Spontaneous loss of T-cell tolerance to glutamic acid decarboxylase in murine insulin-dependent diabetes. *Nature 366:69.*

41. Wegmann, D. R., M. Norbury-Glaser, and D. Daniel. 1994. Insulin-specific T cells are a predominant component of islet infiltrates in pre-diabetic NOD mice. *Eur J Immunol 24:1853.*

42. Atkinson, M. A., D. L. Kaufman, L. Campbell, K. A. Gibbs, S. C. Shah, D. F. Bu, M. G. Erlander, A. J. Tobin, and N. K. Maclaren. 1992. Response of peripheral-blood mononuclear cells to glutamate decarboxylase in insulin-dependent diabetes. *Lancet 339:458.*

43. Keller, R. J. 1990. Cellular immunity to human insulin in individuals at high risk for the development of type I diabetes mellitus. *J Autoimmun 3:321.*

44. Haskins, K., and D. Wegmann. 1996. Diabetogenic T-cell clones. *Diabetes 45:1299.*

45. Eizirik, D. L., and T. Mandrup-Poulsen. 2001. A choice of death--the signal-transduction of immune-mediated beta-cell apoptosis. *Diabetologia 44:2115.*

46. Amrani, A., J. Verdaguer, S. Thiessen, S. Bou, and P. Santamaria. 2000. IL-1alpha, IL-1beta, and IFN-gamma mark beta cells for Fas-dependent destruction by diabetogenic CD4(+) T lymphocytes. *J Clin Invest 105:459.*

47. Su, X., Q. Hu, J. M. Kristan, C. Costa, Y. Shen, D. Gero, L. A. Matis, and Y. Wang. 2000. Significant role for Fas in the pathogenesis of autoimmune diabetes. *J Immunol 164:2523.*

48. Barnett, A. H., C. Eff, R. D. Leslie, and D. A. Pyke. 1981. Diabetes in identical twins. A study of 200 pairs. *Diabetologia 20:87.*

49. Thorsby, E., and K. S. Ronningen. 1993. Particular HLA-DQ molecules play a dominant role in determining susceptibility or resistance to type 1 (insulin-dependent) diabetes mellitus. *Diabetologia 36:371.*

50. Deschamps, I., H. Lestradet, M. Busson, and J. Hors. 1984. Evaluation of recurrence risk in siblings of diabetic children: importance of age and birth order in relation to HLA genotypes. *Diabetes Res 1:125.*

51. She, J. X. 1996. Susceptibility to type I diabetes: HLA-DQ and DR revisited. *Immunol Today 17:323.*

52. Thomson, G. 1983. Investigation of the mode of inheritance of the HLA associated diseases by the method of antigen genotype frequencies among diseased individuals. *Tissue Antigens 21:81.*

53. Baisch, J. M., T. Weeks, R. Giles, M. Hoover, P. Stastny, and J. D. Capra. 1990. Analysis of HLA-DQ genotypes and susceptibility in insulin-dependent diabetes mellitus. *N Engl J Med 322:1836.*

54. Makino, S., K. Kunimoto, Y. Muraoka, Y. Mizushima, K. Katagiri, and Y. Tochino. 1980. Breeding of a non-obese, diabetic strain of mice. *Jikken Dobutsu 29:1.*

55. Belghith, M., J. A. Bluestone, S. Barriot, J. Megret, J. F. Bach, and L. Chatenoud. 2003. TGF-beta-dependent mechanisms mediate restoration of self-tolerance induced by antibodies to CD3 in overt autoimmune diabetes. *Nat Med 9:1202.*

56. Wong, F. S., I. Visintin, L. Wen, R. A. Flavell, and C. A. Janeway, Jr. 1996. CD8 T cell clones from young nonobese diabetic (NOD) islets can transfer rapid onset of diabetes in NOD mice in the absence of CD4 cells. *J Exp Med 183:67.*

57. Sempe, P., M. F. Richard, J. F. Bach, and C. Boitard. 1994. Evidence of CD4+ regulatory T cells in the non-obese diabetic male mouse. *Diabetologia 37:337.*

58. Makhlouf, L., S. T. Grey, V. Dong, E. Csizmadia, M. B. Arvelo, H. Auchincloss, Jr., C. Ferran, and M. H. Sayegh. 2004. Depleting anti-CD4 monoclonal antibody cures new-onset diabetes, prevents recurrent autoimmune diabetes, and delays allograft rejection in nonobese diabetic mice. *Transplantation 77:990.*

59. Mori, Y., M. Suko, H. Okudaira, I. Matsuba, A. Tsuruoka, A. Sasaki, H. Yokoyama, T. Tanase, T. Shida, M. Nishimura, and et al. 1986. Preventive effects of cyclosporin on diabetes in NOD mice. *Diabetologia 29:244.*

60. Christianson, S. W., L. D. Shultz, and E. H. Leiter. 1993. Adoptive transfer of diabetes into immunodeficient NOD-scid/scid mice. Relative contributions of CD4+ and CD8+ T-cells from diabetic versus prediabetic NOD.NON-Thy-1a donors. *Diabetes 42:44.*

61. Soderstrom, I., M. L. Bergman, F. Colucci, K. Lejon, I. Bergqvist, and D. Holmberg. 1996. Establishment and characterization of RAG-2 deficient non-obese diabetic mice. *Scand J Immunol 43:525.*

62. DiLorenzo, T. P., R. T. Graser, T. Ono, G. J. Christianson, H. D. Chapman, D. C. Roopenian, S. G. Nathenson, and D. V. Serreze. 1998. Major histocompatibility complex class I-restricted T cells are required for all but the end stages of diabetes development in nonobese diabetic mice

and use a prevalent T cell receptor alpha chain gene rearrangement. *Proc Natl Acad Sci U S A 95:12538.*

63. Bendelac, A., C. Carnaud, C. Boitard, and J. F. Bach. 1987. Syngeneic transfer of autoimmune diabetes from diabetic NOD mice to healthy neonates. Requirement for both L3T4+ and Lyt-2+ T cells. *J Exp Med 166:823.*

64. Haskins, K., and M. McDuffie. 1990. Acceleration of diabetes in young NOD mice with a CD4+ islet-specific T cell clone. *Science 249:1433.*

65. Rohane, P. W., A. Shimada, D. T. Kim, C. T. Edwards, B. Charlton, L. D. Shultz, and C. G. Fathman. 1995. Islet-infiltrating lymphocytes from prediabetic NOD mice rapidly transfer diabetes to NOD-scid/scid mice. *Diabetes 44:550.*

66. Wicker, L. S., E. H. Leiter, J. A. Todd, R. J. Renjilian, E. Peterson, P. A. Fischer, P. L. Podolin, M. Zijlstra, R. Jaenisch, and L. B. Peterson. 1994. Beta 2-microglobulin-deficient NOD mice do not develop insulitis or diabetes. *Diabetes 43:500.*

67. Kay, T. W., J. L. Parker, L. A. Stephens, H. E. Thomas, and J. Allison. 1996. RIP-beta 2-microglobulin transgene expression restores insulitis, but not diabetes, in beta 2-microglobulin null nonobese diabetic mice. *J Immunol 157:3688.*

68. Serreze, D. V., W. S. Gallichan, D. P. Snider, K. Croitoru, K. L. Rosenthal, E. H. Leiter, G. J. Christianson, M. E. Dudley, and D. C. Roopenian. 1996. MHC class I-mediated antigen presentation and induction of CD8+ cytotoxic T-cell responses in autoimmune diabetes-prone NOD mice. *Diabetes 45:902.*

69. Wang, B., A. Gonzalez, C. Benoist, and D. Mathis. 1996. The role of CD8+ T cells in the initiation of insulin-dependent diabetes mellitus. *Eur J Immunol 26:1762.*

70. Adorini, L., S. Gregori, and L. C. Harrison. 2002. Understanding autoimmune diabetes: insights from mouse models. *Trends Mol Med 8:31.*

71. Lieberman, S. M., A. M. Evans, B. Han, T. Takaki, Y. Vinnitskaya, J. A. Caldwell, D. V. Serreze, J. Shabanowitz, D. F. Hunt, S. G. Nathenson, P. Santamaria, and T. P. DiLorenzo. 2003. Identification of the beta cell antigen targeted by a prevalent population of pathogenic CD8+ T cells in autoimmune diabetes. *Proc Natl Acad Sci U S A 100:8384.*

72. Wicker, L. S., J. A. Todd, and L. B. Peterson. 1995. Genetic control of autoimmune diabetes in the NOD mouse. *Annu Rev Immunol 13:179.*

73. Mora, C., F. S. Wong, C. H. Chang, and R. A. Flavell. 1999. Pancreatic infiltration but not diabetes occurs in the relative absence of MHC class II-restricted CD4 T cells: studies using NOD/CIITA-deficient mice. *J Immunol 162:4576.*

74. Kishimoto, H., and J. Sprent. 2001. A defect in central tolerance in NOD mice. *Nat Immunol 2:1025.*

75. Lesage, S., S. B. Hartley, S. Akkaraju, J. Wilson, M. Townsend, and C. C. Goodnow. 2002. Failure to censor forbidden clones of CD4 T cells in autoimmune diabetes. *J Exp Med 196:1175.*

76. Liston, A., S. Lesage, J. Wilson, L. Peltonen, and C. C. Goodnow. 2003. Aire regulates negative selection of organ-specific T cells. *Nat Immunol 4:350.*

77. Zuklys, S., G. Balciunaite, A. Agarwal, E. Fasler-Kan, E. Palmer, and G. A. Hollander. 2000. Normal thymic architecture and negative selection are associated with Aire expression, the gene defective in the autoimmune-polyendocrinopathy-candidiasis-ectodermal dystrophy (APECED). *J Immunol 165:1976.*

78. Carrasco-Marin, E., J. Shimizu, O. Kanagawa, and E. R. Unanue. 1996. The class II MHC I-Ag7 molecules from non-obese diabetic mice are poor peptide binders. *J Immunol 156:450.*

79. Ridgway, W. M., M. Fasso, and C. G. Fathman. 1999. A new look at MHC and autoimmune disease. *Science 284:749.*

80. Acha-Orbea, H., and H. O. McDevitt. 1987. The first external domain of the nonobese diabetic mouse class II I-A beta chain is unique. *Proc Natl Acad Sci U S A 84:2435.*

81. Tisch, R., and H. McDevitt. 1996. Insulin-dependent diabetes mellitus. *Cell 85:291.*

82. Koarada, S., Y. Wu, G. Olshansky, and W. M. Ridgway. 2002. Increased nonobese diabetic Th1:Th2 (IFN-gamma:IL-4) ratio is CD4+ T cell intrinsic and independent of APC genetic background. *J Immunol 169:6580.*

83. Rapoport, M. J., A. Jaramillo, D. Zipris, A. H. Lazarus, D. V. Serreze, E. H. Leiter, P. Cyopick, J. S. Danska, and T. L. Delovitch. 1993. Interleukin 4 reverses T cell proliferative unresponsiveness and prevents the onset of diabetes in nonobese diabetic mice. *J Exp Med 178:87.*

84. Arreaza, G., K. Salojin, W. Yang, J. Zhang, B. Gill, Q. S. Mi, J. X. Gao, C. Meagher, M. Cameron, and T. L. Delovitch. 2003. Deficient activation and resistance to activation-induced apoptosis of CD8+ T cells is associated with defective peripheral tolerance in nonobese diabetic mice. *Clin Immunol 107:103.*

85. Dahlen, E., G. Hedlund, and K. Dawe. 2000. Low CD86 expression in the nonobese diabetic mouse results in the impairment of both T cell activation and CTLA-4 up-regulation. *J Immunol 164:2444.*

86. Bour-Jordan, H., B. L. Salomon, H. L. Thompson, G. L. Szot, M. R. Bernhard, and J. A. Bluestone. 2004. Costimulation controls diabetes by altering the balance of pathogenic and regulatory T cells. *J Clin Invest 114:979.*

87. Luhder, F., P. Hoglund, J. P. Allison, C. Benoist, and D. Mathis. 1998. Cytotoxic T lymphocyte-associated antigen 4 (CTLA-4) regulates the unfolding of autoimmune diabetes. *J Exp Med 187:427.*

88. Balasa, B., T. Krahl, G. Patstone, J. Lee, R. Tisch, H. O. McDevitt, and N. Sarvetnick. 1997. CD40 ligand-CD40 interactions are necessary for the initiation of insulitis and diabetes in nonobese diabetic mice. *J Immunol 159:4620.*

89. Delovitch, T. L., and B. Singh. 1997. The nonobese diabetic mouse as a model of autoimmune diabetes: immune dysregulation gets the NOD. *Immunity 7:727.*

90. Harrison, L. C., M. Dempsey-Collier, D. R. Kramer, and K. Takahashi. 1996. Aerosol insulin induces regulatory CD8 gamma delta T cells that prevent murine insulin-dependent diabetes. *J Exp Med 184:2167.*

91. Hutchings, P. R., and A. Cooke. 1990. The transfer of autoimmune diabetes in NOD mice can be inhibited or accelerated by distinct cell populations present in normal splenocytes taken from young males. *J Autoimmun 3:175.*

92. Sharif, S., G. A. Arreaza, P. Zucker, and T. L. Delovitch. 2002. Regulatory natural killer T cells protect against spontaneous and recurrent type 1 diabetes. *Ann N Y Acad Sci 958:77.*

93. Lepault, F., and M. C. Gagnerault. 2000. Characterization of peripheral regulatory CD4+ T cells that prevent diabetes onset in nonobese diabetic mice. *J Immunol 164:240.*

94. Wong, F. S., and L. Wen. 2004. What can the HLA transgenic mouse tell us about autoimmune diabetes? *Diabetologia 47:1476.*

95. Rajagopalan, G., Y. C. Kudva, L. Chen, L. Wen, and C. S. David. 2003. Autoimmune diabetes in HLA-DR3/DQ8 transgenic mice expressing the co-stimulatory molecule B7-1 in the beta cells of islets of Langerhans. *Int Immunol 15:1035.*

96. Wen, L., F. S. Wong, J. Tang, N. Y. Chen, M. Altieri, C. David, R. Flavell, and R. Sherwin. 2000. In vivo evidence for the contribution of human histocompatibility leukocyte antigen (HLA)-DQ molecules to the development of diabetes. *J Exp Med 191:97.*

97. Elliott, J. F., J. Liu, Z. N. Yuan, N. Bautista-Lopez, S. L. Wallbank, K. Suzuki, D. Rayner, P. Nation, M. A. Robertson, G. Liu, and K. M. Kavanagh. 2003. Autoimmune cardiomyopathy and heart block develop spontaneously in HLA-DQ8 transgenic IAbeta knockout NOD mice. *Proc Natl Acad Sci U S A 100:13447.*

98. Taylor, J. A., E. Havari, M. F. McInerney, R. Bronson, K. W. Wucherpfennig, and M. A. Lipes. 2004. A spontaneous model for autoimmune myocarditis using the human MHC molecule HLA-DQ8. *J Immunol 172:2651.*

99. Codd, M. B., D. D. Sugrue, B. J. Gersh, and L. J. Melton, 3rd. 1989. Epidemiology of idiopathic dilated and hypertrophic cardiomyopathy. A population-based study in Olmsted County, Minnesota, 1975-1984. *Circulation 80:564.*

100. Rakar, S., G. Sinagra, A. Di Lenarda, A. Poletti, R. Bussani, F. Silvestri, and F. Camerini. 1997. Epidemiology of dilated cardiomyopathy. A prospective post-mortem study of 5252 necropsies. The Heart Muscle Disease Study Group. *Eur Heart J 18:117.*

101. Mestroni, L., E. M. Gilbert, T. J. Bohlmeyer, and M. R. Bristow. 2004. *The Heart.* McGraw-Hill, New York.

102. Roberts, W. C., R. J. Siegel, and B. M. McManus. 1987. Idiopathic dilated cardiomyopathy: analysis of 152 necropsy patients. *Am J Cardiol 60:1340.*

103. Tazelaar, H. D., and M. E. Billingham. 1986. Leukocytic infiltrates in idiopathic dilated cardiomyopathy. A source of confusion with active myocarditis. *Am J Surg Pathol 10:405.*

104. Caforio, A. L., P. J. Keeling, E. Zachara, L. Mestroni, F. Camerini, J. M. Mann, G. F. Bottazzo, and W. J. McKenna. 1994. Evidence from family studies for autoimmunity in dilated cardiomyopathy. *Lancet 344:773.*

105. Kawai, C., and T. Takatsu. 1975. Clinical and experimental studies on cardiomyopathy. *N Engl J Med 293:592.*

106. Anderson, J. L., J. F. Carlquist, and E. H. Hammond. 1982. Deficient natural killer cell activity in patients with idiopathic dilated cardiomyopathy. *Lancet 320:1124.*

107. Fowles, R. E., C. P. Bieber, and E. B. Stinson. 1979. Defective in vitro suppressor cell function in idiopathic congestive cardiomyopathy. *Circulation 59:483.*

108. Gerli, R., P. Rambotti, F. Spinozzi, A. Bertotto, V. Chiodini, P. Solinas, I. Gernini, and S. Davis. 1986. Immunologic studies of peripheral blood from patients with idiopathic dilated cardiomyopathy. *Am Heart J 112:350.*

109. Neumann, D. A., C. L. Burek, K. L. Baughman, N. R. Rose, and A. Herskowitz. 1990. Circulating heart-reactive antibodies in patients with myocarditis or cardiomyopathy. *J Am Coll Cardiol 16:839.*

110. Caforio, A. L., N. J. Mahon, F. Tona, and W. J. McKenna. 2002. Circulating cardiac autoantibodies in dilated cardiomyopathy and myocarditis: pathogenetic and clinical significance. *Eur J Heart Fail 4:411.*

111. Anderson, J. L., J. F. Carlquist, J. R. Lutz, C. W. DeWitt, and E. H. Hammond. 1984. HLA A, B and DR typing in idiopathic dilated cardiomyopathy: a search for immune response factors. *Am J Cardiol 53:1326.*

112. Carlquist, J. F., R. L. Menlove, M. B. Murray, J. B. O'Connell, and J. L. Anderson. 1991. HLA class II (DR and DQ) antigen associations in idiopathic dilated cardiomyopathy. Validation study and meta-analysis of published HLA association studies. *Circulation 83:515.*

113. Herskowitz, A., L. J. Wolfgram, N. R. Rose, and K. W. Beisel. 1987. Coxsackievirus B3 murine myocarditis: a pathologic spectrum of myocarditis in genetically defined inbred strains. *J Am Coll Cardiol 9:1311.*

114. Rose, N. R., L. J. Wolfgram, A. Herskowitz, and K. W. Beisel. 1986. Postinfectious autoimmunity: two distinct phases of coxsackievirus B3-induced myocarditis. *Ann N Y Acad Sci 475:146.*

115. Wolfgram, L. J., K. W. Beisel, and N. R. Rose. 1985. Heart-specific autoantibodies following murine coxsackievirus B3 myocarditis. *J Exp Med 161:1112.*

116. Alvarez, F. L., N. Neu, N. R. Rose, S. W. Craig, and K. W. Beisel. 1987. Heart-specific autoantibodies induced by Coxsackievirus B3: identification of heart autoantigens. *Clin Immunol Immunopathol 43:129.*

117. Neu, N., N. R. Rose, K. W. Beisel, A. Herskowitz, G. Gurri-Glass, and S. W. Craig. 1987. Cardiac myosin induces myocarditis in genetically predisposed mice. *J Immunol 139:3630.*

118. Neumann, D. A., J. R. Lane, S. M. Wulff, G. S. Allen, A. LaFond-Walker, A. Herskowitz, and N. R. Rose. 1992. In vivo deposition of myosin-specific autoantibodies in the hearts of mice with experimental autoimmune myocarditis. *J Immunol 148:3806.*

119. Smith, S. C., and P. M. Allen. 1991. Myosin-induced acute myocarditis is a T cell-mediated disease. *J Immunol 147:2141.*

120. Neu, N., B. Ploier, and C. Ofner. 1990. Cardiac myosin-induced myocarditis. Heart autoantibodies are not involved in the induction of the disease. *J Immunol 145:4094.*

121. Rose, N. R., A. Herskowitz, and D. A. Neumann. 1993. Autoimmunity in myocarditis: models and mechanisms. *Clin Immunol Immunopathol 68:95.*

122. Rayner, D. C., and B. R. Champion. 1995. *Thyroid Autoimmunity.* R.G. Landes Company, Austin.

123. Caturegli, P., P. O. Vidalain, M. Vali, L. A. Aguilera-Galaviz, and N. R. Rose. 1997. Cloning and characterization of murine thyroglobulin cDNA. *Clin Immunol Immunopathol 85:221.*

124. Mariotti, S., and G. Pinna. 2003. Autoimmune Thyroid Diseases. In *Diseases of the Thyroid.* L. E. Braverman, ed. Humana Press Inc., Totowa.

125. Jacobson, D. L., S. J. Gange, N. R. Rose, and N. M. Graham. 1997. Epidemiology and estimated population burden of selected autoimmune diseases in the United States. *Clin Immunol Immunopathol 84:223.*

126. Chang, C. C., C. N. Huang, and L. M. Chuang. 1998. Autoantibodies to thyroid peroxidase in patients with type 1 diabetes in Taiwan. *Eur J Endocrinol 139:44.*

127. Park, D. J., C. S. Cho, S. H. Lee, S. H. Park, and H. Y. Kim. 1995. Thyroid disorders in Korean patients with systemic lupus erythematosus. *Scand J Rheumatol 24:13.*

128. Pongratz, R., W. Buchinger, G. Semlitsch, E. Meister, K. Nadler, and F. Rainer. 2000. [Increased occurrence of autoimmune thyroiditis in patients with chronic rheumatoid arthritis]. *Acta Med Austriaca 27:58.*

129. Niederwieser, G., W. Buchinger, R. M. Bonelli, A. Berghold, F. Reisecker, P. Koltringer, and J. J. Archelos. 2003. Prevalence of autoimmune thyroiditis and non-immune thyroid disease in multiple sclerosis. *J Neurol 250:672.*

130. Poppe, K., and D. Glinoer. 2003. Thyroid autoimmunity and hypothyroidism before and during pregnancy. *Hum Reprod Update 9:149.*

131. Hashimoto, H. 1912. Zur Kenntniss der lymphomatosen Veranderung der Schilddruse (Struma lymphomatosa). *Archiv Klin Chir 97:219.*

132. Rose, N. R., R. Bonita, and C. L. Burek. 2002. Iodine: an environmental trigger of thyroiditis. *Autoimmun Rev 1:97.*

133. Collins, J., and S. Gough. 2002. Autoimmunity in thyroid disease. *Eur J Nucl Med Mol Imaging 29 Suppl 2:S417.*

134. Eguchi, K., N. Matsuoka, and S. Nagataki. 1995. Cellular immunity in autoimmune thyroid disease. *Baillieres Clin Endocrinol Metab 9:71.*

135. Mitsiades, N., V. Poulaki, V. Kotoula, G. Mastorakos, S. Tseleni-Balafouta, D. A. Koutras, and M. Tsokos. 1998. Fas/Fas ligand up-regulation and Bcl-2 down-regulation may be significant in the pathogenesis of Hashimoto's thyroiditis. *J Clin Endocrinol Metab 83:2199.*

136. Mitsiades, N., V. Poulaki, C. S. Mitsiades, D. A. Koutras, and G. P. Chrousos. 2001. Apoptosis induced by FasL and TRAIL/Apo2L in the pathogenesis of thyroid diseases. *Trends Endocrinol Metab 12:384.*

137. Shi, Y., M. Zou, D. Robb, and N. R. Farid. 1992. Typing for major histocompatibility complex class II antigens in thyroid tissue blocks:

association of Hashimoto's thyroiditis with HLA-DQA0301 and DQB0201 alleles. *J Clin Endocrinol Metab 75:943.*

138. Schleusener, H., G. Schernthaner, W. R. Mayr, P. Kotulla, U. Bogner, R. Finke, H. Meinhold, K. Koppenhagen, and K. W. Wenzel. 1983. HLA-DR3 and HLA-DR5 associated thyrotoxicosis--two different types of toxic diffuse goiter. *J Clin Endocrinol Metab 56:781.*

139. Andrada, J. A., N. R. Rose, and J. H. Kite, Jr. 1968. Experimental thyroiditis in the rhesus monkey. IV. The role of thyroglobulin and cellular antigens. *Clin Exp Immunol 3:133.*

140. Ng, H. P., J. P. Banga, and A. W. Kung. 2004. Development of a murine model of autoimmune thyroiditis induced with homologous mouse thyroid peroxidase. *Endocrinology 145:809.*

141. Romball, C. G., and W. O. Weigle. 1987. Transfer of experimental autoimmune thyroiditis with T cell clones. *J Immunol 138:1092.*

142. Flynn, J. C., D. H. Conaway, S. Cobbold, H. Waldmann, and Y. C. Kong. 1989. Depletion of L3T4+ and Lyt-2+ cells by rat monoclonal antibodies alters the development of adoptively transferred experimental autoimmune thyroiditis. *Cell Immunol 122:377.*

143. Kong, Y. M., H. Waldmann, S. Cobbold, A. A. Giraldo, B. E. Fuller, and L. L. Simon. 1989. Pathogenic mechanisms in murine autoimmune thyroiditis: short- and long-term effects of in vivo depletion of CD4+ and CD8+ cells. *Clin Exp Immunol 77:428.*

144. Nabozny, G. H., S. P. Cobbold, H. Waldmann, and Y. C. Kong. 1991. Suppression in murine experimental autoimmune thyroiditis: in vivo inhibition of CD4+ T cell-mediated resistance by a nondepleting rat CD4 monoclonal antibody. *Cell Immunol 138:185.*

145. Gangi, E., C. Vasu, D. Cheatem, and B. S. Prabhakar. 2005. IL-10-producing CD4+CD25+ regulatory T cells play a critical role in granulocyte-macrophage colony-stimulating factor-induced suppression of experimental autoimmune thyroiditis. *J Immunol 174:7006.*

146. Morris, G. P., Y. Yan, C. S. David, and Y. C. Kong. 2005. H2A- and H2E-derived CD4+CD25+ regulatory T cells: a potential role in reciprocal inhibition by class II genes in autoimmune thyroiditis. *J Immunol 174:3111.*

147. Morris, G. P., and Y. C. Kong. 2006. Tolerance to autoimmune thyroiditis: CD4+CD25+ regulatory T cells influence susceptibility but do not supersede MHC class II restriction. *Front Biosci 11:1234.*

148. Vladutiu, A. O., and N. R. Rose. 1971. Autoimmune murine thyroiditis relation to histocompatibility (H-2) type. *Science 174:1137.*

149. Kong, Y. C., L. C. Lomo, R. W. Motte, A. A. Giraldo, J. Baisch, G. Strauss, G. J. Hammerling, and C. S. David. 1996. HLA-DRB1 polymorphism determines susceptibility to autoimmune thyroiditis in transgenic mice: definitive association with HLA-DRB1*0301 (DR3) gene. *J Exp Med 184:1167.*

150. Kong, Y. C., J. C. Flynn, Q. Wan, and C. S. David. 2003. HLA and H2 class II transgenic mouse models to study susceptibility and protection in autoimmune thyroid disease. *Autoimmunity 36:397.*

151. Kong, Y. C., and C. S. David. 2000. New revelations in susceptibility to autoimmune thyroiditis by the use of H2 and HLA class II transgenic models. *Int Rev Immunol 19:573.*

152. Wan, Q., R. Shah, J. C. Panos, A. A. Giraldo, C. S. David, and Y. M. Kong. 2002. HLA-DR and HLA-DQ polymorphism in human thyroglobulin-induced autoimmune thyroiditis: DR3 and DQ8 transgenic mice are susceptible. *Hum Immunol 63:301.*

153. Flynn, J. C., Q. Wan, J. C. Panos, D. J. McCormick, A. A. Giraldo, C. S. David, and Y. C. Kong. 2002. Coexpression of susceptible and resistant HLA class II transgenes in murine experimental autoimmune thyroiditis: DQ8 molecules downregulate DR3-mediated thyroiditis. *J Autoimmun 18:213.*

154. Lahita, R. G. 2000. Textbook of the Autoimmune Diseases. Lippincott Williams & Wilkins.

155. Hala, K., G. Malin, H. Dietrich, U. Loesch, G. Boeck, H. Wolf, B. Kaspers, J. Geryk, M. Falk, and R. L. Boyd. 1996. Analysis of the initiation period of spontaneous autoimmune thyroiditis (SAT) in obese strain (OS) of chickens. *J Autoimmun 9:129.*

156. Dietrich, H. M., R. K. Cole, and G. Wick. 1999. The natural history of the obese strain of chickens--an animal model for spontaneous autoimmune thyroiditis. *Poult Sci 78:1359.*

157. Rasooly, L., C. L. Burek, and N. R. Rose. 1996. Iodine-induced autoimmune thyroiditis in NOD-H-2h4 mice. *Clin Immunol Immunopathol 81:287.*

158. Burek, C. L., R. B. Sharma, and N. R. Rose. 2003. NKT cell regulation of autoimmune thyroiditis. *Autoimmunity 36:405.*

159. Quaratino, S., E. Badami, Y. Y. Pang, I. Bartok, J. Dyson, D. Kioussis, M. Londei, and L. Maiuri. 2004. Degenerate self-reactive human T-cell receptor causes spontaneous autoimmune disease in mice. *Nat Med 10:920.*

160. Quaratino, S., M. Feldmann, C. M. Dayan, O. Acuto, and M. Londei. 1996. Human self-reactive T cell clones expressing identical T cell receptor beta chains differ in their ability to recognize a cryptic self-epitope. *J Exp Med 183:349.*

161. Badami, E., L. Maiuri, and S. Quaratino. 2005. High incidence of spontaneous autoimmune thyroiditis in immunocompetent self-reactive human T cell receptor transgenic mice. *J Autoimmun 24:85.*

CHAPTER 2

IMMUNE MECHANISMS OF NOD.DQ8/Ab^0 MICE

A version of this chapter has been accepted for publication. Hayward, S., Bautista-Lopez, N., Suzuki, K., Atrazhev, A., Dickie, P., and J. Elliott. 2006. Journal of Immunology.

2.1 Introduction

Idiopathic dilated cardiomyopathy (IDCM) is a condition where previously healthy individuals develop life-threatening heart failure associated with cardiac enlargement, but with no apparent underlying cause (1, 2). In humans the cardiac dilation seen typically occurs secondary to an inflammatory process within the heart muscle (i.e. myocarditis); it is thought to be triggered either by a prior sub-clinical viral infection or by a primary autoimmune attack against cardiomyocytes. A better understanding of the immune mechanisms acting to cause myocarditis and IDCM could potentially lead to advances in specific treatments for this disorder, which at the present time are largely supportive and non-specific. Historically two murine models have been used to investigate immune mechanisms of myocarditis: susceptible mouse strains develop post-viral myocarditis following infection with Coxsackievirus B3 (3-5) and (in the same strains) myocarditis can be induced by immunization with cardiac myosin in adjuvant (6-8). Although both models show histological evidence of myocarditis and develop anti-heart autoantibodies, the myocarditis does not arise spontaneously and is typically mild and, in addition, the models are limited because prior virus infection or immunization potentially biases the immune phenotype.

Research into IDCM caused by primary anti-cardiac autoimmune processes has advanced in the past few years by the development of several different lines of transgenic and/or gene knockout mice which develop spontaneous myocarditis and dilated cardiomyopathy. These include: 1) several

lines which over-express TNF-α specifically within cardiomyocytes (9-11); 2) a line of PD-1 receptor knockout mice crossed onto the Balb/c background (12, 13); and 3) several lines of Nonobese Diabetic (NOD) mice which express the human MHC class II molecule HLA-DQ8 (DQA1*0301, DQB1*0302) in the absence of endogenous mouse class II MHC (i.e. NOD.DQ8/Ab^0) (14, 15). Of the three available spontaneous models, the latter displays pathology most similar to what has been observed in humans with IDCM.

Our group was the first to describe a single line of NOD.DQ8/Ab^0 mice where 100% of the animals developed spontaneous anti-cardiac autoimmunity and IDCM. Features of the model include rising titres of anti-cardiac autoantibodies, focal mononuclear cell infiltrates associated with cardiomyocyte destruction in all layers of the myocardium, escalating heart block on ECG, and gradual cardiac dilation with progression to end-stage heart failure (15). Subsequently Lipes and colleagues described three additional independent NOD.DQ8/Ab^0 lines with a similar phenotype. Although Lipes' NOD.DQ8/Ab^0 lines showed somewhat lower disease penetrance, their results indicated that the myocarditis/IDCM phenotype observed in our NOD.DQ8/Ab^0 line was not due to a founder effect. Given the generality of the observation that NOD.DQ8/Ab^0 animals provide an accurate model of spontaneous autoimmune myocarditis/IDCM in humans, we proceeded to characterize the immune mechanisms acting to cause disease in our transgenic line. In undertaking these investigations we assumed it would be of interest to compare the results obtained with what is known about immune mechanisms acting to cause diabetes in NOD

mice, since the same NOD background genes (i.e. genes other than MHC) are likely important for autoimmunity in both models. For these experiments we crossed our animals onto the Rag1 knockout ($Rag1^0$), immunoglobulin heavy chain knockout (IgH^0), and β-2 microglobulin knockout ($\beta2m^0$) backgrounds, all of which were readily available in the NOD genetic background. Here we also utilized a NOD.DQ6/Ab^0 line (originally constructed by our group for studies into diabetes resistance) which is closely matched to the NOD.DQ8/Ab^0 line in every aspect except for the DQ haplotype (DQA1*0102, DQB1*0602 versus DQA1*0301, DQB1*0302). These latter investigations show that DQ6 mice do not develop any cardiac pathology; thus, implicating the DQ8 haplotype as an important contributing factor in the autoimmune myocarditis/IDCM phenotype seen in the DQ8 animals.

Four different cell types (CD4 T cells, CD8 T cells, B lymphocytes and macrophages; (15) and unpublished result) are all found within the mononuclear cell infiltrates observed in older NOD.DQ8/Ab^0 animals with heart block and it is unclear which of these cell types are primarily responsible for the cardiomyocyte destruction. Previously we have shown that adoptive transfer of splenocytes (but not anti-sera) from NOD.DQ8/Ab^0 animals with complete heart block into younger irradiated animals could cause accelerated onset of autoimmune myocarditis and heart block (15); however, the irradiation model is cumbersome and suffers from certain limitations. Here we establish the NOD.DQ8/Ab^0 $Rag1^0$ adoptive transfer model and reproduce results obtained with the irradiation model; we then go on to show that adoptive transfer of CD4 T cells alone can induce disease, whereas

adoptive transfer of purified CD8 T cells or B lymphocytes has no effect. Phenotyping of NOD.DQ8/Ab^0 IgH^0 animals indicates that they still develop complete heart block and myocarditis, but with slightly delayed kinetics, whereas NOD.DQ8/Ab^0 β2m^0 mice fail to develop any cardiac pathology. Taken together these results suggest that CD8 T cells are important for initiating myocarditis in NOD.DQ8/Ab^0 mice (although a role for NK cells cannot be excluded), whereas once autoimmune CD4 T cell responses have been induced, these responses alone are capable of inducing the full disease phenotype, through the recruitment and activation of macrophages. B lymphocytes are not needed for disease to occur (although they may play an ancillary antigen presenting role resulting in slightly earlier disease onset when they are present), and antibodies play little or no role in the disease process. These results have significant parallels with immune mechanisms causing diabetes in NOD mice, and also with the post-Coxsackievirus myocarditis model in mice. The central role of CD4 T cells and macrophages in the final disease process suggests that therapies targeted at these cell subsets may be of most benefit for patients with advanced disease.

2.2 Materials and Methods

2.2.1 Mice

NOD/LtJ mice were purchased from The Jackson Laboratory (JAX; Bar Harbor, ME).

The IAb knockout NOD line (designated NOD/Ab^0) was provided by A.M. Jevnikar (University of Western Ontario, London, ON) and the DQ8 transgenic

NOD line by L. Wicker (University of Cambridge, Cambridge, UK). Details we published previously regarding the construction of this particular DQ8 transgenic NOD line (16) need to be corrected in one aspect (L. Burkly, Biogen Idec Inc, Cambridge, MA; personal communication). The DQA1*0301 and DQB1*0302 genes were not microinjected as two separate genomic fragments (i.e. from cosmids H11A and X10A; (17)), but rather the entire DQ8 gene (containing both α and β segments plus upstream regulatory elements) was injected as a single large DNA fragment, having been isolated from the cosmid pDCβ2 (17). This DQ8 transgenic NOD line has been assigned the formal designation NOD.Tg(CD2-CD4,HLA-DQA1*0301,HLA-DQB1*0302)1Ell. For sake of brevity, we will henceforth refer to this line as NOD.DQ8.

Intercrossing of the NOD.DQ8 and IAb knockout NOD lines to create the NOD.Cg-H2-Ab1^{tm1Gru}Tg(CD2-CD4,HLA-DQA1*0301,HLA-DQB1*0302)1Ell (accession ID MGI:3590082) line has been described (16). In previous publications from our lab (15, 16) the designations 'human CD4, DQA1*0301, DQB1*0302 transgenic IAnull NOD' and subsequently 'HLA-DQ8 transgenic IAb knockout NOD' were used, henceforth this line will be designated NOD.DQ8/Ab^0.

The Rag1 knockout NOD (NOD.129S7(B6)-*Rag1*^{tm1Mom}/J), immunoglobulin heavy chain knockout NOD (NOD.129S2(B6)-*Igh-6*^{tm1Cgn}), and β-2 microglobulin knockout NOD (NOD.129P2(B6)-Beta*2m*^{tm1Unc}/J) lines were all kindly provided by D. Serreze (The Jackson Laboratory, Bar Harbor, ME). The NOD.DQ8/Ab^0 Rag1^0, NOD.DQ8/Ab^0 IgH^0, and NOD.DQ8/Ab^0 β2m^0 lines were created by crossing the NOD.DQ8/Ab^0 animals with the relevant knockout lines,

intercrossing the F1 generation and selecting for desired F2 offspring using flow cytometric analysis and PCR (see below). All breeding colonies were housed in conventional SPF or (in the case of Rag1 knockout) VAF facilities. Care and handling was done in accordance with the guidelines of the Canadian Council on Animal Care and all experimental protocols were approved by our institutional Health Sciences Animal Policy and Welfare Committee.

2.2.2 Establishment of DQ6 Transgenic NOD and DQ6 Transgenic IAb knockout NOD Lines

NOD mice transgenic for both HLA-DQ6 (DQA1*0102, DQB1*0602) and human CD4 were created by microinjecting NOD/LtJ single-cell embryos with a mixture of two different DNA molecules: 1) a human genomic fragment containing the entire DQ6 gene, and 2) a human CD4 minigene construct with mouse CD4 enhancer, previously demonstrated to yield transgenic mice with cell- and tissue-appropriate expression of human CD4 (18). To obtain the DQ6 gene we constructed a bacterial artificial chromosome (BAC) genomic library using DNA from the homozygous B-lymphoblastoid cell line IWB (National Institutes of General Medical Sciences Human Genetic Mutant Cell Repository). Initially 192 separate BAC pools (500 independent BAC clones per pool) were screened by PCR using STS primer pairs for loci 9-10 and 2D7 (19); the two resulting positive pools were then randomly plated and screened by filter hybridization to obtain two positive clones. End sequencing revealed that the most favorable BAC clone (74 kb insert) extended from 30 kb upstream of the DQA1 gene to 12 kb

upstream of the DQB1 gene (both promoters drive inwards). BAC DNA from this clone was purified using a Qiagen 500 column, digested with Not I and the insert was separated from the vector by sedimentation over sucrose gradients (5 to 30% sucrose in a SW 55Ti rotor at 50,000 RPM x 80 min, 18˚C). The buffer was changed to 10mM Tris-HCl pH 8.0, 0.1mM EDTA by passing the insert DNA over a Sephadex G25 column; the resulting material was mixed with an equimolar quantity of the 40 kb human CD4 minigene insert (Not I digested and prepared by the same method as above), and the final concentration of DNA was adjusted to 1 µg/ml in 10 mM Tris-HCl pH 8.0, 0.1 mM EDTA. Embryo harvesting, micro-injection and transfer were all performed using standard methods; we used exclusively NODLtJ embryos derived from animals supplied by JAX, since, in our experience, embryos from other lines of NOD mice from other suppliers cannot be used to create transgenic animals. PCR analysis of tail DNA was used to identify transgenic offspring which were then further characterized for DQ expression levels by staining of peripheral blood mononuclear cells and FACScan analysis using monoclonal SPV-L3 (anti-DQ monomorphic). Of 21 live births arising from 103 transplanted embryos, 8 animals tested positive for the DQ6 transgene by PCR. However, only one animal (female N8) expressed DQ and huCD4 at appropriate levels and this was used to establish the final transgenic line homozygous for both human CD4 and DQ6. This DQ6 transgenic NOD line has been assigned the formal designation NOD.Tg(CD4,HLA-DQA1*0102,HLA-DQB1*0602)1Ell. Again for brevity we will henceforth use the designation NOD.DQ6. I acknowledge A. Atrazhev (University of Alberta,

Edmonton, AB) for the preparation of the DQ6 and hCD4 DNA and P. Dickie (University of Alberta, Edmonton, AB) for performing the microinjections.

To generate IAb knockout NOD.DQ6 animals, IAb knockout NOD animals (see above) were crossed with the NOD.DQ6 line, F1 animals intercrossed and F2 animals screened by flow cytometry for the absence of IA and the presence of two copies of DQ6 and CD4 (animals homozygous for the DQ transgene consistently stained two-fold brighter than hemizygotes). A single breeding pair from the F2 generation was used to establish the NOD.Cg-H2-Ab1^{tm1Gru}Tg(CD4,HLA-DQA1*0102,HLA-DQB1*0602)1Ell (accession ID MGI:3590083) line, for brevity denoted NOD.DQ6/Ab^{0}. (N.B. Both this line and the 'NOD.DQ8/Ab^{0}' line are transgenic for human CD4; the huCD4 transgene is co-integrated with DQ8 or DQ6 and is observed to always transmit alongside of DQ.) I acknowledge K. Suzuki (University of Alberta, Edmonton, AB) for the generation of NOD.DQ6/Ab^{0} strain.

2.2.3 Genotyping

Presence of the HLA-DQ transgene was detected by PCR using the primers TGAGCACAGTGGATTGAG and TGGTAGTTGTCAGGAAGG which target the Locus/STS 9-10 (19). Genomic DNA was prepared from tail biopsies using the DNeasy Tissue Kit (Qiagen Sciences, Maryland, USA), and PCR reactions were done under standard conditions (annealing at 48°C x 1 min.). Additional genotyping experiments as per protocols of Bunce and colleagues (20) were also performed on representative transgenic animals to confirm that the

HLA-DQ8 (DQA1*0301, DQB1*0302) and HLA-DQ6 (DQA1*0102, DQB1*0602) genes were present as expected (Supplementary Figure AI.3).

2.2.4 Antibodies and FACS Analysis

Expression of HLA-DQ, IA, TCR/CD3, CD4, CD8, B220, H-2Kb and/or H-2Kd and CD49b antigens on various cell populations was analyzed by flow cytometry using a FACScan instrument (BD Biosciences, San Jose, CA) and CellQuest software, with gates adjusted for the lymphocyte population. Fluorescently tagged antibodies used for staining were either prepared in house or (where indicated) purchased commercially. They included: SPV-L3 (mouse anti-human DQ monomorphic); 10-3-6 (mouse anti-mouse IA); H57-597 (hamster anti-mouse TCR); GK1.5 (rat anti-mouse CD4); OKT4 (rat anti-human CD4), CL169F (rat anti-mouse CD8; Cedarlane, Hornby, ON); RA3-6B2 (rat anti-mouse B220); CL9013 (mouse anti-mouse H-2Kb; Cedarlane); SF1-1.1 (mouse anti-mouse H-2Kd); and DX5 (rat anti-mouse CD49b; BD Pharmingen, Missisauga, ON). In generating the NOD.DQ8/Ab^0 $Rag1^0$ line, as well as screening for the absence of IA, we also followed the animals for the presence of H-2Kb and the absence of H-2Kd. Since the IAb knockout was generated in the 129 strain, the interrupted IAb gene has H-2Kb nearby, whereas any animals retaining an intact copy of IAb would have derived it from NOD, which has H-2Kd nearby.

2.2.5 Bone Marrow Derived Dendritic Cells

Bone marrow cells were washed out from dissected, open ended femurs

of 6-8 week old mice, suspended in endotoxin-free RPMI 1640 medium (Invitrogen Inc., Burlington, ON) and collected by centrifugation (250 *x g*, 5min, 20°C). The cells were resuspended in 'dendritic cell culture medium' (RPMI supplemented with 10% FCS [Invitrogen], 10ng/ml mouse IL-4 and 10ng/ml mouse GM-CSF [both cytokines from Peprotech Inc, Rocky Hill, NJ]), diluted to 1 x 10^6 cells/ml and plated in 6 well tissue culture treated plates at 4 x 10^6 cells/well. The cells were incubated at 5% CO_2 and 37°C and 24h later all the media in each well was gently aspirated and replaced with fresh medium. On days 2, 4 and 6 half of the media in each well was gently aspirated and replaced. On day 8 the culture was stimulated with mouse TNF-α (Peprotech) and LPS (Sigma, St.Louis, MO) (both at 10ng/ml). On day 9 the remaining cells were harvested and triply stained for the dendritic cell marker CD11c (monoclonal HL3, BD Pharmingen, San Diego, CA), HLA-DQ (monoclonal SPV-L3) and mouse IA (monoclonal 10-3-6) and then analyzed by FACScan.

2.2.6 Superantigen Induced T cell Proliferation

Spleens were removed from NOD.DQ6/Ab^0, NOD.DQ8/Ab^0 and wild-type NOD mice and the splenocytes were purified using lympholyte-M (Cedarlane, Hornby, ON) and prepared as a suspension. Cells (0.5x10^6/well) were triplicately cultured in 200µl/well of DMEM medium containing 5% FCS, 5x10^{-5}M βME, 2mM L-glutamine and 100U/ml of penicillin and 100µg of streptomycin (Invitrogen Inc., Burlington, ON). Cultures were incubated in the presence of varied concentrations of *Staphylococcus aureus* endotoxin B (SEB; Sigma, St. Louis,

MO) or toxic shock syndrome toxin (TSST; Sigma) for 56 hours at 37°C in 7.2% CO_2. ^{3}H-thymidine (Amersham) was then added at 0.5μCi/well and incubated under the same conditions for 16 hours. The cultures were then harvested onto glass fiber mats using a cell harvester. Radioactivity was then counted using a scintillation counter. The proliferative response was measured as the 3H-thymidine incorporation expressed as mean counts per minute (cpm). Stimulation index (SI) was calculated as the proliferative response in the presence of superantigen divided by the proliferative response in the absence of superantigen.

2.2.7 Proliferation Blocking Assay

T cell proliferation was measured as described above; however, the following monoclonal antibodies were added (50μg/ml) at the same time as the superantigen: anti-DQ Monomorphic (FN81-1); anti-DQ8 (4D12); anti-DQ6 (G2a.5); and anti-hepatitis B virus surface antigen (H25B10) as an isotype control.

2.2.8 Lymphocyte Recall Response

NOD and NOD.DQ6/Ab^0 mice were injected interperitoneally (I.P.) with 100μg of ovalbumin or hen egg lysozyme premixed with complete freunds adjuvant (protein in PBS to 150μl mixed with 150μl CFA; Sigma, St. Louis, MO). After two weeks, the mice received an I.P. boost of the same amount of protein, but this time in incomplete freunds adjuvant (Sigma). After another two weeks

their spleens were removed and the splenic lymphocytes were purified using lympholyte-M gradients (Cedarlane, Hornby, ON) and prepared as a suspension. Cells ($0.5x10^6$/well) were triplicately cultured in 200µl/well of DMEM medium containing 5% FCS, $5x10^{-5}$M βME, 2mM L-glutamine and 100U/ml of penicillin and 100µg of streptomycin (Invitrogen Inc., Burlington, ON). Cultures were incubated in the presence of varied concentrations (0, 5, 10, 20, 50, 100 and 250µg/ml) of ovalbumin or hen egg lysozyme for 56 hours at 37°C in 7.2% CO_2. ^{3}H-thymidine (Amersham) was then added at 0.5µCi/well and incubated under the same conditions for 16 hours. The cultures were then harvested onto glass fiber mats using a cell harvester and radioactivity was then counted using a scintillation counter. The proliferative response was measured as the ^{3}H-thymidine incorporation expressed as mean counts per minute (cpm). Stimulation index (SI) was calculated as the proliferative response in the presence of the recall antigen divided by the proliferative response in the absence of the antigen.

2.2.9 Monitoring Mice for Myocarditis by Electrocardiogram (ECG)

These methods have been described previously (see Supporting Text for (15)). In brief, non-sedated mice were placed in a syringe barrel which had been modified to allow access to the feet. Electrodes, with limb leads attached, were clipped to each of the four foot pads and ECG leads I, II, III, AVR and AVL were simultaneously recorded (Supplementary Figure AI.1.A). Parameters measured included sinus rate (P-P interval), PR interval (onset of P wave to onset of QRS

complex) and ventricular rate (QRS-QRS interval). First degree heart block was defined as a PR interval greater than 36msec, a value that is >3 SD above the mean for a large group of normal animals (Supplementary Figure A1.2). Complete heart block was diagnosed whenever the P waves (i.e. atrial depolarization events) were completely dissociated from the QRS complexes (i.e. ventricular depolarization events) (Supplementary Figure AI.1.B).

2.2.10 ELISA for Cardiac Myosin Autoantibodies

Falcon 353911 microtitre plates (Becton Dickinson Labware, Franklin Lakes, NJ) were coated overnight at 4°C with 50µl per well of 5µg/ml porcine cardiac myosin (Sigma, St.Louis, MO) in PBS. The plates were washed with PBS + 0.1% Tween 20 (PBS-T), blocked with 1% w/v BSA in PBS-T and incubated with mouse sera (various dilutions in PBS-T). The plates were then incubated with horseradish peroxidase-conjugated goat anti-mouse IgG (H+L; 1:5,000; Jackson ImmunoResearch, West Grove, PA) and developed by using ABTS (Sigma) as a substrate. OD 405nm minus OD 490nm was measured on a plate reader and expressed as the mean of triplicate wells.

2.2.11 Adoptive Transfers

Donor lymphocytes were harvested from 16-24 week old NOD.DQ8/Ab^0 mice demonstrating at least first degree heart block. Splenic lymphocytes were obtained by passing total splenocytes over lympholyte-M gradients (Cedarlane, Hornby, ON); these cells or enriched lymphocyte populations (see below) were

washed in RPMI 1640, pelleted and finally resuspended in PBS and adoptive transfers were accomplished by tail vein injection into 8 week old NOD.DQ8/Ab^0 Rag1^0 mice. Onset of heart block in recipients was monitored via biweekly ECG.

2.2.12 Echocardiography

M-mode echocardiograms were performed on non-sedated animals using a 15mHz probe and SONOS 5500 instrument (Agilent Technologies, Palo Alto, CA). Moistened fur on the left thorax was shaved using a scalpel blade and LiquaSonic ultrasound transmission gel (Chester Labs, Cincinnati, OH) was applied to the bare skin prior to probing. The left ventricle was visualized in diastole and the 2D parasternal short axis was measured.

2.2.13 MACS enrichment for CD4 T cells

A Mouse CD4+ T Cell Isolation Kit (Miltenyi Biotec, Auburn, CA) was initially used to obtain a population of enriched CD4 T cells from the spleens of NOD.DQ8/Ab^0 mice with heart block. This method accomplishes enrichment by magnetic depletion of non-CD4 T cells, including CTLs, B cells, NKs, DCs, MΦs, granulocytes and erythroid cells, using a cocktail of 5 different biotin-conjugated antibodies (CD8α/Ly-2, CD45R/B220, DX5, CD11b/Mac-1 and Ter119) against relevant cell surface markers in combination with ferromagnetic anti-biotin microbeads. Lymphocytes were purified from spleens using lympholyte-M gradients (Cedarlane, Hornby, ON). In accordance with the kit instructions, the cells were incubated with the cocktail of biotinylated antibodies, washed,

incubated with the anti-biotin microbeads and finally passed over a MS column mounted within the magnetic field of a MACS separator (Miltenyi Biotec). Purity of the enriched CD4 cells which passed through the column was evaluated by flow cytometry (FACScan, BD Biosciences, San Jose, CA) using antibodies against mouse CD4, CD8, TCR and B220. Cell populations enriched by this method consisted of 91% CD4 T cells and 9% B220 cells (the latter being negative for the three other surface markers).

2.2.14 Cell Enrichment by Fluorescent Cell Sorting

Splenic lymphocytes from NOD.DQ8/Ab^0 mice with heart block were obtained using lympholyte-M gradients (Cedarlane, Hornby, ON). Lymphocytes from 5-10 animals were pooled and aliquots of cells incubated with fluorescently tagged anti-mCD4, anti-mCD8, or anti-B220 and then positively sorted on a FACS Aria instrument (BD Biosciences, San Jose, CA). Purity of cell populations selected by this method was ≥99% as assessed FACS.

2.2.15 Histology/Immunohistochemistry

For H&E staining, hearts were fixed in 10% buffered formalin (Fisher, Fair Lawn, NJ), embedded in paraffin, sectioned and stained with hematoxylin and eosin using standard methods. For CD4 and CD11b staining, frozen sections were made using O.C.T Tissue Tek compound (Fisher) and slides were fixed in ice cold acetone, blocked in 2% FCS/PBS and treated with both avidin and biotin solutions (Vector Labs, Burlington, ON). Rat anti-mouse CD4 (H129.19; BD

Pharmingen, Mississauga, ON) and CD11b (M1/70; BD Pharmingen) were used at 1:100 and 1:500, respectively, and detected using a biotin conjugated goat anti-rat IgG (H+L) at 1:200. Staining was visualized using ABC kit (Vector Labs, Burlington, ON) followed by DAB (Sigma, St.Louis, MO) and the slide was counterstained with hematoxylin, dehydrated and mounted.

2.2.16 Preparation of RNA

RNA was prepared from NOD.DQ8$^{+/-}$/Ab$^{+/-}$ tissues using a Qiagen Midi RNeasy kit and their protocol was followed (Qiagen, Mississauga, ON). In brief, liquid N_2 snap frozen tissues were placed in 4ml RNeasy lysis buffer (containing βME) and crushed with a sterile pestle. The lysate was further homogenized by passing it through a 23 gauge needle. Lysates were spun for 10 minutes at 3000 *x g*, the supernatant removed and then 4ml of 70% ethanol was added to the supernatant and shaken. The sample was loaded and spun in kit spin columns (3000 *x g*, 6min). The column was then washed with 4ml of Buffer RW1 (3000 *x g*, 6min), followed by 2.5ml of RPE buffer (3000 *x g*, 2min) and then another 2.5ml RPE (3000 *x g*, 5min). RNA was eluted from the column by twice using 250µl RNAse free water (3000 *x g*, 3min). RNA was either stored at -70°C or -20°C depending on use.

RNA purity was checked using a 1% agarose formaldehyde gel and it was prepared as follows. 44ml of milliQ water was added to 0.5g of agarose and the agarose was melted. The agarose solution was allowed to cool to 70°C and then 5ml of 10X MOPS buffer (400mM MOPS, pH7.0; 0.1M Sodium Acetate; 0.01M

EDTA), 1.5mL of formaldehyde solution (37%), and 2µl of ethidium bromide were added. The gel was allowed to harden and was run in 1X MOPS with 1µl ethidium bromide in the tank (Supplementary Figure AI.4.E).

The RNA was prepared and run as follows: 20µl of RNA sample (~1.5-2µg RNA + DEPC treated and autoclaved H_2O) was added to RNA treatment (2 volumes 10X MOPS, 3 volumes 37% formaldehyde, 10 volumes of deionized formamide) and then heated to 55°C for 15 minutes. The samples were then cooled on ice and then 1/10 volume RNA load dye (50% glycerol, 1mM EDTA) was added and 20µl of the sample was loaded and the gel was run at 60-70volts.

2.2.17 Generation of Probe Templates

Starting vectors were already available in the lab for DQ8α, DQ8β, DQ6α, DQ6β, IAα, and IAβ. Vectors were linearized by Not I digest (0.5µg vector, 4µl 10X buffer #3, 0.5µl BSA, 1µl Not I (NEB) and water to 40µl). Digests were incubated at 37°C for approximately 4hours and aliquots were analyzed on a 1% agarose gel (Supplementary Figure AI.4.A). The linearized templates were then amplified by PCR using standard conditions with primers designed to amplify the MHC class II and also to insert Sfi I restriction sites onto each end (see Supplementary Table AI.1). PCR program: 25 times (94°C 1 minute, 56°C 1 minute, 72°C 2 minutes); an aliquot was analyzed on a 1% agarose gel (Supplementary Figure AI.4.B). PCR products were cleaned using a Qiagen Qiaquick kit (Mississauga, ON) and then reprecipitated using 3M NaOAC, pH 5.2 and ethanol. A pJFE7s CMV vector, as well as the PCR products, were

linearized using the restriction enzyme Sfi I (NEB). After overnight digestion, the vector was treated with calf intestine alkaline phosphatase (1µl added, room temperature, 5min, addition of 1µl of 0.5M EDTA, pH 8.0, and 70°C, 10 min). Linearized vector, as well as the PCR inserts, were run on a 0.8% low melting point agarose gel and the inserts and vector were cut out of the gel (Supplementary Figure AI.4.C). 60µl DEPC treated and autoclaved H_2O was added to each slice and then the gel slices were melted at 70°C. The insert and vector were ligated by combining (4µl vector, 4µl insert, 4µl 10X ligase buffer, 1µl T4 DNA ligase and 27µl DEPC treated and autoclaved H_2O and then by incubating at room temperature for approximately 2 hours. XL-2 blue competent cells prepared by K.Suzuki (University of Alberta, Edmonton, AB) were thawed on ice and 100µl was combined with 10µl of each ligation. The mixture was iced (10 min), heat shocked at 37°C (2min), iced (10 min) and them 1ml of YT broth (Sigma, St. Louis, MO) was added. The samples were then placed on a rotator wheel for 1 hour at 37°C. A 100µl was spread on a YT agar (Invitrogen, Burlington, ON) 1X ampicillan (AMP; 100ug/ml; Sigma, St.Louis, MO) plate and then the remaining sample (spun down, aspirated and resuspended in residual) was spread on another YT agar AMP plate. The plates were incubated overnight at 37°C. Colonies were counted and compared to control plates (vector alone ligation). A colony was picked and added to 3.5ml of YT-AMP and incubated overnight at 37°C. A miniprep/wizard was performed using a SV Miniprep kit (Promega, Madison, WI) and the manufacture's protocol was followed. The miniprep was spun down and 250µl SV resuspension buffer was added followed

by 250µl of lysis solution. Samples were gently inverted 4 times and then incubated at room temperature (4min). 10µl alkaline protease solution was added, samples were gently inverted 4 more times and then incubated at room temperature (5min). 350µl of neutralization solution was added, samples were gently inverted 4 times and then spun (16,000 *x g*, 10min, 4°C). Samples were loaded onto columns (connected to a vacuum) and DNA was collected and washed with wash solution. DNA was eluted from the columns using 100µl 0.1TE buffer (16,000 *x g*, 1min, room temperature) and samples were stored at -20°C. Wizard minipreps were assessed for proper vector/insert composition on a 1% agarose gel after digestion with restriction enzyme Sfi I (NEB) (Supplementary Figure AI.4.D). Wizard minipreps were also checked for correct insert sequence by sequencing using T3 and T7 sequencing primers. Large aliquots of correct DNA templates were prepared using a Qiagen maxiprep (Mississauga, ON) following their protocol and then followed by reprecipitation with 3M NaOAc, pH 5.2 and ethanol and resuspension in 0.1 TE in DEPC treated and autoclaved H_2O.

2.2.18 Generation of RNA probes

The following were combined to generate a probe: 1µl RNasin; 2µl of 5X T3 RNA polymerase buffer; 1µl DTT; 0.5µl each of 10mM ATP, CTP, and GTP; 0.3-0.8µl UTP (0.1mM; volume depends on probe size); 2.5µl α^{32}P rUTP (Amersham); 0.5µl template; and 2µl T3 polymerase. The mixture was incubated at 37°C for 1 hour 15 minutes. 0.1µl RNase Free DNase and 0.25µl each of

0.2M NaCl and $CaCl_2$ were then added and incubated at 37°C for 20 minutes. 90µl of RPA elution buffer (Ambion) was added and it was loaded onto a drip column prepared as follows: The bottom of the reservoir section of a 5.5" unplugged Pasteur pipet was "plugged" with glass wool. A column of G50 fine sephadex slurry was made in the reservoir section of the pipet. The buffer was then exchanged to RPA elution buffer by running the buffer through the column. 100µl elution buffer aliquots were loaded onto the top of the drip column pushing the probe solution through separating the incorporated ^{32}P UTP from the unincorporated. Fractions were collected and aliquots were analyzed (by cpm counts). Probe purity was also checked by autoradiogram after running the probe in a 4% acrylamide gel.

2.2.19 RNAse Protection Assay

RNAse protection assays were performed using Ambion's RPA III™ Ribonuclease Protection Assay Kit (#1414); Ambion's protocol was followed. In brief, RNA and probes were mixed and the volume was adjusted to 0.5M NH_4OAc. 2.5 volumes of 100% ethanol were added to each tube and then placed at -20°C (20min). The samples were then spun (16,000 *x g*, 15min, 4°C), ethanol was aspirated and the sample was dried (5 min). 10µl hybridization buffer was added, the sample vortexed and spun and then incubated at 95°C (3min), vortexed and spun and incubated at 42°C (2.5 hours to overnight). Digestion buffer was thawed and RNAse A/T1 was added. This solution was added to the samples, incubated at 37°C (30min) and then 225µl RNAse

inactivation/precipitation buffer was added and incubated at -20°C (15min). The samples were then spun (16,000 *x g*, 15min, 4°C), the supernatant was removed, the sample was respun and remaining supernatant was removed. The pellet was resuspended in 6µl of load dye, incubated at 95°C (3min) and then loaded onto a 4% acrylamide gel. The gel was run at 250 volts for approximately 1-1.5 hours and then was visualized by autoradiogram.

2.3 Results

To provide a DQ control strain which could be directly compared to our NOD.DQ8 animals, we made use of a second transgenic line that expressed DQ6 (DQA1*0102, DQB1*0602) rather than DQ8, but which we anticipated would be closely matched in all other aspects. Splenocytes and bone marrow derived dendritic cells (DCs) from the two different transgenic lines showed appropriate expression of their respective DQ transgenes, (i.e. mouse class II MHC (IA) and human class II MHC (DQ) were expressed on the same cells; Figure 2-1, panels A and B and Figure 2-2, panels A and B), and levels of DQ were comparable between the two lines. Crossing of the NOD.DQ8 and NOD.DQ6 lines with NOD/Ab^0 mice (i.e. IAb knockout) resulted in lines expressing the expected human MHC, but without IA (Figure 2-1, panels C and D and Figure 2-2, panels C and D). The NOD.DQ8/Ab^0 and NOD.DQ6/Ab^0 lines had comparable levels of DQ expression on both splenocytes and DCs and they had comparable numbers of CD3, CD4 and CD8 T cells, as well as B cells, with these numbers being close to those found in wild-type NOD mice (Table 2-1). The NOD.DQ8/Ab^0 and

NOD.DQ6/Ab^0 lines were also comparable in terms of proliferative responses to the superantigens SEB and TSST-1 (Figure 2-3; and these responses could be blocked with anti-DQ monoclonal antibodies, Figure 2-4) and to recall antigens (Figure 2-5).

The NOD.DQ8/Ab^0 and NOD.DQ6/Ab^0 lines were compared for development of spontaneous anti-cardiac autoimmunity using two criteria: 1) appearance of heart block as assessed by ECG (Figure 2-6-A); and 2) appearance of autoantibodies against cardiac myosin as assessed by solid-phase ELISA (Figure 2-6-B). Nearly all of the NOD.DQ8/Ab^0 animals developed heart block by 24 weeks of age (similar to (15)), whereas a concurrent cohort of NOD.DQ6/Ab^0 animals failed to develop heart block at any age (Figure 2-6-A). Similarly, NOD.DQ8/Ab^0 animals produced high-titre anti-cardiac myosin autoantibodies by 12 weeks of age, whereas the NOD.DQ6/Ab^0 animals showed no anti-cardiac myosin autoantibodies at any age (Figure 2-6-B). Gross and microscopic examination of NOD.DQ6/Ab^0 hearts from animals at a variety of ages (up to 50 weeks) showed complete absence of any cardiac pathology.

To further define the nature of the pathogenic lymphocytes in the NOD.DQ8/Ab^0 animals, we crossed them with Rag1 knockout NOD mice to establish a NOD.DQ8/Ab^0 Rag1^0 line (Figure 2-7, A-C) to be used in adoptive transfer studies. As expected, NOD.DQ8/Ab^0 Rag1^0 animals had normal sized hearts (echocardiographic data Figure 2-8-B and gross specimen Figure 2-10-A, left) with normal ECG conduction parameters (P-R interval normal at all ages, Figure 2-7-D) and no other signs of anti-cardiac autoimmunity (anti-cardiac

autoantibodies and intra-myocardial mononuclear cell infiltrates were not seen; Figure 2-8-C and 2-10-C respectively). Adoptive transfer of splenic lymphocytes (1×10^6) from older NOD.DQ8/Ab^0 mice with heart block to younger NOD.DQ8/Ab^0 $Rag1^0$ animals triggered myocarditis in 100% of the recipients (Figure 2-8-A). First degree heart block (i.e. PR interval >36msec) appeared as early as 2 weeks after cell transfer, with half of the animals progressing to complete heart block within 8 weeks and the remainder by 12 weeks post transfer. In addition to ECG changes, the recipient animals developed cardiomegaly with dilated cardiac chambers (echocardiographic data Figure 2-8-B and gross specimen Figure 2-10-A, middle), mononuclear cell infiltrates within the heart wall (Figure 2-10-D), and anti-cardiac myosin autoantibodies (ELISA titres reached at least 1:10,000 by 12 weeks post transfer in all animals; Figure 2-8-C). In parallel experiments younger NOD.DQ8/Ab^0 $Rag1^0$ animals were also injected with pooled serum from older NOD.DQ8/Ab^0 mice with heart block (150µl/animal by I.P. injection); ECG parameters and cardiac pathology remained the same as non-manipulated NOD.DQ8/Ab^0 $Rag1^0$ animals (see Figure 2-7D and 2-10C).

CD4 T lymphocytes play a central role in the pathogenesis of many organ-specific autoimmune diseases. To determine whether CD4 T cells represent a critical subset capable of causing myocarditis in our DQ8 animal model, we used two different methods to specifically enrich for these cells from older NOD.DQ8/Ab^0 animals with heart block. The enriched cell populations were then adoptively transferred to young NOD.DQ8/Ab^0 $Rag1^0$ mice and the animals

followed by serial ECG measurements. For these experiments we used the appearance of complete heart block as the end-point, since this ECG abnormality indicates widespread, advanced and essentially irreversible cardiac damage.

In the first series of experiments CD4 T cell enrichment was achieved using a negative selection strategy, which employed a mixture of monoclonal antibodies and Miltenyi Biotec ferromagnetic microbeads. One million CD4 splenic lymphocytes enriched by this method were adoptively transferred to 8 week old NOD.DQ8/Ab^0 Rag1^0 mice via tail vein injection and results for a representative experiment are shown in Figure 2-9-A. The recipients began to develop complete heart block as early as 4 weeks post transfer and by 12 weeks the entire cohort had developed disease (Figure 2-9-A). Although disease onset appeared to be somewhat accelerated in the animals that received the CD4 enriched cells compared to animals who received the same number of total lymphocytes (total lymphocytes and CD4 cells were taken from the same pool of donor splenocytes), at only one time point (8 weeks) did the difference between the two groups reach statistical significance ($p<0.02$). All recipient mice were euthanized at 14 weeks post transfer and the hearts were examined for gross and microscopic pathology. Interestingly, hearts from animals that had received the CD4 enriched cell populations were consistently larger than those found in animals that had received the same number of whole splenocytes (Figure 2-10-A, right). In fact, hearts from the Rag1^0 animals that received the CD4 enriched cell transfers were often larger than those typically seen in NOD.DQ8/Ab^0 mice undergoing spontaneous disease (15). Histopathological examination of the

myocardium from animals that had received the CD4 enriched cell transfers showed that mononuclear cells were more numerous and lymphocyte infiltrates more widespread/generalized than those seen in animals receiving transfer of the same number of total splenocytes (Figure 2-10, panel E versus D).

FACScan analysis of the 'CD4 enriched' cell population purified using the Miltenyi Biotec negative selection strategy and described above revealed that CD4 T cells comprised 91% of the enriched population, with the remaining 9% being almost entirely B220 lymphocytes (Figure 2-11). This level of contaminating B220 cells was repeatedly obtained using the Miltenyi kit, and therefore an additional series of adoptive transfer experiments were performed using cell populations positively selected by FACS sorting; purity was consistently ≥99% (Figure 2-12). Additional cell populations were also obtained by this positive selection strategy; thus, our experiments included CD4 T cells, CD8 T cells, and B cells (Figure 2-9-B). Consistent with our previous results, adoptive transfer of 1 x 10^6 CD4 T cells, selected by FACS sorting, induced complete heart block, with kinetics that were essentially identical to concurrent experiments using the same number of total splenocytes (Figure 2-9-B; total lymphocytes and CD4 cells again being taken from the same pool of donor splenocytes). In contrast, adoptive transfer of 1 x 10^6 CD8 T cells or B cells induced no ECG changes at any time post transfer, nor was any cardiac pathology noted upon gross and microscopic examination. Hearts from animals which received FACS sorted CD4 T cells were examined 16 weeks after transfer and they were found to be larger on average than hearts from concurrent

controls that received total splenocytes; histopathological examination again showed lymphocyte infiltrates to be more widespread/generalized in the animals that had received the sorted CD4 T cells (i.e. results were very similar to those shown in Figure 2-10-E for animals that received magnetically enriched CD4 T cells).

The mononuclear cell infiltrates present in the hearts of NOD.DQ8/Ab^0 $Rag1^0$ recipients of splenic CD4 T cells were further analyzed by immunohistochemistry (Figure 2-13). Staining revealed the presence of scattered CD4 T cells (Figure 2-13, panels B, E, and H), whereas the predominant cell types stained positive for CD11b (Figure 2-13, panels C, F, and I). Examination of these infiltrates at high magnification revealed predominance of macrophages and, to a lesser extent, lymphocytes, with only the occasional neutrophils observed.

Although purified CD8 T cells or B lymphocytes were not capable of inducing myocarditis in our Rag1 knockout adoptive transfer model, it is still possible that these immune cells play a critical role in initiating the anti-cardiomyocyte autoimmune response in immune competent NOD.DQ8/Ab^0 mice. To test this possibility we crossed our NOD.DQ8/Ab^0 animals with two different knockout lines: 1) a NOD immunoglobulin heavy chain knockout (IgH^0) line; and 2) a NOD β-2 microglobulin knockout ($\beta 2m^0$) line. As expected, the resulting NOD.DQ8/Ab^0 IgH^0 mice were deficient in B lymphocytes (Figure 2-14-A). Cohorts of NOD.DQ8/Ab^0 IgH^0 animals at four different ages (8, 12, 18, and 24 weeks) were first assessed for the presence of heart block by ECG (Figure 2-14-

C) and then sacrificed and their hearts examined for gross and microscopic pathology (Figure 2-15-A). The appearance of heart block was slightly delayed in the IgH^0 animals compared to a concurrent group of NOD.DQ8/Ab^0 animals (Figure 2-14-C); this difference did not reach statistical significance ($p>0.1$). Histological examination of NOD.DQ8/Ab^0 IgH^0 hearts from 22 week old animals showed mononuclear cell infiltrates which were very similar to those seen in NOD.DQ8/Ab^0 animals (Figure 2-15-A versus Figure 2-10-B), and the magnitude of cardiac enlargement was also comparable between the two groups.

Once the NOD.DQ8/Ab^0 $\beta2m^0$ line was established, FACScan analysis demonstrated that these animals were deficient in CD8 T cells (Figure 2-14-B). Cohorts of NOD.DQ8/Ab^0 $\beta2m^0$ mice at four different ages (8, 12, 18, and 24 weeks) were first assessed for the presence of heart block by ECG (Figure 2-14-C) and then they were sacrificed and their hearts examined for gross and microscopic pathology (Figure 2-15-B). None of the NOD.DQ8/Ab^0 $\beta2m^0$ animals developed complete heart block and only one animal (in the 18 week cohort) demonstrated first degree heart block at sacrifice (PR interval 39msec). Serum acquired at necropsy showed that anti-cardiac myosin autoantibodies did not appear above background levels in the NOD.DQ8/Ab^0 $\beta2m^0$ animals (Figure 2-14-D). Histological examination of NOD.DQ8/Ab^0 $\beta2m^0$ hearts from 22 week old animals showed minimal or absent mononuclear cell infiltrates (Figure 2-15-B) and on gross examination no cardiac enlargement was observed.

2.4 Discussion

Previous members of the Elliott lab serendipitously discovered that NOD.DQ8/Ab^0 animals develop spontaneous anti-cardiomyocyte autoimmunity and fatal dilated cardiomyopathy. With only one transgenic line, our initial hypothesis was that this was due to a founder effect, arising possibly because the transgene integration site caused inappropriate overexpression of the DQ within cardiomyocytes. Although RNAse protection experiments quickly ruled out elevated levels of DQ mRNA within the heart (Figure 2-16), definitive evidence that the myocarditis was not due to a founder effect came from the work of Lipes and colleagues (14). All three of their independently derived DQ8 transgenic lines developed spontaneous myocarditis and fatal dilated cardiomyopathy. When the three lines described by the Lipes group (14) are considered together with our line, mortality rates appear to be roughly correlated with levels of DQ8 transgene expression. In one published NOD.DQ8/Ab^0 line myocarditis was not reported (21) and we speculate that transgene expression levels in these mice are insufficient to induce an autoimmune response against cardiomyocytes which may reflect unbalanced expression of the two DQ chains (a mixture of DQ8 α and DQ8 β genomic fragments was microinjected, in contrast to our model in which a large human genomic fragment, containing, on a single DNA insert, all DQα and DQβ coding exons as well as corresponding human promoters and upstream regulatory elements, was used).

In NOD.DQ8/Ab^0 mice there is no apparent reason why the cardiomyocyte is targeted and with our present understanding we could not have predicted this

outcome. Therefore we hypothesized that, in the NOD/Ab^0 background, perhaps expression of any one of a number of different DQ molecules (i.e. encoded by different haplotypes) would lead to autoimmune myocarditis. To address this possibility we examined another DQ transgenic line (NOD.DQ6/Ab^0) for signs of anti-cardiac autoimmunity (N.B. The DQ6 animals provide a control for the DQ8 with respect to mouse class I and class III MHC genes). Despite being matched closely to the NOD.DQ8/Ab^0 line in every aspect except DQ itself, NOD.DQ6/Ab^0 animals failed to show any signs of myocarditis providing additional evidence that it is the DQ8 molecule which dictates the 'choice' of cellular target for the autoimmune response. Although absence of myocarditis in our NOD.DQ6/Ab^0 mice could again be due to a founder effect, the idea that non-DQ8 haplotypes do not develop myocarditis in this animal model is also supported by preliminary results from our most recent DQ transgenic NOD/A_b^0 animals, where two independent founder lines (both NOD.DQ8aDQ2b/Ab^0, i.e. expressing the trans-heterodimer DQA1*0301, DQB1*0201) have shown no cardiac pathology (K. Suzuki and J. Elliott, unpublished observations).

Direct experimental evidence regarding the role of lymphocytes and various lymphocyte subsets in mediating myocarditis in our NOD.DQ8/Ab^0 animals was obtained by establishing a Rag1 knockout adoptive transfer model. In their initial publication Lipes and colleagues also determined that splenocytes, but not serum, could transfer disease, with disease appearance assessed by gross and microscopic pathology and (with cell transfers) by the occurrence of anti-cardiac myosin autoantibodies. Although these authors injected a different

number of splenocytes than we used in our experiments (1.5 – 2 fold more, or possibly 15-20 fold more as cited later in the manuscript), the fact that our results are very similar to theirs supports the notion that the basic immunological mechanism of myocarditis in the NOD.DQ8/Ab^0 model will be the same for DQ8 transgenic animals from diverse origins.

CD4 T cells are very likely to play a role in the autoimmune myocarditis of NOD.DQ8/Ab^0 mice based on the simple fact that this particular autoimmune phenotype requires DQ8; a molecule whose function it is to present processed antigen to CD4 T cells. Our adoptive transfer model allowed us to demonstrate that indeed purified CD4 T cells alone could induce disease, whereas purified CD8 T cells or B lymphocytes did not. These findings are virtually identical to those described previously for the adoptive transfer of type 1 diabetes in NOD mice (22) and they suggest that in both disease models, once the autoimmune response has become established, CD4 T cells alone are sufficient to orchestrate the destruction of the target cells or tissues (23). In NOD.DQ8/Ab^0 animals the destruction is likely accomplished through a pro-inflammatory DTH-like mechanism (Figure 2-17), whereby pathogenic CD4 T cells entering the myocardium secrete a number of cytokines including IFN-γ and IL-17 and these, in turn, cause the recruitment and activation of macrophages (24, 25). Inflammation and tissue destruction then ensue via the production of additional pro-inflammatory cytokines by the macrophages (e.g. TNF-α) and through the release of proteolytic enzymes and reactive oxygen species from macrophages and occasional granulocytes. Immunohistochemical analysis of hearts from

NOD.DQ8/Ab^0 Rag1^0 animals that had received purified CD4 T cells yielded images entirely consistent with the scenario outlined above. The predominance of macrophages bears some resemblance to the myocarditis seen in transgenic mice with cardiomyocyte-specific overexpression of TNF-α (9, 11) and suggests that the TNF-α and DQ8 transgenic models may share some downstream cellular effector mechanisms. In addition to macrophage-mediated damage, it has been shown in experimental autoimmune myocarditis that CD4 T cells within the myocardial infiltrates express high levels of FasL (26) and this may be another complementary mechanism acting in NOD.DQ8/Ab^0 animals to cause direct cardiomyocyte destruction and inflammatory cell recruitment.

In comparison to adoptive transfer of total splenocytes, adoptive transfer of purified CD4 T cells into NOD.DQ8/Ab^0 Rag1^0 mice consistently induced a greater degree of cardiac enlargement and more extensive mononuclear cell infiltration. There are several possible explanations for this phenomenon. The simplest is that in purified form, 4-fold more of the pathogenic CD4 T cells were actually transferred (i.e. 1 x 10^6 cells were transferred in each experiment, but spleens contain only about 25% CD4 T cells) and the larger number of cells caused more pronounced cardiac destruction. However, other possible explanations can be envisaged, such as a suppressive effect mediated by CD8 T cells which are co-transferred in the total splenocyte populations. This effect might be analogous to what has been observed in rheumatoid arthritis where CD8 T cells are known to have a regulatory or protective effect (27). These ideas

could potentially be tested in the future by adoptive transfer of specific mixtures of purified cell populations.

For the CD4 adoptive transfer experiments we used both a negative selection strategy involving magnetic microbeads and FACS sorting to obtain enriched CD4 T cells. Interestingly the magnetically enriched CD4 T cells (with contaminating B cells) appeared to induce disease slightly faster than total splenocytes, whereas with the more highly purified CD4 T cells disease occurred with slightly delayed kinetics. Although these differences were not statistically significant (except at one data point), they suggest that B cells may play a minor, ancillary role in disease pathogenesis, likely by presenting cardiac antigens to CD4 T cells.

Results obtained with NOD.DQ8/Ab^0 mice crossed onto the Ig heavy chain knockout showed that B lymphocytes are not needed to generate myocarditis, although disease onset was slightly delayed in the NOD.DQ8/Ab^0 IgH^0 animals, again suggesting that B lymphocytes may play an ancillary role in disease pathogenesis. Our results are similar to those described for experimental autoimmune myocarditis (28), as well as for several other murine autoimmune models, where the full disease phenotype can occur in the absence of B lymphocytes. This finding appears to be in contrast to what is generally reported for NOD mice; Ig heavy chain knockout animals fail to develop autoimmune diabetes (29, 30). We suggest that this difference in the apparent requirement for B cells is due to differing threshold requirements for B cell antigen presentation to reach the respective endpoints. In NOD.DQ8/Ab^0 animals the

autoimmune response against cardiomyocytes appears to be very robust with 100% of animals developing fatal disease. In these animals dendritic cells alone (or in concert with macrophages) can apparently present sufficient cardiac antigens to initiate and amplify a lethal CD4 autoimmune response. The APC function of B lymphocytes is not required; although, if present, it can contribute to earlier onset of heart block and cardiac failure. In contrast, a certain proportion of wild-type NOD mice (15-50% depending on the colony) never progress to diabetes. Thus, the CD4 autoimmune response in NOD is not as robust and we infer that the APC activity provided by B lymphocytes is needed in nearly all animals to stimulate CD4 autoimmune responses beyond the critical threshold needed to trigger diabetes. This idea is consistent with reports that in NOD mice it is the APC activity of B lymphocytes (rather than antibody production) that is required to achieve the full diabetes phenotype (31-33). Thus we hypothesize that the differential requirement for B lymphocytes between NOD.DQ8/Ab^0 IgH^0 and NOD/IgH^0 animals relates to the fact that the NOD requires the highly efficient APC function of B lymphocytes for diabetes whereas, for cardiomyopathy, this same function is detectable, but not critical, in the NOD.DQ8/$A_b{}^o$ animals.

The results obtained with NOD.DQ8/Ab^0 $\beta 2m^0$ mice suggest that CD8 T cells, NKT cells, or NK cells are critical for the spontaneous anti-cardiomyocyte autoimmune response to arise. Absence of NKT cells (which recognize antigen on CD1d) seems least likely to be the cause of the myocarditis-free phenotype. Both NOD mice (34, 35) and our NOD.DQ8/Ab^0 mice (Table 2-2) are already

deficient in NKT cells and it has been shown that a further reduction in NKT cells tends to exacerbate rather than mitigate anti-islet autoimmunity in the NOD (34-37). Future experiments treating NOD.DQ8/Ab^0 animals with anti-CD8 monoclonal antibodies would potentially address whether the absence of myocarditis in NOD.DQ8/Ab^0 $\beta2m^0$ animals is indeed a reflection of the absence of CD8 T cells and not the absence of NKT cells. Recently Yokoyama and colleagues have shown that NK cells acquire functional competence through a specific interaction with self-MHC molecules (termed 'licensing'; (38)). In the absence of class I MHC licensing will not occur; thus, absence of myocarditis in our NOD.DQ8/Ab^0 $\beta2m^0$ mice could potentially be due to some defect in NK cell development and this idea remains to be explored. On the other hand, a central role for CD8 T cells would be consistent with the role that these cells are thought to play in autoimmune diabetes in NOD mice, where NOD/$\beta2m^0$ animals fail to develop insulitis or diabetes and the cloning of islet-infiltrating CD8 T cells has shown them to play a key role in early disease pathogenesis (39-42). From our results (and by analogy with what is thought to happen in NOD mice), we hypothesize that it is autoreactive CD8 cells which are responsible for the initial killing of cardiomyocytes around the pulmonary veins and within the atria of young NOD.DQ8/Ab^0 animals. This releases significant quantities of cardiac antigens, which are presented to CD4 T cells in the context of DQ8 by APCs, triggering and amplifying the CD4 autoimmune response. With time the CD4 autoimmune response becomes self-perpetuating and CD8 T cells are no longer

required; although, they likely continue to have some cytotoxic activity against cardiomyocytes.

In comparing the cellular pathogenic mechanisms and progression of autoimmunity in NOD versus NOD.DQ8/Ab^0 mice, we favor the simple hypothesis that because the two strains share the NOD background, the same types of autoimmune effector cells, arising in the same basic temporal sequence will occur in both types of mice. In this context the key similarities between the NOD and NOD.DQ8/Ab^0 include: 1) a critical role for CD8 T cells early in the autoimmune process; 2) a central role for CD4 T cells in orchestrating the final tissue destruction; and 3) little or no role for antibodies in the disease process. As discussed above, the difference between NOD and NOD.DQ8/Ab^0 with respect to the requirement for B lymphocytes appears to be quantitative rather than qualitative and it does not reflect a fundamental difference in the cellular pathogenic mechanisms acting to cause autoimmunity in the two different strains. The question as to why β cells are targeted in the NOD and cardiomyocytes in NOD.DQ8/Ab^0 has no answer at the present time. This difference in 'target organ selection' must arise in part from differences in MHC class II molecules (IAg7 versus DQ8), since CD4 T cells are involved and since NOD.DQ6/Ab^0 animals (matched at class I MHC) do not develop anti-cardiomyocyte autoimmunity. However, since CD8 cells are also involved in pathogenesis, differences in MHC class I molecules (Kd in NOD versus Kb in NOD.DQ8/Ab^0; both strains express Db) may well play a role as well. In this context it is interesting that Kb is considered to be protective against diabetes in wild-type NOD mice (43). If IAg7

knockout/DQ8 knockin transgenic NOD animals (i.e. replace IAg7 with DQ8 directly in the NOD MHC locus) can be generated, they will be useful to resolve the issue.

In humans, idiopathic dilated cardiomyopathy (IDCM) is a diagnosis of exclusion, reserved for patients in whom no apparent cause for the myocarditis and downstream cardiac dilation can be identified. Although there are likely a variety of root causes for IDCM (eg. prior inapparent viral infection, de novo anti-cardiac autoimmune response, etc.), by the time the patient presents to the clinic these may be impossible to discern. Therefore, at a practical level the challenge for the field is to develop an approach to sub-classify the disease based on the dominant cellular immune mechanism causing cardiac damage at the time of presentation and to test therapies that are most likely to affect the relevant immune pathways. We suggest that the end stage CD4 T cell driven, macrophage-mediated damage seen in NOD.DQ8/Ab^0 mice may be representative of one form of immune pathology seen in a subset of humans (arbitrarily named 'immunotype 1 myocarditis' for sake of discussion). In such patients with active disease, we would predict that therapies which inhibit macrophage function and signaling (e.g. agents that block TNF-α and/or IL-1β signaling) would be of greatest immediate benefit, therapies that inhibit CD4 T cell activation and function would be useful in the slightly longer term and therapies that primarily affect antibody production would be of little value. These ideas can now be tested using our NOD.DQ8/Ab^0 and NOD.DQ8/Ab^0 $Rag1^0$ adoptive transfer models at various stages of disease progression. Although it is

possible that HLA-DQ8 will be found more often in patients with 'immunotype 1 myocarditis', it is difficult to extrapolate from our NOD.DQ8/Ab^0 animals to the human situation. A number of reports have suggested that the DQ8 haplotype (or linked DR4) is associated with idiopathic myocarditis or dilated cardiomyopathy in humans (44-47), while other studies have implicated non-DQ8/non-DR4 haplotypes (48-50). There is no consensus on this issue, perhaps a reflection of the fact that in humans other class II MHC molecules (i.e. a second DQ molecule as well as DP and DR molecules) are always expressed alongside of the DQ8, and these may have a significant influence on the global CD4 T cell repertoire. Since the autoimmunity occurs rapidly and reproducibly in the NOD.DQ8/Ab^0 and NOD.DQ8/Ab^0 Rag1^0 adoptive transfer models, and because ECG provides a powerful non-invasive method to monitor disease progression, the animals provide a useful in vivo system to test new immunosuppressive agents, either DQ8 specific agents (e.g. copolymers) or general agents (e.g. small molecules, co-stimulatory blocking agents, etc.).

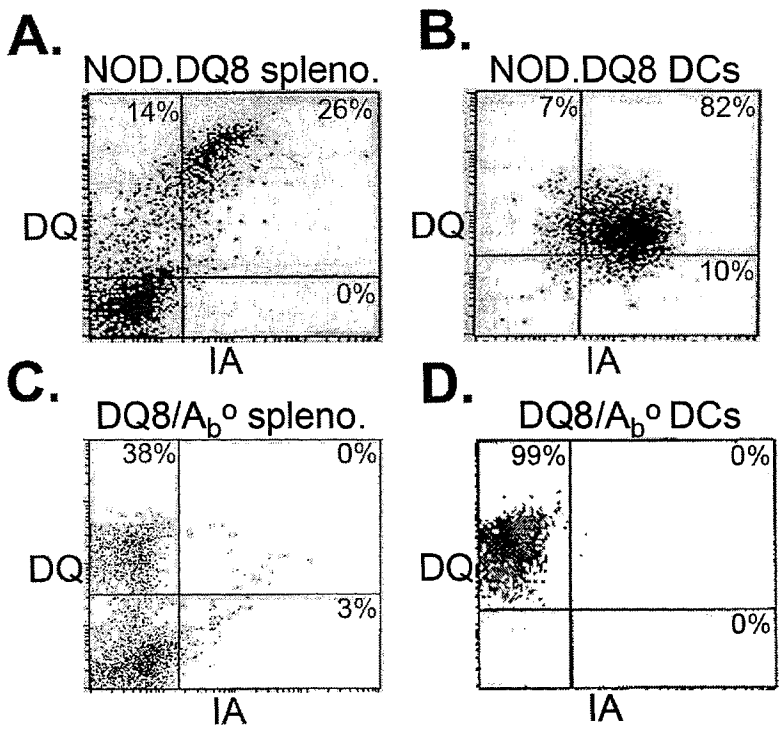

Figure 2-1: DQ8 transgenic mice show tissue appropriate expression of the MHC class II transgene. MHC -IA and -DQ expression levels on (A) splenocytes and (B) bone marrow derived dendritic cells (DCs) from NOD.DQ8 animals; (C,D) IA versus DQ expression levels on splenocytes and DCs from NOD.DQ8/Ab^{o} animals [i.e. animals shown in A and B above, crossed onto the IAb knockout NOD background].

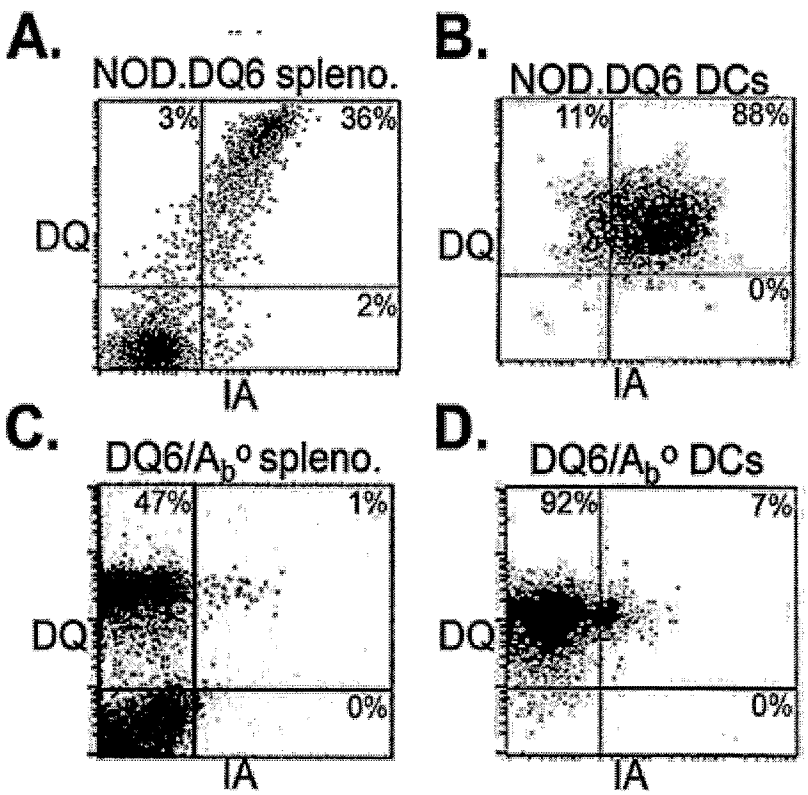

Figure 2-2: DQ6 transgenic mice show tissue appropriate expression of the MHC class II transgene. MHC -IA and -DQ expression levels on (A) splenocytes and (B) bone marrow derived dendritic cells (DCs) from NOD.DQ6 animals; (C,D) IA versus DQ expression levels on splenocytes and DCs from NOD.DQ6/Ab^{o} animals [i.e. animals shown in A and B above, crossed onto the IAb knockout NOD background].

	CD3	CD8	CD4	B220
PBLs				
NOD	44 ± 3%	20 ± 5%	29 ± 4%	40 ± 4%
NOD/Ab^0	23 ± 4%	21 ± 7%	1 ± 0%	41 ± 5%
NOD.DQ8/Ab^0	46 ± 7%	17 ± 4%	28 ± 3%	40 ± 6%
NOD.DQ6/Ab^0	42 ± 4%	20 ± 3%	21 ± 4%	44 ± 7%
Splenocytes				
NOD	42 ± 1%	8 ± 3%	32 ± 5%	49 ± 3%
NOD/Ab^0	17 ± 3%	11 ± 2%	6 ± 1%	48 ± 6%
NOD.DQ8/Ab^0	38 ± 5%	10 ± 3%	26 ± 2%	54 ± 6%
NOD.DQ6/Ab^0	36 ± 8%	7 ± 3%	28 ± 2%	51 ± 4%

Table 2-1: Relative abundance of various lymphocyte subsets in progenitor strains and DQ Transgenic IAb knockout lines. Peripheral blood lymphocytes (PBLs) and splenic lymphocytes were purified by passage over lympholyte-M gradients. These were stained with antibodies against the indicated markers and analyzed by FACScan. Data represents the average of three independent experiments, given as a percentage of total lymphocytes +/- standard deviation. The CD4 population represents cells expressing mouse CD4, although these cells also co-express human CD4. It has been shown that mouse CD4 is able to bind and interact with human MHC class II (14, 51).

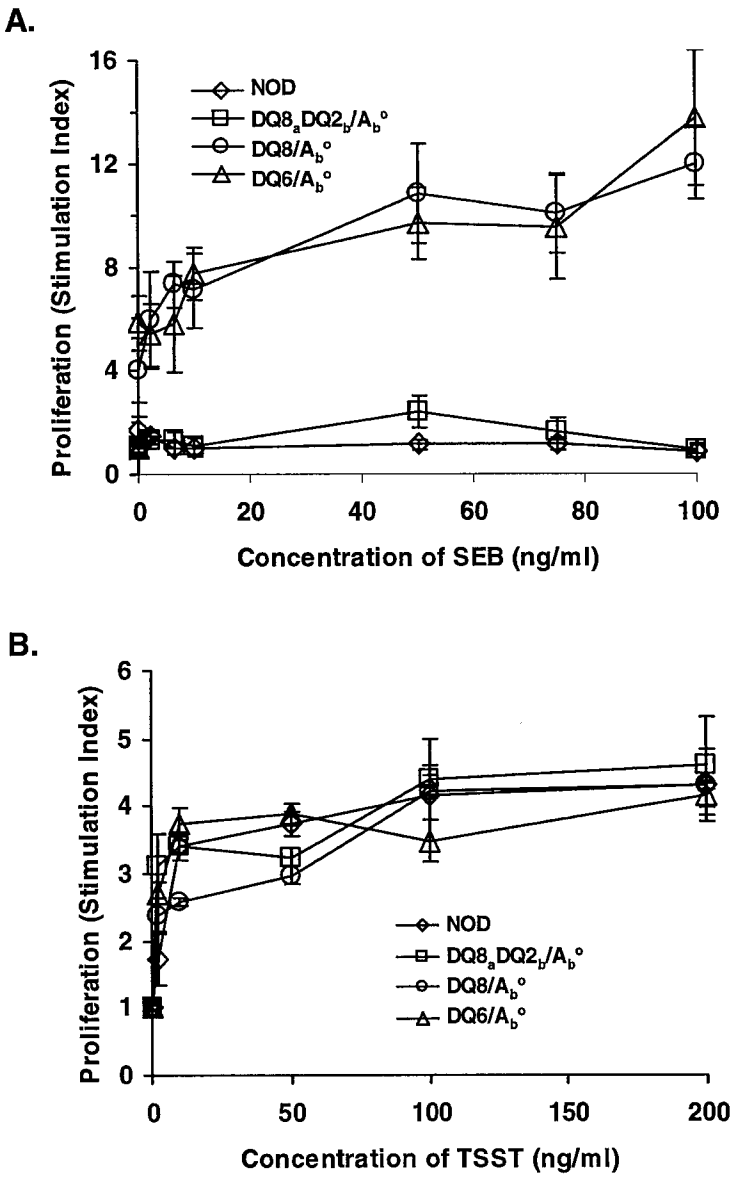

Figure 2-3: Proliferative responses of splenocytes from NOD.DQ8/Ab^0, NOD.DQ6/Ab^0, NOD and NOD.DQ8aDQ2b/Ab^0 mice to the superantigens SEB and TSST. A standard 3H thymidine uptake proliferation assay was performed. (A) Response to SEB. (B) Response to TSST. These are representative results (of 5 experiments each) analyzed in triplicate. Error bars represent standard deviation. NOD mice have been shown previously to respond to TSST, but not SEB (52). NOD.DQ8aDQ2b Ab^0 mice, like NOD mice, develop insulitis and diabetes (53). For each experiment a SI of one was set for the proliferation of NOD splenic lymphocytes in the absence of superantigen and NOD.DQ6/Ab^0 and NOD.DQ8/Ab^0 splenic lymphocytes have a higher background proliferation to those of NOD.

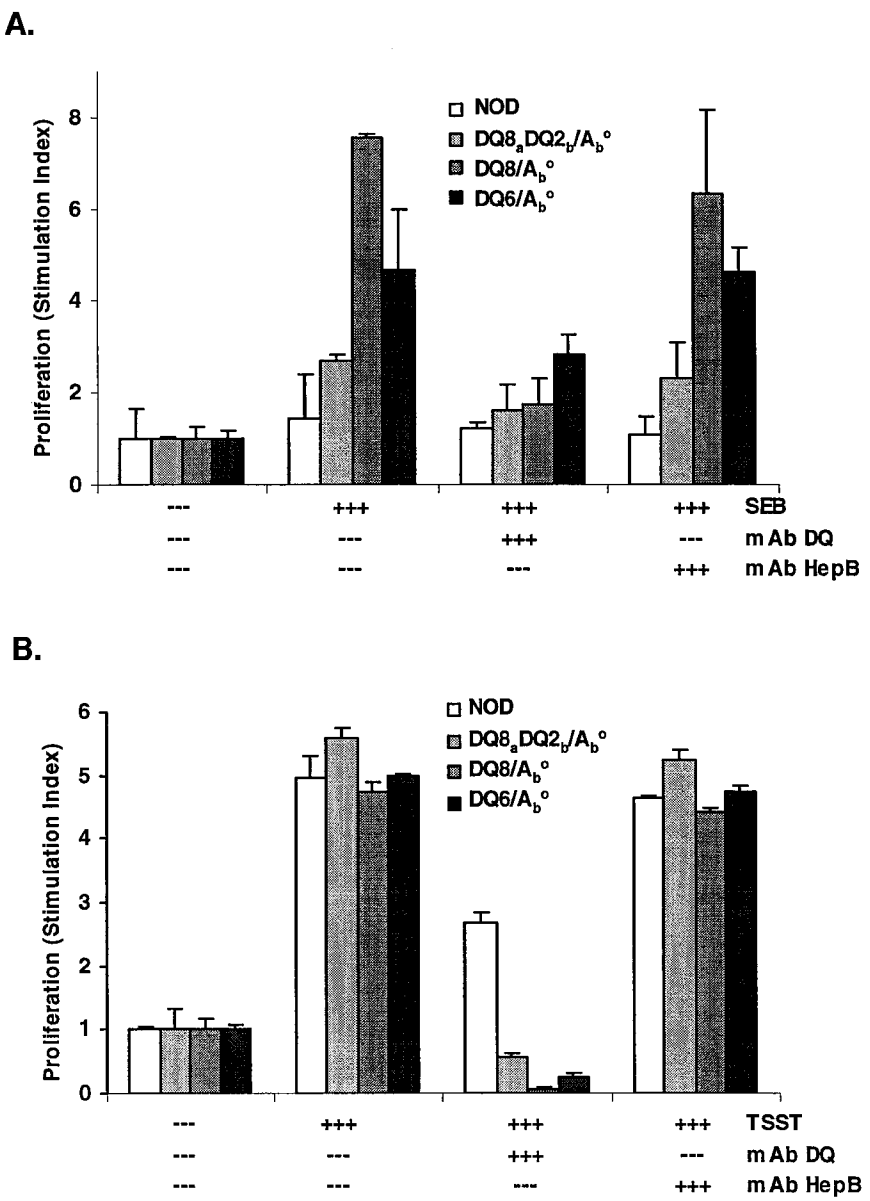

Figure 2-4: An anti-DQ monoclonal antibody can block superantigen stimulation of DQ-transgenic splenocytes. A standard ^{3}H thymidine uptake proliferation assay was performed at 50ng/ml superantigen in the absence and presence of an anti-DQ monoclonal antibody or a control anti-hepatitis B antigen antibody. (A) SEB stimulation. (B) TSST stimulation. These are representative results (of 3 experiments each) analyzed in triplicate. Error bars represent standard deviation. For details on NOD.DQ8aDQ2b Ab^{0} mice see (53).

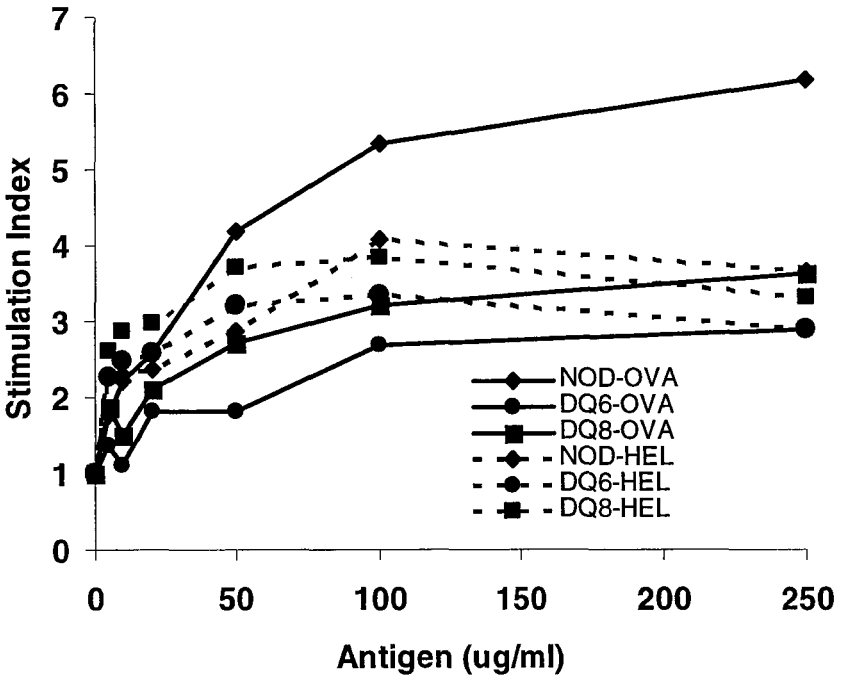

Figure 2-5: NOD.DQ8/Ab^0 and NOD.DQ6/Ab^0 mice have similar recall responses to ovalbumin and hen egg lysozyme. Splenocytes from pre-immunized mice were stimulated with various concentrations of the immunization antigen, ovalbumin (OVA) or hen egg lysozyme (HEL), and proliferation was measured by ^{3}H thymidine uptake. Each condition was done in triplicate and this is a representative experiment of three experiments.

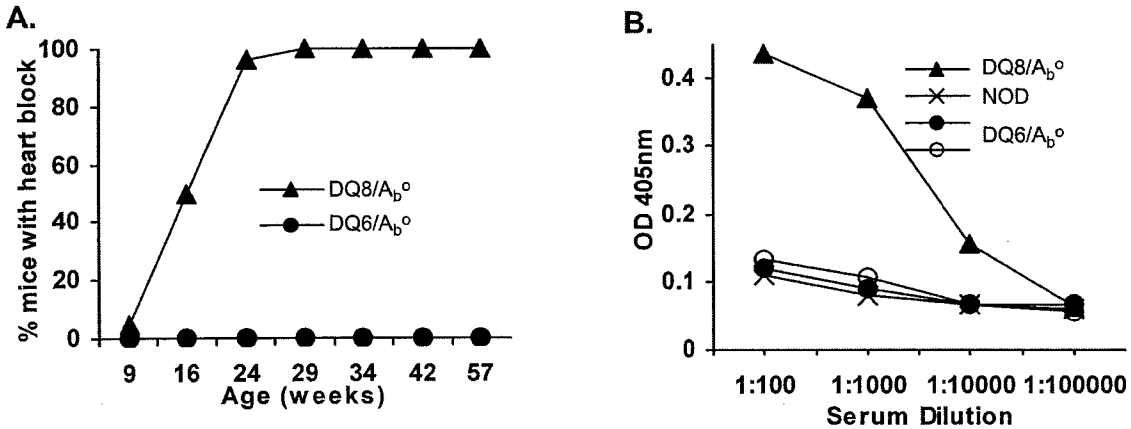

Figure 2-6: NOD.DQ6/Ab^0 mice do not develop autoimmune myocarditis. (A) Incidence of heart block (first or second degree; via ECG) versus age in the NOD.DQ8/Ab^0 line was compared to the NOD.DQ6/Ab^0 NOD line (n=16 animals in each group). (B) Titres of anti-cardiac myosin autoantibodies, determined by ELISA using sera of NOD.DQ8/Ab^0 mice compared to NOD wild-type (at 12 weeks), and to NOD.DQ6/Ab^0 mice at two different ages (24 weeks = closed circles, 40 weeks=open circles).

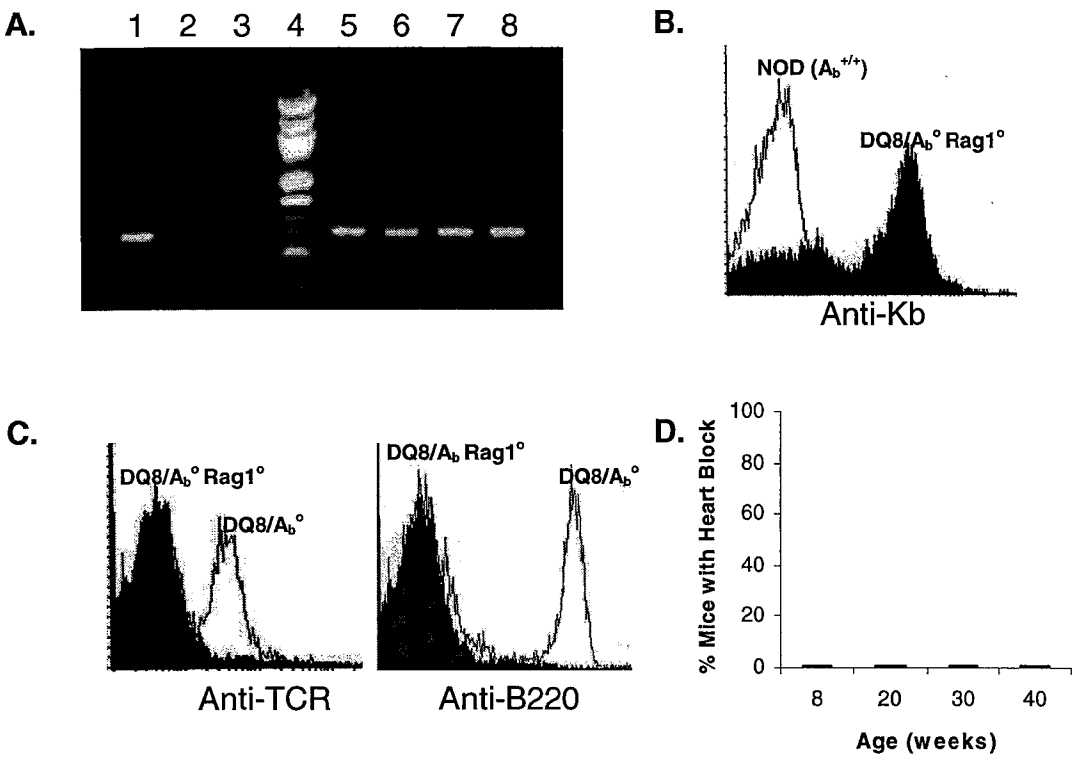

Figure 2-7: NOD.DQ8/Ab^0 Rag1^0 mice do not develop autoimmune myocarditis. NOD.DQ8/Ab^0 Rag1^0 mice were established by crossing NOD.DQ8/Ab^0 mice with NOD Rag1^0 mice and screening for the presence of DQ by PCR (A) and for the absence of IA (B), T cells (C) and B cells (C) by FACs. (A) Representative DQ screening by PCR of tail DNAs. Lane 1: Positive control, NOD.DQ8/Ab^0, Lane 2: Negative control, wild-type NOD, Lane 3: Negative control, NOD Rag1^0, Lane 4: MW markers, Lane 5-8 NOD.DQ8/Ab^0 Rag1^0 mice. (B) Representative FACs histogram of class I haplotype screening of NOD.DQ8/Ab^0 Rag1^0 mice. NOD mice are MHC class I, K^d, the IAb^0 is linked with the MHC class I K^b. Therefore NOD.DQ8/Ab^0 Rag1^0 mice are K^b. (C) Representative FACs profiles showing the absence of T cells and B cells in NOD.DQ8/Ab^0 Rag1^0 mice. (D) ECG analysis of NOD.DQ8/Ab^0 Rag1^0 mice at various ages.

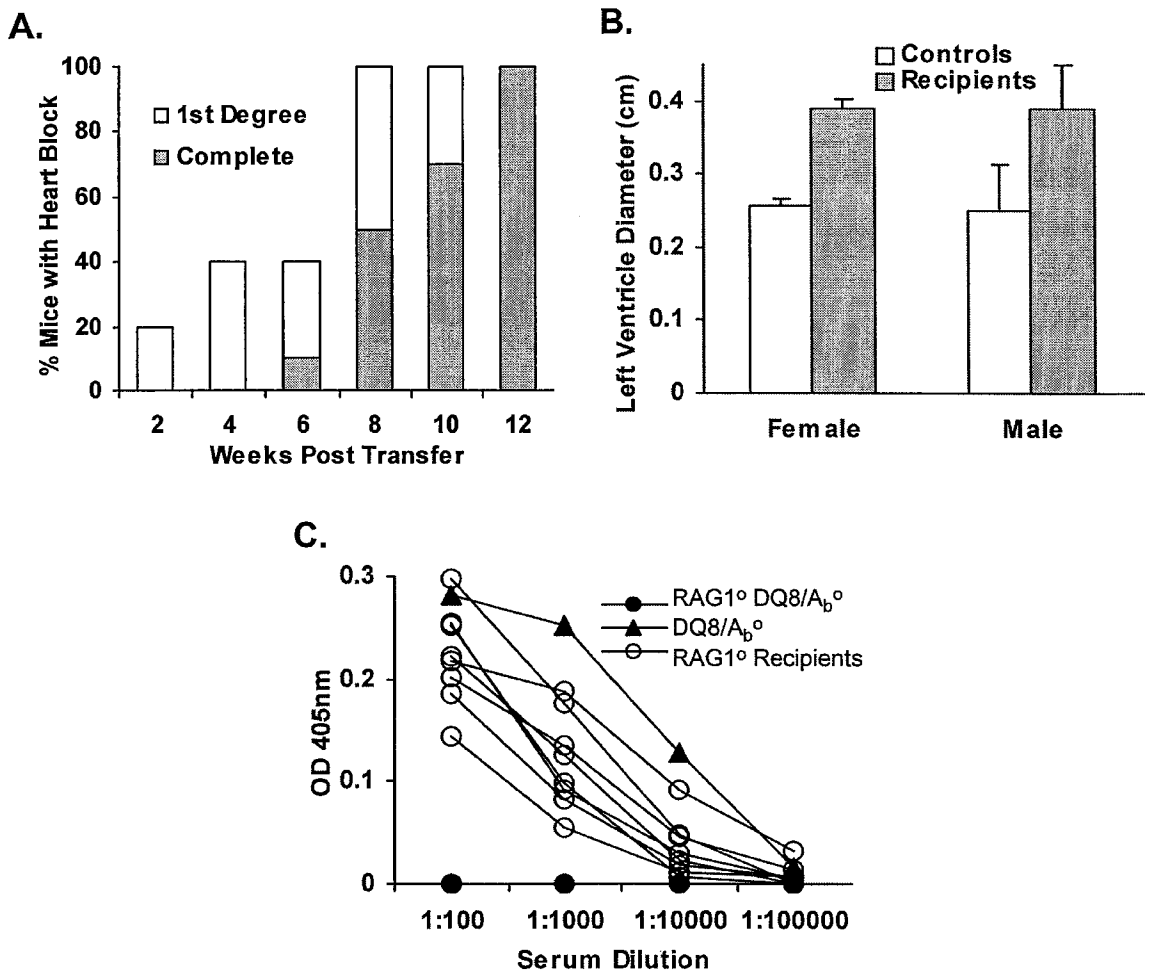

Figure 2-8: The autoimmune myocarditis of NOD.DQ8/Ab^0 mice can be adoptively transferred to NOD.DQ8/Ab^0 Rag1^0 mice. (A) Incidence of heart block for 12 weeks post transfer of 1 x 10^6 splenocytes from >12 week old NOD.DQ8/Ab^0 mice to 8 week old NOD.DQ8/Ab^0 Rag1^0 mice (n=8). (B) Echocardiography data from the experiment in (A). Non-sedated echocardiographs were taken and the diameter of the left ventricle was measured at 14 weeks post transfer. (n=4 for each sex). (C) Titres of anti-cardiac myosin autoantibodies in the serum of the recipients of (A) at 14 weeks post transfer (n=8) as compared to an age matched NOD.DQ8/Ab^0 mouse (positive control) and a NOD.DQ8/Ab^0 Rag1^0 mouse (negative control).

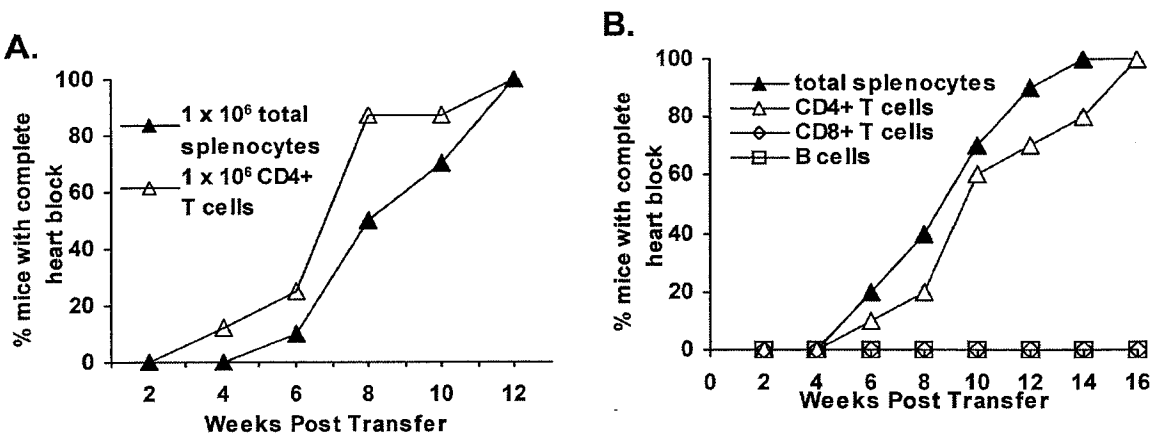

Figure 2-9: CD4 T cells alone can adoptively transfer myocarditis from NOD.DQ8/Ab^0 mice to NOD.DQ8/Ab^0 Rag1^0 mice. (A) Incidence of complete heart block for 12 weeks post transfer of 1 x 10^6 magnetic sorted CD4 enriched splenocytes (91% CD4+, 9% B220+) as compared to 1 x 10^6 whole splenocytes from >12 week old NOD.DQ8/Ab^0 mice into 8 week old NOD.DQ8/Ab^0 Rag1^0 mice (n=8). (B) Incidence of complete heart block for 16 weeks post transfer of 1x10^6 whole splenocytes or FACs sorted CD4 T cells, CD8 T cells, or B cells from >12 week old NOD.DQ8/Ab^0 mice into 8 week old NOD.DQ8/Ab^0 Rag1^0 mice (n=5).

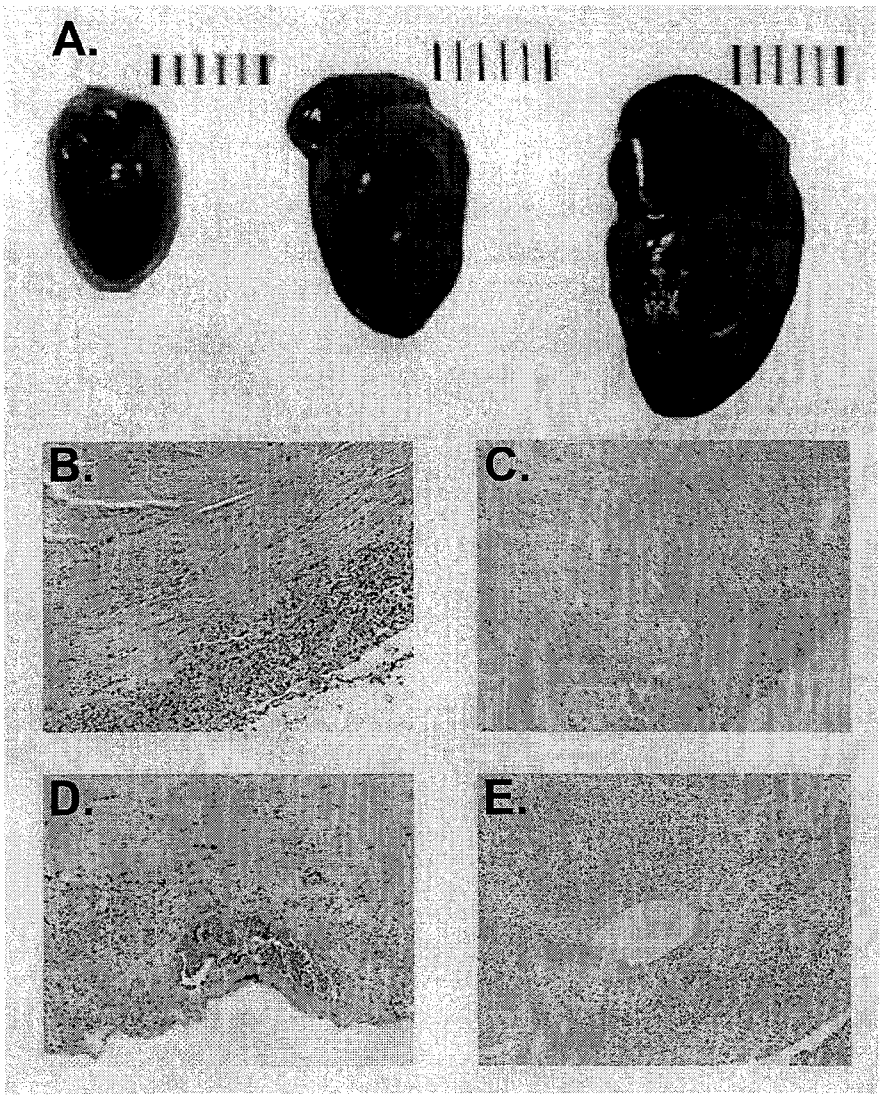

Figure 2-10: Adoptive transfer of CD4 T cells alone produces a more profound disease than adoptive transfer of total splenocytes. (A) Photograph of a heart from a NOD.DQ8/Ab^0 Rag1^0 mouse (left), a NOD.DQ8/Ab^0 Rag1^0 mouse 12 weeks after receiving 1 x 10^6 splenocytes from NOD.DQ8/Ab^0 mice (middle) and a NOD.DQ8/Ab^0 Rag1^0 mouse 12 weeks after receiving 1 x 10^6 CD4 enriched splenocytes from NOD.DQ8/Ab^0 mice (right). The scale bar represents 0.5cm. (B-E) H&E stained cardiac sections of a NOD.DQ8/Ab^0 mouse (B), a NOD.DQ8/Ab^0 Rag1^0 mouse (C), a NOD.DQ8/Ab^0 Rag1^0 mouse 14 weeks after receiving 1 x 10^6 splenocytes from a NOD.DQ8/Ab^0 mouse (D), a NOD.DQ8/Ab^0 Rag1^0 mouse 14 weeks after receiving 1 x 10^6 CD4 enriched splenocytes from a NOD.DQ8/Ab^0 mouse (E). Histological sections are at 200x.

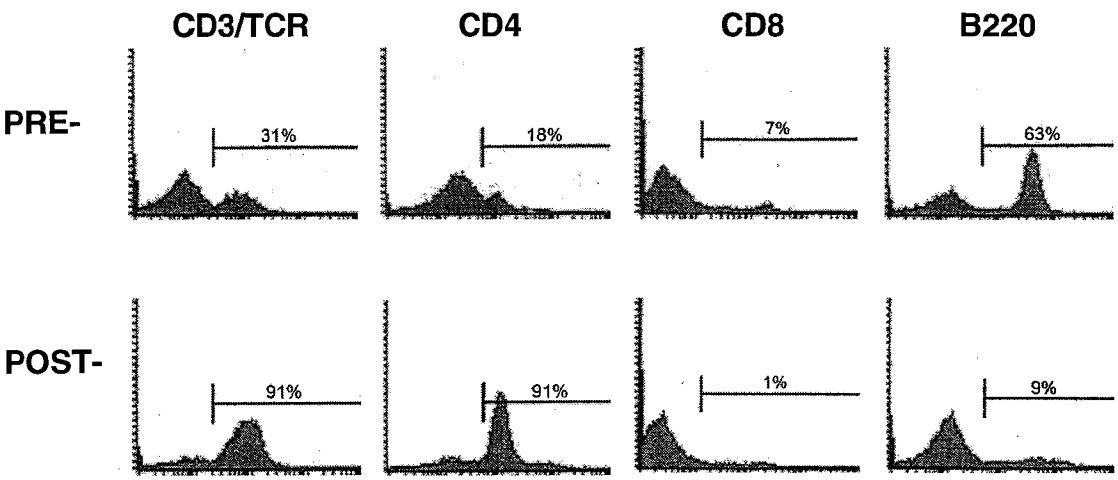

Figure 2-11: Analysis of cells separated by magnetic selection. Representative flow cytometry profiles of lympholyte-M purified splenic lymphocytes from a NOD.DQ8/Ab^0 mouse before enrichment (Pre) and after negative selection of CD4 T cells using a Miltenyi Biotec mouse CD4+ T cell isolation kit (Post). Antibodies CD8α/Ly-2, CD45R/B220, DX5, CD11b/Mac-1 and ter-119 were used to remove the non-CD4 population. Anti-TCR (H57-597), anti-CD4 (GK1.5), anti-CD8 (CL169F), and anti-B220 (RA3-6B2) were used to assess the quality of the separation.

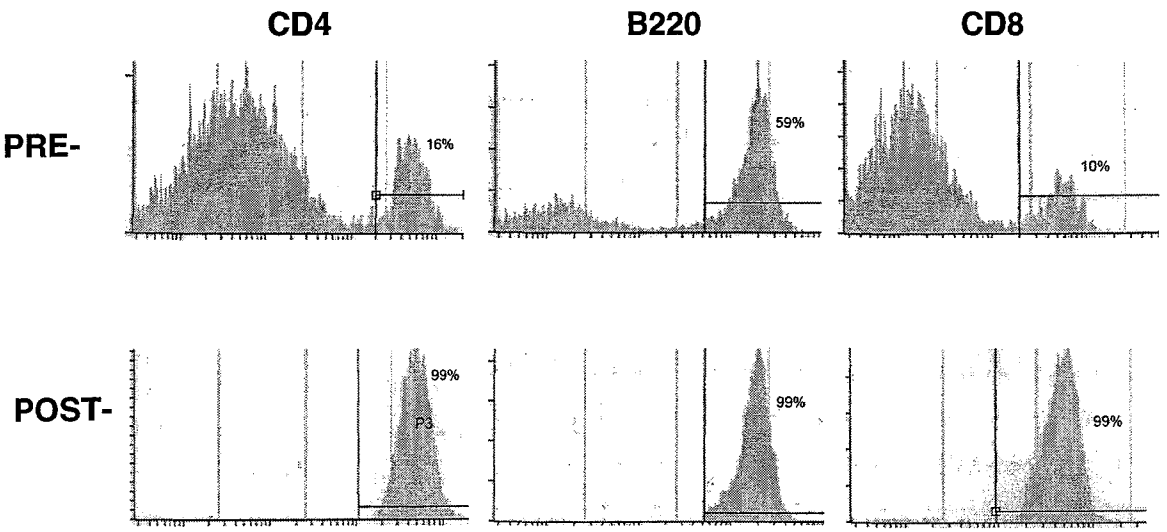

Figure 2-12: Analysis of cells separated by fluorescent Cell Sorting. Representative flow cytometry profiles of singly stained lympholyte-M purified splenic lymphocytes from a NOD.DQ8/Ab^0 mouse. Splenic lymphocytes were either stained with Anti-CD4 (GK1.5), anti-B220 (RA3-6B2) or anti-CD8 (CL169F). "Pre" represents the CD4, B220, or CD8 staining prior to FACS sorting. "Post" represents the purity of the cell type of interest in each of the three FACS sorted populations.

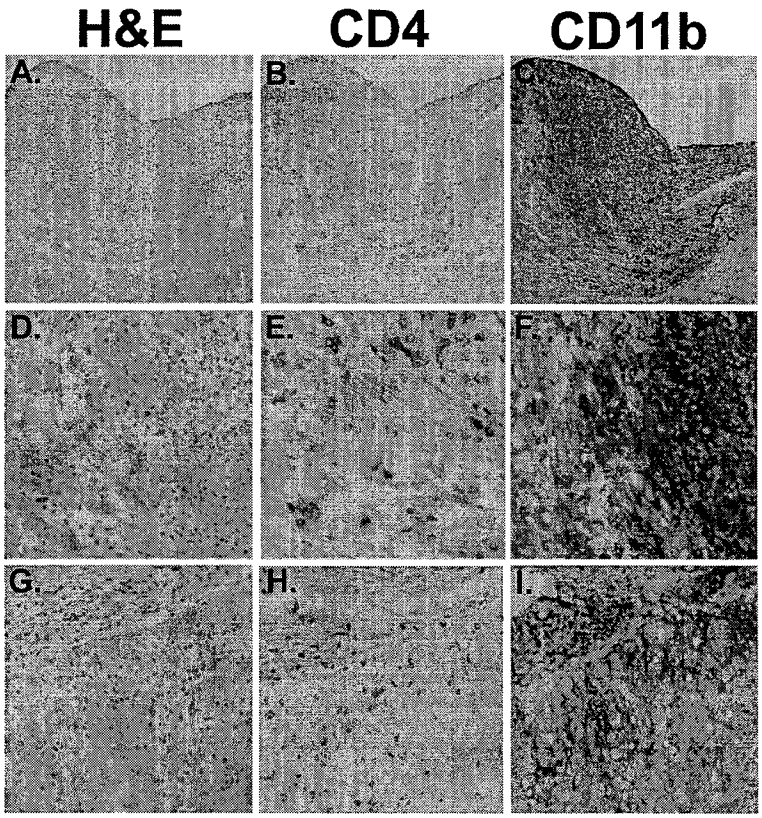

Figure 2-13: Macrophages predominate in the mononuclear cell infiltrate seen in the hearts of NOD.DQ8/Ab^0 Rag1^0 mice that received CD4 T cell transfers. (A-C) Infiltrate at 100x magnification stained by either H&E (A), or by immunohistochemistry staining for anti-CD4 (B), or anti-CD11b (C). (D-I) Infiltrate at 200x magnification stained by H&E (D/G), or by immunohistochemistry staining for anti-CD4 (E/H), or anti-CD11b (F/I).

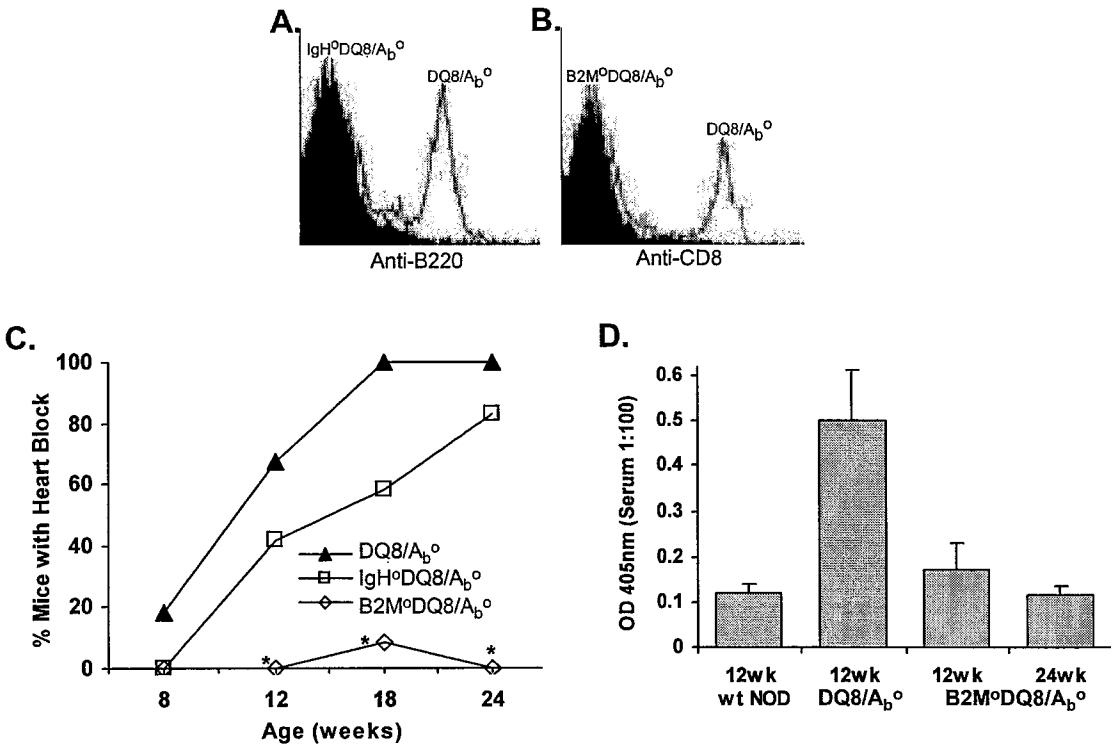

Figure 2-14: CD8 T cells, but not B cells, are critical to the induction of autoimmune myocarditis in NOD.DQ8/Ab^0 mice. (A) Comparison of B cell populations in NOD.DQ8/Ab^0 mice with those in immunoglobulin heavychain knockout NOD.DQ8/Ab^0 mice. (B) Comparison of CD8 T cell populations in NOD.DQ8/Ab^0 mice with those in β2-microglobulin knockout DQ8/Ab^0 mice. (C) Incidence of heart block in NOD.DQ8/Ab^0 mice, immunoglobulin heavychain knockout NOD.DQ8/Ab^0 mice and β2-microglobulin knockout NOD.DQ8/Ab^0 mice at various ages. (D) Titres of anti-cardiac myosin autoantibodies in serum of 12 week old NOD mice (n=3), 12 week old NOD.DQ8/Ab^0 mice (n=3), and β2-microglobulin knockout NOD.DQ8/Ab^0 mice (n=12) at two different ages.

A. B.

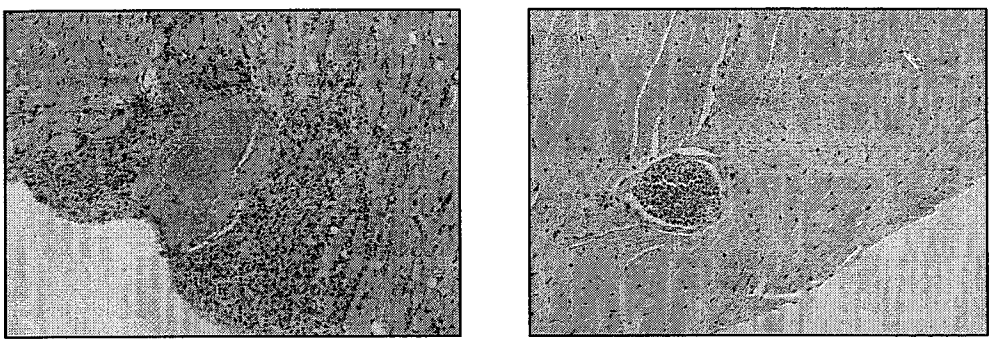

Figure 2-15: Histology results for NOD.DQ8/Ab^0 IgH^0 and NOD.DQ8/Ab^0 β2m^0 mice. H&E stained cardiac sections (200x) of an immunoglobulin heavychain knockout NOD.DQ8/Ab^0 mouse (A), and a β-2 microglobulin knockout NOD.DQ8/Ab^0 mouse (B).

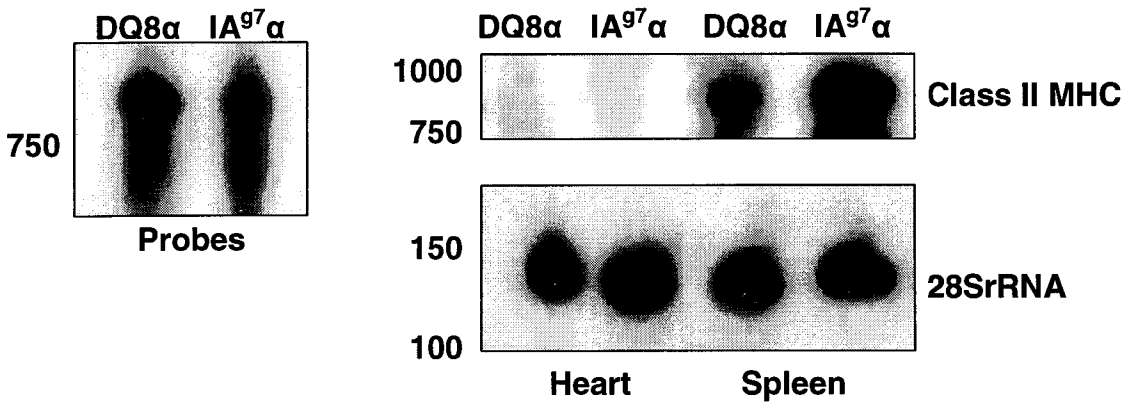

Figure 2-16: DQ mRNA levels are not abnormally elevated in the hearts of NOD.DQ8$^{+/-}$/Ab$^{+/-}$ mice. DQ8α, IAα and 28SrRNA RNA probes were made (see materials and methods) and used to probe various NOD.DQ8$^{+/-}$/Ab$^{+/-}$ tissues, including the heart and spleen shown here, using a RNAse Protection Assay. Identical results were seen with probes for the beta chains. (Note: the mice are a result of a F1 cross and do not develop myocarditis. The cross was made so that levels of DQ and IA mRNA could be compared in the same RNA samples. These experiments disprove the hypothesis that heart disease in the NOD.DQ8/Ab^{0} mice might be due to an abnormally high/aberrant expression of the DQ transgene specifically within the heart.)

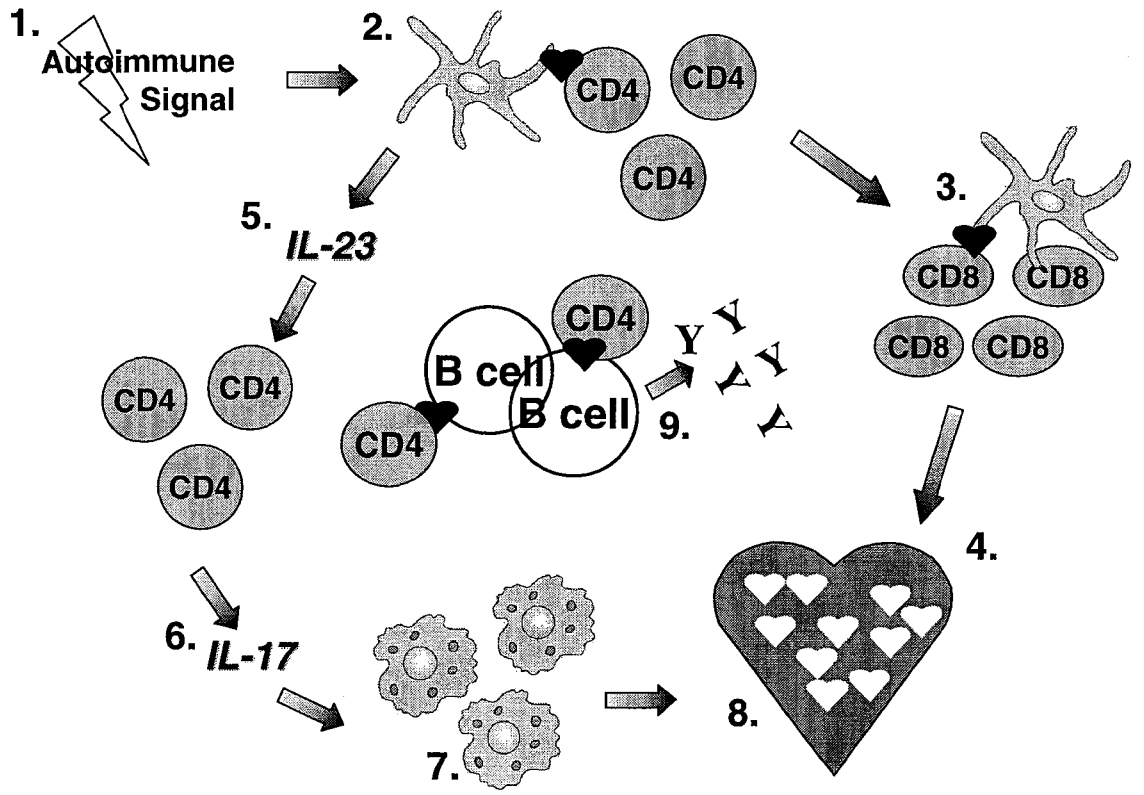

Figure 2-17: Proposed Immune Mechanism for Autoimmunity in NOD.DQ8/Ab^0 mice. **1.** An unknown autoimmune trigger breaks self tolerance. **2.** APCs such as dendritic cells present heart antigen to CD4 cells via DQ8. **3.** Cytokines and presentation of heart antigen via MHC class I recruits CD8 T cells to the heart. **4.** CD8 CTLs begin to attack the heart releasing vast quantities of cardiac antigens which get presented to CD4 T cells in the context of DQ8. **5.** Activated dendritic cells release IL-23. **6.** IL-23 induces a subset of CD4 T cells to release IL-17. **7.** IL-17 recruits macrophages. **8.** Macrophages through phagocytosis and inflammatory cytokines take over the destruction of the heart. **9.** Meanwhile, in addition to playing a minor role as APCs, B cells become activated and release autoantibodies.

	DX5 SP	CD3 SP	DX5 CD3 DP
Balb/c	2.2%	38%	0.4%
NOD	2.5%	44%	<0.1%
NOD.DQ8/Ab^0	2.0%	46%	<0.1%

Table 2-2: Like NODs, NOD.DQ8/Ab^0 animals have reduced numbers of NKT cells. Splenic lymphocytes were purified by passage over lympholyte-M gradients. These were stained with antibodies against the indicated markers and analyzed by FACScan. Results presented are of a representative experiment. DX5 and CD3 single positive (SP) cells represent NK and T cells, respectively. DX5 CD3 double positive (DP) cells represent NKT cells. (Note: DX5 was used as NOD mice do not express NK1.1.)

2.5 References

1. Dec, G. W., and R. W. DeSanctis. 1998. In *Scientific American Medicine.* D. C. Dale, and D. D. Federman, eds. Scientific American, New York.

2. Manolio, T. A., K. L. Baughman, R. Rodeheffer, T. A. Pearson, J. D. Bristow, V. V. Michels, W. H. Abelmann, and W. R. Harlan. 1992. Prevalence and etiology of idiopathic dilated cardiomyopathy (summary of a National Heart, Lung, and Blood Institute workshop. *Am J Cardiol 69:1458.*

3. Herskowitz, A., L. J. Wolfgram, N. R. Rose, and K. W. Beisel. 1987. Coxsackievirus B3 murine myocarditis: a pathologic spectrum of myocarditis in genetically defined inbred strains. *J Am Coll Cardiol 9:1311.*

4. Rose, N. R., L. J. Wolfgram, A. Herskowitz, and K. W. Beisel. 1986. Postinfectious autoimmunity: two distinct phases of coxsackievirus B3-induced myocarditis. *Ann N Y Acad Sci 475:146.*

5. Wolfgram, L. J., K. W. Beisel, and N. R. Rose. 1985. Heart-specific autoantibodies following murine coxsackievirus B3 myocarditis. *J Exp Med 161:1112.*

6. Neu, N., N. R. Rose, K. W. Beisel, A. Herskowitz, G. Gurri-Glass, and S. W. Craig. 1987. Cardiac myosin induces myocarditis in genetically predisposed mice. *J Immunol 139:3630.*

7. Neu, N., B. Ploier, and C. Ofner. 1990. Cardiac myosin-induced myocarditis. Heart autoantibodies are not involved in the induction of the disease. *J Immunol 145:4094.*

8. Smith, S. C., and P. M. Allen. 1991. Myosin-induced acute myocarditis is a T cell-mediated disease. *J Immunol 147:2141.*

9. Kubota, T., C. F. McTiernan, C. S. Frye, S. E. Slawson, B. H. Lemster, A. P. Koretsky, A. J. Demetris, and A. M. Feldman. 1997. Dilated cardiomyopathy in transgenic mice with cardiac-specific overexpression of tumor necrosis factor-alpha. *Circ Res 81:627.*

10. Kubota, T., C. F. McTiernan, C. S. Frye, A. J. Demetris, and A. M. Feldman. 1997. Cardiac-specific overexpression of tumor necrosis factor-alpha causes lethal myocarditis in transgenic mice. *J Card Fail 3:117.*

11. Bryant, D., L. Becker, J. Richardson, J. Shelton, F. Franco, R. Peshock, M. Thompson, and B. Giroir. 1998. Cardiac failure in transgenic mice with myocardial expression of tumor necrosis factor-alpha. *Circulation 97:1375.*

12. Nishimura, H., T. Okazaki, Y. Tanaka, K. Nakatani, M. Hara, A. Matsumori, S. Sasayama, A. Mizoguchi, H. Hiai, N. Minato, and T. Honjo. 2001. Autoimmune dilated cardiomyopathy in PD-1 receptor-deficient mice. *Science 291:319.*

13. Okazaki, T., Y. Tanaka, R. Nishio, T. Mitsuiye, A. Mizoguchi, J. Wang, M. Ishida, H. Hiai, A. Matsumori, N. Minato, and T. Honjo. 2003. Autoantibodies against cardiac troponin I are responsible for dilated cardiomyopathy in PD-1-deficient mice. *Nat Med 9:1477.*

14. Taylor, J. A., E. Havari, M. F. McInerney, R. Bronson, K. W. Wucherpfennig, and M. A. Lipes. 2004. A spontaneous model for autoimmune myocarditis using the human MHC molecule HLA-DQ8. *J Immunol 172:2651.*

15. Elliott, J. F., J. Liu, Z. N. Yuan, N. Bautista-Lopez, S. L. Wallbank, K. Suzuki, D. Rayner, P. Nation, M. A. Robertson, G. Liu, and K. M. Kavanagh. 2003. Autoimmune cardiomyopathy and heart block develop spontaneously in HLA-DQ8 transgenic IAbeta knockout NOD mice. *Proc Natl Acad Sci U S A 100:13447.*

16. Liu, J., L. E. Purdy, S. Rabinovitch, A. M. Jevnikar, and J. F. Elliott. 1999. Major DQ8-restricted T-cell epitopes for human GAD65 mapped using human CD4, DQA1*0301, DQB1*0302 transgenic IA(null) NOD mice. *Diabetes 48:469.*

17. Okada, K., J. M. Boss, H. Prentice, T. Spies, R. Mengler, C. Auffray, J. Lillie, D. Grossberger, and J. L. Strominger. 1985. Gene organization of DC and DX subregions of the human major histocompatibility complex. *Proc Natl Acad Sci U S A 82:3410.*

18. Killeen, N., S. Sawada, and D. R. Littman. 1993. Regulated expression of human CD4 rescues helper T cell development in mice lacking expression of endogenous CD4. *Embo J 12:1547.*

19. Ellis, M. C., A. H. Hetisimer, D. A. Ruddy, S. L. Hansen, G. S. Kronmal, E. McClelland, L. Quintana, D. T. Drayna, M. S. Aldrich, and E. Mignot. 1997. HLA class II haplotype and sequence analysis support a role for DQ in narcolepsy. *Immunogenetics 46:410.*

20. Bunce, M., C. J. Taylor, and K. I. Welsh. 1993. Rapid HLA-DQB typing by eight polymerase chain reaction amplifications with sequence-specific primers (PCR-SSP). *Hum Immunol 37:201.*

21. Kudva, Y. C., G. Rajagopalan, R. Raju, R. S. Abraham, M. Smart, J. Hanson, and C. S. David. 2002. Modulation of insulitis and type 1 diabetes by transgenic HLA-DR3 and DQ8 in NOD mice lacking endogenous MHC class II. *Hum Immunol 63:987.*

22. Christianson, S. W., L. D. Shultz, and E. H. Leiter. 1993. Adoptive transfer of diabetes into immunodeficient NOD-scid/scid mice. Relative contributions of CD4+ and CD8+ T-cells from diabetic versus prediabetic NOD.NON-Thy-1a donors. *Diabetes 42:44.*

23. DiLorenzo, T. P., R. T. Graser, T. Ono, G. J. Christianson, H. D. Chapman, D. C. Roopenian, S. G. Nathenson, and D. V. Serreze. 1998. Major histocompatibility complex class I-restricted T cells are required for all but the end stages of diabetes development in nonobese diabetic mice and use a prevalent T cell receptor alpha chain gene rearrangement. *Proc Natl Acad Sci U S A 95:12538.*

24. Park, H., Z. Li, X. O. Yang, S. H. Chang, R. Nurieva, Y. H. Wang, Y. Wang, L. Hood, Z. Zhu, Q. Tian, and C. Dong. 2005. A distinct lineage of CD4 T cells regulates tissue inflammation by producing interleukin 17. *Nat Immunol.*

25. Witowski, J., K. Ksiazek, and A. Jorres. 2004. Interleukin-17: a mediator of inflammatory responses. *Cell Mol Life Sci 61:567.*

26. Ishiyama, S., M. Hiroe, T. Nishikawa, T. Shimojo, S. Abe, H. Fujisaki, H. Ito, K. Yamakawa, N. Kobayashi, T. Kasajima, and F. Marumo. 1998. The

Fas/Fas ligand system is involved in the pathogenesis of autoimmune myocarditis in rats. *J Immunol 161:4695.*

27. Taneja, V., N. Taneja, T. Paisansinsup, M. Behrens, M. Griffiths, H. Luthra, and C. S. David. 2002. CD4 and CD8 T cells in susceptibility/protection to collagen-induced arthritis in HLA-DQ8-transgenic mice: implications for rheumatoid arthritis. *J Immunol 168:5867.*

28. Malkiel, S., S. Factor, and B. Diamond. 1999. Autoimmune myocarditis does not require B cells for antigen presentation. *J Immunol 163:5265.*

29. Serreze, D. V., H. D. Chapman, D. S. Varnum, M. S. Hanson, P. C. Reifsnyder, S. D. Richard, S. A. Fleming, E. H. Leiter, and L. D. Shultz. 1996. B lymphocytes are essential for the initiation of T cell-mediated autoimmune diabetes: analysis of a new "speed congenic" stock of NOD.Ig mu null mice. *J Exp Med 184:2049.*

30. Akashi, T., S. Nagafuchi, K. Anzai, S. Kondo, D. Kitamura, S. Wakana, J. Ono, M. Kikuchi, Y. Niho, and T. Watanabe. 1997. Direct evidence for the contribution of B cells to the progression of insulitis and the development of diabetes in non-obese diabetic mice. *Int Immunol 9:1159.*

31. Serreze, D. V., S. A. Fleming, H. D. Chapman, S. D. Richard, E. H. Leiter, and R. M. Tisch. 1998. B lymphocytes are critical antigen-presenting cells for the initiation of T cell-mediated autoimmune diabetes in nonobese diabetic mice. *J Immunol 161:3912.*

32. Serreze, D. V., and P. A. Silveira. 2003. The role of B lymphocytes as key antigen-presenting cells in the development of T cell-mediated autoimmune type 1 diabetes. *Curr Dir Autoimmun 6:212.*

33. Wong, F. S., L. Wen, M. Tang, M. Ramanathan, I. Visintin, J. Daugherty, L. G. Hannum, C. A. Janeway, Jr., and M. J. Shlomchik. 2004. Investigation of the role of B-cells in type 1 diabetes in the NOD mouse. *Diabetes 53:2581.*

34. Poulton, L. D., M. J. Smyth, C. G. Hawke, P. Silveira, D. Shepherd, O. V. Naidenko, D. I. Godfrey, and A. G. Baxter. 2001. Cytometric and functional analyses of NK and NKT cell deficiencies in NOD mice. *Int Immunol 13:887.*

35. Yang, Y., M. Bao, and J. W. Yoon. 2001. Intrinsic defects in the T-cell lineage results in natural killer T-cell deficiency and the development of diabetes in the nonobese diabetic mouse. *Diabetes 50:2691.*

36. Beaudoin, L., V. Laloux, J. Novak, B. Lucas, and A. Lehuen. 2002. NKT cells inhibit the onset of diabetes by impairing the development of pathogenic T cells specific for pancreatic beta cells. *Immunity 17:725.*

37. Falcone, M., F. Facciotti, N. Ghidoli, P. Monti, S. Olivieri, L. Zaccagnino, E. Bonifacio, G. Casorati, F. Sanvito, and N. Sarvetnick. 2004. Up-regulation of CD1d expression restores the immunoregulatory function of NKT cells and prevents autoimmune diabetes in nonobese diabetic mice. *J Immunol 172:5908.*

38. Kim, S., J. Poursine-Laurent, S. M. Truscott, L. Lybarger, Y. J. Song, L. Yang, A. R. French, J. B. Sunwoo, S. Lemieux, T. H. Hansen, and W. M. Yokoyama. 2005. Licensing of natural killer cells by host major histocompatibility complex class I molecules. *Nature 436:709.*

39. Serreze, D. V., E. H. Leiter, G. J. Christianson, D. Greiner, and D. C. Roopenian. 1994. Major histocompatibility complex class I-deficient NOD-B2mnull mice are diabetes and insulitis resistant. *Diabetes 43:505.*

40. Sumida, T., M. Furukawa, A. Sakamoto, T. Namekawa, T. Maeda, M. Zijlstra, I. Iwamoto, T. Koike, S. Yoshida, H. Tomioka, and et al. 1994. Prevention of insulitis and diabetes in beta 2-microglobulin-deficient non-obese diabetic mice. *Int Immunol 6:1445.*

41. Wicker, L. S., E. H. Leiter, J. A. Todd, R. J. Renjilian, E. Peterson, P. A. Fischer, P. L. Podolin, M. Zijlstra, R. Jaenisch, and L. B. Peterson. 1994. Beta 2-microglobulin-deficient NOD mice do not develop insulitis or diabetes. *Diabetes 43:500.*

42. DiLorenzo, T. P., and D. V. Serreze. 2005. The good turned ugly: immunopathogenic basis for diabetogenic CD8+ T cells in NOD mice. *Immunol Rev 204:250.*

43. Serreze, D. V., T. M. Holl, M. P. Marron, R. T. Graser, E. A. Johnson, C. Choisy-Rossi, R. M. Slattery, S. M. Lieberman, and T. P. DiLorenzo. 2004. MHC class II molecules play a role in the selection of autoreactive class I-

restricted CD8 T cells that are essential contributors to type 1 diabetes development in nonobese diabetic mice. *J Immunol 172:871.*

44. McKenna, C. J., M. B. Codd, H. A. McCann, and D. D. Sugrue. 1997. Idiopathic dilated cardiomyopathy: familial prevalence and HLA distribution. *Heart 77:549.*

45. Carlquist, J. F., R. H. Ward, D. Husebye, M. Feolo, and J. L. Anderson. 1994. Major histocompatibility complex class II gene frequencies by serologic and deoxyribonucleic acid genomic typing in idiopathic dilated cardiomyopathy. *Am J Cardiol 74:918.*

46. Carlquist, J. F., R. L. Menlove, M. B. Murray, J. B. O'Connell, and J. L. Anderson. 1991. HLA class II (DR and DQ) antigen associations in idiopathic dilated cardiomyopathy. Validation study and meta-analysis of published HLA association studies. *Circulation 83:515.*

47. Limas, C. J. 1996. Autoimmunity in dilated cardiomyopathy and the major histocompatibility complex. *Int J Cardiol 54:113.*

48. Hiroi, S., H. Harada, H. Nishi, M. Satoh, R. Nagai, and A. Kimura. 1999. Polymorphisms in the SOD2 and HLA-DRB1 genes are associated with nonfamilial idiopathic dilated cardiomyopathy in Japanese. *Biochem Biophys Res Commun 261:332.*

49. Harcombe, A. A., L. Sharples, S. R. Large, J. Wallwork, P. L. Weissberg, and V. Joysey. 1999. HLA antigen frequencies in end-stage idiopathic and ischaemic cardiomyopathy. *Int J Cardiol 68:31.*

50. Lozano, M. D., R. J. Rubocki, J. E. Wilson, B. M. McManus, and J. L. Wisecarver. 1997. Human leukocyte antigen class II associations in patients with idiopathic dilated cardiomyopathy. Myocarditis Treatment Trial Investigators. *J Card Fail 3:97.*

51. Cheng, S., M. Smart, J. Hanson, and C. S. David. 2003. Characterization of HLA DR2 and DQ8 transgenic mouse with a new engineered mouse class II deletion, which lacks all endogenous class II genes. *J Autoimmun 21:195.*

52. Radons, J., V. Burkart, and H. Kolb. 1997. MHC class II-dependent abnormal reactivity toward bacterial superantigens in immune cells of NOD mice. *Diabetes 46:379.*

53. Dawson, L. A. 2005. Characterization of HLA-DQ8a/DQ2b Transgenic IAb null NOD Mice as a Model for Type 1 Diabetes. In *Department of Medical Microbiology and Immunology*. University of Alberta, Edmonton.

CHAPTER 3

NOD.DQ6/Ab^0 MICE: AN ANIMAL MODEL OF SPONTANEOUS AUTOIMMUNE THYROIDITIS

A version of this chapter has been submitted for publication. Hayward, S., Billesberger, L., Suzuki, K., and J. Elliott. 2006. Journal of Immunology.

3.1 Introduction

Hypothyroidism is a condition where the thyroid gland is unable to produce sufficient quantities of thyroid hormone. This insufficiency can be caused by radiation, drug therapy, surgery, or, more commonly, autoimmunity. Seventy percent of hypothyroidism cases are caused by Hashimoto's thyroiditis (1). Symptoms of Hashimoto's disease include tightness of the throat, fatigue, slow heart rate, depression, weight gain and intolerance to cold (2). A role for autoimmunity in the pathogenesis of Hashimoto's disease is supported by the findings of: 1) diffuse lymphocytic infiltrates within the thyroid glandon biopsy; 2) circulating anti-thyroid autoantibodies in nearly all patients (3); and 3) in many patients, presence in the blood of activated CD4 and CD8 T cells specific for thyroid antigens (4, 5). In addition, animal models which closely mimic Hashimoto's disease can be created by immunization with thyroid antigens (6).

In some patients with autoimmune thyroiditis the thyroid gland can be enlarged (150–300% of normal size; a goiter) while in other patients the thyroid remains normal in size (7, 8). A stronger indicator of autoimmune thyroiditis is the presence of autoantibodies. Anti-thyroid peroxidase antibodies are present in 95% of affected individuals, whereas anti-thyroglobulin antibodies are present in only 60% (9). These autoantibodies have been strongly associated with an elevated concentration of thyroid stimulating hormone (TSH) in the serum and measurement of TSH levels is a common diagnostic test (10).

In humans autoimmune thyroiditis has been associated with a variety of MHC haplotypes, including DR3/DR4 (11, 12), DR5 (12) and DQ8 (13). In mice,

the H-2 haplotype appears to dictate susceptibility to experimental autoimmune thyroiditis (EAT). For example, EAT can be induced in H-2k and H-2s animals, but not in H-2f strains (14, 15). Using a variety of transgenic lines, Chella David's group has investigated several different mouse or human MHC class II molecules for their permissiveness for EAT. Addition of susceptible class II molecules, such as H-2Ak or HLA-DR3, to resistant strains converts them to a susceptible phenotype (16). In transgenic studies in the IAb knockout background, David's group has characterized the contribution of human class II alleles, showing that that DR3 (DRB1*0301), but not DR2 (DRB1*0502) or DR4 (DRB1*0401) and DQ8, but not DQ6 (DQA1*0103, DQB1*0601; one variant of DQ6) are permissive for EAT (13, 16, 17).

In this chapter a new mouse model of spontaneous autoimmune thyroiditis is presented. HLA-DQ6 (DQA1*0102, DQB1*0602) transgenic IAb knockout NOD mice (abbreviated NOD.DQ6/Ab^0) consistently show mononuclear cell infiltrates within the thyroid glands. These animals develop autoantibodies to both thyroid peroxidase (TPO) and thyroglobulin (Tg), they show elevated TSH and low T4 hormone levels and a subset of animals (~25%) develop goiter. In addition, the thyroid disease can be adoptively transferred to an immunodeficient syngeneic line (NOD.DQ6Ab^0 Rag1^0).

3.2 Materials and Methods

3.2.1 Mice

NOD-Lt/J mice were purchased from The Jackson Laboratory (JAX; Bar

Harbor, ME) and Balb/c mice were provided in-house by Health Sciences Laboratory Animals Services, (University of Alberta, Edmonton, AB).

The origins of the NOD.DQ8/Ab^0, NOD.DQ8/Ab^0 Rag1^0, and NOD.DQ6/Ab^0 lines have all been described previously ((18) and Chapter 2); all are human HLA transgenic IAb knockout NOD mice.

The Rag1 knockout NOD line (NOD.129S7(B6)-*Rag1*^{tm1Mom}/J) was kindly provided by D. Serreze (The Jackson Laboratory, Bar Harbour, ME). The NOD.DQ6/Ab^0 Rag1^0 line was created by crossing the NOD.DQ6/Ab^0 animals with the Rag1 knockout NOD line, intercrossing the F1 generation and selecting for desired F2 offspring using flow cytometric analysis and PCR (as per Chapter 2). I acknowledge L. Billesberger (University of Alberta, Edmonton, AB) for her assistance in the screening of the offspring.

All breeding colonies were housed in conventional SPF or (in the case of Rag1 knockout) VAF facilities. Care and handling was done in accordance with the guidelines of the Canadian Council on Animal Care, and all experimental protocols were approved by our institutional Health Sciences Animal Policy and Welfare Committee.

3.2.2 Histology/Immunohistochemistry

For H&E staining, thyroids were fixed in 10% buffered formalin (Fisher, Fair Lawn, NJ), embedded in paraffin, sectioned and stained with hematoxylin and eosin using standard methods. For CD4, CD8 and B220 staining, frozen sections were made using O.C.T Tissue Tek compound (Fisher) and slides were

fixed in ice cold acetone, blocked in 2% FCS/PBS and treated with both avidin and biotin solutions (Vector Labs, Burlington, ON). Rat anti-mouse CD4 (H129.19; BD Pharmingen, Mississauga, ON), CD8 (53-6.7; BD Pharmingen) and B220 (RA3-6B2; in house antibody) were used at 1:100 and detected using a biotin conjugated goat anti-rat IgG (H+L; Jackson Immunoresearch, West Grove, PA) at 1:200. Staining was visualized using an ABC kit (Vector Labs) followed by DAB (Sigma, St.Louis, MO) and the slide was counterstained with hematoxylin, dehydrated and mounted.

3.2.3 Indirect Immunofluorescence

Frozen sections of thyroids from NOD.Rag1^0 mice were fixed with ice cold acetone, antigen retrieved with 1% SDS/PBS, blocked with 1% BSA/PBS and stained with mouse serum (1:200). Staining was visualized with rhodamine-conjugated goat anti-mouse IgG (1:200; Jackson ImmunoResearch, West Grove, PA) and observation under a fluorescent microscope.

3.2.4 Radioligand Binding Assay

A detailed protocol can be found in Chapter 4, but, in brief, ^{3}H mouse TPO was generated using an *in vitro* transcription/translation system (*Promega*; TnT®SP6 coupled wheat germ extract system) and then used in a radioligand binding assay. Mouse serum was mixed with ^{3}H TPO (1/25 v/v) and autoantibody which had bound ^{3}H TPO was secondarily captured using Protein

G-sepharose and a Millipore Filter Plate for high throughput separation. Captured ^{3}H TPO was then counted in a β counter.

3.2.5 Mouse Thyroid Lysates

14 week old IAb knockout NOD mice were maintained on 0.1% 3-amino-1,2,4-triazole (ATA; Sigma, St.Louis, MO) in their drinking water for 10 weeks. ATA is an insecticide which inhibits thyroid peroxidase and thereby induces thyroid hypertrophy (19). After 10 weeks, mice were euthanized and their hypertrophied thyroids removed. These larger thyroids were easier to dissect, yielded more tissue and, because of their size, the amount of contaminating non-thyroid tissue carried along with the dissection was minimized.

3.2.6 FRTL-5 Cells

The FRTL-5 rat thyroid cell line (ATCC# CRL-1468) was obtained from the J. Ginsberg Lab (University of Alberta, Edmonton, AB). FRTL-5 cells are an epithelial-like adherent cell line which grows in F12 COON's modification medium (plus sodium carbonate and pH adjusted to 7.35 with HCl) containing insulin (10µg/ml), Gly-His-Lys peptide (10ng/ml), cortisol (10nM), transferrin (5µg/ml), TSH (10mU/ml) and somatostatin (10ng/ml), all purchased from Sigma, St. Louis, MO. 10% heat inactivated fetal calf serum and 1X penicillin/streptomycin (both from Invitrogen, Burlington, ON) were also added. For lysates, cells were released from the flask with CTC solution which is composed of collagenase (20U/ml), trypsin-EDTA (0.076%) and heat-inactivated chicken serum (2%) in

F12 COON's modification medium. Cells were harvested, washed, frozen and thawed through three cycles and homogenized by passing through a 18 gauge needle in the presence of EDTA-free protease inhibitor cocktail (Roche, Mississauga, ON).

3.2.7 SDS-PAGE and Western Blots

Antigens were loaded at 10µg/well into 7.5% polyacrylamide gels and run at 100V. The gel was either stained with coomassie blue or the proteins were directly transferred onto a nitrocellulose membrane at 250mA constant for 1 hour. The membrane was blocked for 1 hour with 5% skim milk-PBS at room temperature, incubated with mouse serum diluted 1:200 in 5% skim milk-PBS overnight at 4°C, washed with PBS + 1% Tween-20 (PBS-T) and finally incubated with goat anti-mouse IgG-HRP diluted 1:2000 in 5% skim milk-PBS for 1 hour at room temperature. After washing with PBS-T, the membrane was developed with ECL (Amersham Biosciences, Piscataway, NJ) and Kodak Biomax MR film.

3.2.8 Non-rodent thyroids

Thyroid glands from cow, pig and sheep were obtained from a slaughter house in the vicinity (Camrose Packers). The glands were dissected away from surrounding neck strap muscles and transported to the lab on dry ice. Upon arrival, tissue was cut (on dry ice) into sections and frozen at -80°C. The tissues were each homogenized with 1ml SDS-PAGE stacking buffer and then passed

through a 18 gauge needle 10 times. The lysates were then centrifuged at 6,000 *x g* for 10 minutes and the supernatants were used. I acknowledge K. Suzuki (University of Alberta, Edmonton, AB) for the preparation of these lysates.

3.2.9 Preparation of mouse thyroglobulin

Mouse thyroids (Pel-Freeze Biologicals, Rogers, AR) were homogenized on ice in extraction buffer (50mM Tris-HCl, 1mM EDTA, protease inhibitor cocktail, Roche, Mississauga, ON). Homogenates were ultracentrifuged for 1h at ~100,000 x *g* at 4°C using thick walled polyallomer tubes in a SW55 swinging bucket rotor (Beckman, Mississauga, ON). The supernatant was removed and loaded onto a 200cm^3 superdex-200 column (Amersham Biosciences, Piscataway, NJ) and run at 8ml/hour in Tris-HCl Buffer (10mM Tris-HCl, pH 7.5, 1mMEDTA, protease inhibitor cocktail (Roche, Mississauga, ON)). Aliquots of each 2ml fraction were screened by SDS-PAGE followed by coomassie staining. Those fractions positive for thyroglobulin alone were pooled and used in autoantibody assays (Western blot and ELISA).

3.2.10 ELISA for thyroglobulin autoantibodies

Falcon 353911 microtitre plates (Becton Dickinson Labware, Franklin Lakes, NJ) were coated overnight at 4°C with 50µl per well of 15µg/ml mouse thyroglobulin in PBS. The plates were washed with PBS-T, blocked for 1h at room temperature with 1% w/v BSA in PBS-T and incubated with mouse sera (various dilutions in PBS-T) overnight at 4°C. The plates were then incubated

with horseradish peroxidase (HRP) conjugated goat anti-mouse IgG (H+L; 1:5,000; Jackson ImmunoResearch, West Grove, PA) and developed by using TMB (Sigma, St.Louis, MO) as a substrate. OD 450nm was measured on a plate reader and expressed as the mean of triplicate wells.

3.2.11 TSH Radioimmunoassay

Sera collected from mice of various ages were shipped on dry ice to Dr. A.F. Parlow of the National Peptide and Hormone Program, Harbor-UCLA Medical Center, Torrance, California. The serum TSH levels were analyzed by a standard radioimmunoassay using Rat TSH as the iodinated antigen and anti-mouse TSH as the antiserum.

3.2.12 TSH ELISA

Serum TSH levels was also analyzed using a Rodent Thyroid Stimulating Hormone (TSH) ELISA Test Kit purchased from Endocrine Technologies, California. In brief, the microtiter wells included with the kit are coated with affinity purified anti-TSH antibody; serum and a constant amount of anti-TSH antibody conjugated with HRP (provided with kit) were added to those pre-coated wells. During incubation, the serum TSH reacts simultaneously with the two antibodies, resulting in the TSH being sandwiched between the solid-phase and enzyme-linked antibodies. Any unbound HRP-labelled TSH antibodies were washed away, TMB solution was added and the reaction stopped using 2N HCl. Absorbance was measured at 450nm. A series of TSH standards included in the

kit were also analyzed, a standard curve constructed and the concentration of TSH in the serum calculated using this curve.

3.2.13 T4 ELISA

Analysis of serum T4 levels was done using a Rodent Thyroxin (T4) ELISA Test Kit purchased from Endocrine Technologies, California. In brief, the microtiter wells included with the kit are coated with anti-T4 antibody; serum and a constant amount of T4 conjugated with HRP (provided with kit) was added to each of the pre-coated wells. During incubation the serum T4 and the HRP-conjugated T4 compete for the limited binding sites on the anti-T4 antibody. Any unbound T4-conjugate was washed away, TMB solution was added and the reaction was stopped using 2N HCl. The absorbance was measured at 450nm. A series of T4 standards were also analyzed, a standard curve constructed and the concentration of T4 in the serum calculated.

3.2.14 Adoptive Transfers

Donor lymphocytes or serum were harvested from >20 week old NOD.DQ6/Ab^0 mice. Splenic lymphocytes were obtained by passing total splenocytes over lympholyte-M gradients (Cedarlane, Hornby, ON); these cells were washed in RPMI 1640, pelleted and finally resuspended in PBS. Adoptive transfers of lymphocytes were accomplished by tail vein injection into 8 week old NOD.DQ6/Ab^0 $Rag1^0$ mice.

Adoptive transfer of serum involved injection I.P. of 150µl serum from >20

week old NOD.DQ6/Ab^0 animals into 8 week old NOD.DQ6/Ab^0 Rag1^0 recipients.

For adoptive transfer of lymphocyte subsets, splenic lymphocytes from >20 week old NOD.DQ6/Ab^0 mice were obtained using lympholyte-M gradients (Cedarlane, Hornby, ON). Lymphocytes from 5-10 animals were pooled and aliquots of cells incubated with fluorescently tagged anti-mCD4, anti-mCD8, or anti-B220 and then positively sorted on a FACS Aria instrument (BD Biosciences, San Jose, CA). Purity of cell populations selected by this method was ≥99% as assessed FACS. Adoptive transfers of lymphocyte subsets were accomplished by tail vein injection into 8 week old NOD.DQ6/Ab^0 Rag1^0 mice.

Adoptive transfer recipients were tail bled bi-weekly for analysis of hormone changes and/or presence of anti-thyroid autoantibodies.

3.3 Results

3.3.1 Thyroid Infiltrates, Fibrosis, and Goiter.

A subset of NOD.DQ6/Ab^0 mice show grossly enlarged thyroid glands and mononuclear cell infiltrates develop within the thyroids of virtually all animals. Approximately 25% of this mouse population develops a grossly enlarged thyroid or goiter (Figure 3-1, panel B versus panel A; Figure 3-1-I). Histological examination of these goiters reveals the presence of mononuclear cell infiltrate, the complete absence of thyroid follicle architecture and massive fibrosis (Figure 3-1, panels G and H versus panels C and D). Examination of thyroids from these NOD.DQ6/Ab^0 mice reveals that, even though they do not all develop goiter, all show thyroid infiltrate and the severity increases with age (Figure 3-1-I).

Destruction of the thyroid follicles usually begins on the periphery of the thyroid and progresses inwards towards the tracheal side of the thyroid (Figure 3-1, panels E and F).

3.3.2 CD8 T cells Predominate in Goiter Infiltrates

Immunohistochemical staining of the thyroid infiltrate in non-goiter NOD.DQ6/Ab^0 animals reveals the presence of primarily B cells (Figure 3-2-D) and CD4 T cells (Figure 3-2-C) with lesser numbers of CD8 T cells (Figure 3-2-B). Examination of the goiters from NOD.DQ6/Ab^0 mice shows that although CD4 T cells and B cells are present (Figure 3-2, panels H and I, respectively), CD8 T cells predominate in the infiltrate (Figure 3-2-G). These CD8+ cells were confirmed to be CD8 T cells, and not NK or NKT cells, as they did not co-stain for DX5 (Figure 3-2, E and J).

3.3.3 Anti-Thyroid Autoantibodies Arise Spontaneously.

The histological picture of thyroiditis seen in the NOD.DQ6/Ab^0 mice, in addition to the autoimmune history of NOD and NOD.DQ8/Ab^0 animals, suggested that the disease process might be autoimmune in origin. Therefore, we investigated these animals for anti-thyroid autoantibodies. Frozen sections of normal mouse thyroid were tested by indirect immunofluorescence using serum from >20 week old NOD.DQ6/Ab^0 mice. Staining of thyroid follicle membranes was seen (Figure 3-3-A) and was not seen when control serum was used (Figure 3-3, B and C) or when secondary antibody alone was used (Figure 3-3-D).

Classically such staining is assumed to be anti-TPO staining, but we performed a further autoantibody assay to confirm this assumption. NOD.DQ6/Ab^0 sera, but not control sera, were able to bind and capture ^{3}H TPO (Figure 3-4). NOD.DQ6/Ab^0 mice do not all develop the same titres of anti-TPO autoantibodies, but they consistently develop titres greater than other strains of mice (Figure 3-4).

The production of a frozen section generally causes the destruction of the colloid (center) of the thyroid and as such this process prevents the examination of autoantigens located within the colloid. Therefore, we addressed other autoantigens via Western blot and ELISA (Figures 3-5 and 3-6). Mouse thyroids were collected from NOD.Ab^0 mice that had been maintained for 10 weeks with 0.1% 3-amino-1,2,4-triazole (ATA) in their water to chemically induce enlarged thyroids (Supplementary Figure AI.6.A). Rat thyroids were dissected from retired Sprague-Dawley female breeders (a gift from the Davidge Lab, University of Alberta, Edmonton, AB). Thyroids were snap frozen and homogenized in the presence of protease inhibitors. The rat FRTL-5 thyroid cell line (ATCC# CRL-1468) was utilized as a "pure" source of thyroid antigens, e.g. void of muscle tissue (Supplementary Figure AI.6.B). 10µg of protein was loaded per sample and run on SDS-PAGE and then transferred to nitrocellulose. Staining of the nitrocellulose membranes with mouse serum reveals the presence of anti-thyroid autoantibodies in NOD.DQ6/Ab^0 serum, but not in control mouse serum (Figure 3-5). The anti-thyroid autoantibodies of NOD.DQ6/Ab^0 serum appear to be specific to rodent antigens as analysis using bovine, sheep, or pig thyroid lysates

was negative (Supplementary Figure AI-7). Mouse thyroglobulin makes up >75% of the thyroid and thus, was easily prepared from mouse thyroids. 10μg of purified thyroglobulin or commercial bovine serum albumin (BSA) was run on SDS-PAGE (Figure 3-6-A) and transferred to nitrocellulose and probed with NOD.DQ6/Ab^0 serum. Blotting revealed the presence of anti-thyroglobulin, but not anti-BSA autoantibodies (Figure 3-6-B).

The anti-Tg autoantibodies from NOD.DQ6/Ab^0 animals were investigated further. We used our semi-purified mouse Tg to establish a solid-phase ELISA to measure anti-Tg IgG autoantibody titres in sera from NOD.DQ6/Ab^0 of various ages. These autoantibodies increased with age (Figure 3-7-B) and titres of 1/10,000 were seen as compared to 1/00 in Balb/c mice (Figure 3-7-A).

3.3.4 Thyroid Hormone and TSH Levels are Altered

Thyroid function is tightly regulated by release of thyroid stimulating hormone (TSH) from the pituitary gland. Thyroid stimulation by TSH induces the production and release of the thyroid hormones T3 and T4. T3 and T4 then proceed to have metabolic effects in various areas of the body. Destruction of the thyroid by autoimmune thyroiditis results in the reduced capacity for the production of the thyroid hormones T3 and T4. Feedback loops signal to the pituitary this lack of production and consequently the pituitary releases more TSH. The thyroid is still incapable of producing sufficient levels of T4 and thus more TSH is released. The hypothyroidism resulting from autoimmune thyroiditis is characterized by elevated TSH and reduced T4 levels. NOD.DQ6/Ab^0 mice

have this characteristic profile. TSH serum levels were found to be higher than controls using both radioimmunoassay and ELISA methods (Figure 3-8, panels A and B, respectively) and T4 levels were found to be lower than controls (ELISA; Figure 3-9).

3.3.5 Thyroiditis Can Be Adoptively Transferred

To confirm that the immune system plays a causative role in the hypothyroidism which occurs in these mice adoptive transfer experiments were performed, transferring splenic lymphocytes from >20wk old NOD.DQ6/Ab^0 mice into 6wk old NOD.DQ6/Ab^0 Rag1^0 mice. The mice were bled bi-weekly and assessed for appearance of anti-thyroid autoantibodies and altered hormone levels. Analysis of sera (1:200) from these mice (n=16) by Western blot revealed that, by 4 weeks post transfer, 69% of the mice show anti-thyroid autoantibodies at a dilution of 1:200 and that by 8 weeks post transfer all animals have developed these autoantibodies (Figure 3-10). Sera from the recipients were also examined by ELISA for anti-Tg autoantibodies and titres were shown to increase with weeks post transfer (Figure 3-11-A). This increase in titres was not an artifact of the adoptive transfer as sera from NOD.DQ8/Ab^0 Rag1^0 recipients of NOD.DQ8/Ab^0 splenocytes did not show significantly elevated titres (i.e. titres were equivalent to NOD.DQ8/Ab^0 background levels; 3-11-B).

ELISA analysis of the sera from the recipients also revealed that their TSH levels increased post transfer (Figure 3-12-A) and that their T4 levels significantly declined (Figure 3-13-A). These changes in hormone levels are not an artifact of

adoptive transfer as again identical experiments were performed with NOD.DQ8/Ab^0 splenocytes into NOD.DQ8/Ab^0 Rag1^0 recipients and their TSH and T4 levels remained unchanged (Figures 3-12-B and 3-13-B, respectively).

At 14 weeks post transfer all animals were euthanized and their thyroids were examined microscopically. NOD.DQ6/Ab^0 Rag1^0 recipients did not develop goiter, but 83% showed thyroid infiltrate comparable to that seen in initial stages of thyroid destruction in NOD.DQ6/Ab^0 mice (Table 3-1; Figure 3-15).

The adoptive transfer of autoimmune thyroiditis from NOD.DQ6/Ab^0 mice to NOD.DQ6/Ab^0 Rag1^0 recipients was confirmed to be cell-mediated in that serum alone was not able to transfer the autoimmune thyroiditis or hypothyroidism (Figure 3-14); although the disease incidence from transfer was slightly more severe when splenocytes and serum were transferred as opposed to splenocytes alone (Figure 3-14).

Preliminary adoptive transfer experiments using lymphocyte subsets suggests that CD4 T cells alone may be able to adoptively transfer the thyroiditis (Table 3-1; Figure 3-15B); however, in addition, 2 out of 8 mice that received CD8 T cells alone showed minor infiltrate (Table 3-1). TSH levels in all subset adoptive transfers remained stable.

3.4 Discussion

Many animal models of experimental autoimmune thyroiditis (EAT) are known (20). EAT may be induced by injection of homologous or autologous thyroid antigen in virtually all animal species including rabbit (21), guinea pig (22),

mouse (23), rat (24), dog (25), monkey (26) and chicken (27). The most abundant antigen in crude thyroid extracts is Tg (>75% of the protein mass) (28) and many EAT models make use of purified Tg. EAT has also been induced using peptides of Tg, again from a variety of species (29, 30), heat-inactivated Tg (31, 32) and Tg pulsed dendritic cells (33). Finally another less abundant, membrane-bound thyroid antigen, TPO, has also been used to induce EAT (34, 35) and more recently intramuscular DNA injections of a TPO expression plasmid have also been used successfully (36).

EAT models vary in both their symptoms and pathogenesis. Most show some permanent lymphocytic infiltrate, but in some the infiltrate is only transient (37). Most models develop autoantibodies to Tg, but anti-TPO autoantibodies have not been detected except in cases where animals were immunized with TPO (34, 35) or in the experimentally-induced rhesus monkey model of EAT (26). Models that show mononuclear cell infiltrates and autoantibodies do not necessarily show decreased thyroid hormone levels (i.e. T4; (38)) and TSH levels have typically not been measured in EAT. As well as depending on the genetic background of the host, variability in severity of thyroiditis in mouse EAT may reflect the use of different inducing antigens. In nearly all mouse models of EAT the thyroid disease is very mild and can only be diagnosed by histopathology; obvious enlargement of the thyroid gland (goiter) has not been reported. Although these EAT models have, and will continue to provide valuable information about autoimmune thyroiditis, our NOD.DQ6/Ab^0 animals appear to be more similar to the human disease (Table 3-2).

Our NOD.DQ6/Ab^0 line was not the first spontaneous autoimmune thyroiditis model. The first spontaneous model discovered was the obese chicken (39). This inbred strain develops a disease that is very close to Hashimoto's thyroiditis in humans—in all of its clinical, histopathological, serological and endocrinological aspects (40, 41). More recently NOD-H2h4 mice (I-Ak congenic on the NOD background) were found to develop spontaneous autoimmune thyroiditis (SAT) and anti-mouse Tg autoantibodies were observed in nearly all animals 6-8 weeks after administration of 0.05% NaI in their drinking water. After reaching maximum severity, inflammation in these mice remains chronic over the next 3-4 months. Since iodine is a key component of thyroid metabolism, this emphasizes the importance of environmental factors in affecting the disease process; a phenomenon which is well known in humans (38, 42). It would be of interest to determine if the severity of NOD.DQ6/Ab^0 autoimmune thyroiditis and hypothyroidism could be increased if the animals were given iodine in their water.

In 2004, Quaratino and colleagues described a second mouse model of spontaneous autoimmune thyroiditis. In this model the animals are transgenic for a human T cell receptor derived from a thyroid-infiltrating T cell, originally cloned from a patient suffering from autoimmune thyroiditis (43). The T cell was found to be specific for two TPO epitopes: an agonistic highly stimulatory epitope ($TPO_{536-547}$) which is preferentially displayed after endogenous processing during inflammation (43, 44) and an antagonistic epitope ($TPO_{537-548}$) which is preferentially displayed when whole TPO is presented (43, 45). The TCR

transgenic mouse line (called "TAZ10") displayed most of the key features of human Hashimoto's thyroiditis (clinical, histological and endocrinological); however, the animals did not develop autoantibodies—a reflection of the fact that the transgene was expressed in the Rag1 knockout background (43). Further studies on this TCR transgenic, but in an immune competent background, have now been carried out (46). For these latter animals the spontaneous anti-thyroid autoimmunity was delayed (occurring at 20 weeks of age rather than 12), but the affected mice still showed clinical and histological characteristics of autoimmune thyroiditis (46). The authors speculate that the development of autoimmunity in the immunocompetent background may be related to a dramatic reduction in the number of circulating regulatory T cells.

The TPO-specific TAZ10 TCR is restricted to DQ6 (DQA1*0102, DQB1*0602) (44); the same MHC molecule that is expressed in our NOD.DQ6/Ab^0 animals which develop spontaneous autoimmune thyroiditis. However, although DQA1*0102, DQB1*0602 has been linked to a number of autoimmune diseases (notably multiple sclerosis (47, 48) and narcolepsy (49, 50)), it has not, to our knowledge, been linked to autoimmune thyroiditis (although the thyroiditis patient from whom the TAZ10 T cell clone originated was of this DQ6 haplotype) (51, 52). It would be of great interest to see if NOD.DQ6/Ab^0 animals show a response to the TPO epitopes (both mouse and human) seen by the transgenic TAZ10 TCR. Worth noting as well is that the TAZ10 TCR is also able to see the TPO epitope in the mouse class II MHC, H-

2Ak and this mouse MHC class II is linked to protection from diabetes and susceptibility to thyroiditis, very reminiscent to what we have seen with the HLA-DQ6 (DQA1*0102, DQB1*0602). Perhaps NOD IAg7 is the mouse equivalent of the HLA-DQ8 (DQA1*0301, DQB1*0302)—both linked to diabetes susceptibility and H-2Ak is the mouse equivalent of HLA-DQ6—both linked to diabetes resistance and thyroiditis susceptibility.

Although 70% of hypothyroidism cases arise from Hashimoto's thyroiditis (1), only about 10% of Hashimoto's patients actually develop hypothyroidism and as such it has not been surprising that EAT models do not develop elevated TSH or lowered T4 serum levels. It is interesting that the spontaneous models, with high incidence rates without environmental manipulation (e.g. addition of iodine), such as the obese chicken, the TAZ10 TCR transgenic mice and our NOD.DQ6/Ab^0 animals, are the only models to progress to hypothyroidism. In fact, some of the TSH levels seen in our NOD.DQ6/Ab^0 are believed to be some of the highest recorded (8375 ng/ml and 16,900ng/ml; personal communication with A.F. Parlow, National Hormone and Peptide Program, California). Initially the fact that the adoptive transfer recipients did not show a more dramatic change in their thyroid hormones was disappointing, but this was probably to be expected. Not only must the disease be severe enough to cause hypothyroidism (likely longer than 14 weeks post transfer), but the thyroid can store enough thyroglobulin for making thyroid hormones to last for two months or more (53).

It appears that, similar to the autoimmune myocarditis of NOD.DQ8/Ab^0 animals (Chapter 3), CD4 T cells alone can adoptively transfer the anti-thyroid

autoimmunity in NOD.DQ6/Ab^0 animals; although, at least by 14 weeks post transfer, the CD4 T cell transfer of autoimmune thyroiditis is not as robust as the myocarditis model. However, the only difference between the mice is the MHC class II molecule which suggests that CD4, like in NOD.DQ8/Ab^0 animals, would be very important. Perhaps the difference in the adoptive transfer results between the two DQ transgenic lines is a reflection of the size of the target organ and the severity of the disease in the immunocompetent strains. The incidence and potency of the DQ8 autoimmune myocarditis is different to that of the DQ6 autoimmune thyroiditis. Perhaps the CD4 T cells in DQ6 autoimmune thyroiditis require a stronger co-operation with CD8 cells (and/or B cells) than those of DQ8 autoimmune myocarditis and the predominate presence of CD8 cells in DQ6 goiters and the fact that minor infiltrate was seen in some recipients when CD8 cells alone were transferred supports this hypothesis. It is also possible that the CD8 T cells predominating within the goiter infiltrate are in fact regulatory cells. There is a granulomatous form of experimental autoimmune thyroiditis which is characterized by follicular cell proliferation, large numbers of histocytes and multinucleated giant cells and variable numbers of neutrophils are observed in addition CD4 T cells. Although CD4 T cells are thought to be the primary effector cells in granulomatous thyroiditis (54, 55), CD8 T cells vastly out number the CD4 T cells (56) and it has been shown that deletion of CD8 T cells in recipient mice delays the resolution of the granulomatous lesions (57). Future studies involving multi-subset adoptive transfers, longer term transfers and adoptive transfers using lymphocytes isolated from NOD.DQ6/Ab^0 thyroids, along

with cytokine profiling, should address these issues.

And so, in conclusion, NOD.DQ6/Ab^0 mice are a new spontaneous mouse model for Hashimoto's thyroiditis that not only develops all aspects of autoimmune thyroiditis (infiltrate, goiter, anti-thyroglobulin and anti-thyroid peroxidase autoantibodies), but also develops hypothyroidism (elevated TSH and lowered T4). NOD.DQ6/Ab^0 animals will be invaluable for understanding immune pathogenesis in Hashimoto's thyroiditis and for designing and testing new therapies.

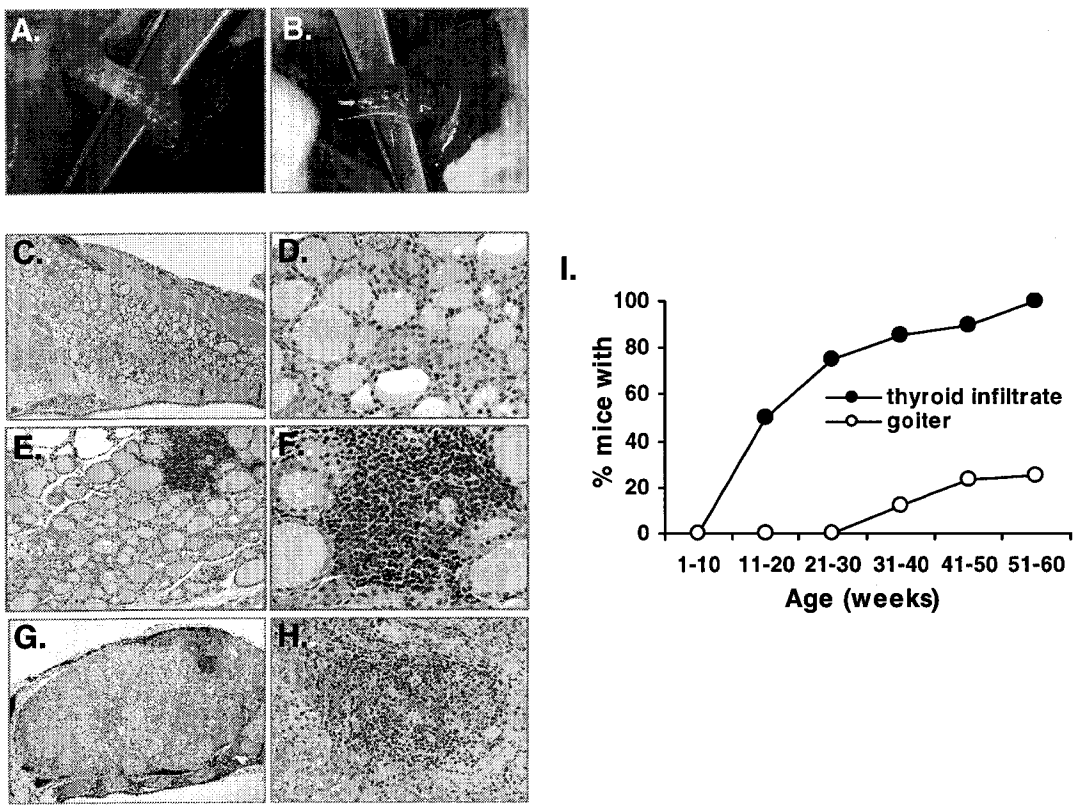

Figure 3-1: NOD.DQ6/Ab^0 mice show mononuclear cell infiltration of the thyroid and a subset of animals develop goiter. Gross pathology of upper trachea and attached structures from two different NOD.DQ6/Ab^0 animals, showing that thyroid glands range in size from normal (A; thyroid is too small to be clearly seen) to grossly enlarged (B; also known as goitre). Histology of thyroid tissue from a healthy Balb/c mouse (C) compared to tissue from NOD.DQ6/Ab^0 mice at various stages of thyroid infiltration, from early (D), to intermediate (E and F), to late (G and H), the latter sample being taken from an animal with obvious goitre. Sections were stained with H&E and photographed at magnifications of 100x (C and G) and 200x (E) and 400x (D, F, and H). (I) Incidence of thyroid infiltrate and goiter at different ages of NOD.DQ6/Ab^0 mice (n=54). Goiter is defined as a clearly visible thyroid that it is firm and light grey/yellow in color.

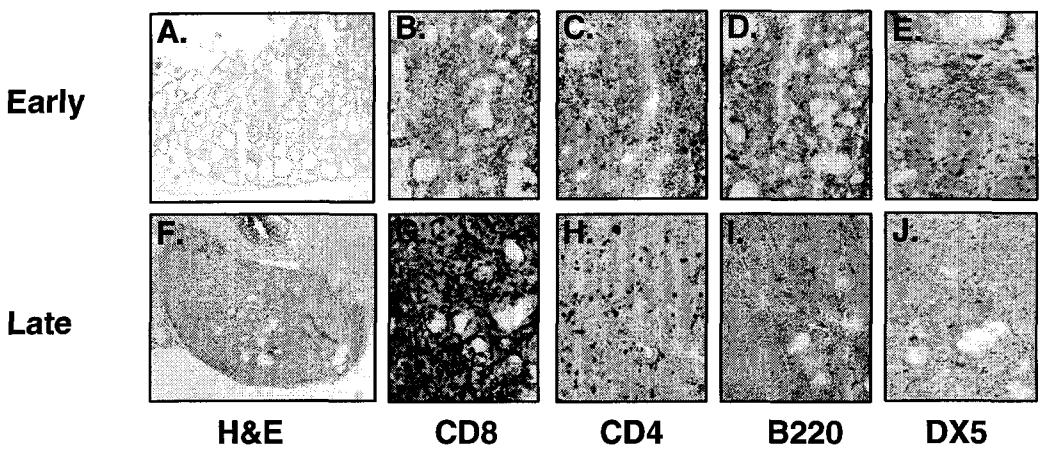

Figure 3-2: A variety of immune cells can be detected within the thyroids of NOD.DQ6/Ab^0 mice, but CD8 T cells predominate in end stage goiters. Frozen sections of thyroids from NOD.DQ6/Ab^0 mice were either H&E stained (A/F; 100X) or incubated with antibodies against CD8 (B/G; 200X), CD4 (C/H; 200X), B220 (D/I; 200X), or DX5 (E/J; 200X). Antibody binding was detected using an ABC kit (Vector) and DAB substrate (Sigma). Slides were counterstained with hematoxylin.

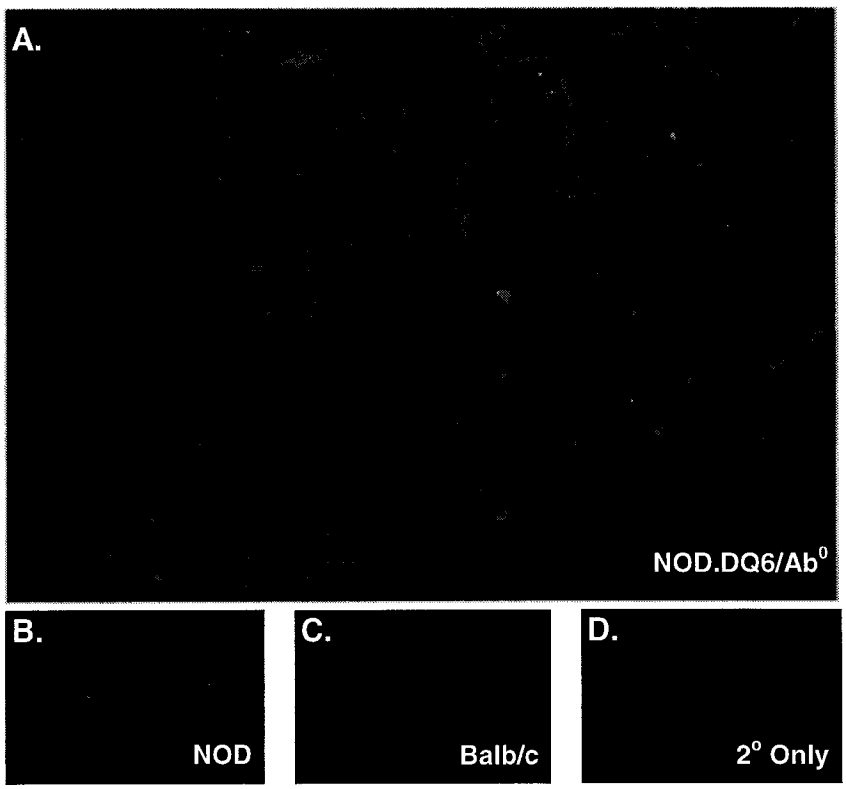

Figure 3-3: Anti-thyroid membrane autoantibodies can be detected in NOD.DQ6/Ab^0 serum by indirect immunofluorescence. Frozen sections of thyroids from NOD.RAG1^0 mice were incubated with sera from various strains of mice: (A) NOD.DQ6/Ab^0, (B) NOD, (C) Balb/c, and (D) secondary antibody alone. Bound antibodies were detected using a rhodamine-conjugated goat anti-mouse IgG secondary antibody. Photographs were taking at a magnification of 200X.

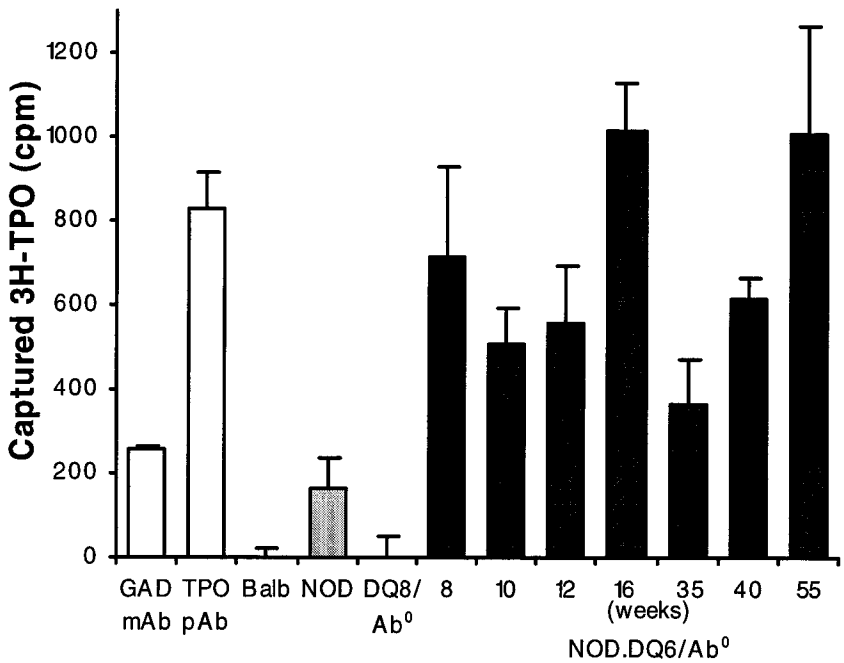

Figure 3-4: NOD.DQ6/Ab^0 mice develop anti-thyroid peroxidase autoantibodies. Serum from NOD.DQ6/Ab^0 mice, but not from control strains, was able to bind thyroid peroxidase in a radioligand binding assay. All samples were run in triplicate and results of one representative experiment are shown. All serum was used at a serum to antigen v/v ratio of 1/25. The GAD monoclonal antibody was used at 5µg/20,000cpm of protein and the TPO polyclonal was used at 0.1µg/20,000cpm of protein.

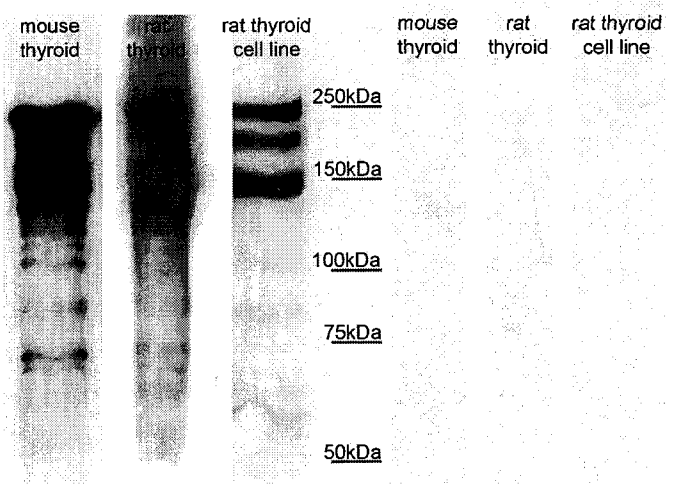

Figure 3-5: NOD.DQ6/Ab^0 mice develop anti-thyroid autoantibodies as measured by Western blot. 10µg of crude mouse thyroid lysate, crude rat thyroid lysate, and rat thyroid cell line (FRTL-5) lysate were loaded onto 7.5 % polyacrylamide gels. Proteins were transferred to nitrocellulose and probed with either NOD.DQ6/Ab^0 serum or Balb/c serum (1:200 in 5% skim milk/PBS). A representative blot is shown, with a very similar result obtained in a total of 10 experiments.

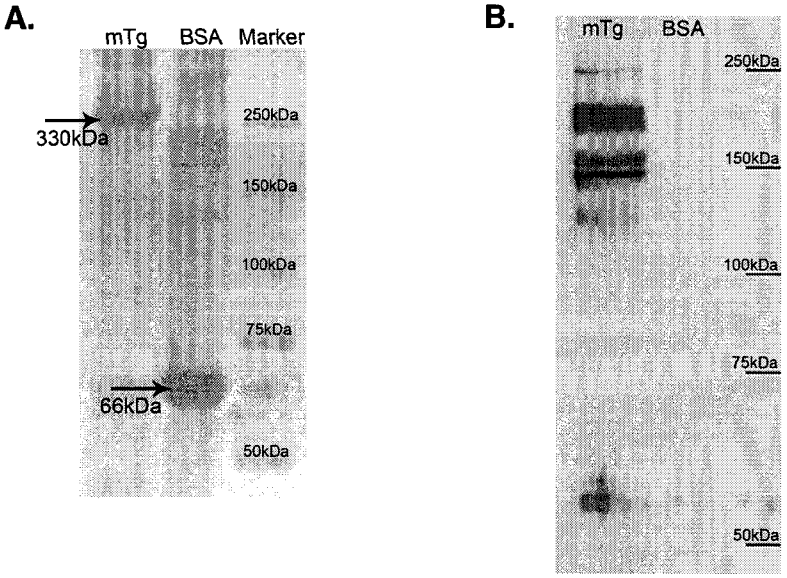

Figure 3-6: NOD.DQ6/Ab^0 mice develop anti-thyroglobulin autoantibodies. 10µg of crude mouse thyroglobulin (mTg) or bovine serum albumin (BSA; Sigma) was loaded in each well of 7.5% SDS-PAGE gels. (A) Gel was stained with Coomassie R250. This is a representative gel (n=3). (B) Proteins were transferred to nitrocellulose and probed with NOD.DQ6/Ab^0 serum (1:200 in 5% skim milk/PBS) and visualized using a HRP-conjugated goat anti-mouse IgG, ECL, and autoradiography. This is a representative blot (n=5). The marker was Precision Plus Protein Standards (Biorad).

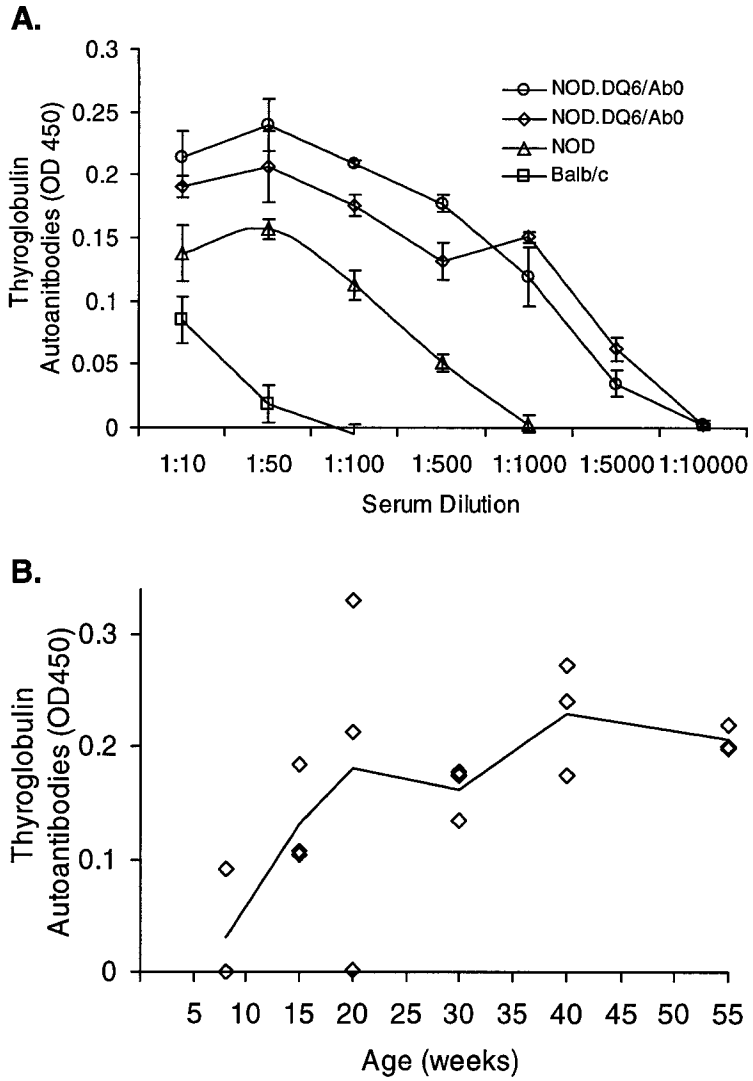

Figure 3-7: Serum titres of anti-thyroglobulin autoantibodies increase with age in NOD.DQ6/Ab^0 mice. (A) Various dilutions of Balb/c, NOD, and NOD.DQ6/Ab^0 serum were tested using a mouse thyroglobulin ELISA. Balb/c animals show a titre of 1:100, NOD a titre of 1:1000, and NOD.DQ6/Ab^0 mice a titre of 1:10,000. Data for a representative experiment are shown, with error bars representing standard deviation of triplicate analysis. (B) Serum collected from NOD.DQ6/Ab^0 animals of various ages were tested for anti-thyroglobulin autoantibodies using an ELISA. Each diamond represents data for one animal.

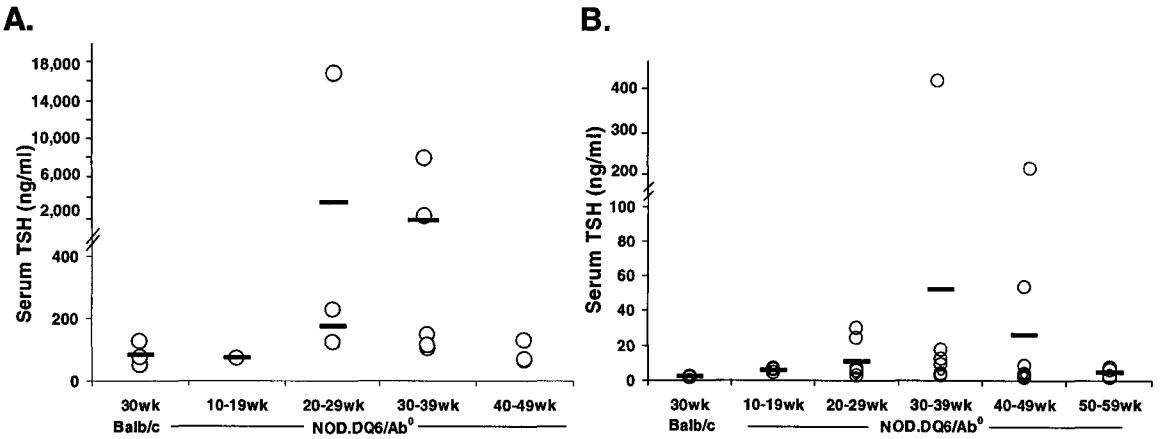

Figure 3-8: A subset of NOD.DQ6/Ab^0 mice show elevated serum thyroid stimulating hormone (TSH) levels. (A) TSH levels assayed by Dr. A.F. Parlow (National Hormone and Peptide Program, California) using a radioimmunoassay for TSH. (B) Serum TSH assayed using a rodent TSH ELISA kit (Endocrine Technologies, Californina). Each symbol represents an individual mouse.

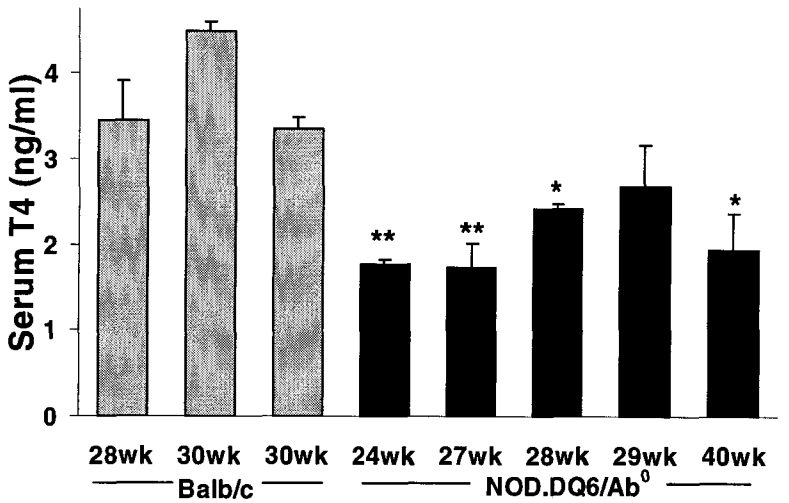

Figure 3-9: NOD.DQ6/Ab^0 mice show reduced T4 hormone levels. Serum T4 was assayed in various Balb/c and NOD.DQ6/Ab^0 mice using a rodent T4 ELISA kit (Endocrine Technologies, California). *p<0.05 **p<0.01

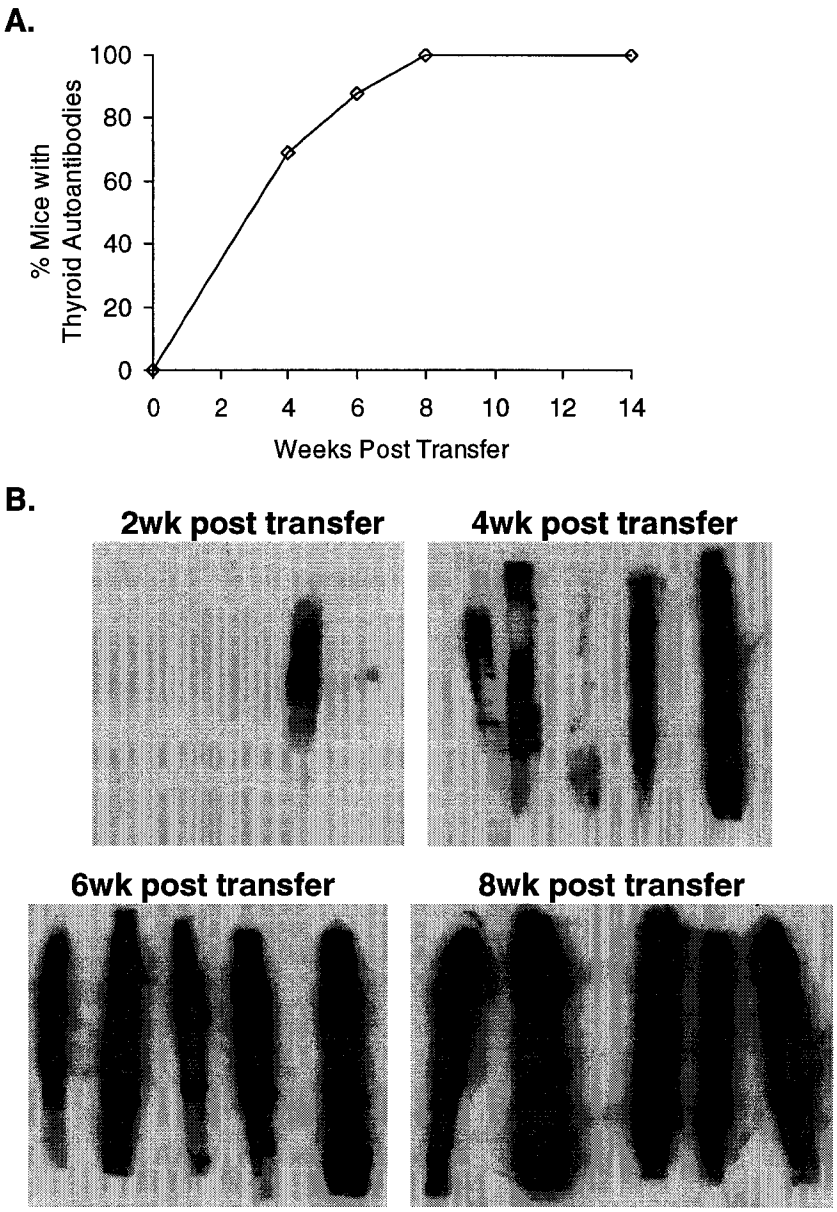

Figure 3-10: The autoimmune thyroiditis of NOD.DQ6/Ab^0 mice can be adoptively transferred to syngeneic Rag1^0 recipients. 1 x 10^6 splenic lymphocytes from >20week old NOD.DQ6/Ab^0 mice were adoptively transferred to 6 week old NOD.DQ6/Ab^0 Rag1^0 recipients. Mice were bled bi-weekly for anti-thyroid autoantibody analysis. (A) Incidence data based on the experiment represented in (B). By 8 weeks post transfer 100% of mice were positive for anti-thyroid autoantibodies (n=16). (B) Rat thyroid lysates were run on 7.5% SDS polyacrylamide gels and probed with recipient serum (1:200 dilution) collected at 2, 4, 6, and 8 wks post transfer. Representative blots for five recipients at each time point are shown.

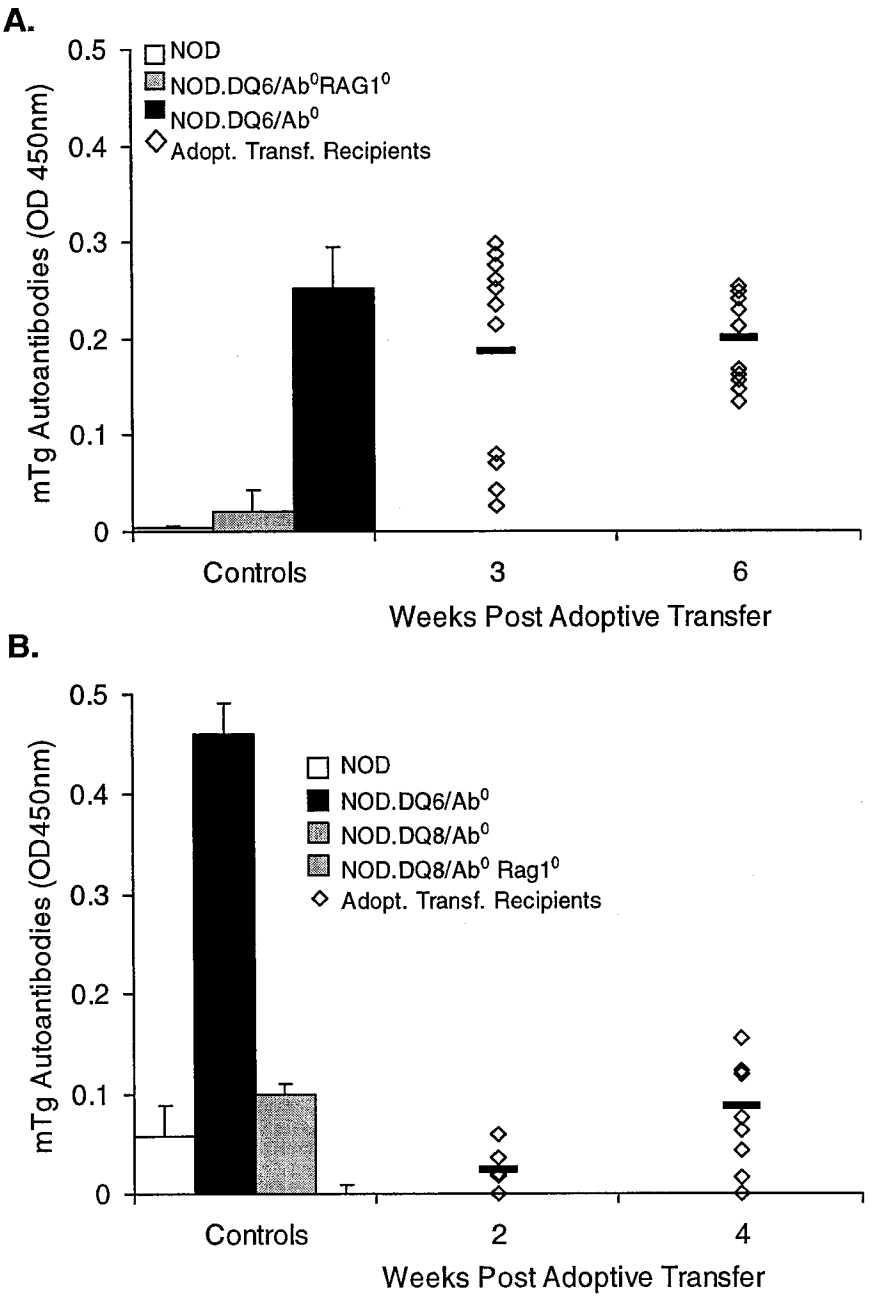

Figure 3-11: Adoptive transfer of NOD.DQ6/Ab^0 lymphocytes into NOD.DQ6/Ab^0 Rag1^0 recipients induces anti-thyroglobulin autoantibodies. (A) NOD.DQ6/Ab^0 splenocytes were adoptively transferred into NOD.DQ6/Ab^0 Rag1^0 mice. (B) NOD.DQ8/Ab^0 splenocytes were adoptively transferred to NOD.DQ8/Ab^0 Rag1^0 recipients. Serum from tail bleeds of adoptive transfer recipients was analyzed using a mouse thyroglobulin ELISA.

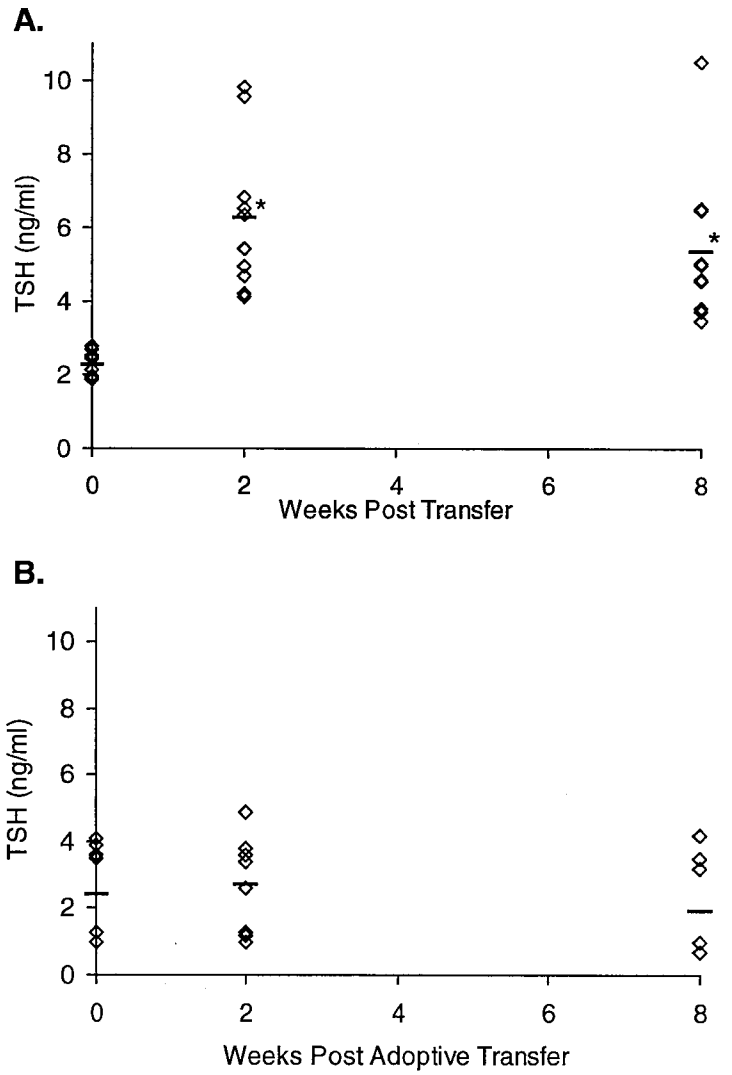

Figure 3-12: NOD.DQ6/Ab^0 Rag1^0 recipients of NOD.DQ6/Ab^0 splenocytes develop elevated TSH levels. (A) NOD.DQ6/Ab^0 splenocytes were adoptively transferred into NOD.DQ6/Ab^0 Rag1^0 mice. (B) NOD.DQ8/Ab^0 splenocytes were adoptively transferred to NOD.DQ8/Ab^0 Rag1^0 recipients. Serum from tail bleeds of adoptive transfer recipients was analyzed using a rodent TSH ELISA (Endocrine Technologies, California). *$p<0.001$

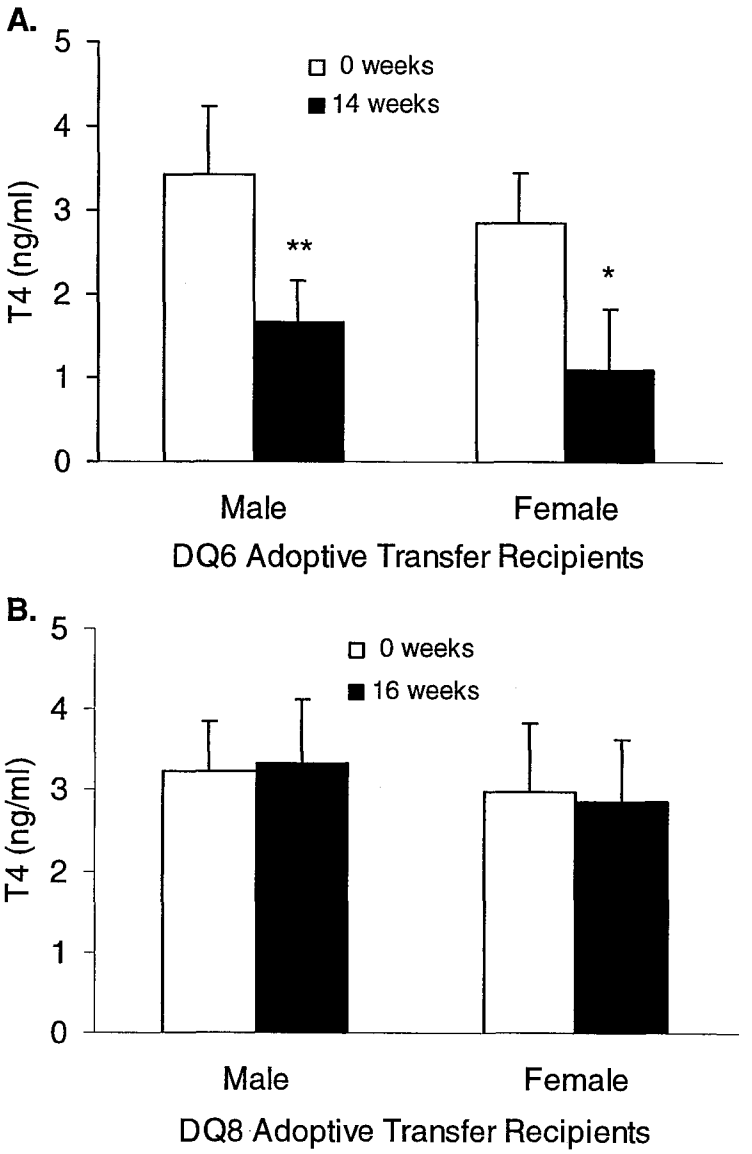

Figure 3-13: NOD.DQ6/Ab^0 Rag1^0 recipients of NOD.DQ6/Ab^0 splenocytes develop reduced T4 hormone levels. (A) NOD.DQ6/Ab^0 splenocytes were adoptively transferred into NOD.DQ6/Ab^0 Rag1^0 mice. (B) NOD.DQ8/Ab^0 splenocytes were adoptively transferred to NOD.DQ8/Ab^0 Rag1^0 recipients. Serum from tail bleeds of adoptive transfer recipients was analyzed using a rodent T4 ELISA (Endocrine Technologies, California). *p=0.01 **p=0.001

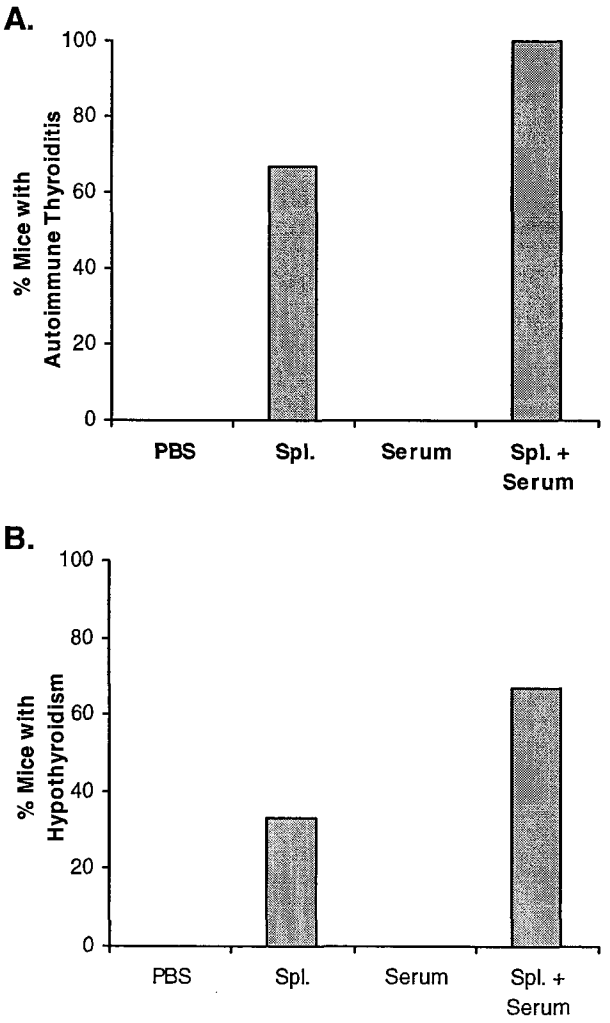

Figure 3-14: NOD.DQ6/Ab^0 splenocytes, but not serum, can adoptively transfer autoimmune thyroiditis and hypothyroidism to NOD.DQ6/Ab^0 Rag1^0 mice. (A) Incidence of autoimmune thyroiditis (infiltrate) or (B) Incidence of hypothyroidism (elevated TSH and low T4) in NOD.DQ6/Ab^0 recipients of 1 x 10^6 splenic lymphocytes (I.V.), 150µl serum (I.P.), or both from NOD.DQ6/Ab^0 animals. n=3/cohort.

	n=	No Infiltrate	Minor Infiltrate	Moderate Infiltrate	Elevated TSH
Splenocytes	**12**	4/12	5/12	3/12	10/12
CD4	**8**	2/8	4/8	2/8	0/8
CD8	**8**	6/8	2/8	0/8	0/8
B220	**8**	8/8	0/8	0/8	0/8

Table 3-1: NOD.DQ6/Ab^0 Rag1^0 recipients of total lymphocytes or CD4 T lymphocytes from NOD.DQ6/Ab^0 mice develop autoimmune thyroiditis. Scoring of thyroid infiltrate and evaluation of TSH changes of NOD.DQ6/Ab^0 Rag1^0 recipients 14 weeks after receiving 1 x 10^6 splenic lymphocytes (total or CD4, CD8, or B220 FACS sorted) from >20 week old NOD.DQ6/Ab^0 mice.

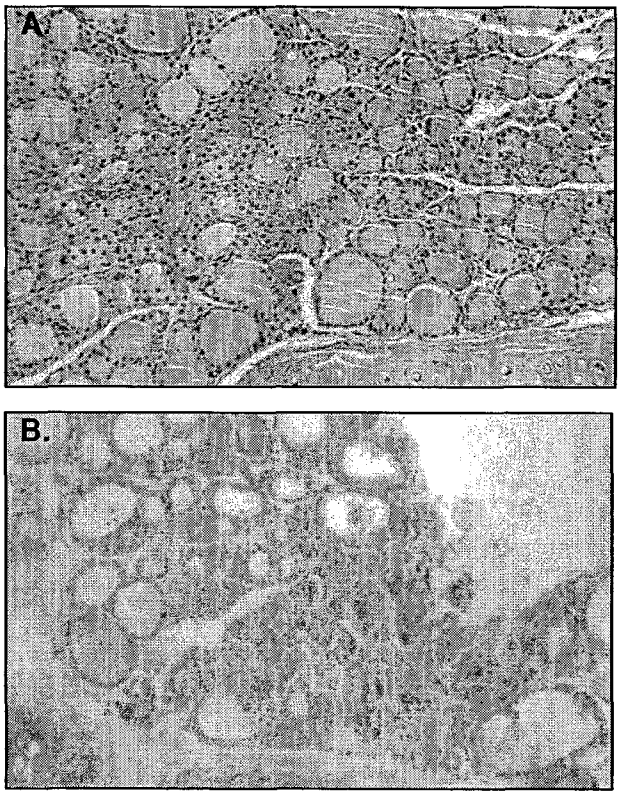

Figure 3-15: NOD.DQ6/Ab^0 Rag1^0 recipients of total lymphocytes or CD4 T lymphocytes from NOD.DQ6/Ab^0 mice develop thyroid infiltrate. (A) H&E stained thyroid section from a NOD.DQ6/Ab^0 Rag1^0 recipient 14 weeks after receiving 1 x 10^6 splenic lymphocytes from >20 week old NOD.DQ6/Ab^0 mice. (B) H&E stained thyroid section from a NOD.DQ6/Ab^0 Rag1^0 recipient 14 weeks after receiving 1 x 10^6 CD4 FACs sorted splenic lymphocytes from >20 week old NOD.DQ6/Ab^0 mice. Magnification: 200X.

	EAT in mice (Tg or thyroid lysate)	NOD.DQ6/Ab^0 Mice	Humans
Autoimmune Thyroiditis			
Thyroid Infiltrate	Most	Yes	Yes
Goiter	No	Some	Some
Anti-Tg autoAbs	Yes	Yes	Most
Anti-TPO autoAbs	No	Yes	Most
Iodine Responsive	Yes	n/a	Yes
Hypothyroidism			
Elevated TSH	No	Some	Some
Low T4	No	Some	Some

Table 3-2: Comparison of the thyroid autoimmunity in mouse EAT, NOD.DQ6/Ab^0 mice and humans. Phenotypic data is based on the literature and the data presented in this chapter (Mouse EAT (1, 20, 23); Humans (1-3, 8-10)). n/a = data not collected

3.5 References

1. Mariotti, S., and G. Pinna. 2003. Autoimmune Thyroid Diseases. In *Diseases of the Thyroid.* L. E. Braverman, ed. Humana Press Inc., Totowa.

2. Rosenthal, M. S. 1998. *The Thyroid Source Book.* Lowell House, Los Angelas.

3. Amino, N., S. R. Hagen, N. Yamada, and S. Refetoff. 1976. Measurement of circulating thyroid microsomal antibodies by the tanned red cell haemagglutination technique: its usefulness in the diagnosis of autoimmune thyroid diseases. *Clin Endocrinol (Oxf) 5:115.*

4. Watanabe, M., N. Yamamoto, H. Maruoka, H. Tamai, F. Matsuzuka, A. Miyauchi, and Y. Iwatani. 2002. Independent involvement of CD8+ CD25+ cells and thyroid autoantibodies in disease severity of Hashimoto's disease. *Thyroid 12:801.*

5. Ohashi, H., T. Okugawa, and M. Itoh. 1991. Circulating activated T cell subsets in autoimmune thyroid diseases: differences between untreated and treated patients. *Acta Endocrinol (Copenh) 125:502.*

6. Stafford, E. A., and N. R. Rose. 2000. Newer insights into the pathogenesis of experimental autoimmune thyroiditis. *Int Rev Immunol 19:501.*

7. Weiss, R. E., and S. Refetoff. 2000. Resistance to thyroid hormone. *Rev Endocr Metab Disord 1:97.*

8. Katz, S. M., and A. L. Vickery, Jr. 1974. The fibrous variant of Hashimoto's thyroiditis. *Hum Pathol 5:161.*

9. Huang, S. A., H. M. Tu, J. W. Harney, M. Venihaki, A. J. Butte, H. P. Kozakewich, S. J. Fishman, and P. R. Larsen. 2000. Severe hypothyroidism caused by type 3 iodothyronine deiodinase in infantile hemangiomas. *N Engl J Med 343:185.*

10. Hollowell, J. G., N. W. Staehling, W. D. Flanders, W. H. Hannon, E. W. Gunter, C. A. Spencer, and L. E. Braverman. 2002. Serum TSH, T(4), and

thyroid antibodies in the United States population (1988 to 1994): National Health and Nutrition Examination Survey (NHANES III). *J Clin Endocrinol Metab 87:489.*

11. Jenkins, D., M. A. Penny, J. A. Fletcher, K. H. Jacobs, C. H. Mijovic, J. A. Franklyn, and M. C. Sheppard. 1992. HLA class II gene polymorphism contributes little to Hashimoto's thyroiditis. *Clin Endocrinol (Oxf) 37:141.*

12. Farid, N. R., L. Sampson, H. Moens, and J. M. Barnard. 1981. The association of goitrous autoimmune thyroiditis with HLA-DR5. *Tissue Antigens 17:265.*

13. Wan, Q., R. Shah, J. C. Panos, A. A. Giraldo, C. S. David, and Y. M. Kong. 2002. HLA-DR and HLA-DQ polymorphism in human thyroglobulin-induced autoimmune thyroiditis: DR3 and DQ8 transgenic mice are susceptible. *Hum Immunol 63:301.*

14. Beisel, K. W., C. S. David, A. A. Giraldo, Y. M. Kong, and N. R. Rose. 1982. Regulation of experimental autoimmune thyroiditis: mapping of susceptibility to the I-A subregion of the mouse H-2. *Immunogenetics 15:427.*

15. Vladutiu, A. O., and N. R. Rose. 1971. Autoimmune murine thyroiditis relation to histocompatibility (H-2) type. *Science 174:1137.*

16. Kong, Y. C., J. C. Flynn, Q. Wan, and C. S. David. 2003. HLA and H2 class II transgenic mouse models to study susceptibility and protection in autoimmune thyroid disease. *Autoimmunity 36:397.*

17. Kong, Y. C., L. C. Lomo, R. W. Motte, A. A. Giraldo, J. Baisch, G. Strauss, G. J. Hammerling, and C. S. David. 1996. HLA-DRB1 polymorphism determines susceptibility to autoimmune thyroiditis in transgenic mice: definitive association with HLA-DRB1*0301 (DR3) gene. *J Exp Med 184:1167.*

18. Elliott, J. F., J. Liu, Z. N. Yuan, N. Bautista-Lopez, S. L. Wallbank, K. Suzuki, D. Rayner, P. Nation, M. A. Robertson, G. Liu, and K. M. Kavanagh. 2003. Autoimmune cardiomyopathy and heart block develop spontaneously in HLA-DQ8 transgenic IAbeta knockout NOD mice. *Proc Natl Acad Sci U S A 100:13447.*

19. Champion, B. R., D. C. Rayner, P. G. Byfield, K. R. Page, C. T. Chan, and I. M. Roitt. 1987. Critical role of iodination for T cell recognition of thyroglobulin in experimental murine thyroid autoimmunity. *J Immunol 139:3665.*

20. Weetman, A. P., and A. M. McGregor. 1994. Autoimmune thyroid disease: further developments in our understanding. *Endocr Rev 15:788.*

21. Weigle, W. O. 1965. The production of thyroiditis and antibody following injection of unaltered thyroglobulin without adjuvant into rabbits previously stimulated with altered thyroglobulin. *J Exp Med 122:1049.*

22. Flax, M. H. 1963. Experimental allergic thyroiditis in the guinea pig. II. Morphologic studies of development of disease. *Lab Invest 12:199.*

23. Vladutiu, A. O., and N. R. Rose. 1972. Murine thyroiditis. 3. Influence of syngeneic and allogeneic thyroid antigen on induction of the disease. *Clin Exp Immunol 11:245.*

24. Jones, H. E., and I. M. Roitt. 1961. Experimental auto-immune thyroiditis in the rat. *Br J Exp Pathol 42:546.*

25. Haines, D. M., and W. J. Penhale. 1985. Experimental thyroid autoimmunity in the dog. *Vet Immunol Immunopathol 9:221.*

26. Andrada, J. A., N. R. Rose, and J. H. Kite, Jr. 1968. Experimental thyroiditis in the rhesus monkey. IV. The role of thyroglobulin and cellular antigens. *Clin Exp Immunol 3:133.*

27. Wick, G., and H. Burger. 1971. Comparison of experimental allergic thyroiditis and spontaneous hereditary autoimmune thyroiditis in chickens. *Z Immunitatsforsch Exp Klin Immunol 142:54.*

28. Charreire, J. 1989. Immune mechanisms in autoimmune thyroiditis. *Adv Immunol 46:263.*

29. Verginis, P., M. M. Stanford, and G. Carayanniotis. 2002. Delineation of five thyroglobulin T cell epitopes with pathogenic potential in experimental autoimmune thyroiditis. *J Immunol 169:5332.*

30. Carayanniotis, G., and Y. C. Kong. 2000. Pathogenic thyroglobulin peptides as model antigens: insights on the induction and maintenance of autoimmune thyroiditis. *Int Rev Immunol 19:557.*

31. Brazillet, M. P., F. Batteux, O. Abehsira-Amar, F. Nicoletti, and J. Charreire. 1999. Induction of experimental autoimmune thyroiditis by heat-denatured porcine thyroglobulin: a Tc1-mediated disease. *Eur J Immunol 29:1342.*

32. Brazillet, M. P., K. Mignon-Godefroy, and J. Charreire. 1996. Induction of experimental autoimmune thyroiditis (EAT) by heat-denaturated thyroglobulin (Tg). *Exp Clin Endocrinol Diabetes 104 Suppl 3:23.*

33. Watanabe, H., M. Inaba, Y. Adachi, K. Sugiura, H. Hisha, T. Iguchi, T. Ito, R. Yasumizu, K. Inaba, T. Yamashita, and S. Ikehara. 1999. Experimental autoimmune thyroiditis induced by thyroglobulin-pulsed dendritic cells. *Autoimmunity 31:273.*

34. Kotani, T., K. Umeki, K. Hirai, and S. Ohtaki. 1990. Experimental murine thyroiditis induced by porcine thyroid peroxidase and its transfer by the antigen-specific T cell line. *Clin Exp Immunol 80:11.*

35. Ng, H. P., J. P. Banga, and A. W. Kung. 2004. Development of a murine model of autoimmune thyroiditis induced with homologous mouse thyroid peroxidase. *Endocrinology 145:809.*

36. Flynn, J. C., A. Gardas, Q. Wan, M. Gora, G. Alsharabi, W. Z. Wei, A. A. Giraldo, C. S. David, Y. M. Kong, and J. P. Banga. 2004. Superiority of thyroid peroxidase DNA over protein immunization in replicating human thyroid autoimmunity in HLA-DRB1*0301 (DR3) transgenic mice. *Clin Exp Immunol 137:503.*

37. Romball, C. G., and W. O. Weigle. 1987. Transfer of experimental autoimmune thyroiditis with T cell clones. *J Immunol 138:1092.*

38. Rasooly, L., C. L. Burek, and N. R. Rose. 1996. Iodine-induced autoimmune thyroiditis in NOD-H-2h4 mice. *Clin Immunol Immunopathol 81:287.*

39. Witebsky, E., J. H. Kite, Jr., G. Wick, and R. K. Cole. 1969. Spontaneous thyroiditis in the obese strain of chichens. I. Demonstration of circulating autoantibodies. *J Immunol 103:708.*

40. Dietrich, H. M., A. J. Oliveira-dos-Santos, and G. Wick. 1997. Development of spontaneous autoimmune thyroiditis in Obese strain (OS) chickens. *Vet Immunol Immunopathol 57:141.*

41. Sundick, R. S., N. Bagchi, and T. R. Brown. 1996. The obese strain chicken as a model for human Hashimoto's thyroiditis. *Exp Clin Endocrinol Diabetes 104 Suppl 3:4.*

42. Braley-Mullen, H., G. C. Sharp, B. Medling, and H. Tang. 1999. Spontaneous autoimmune thyroiditis in NOD.H-2h4 mice. *J Autoimmun 12:157.*

43. Quaratino, S., E. Badami, Y. Y. Pang, I. Bartok, J. Dyson, D. Kioussis, M. Londei, and L. Maiuri. 2004. Degenerate self-reactive human T-cell receptor causes spontaneous autoimmune disease in mice. *Nat Med 10:920.*

44. Quaratino, S., M. Feldmann, C. M. Dayan, O. Acuto, and M. Londei. 1996. Human self-reactive T cell clones expressing identical T cell receptor beta chains differ in their ability to recognize a cryptic self-epitope. *J Exp Med 183:349.*

45. Quaratino, S., L. P. Duddy, and M. Londei. 2000. Fully competent dendritic cells as inducers of T cell anergy in autoimmunity. *Proc Natl Acad Sci U S A 97:10911.*

46. Badami, E., L. Maiuri, and S. Quaratino. 2005. High incidence of spontaneous autoimmune thyroiditis in immunocompetent self-reactive human T cell receptor transgenic mice. *J Autoimmun 24:85.*

47. Hillert, J. 1994. Human leukocyte antigen studies in multiple sclerosis. *Ann Neurol 36 Suppl:S15.*

48. Spurkland, A., E. G. Celius, I. Knutsen, A. Beiske, E. Thorsby, and F. Vartdal. 1997. The HLA-DQ(alpha 1*0102, beta 1*0602) heterodimer may

confer susceptibility to multiple sclerosis in the absence of the HLA-DR(alpha 1*01, beta 1*1501) heterodimer. *Tissue Antigens 50:15.*

49. Mignot, E., X. Lin, J. Arrigoni, C. Macaubas, F. Olive, J. Hallmayer, P. Underhill, C. Guilleminault, W. C. Dement, and F. C. Grumet. 1994. DQB1*0602 and DQA1*0102 (DQ1) are better markers than DR2 for narcolepsy in Caucasian and black Americans. *Sleep 17:S60.*

50. Planelles, D., N. Puig, A. Beneto, E. Gomez, P. Rubio, V. Mirabet, S. Bonanad, I. Blasco, and J. A. Montoro. 1997. HLA-DQA, -DQB and -DRB allele contribution to narcolepsy susceptibility. *Eur J Immunogenet 24:409.*

51. Dayan, C. M., M. Londei, A. E. Corcoran, B. Grubeck-Loebenstein, R. F. James, B. Rapoport, and M. Feldmann. 1991. Autoantigen recognition by thyroid-infiltrating T cells in Graves disease. *Proc Natl Acad Sci U S A 88:7415.*

52. Londei, M., G. F. Bottazzo, and M. Feldmann. 1985. Human T-cell clones from autoimmune thyroid glands: specific recognition of autologous thyroid cells. *Science 228:85.*

53. Braverman, L. E., and R. D. Utiger. 2005. Werner & Ingbar's The Thyroid: A Fundamental and Clinical Text. Lippincott Williams and Wilkins, Philadelphia.

54. Braley-Mullen, H., G. C. Sharp, J. T. Bickel, and M. Kyriakos. 1991. Induction of severe granulomatous experimental autoimmune thyroiditis in mice by effector cells activated in the presence of anti-interleukin 2 receptor antibody. *J Exp Med 173:899.*

55. Braley-Mullen, H., G. C. Sharp, H. Tang, K. Chen, M. Kyriakos, and J. T. Bickel. 1998. Interleukin-12 promotes activation of effector cells that induce a severe destructive granulomatous form of murine experimental autoimmune thyroiditis. *Am J Pathol 152:1347.*

56. McMurray, R. W., G. C. Sharp, and H. Braley-Mullen. 1994. Intrathyroidal cell phenotype in murine lymphocytic and granulomatous experimental autoimmune thyroiditis. *Autoimmunity 18:93.*

57. Braley-Mullen, H., R. W. McMurray, G. C. Sharp, and M. Kyriakos. 1994. Regulation of the induction and resolution of granulomatous experimental autoimmune thyroiditis in mice by CD8+ T cells. *Cell Immunol 153:492.*

CHAPTER 4

A RADIOLIGAND BINDING ASSAY TO MEASURE ANTI-THYROID PEROXIDASE AUTOANTIBODIES IN MICE

A version of this chapter has been submitted for publication. Hayward, S., Suzuki, K., and J. Elliott. 2006. Journal of Immunological Methods

4.1 Introduction

Hashimoto's thyroiditis, also called autoimmune thyroiditis, is a chronic inflammatory disease which leads to thyroid destruction and can lead to a deficiency in thyroid hormone production. Autoimmune thyroiditis occurs in more than 3% of the population and symptoms include fatigue, weight gain and, in some cases, a gradual enlargement of the thyroid gland (goiter). Currently, there is no known intervention that can prevent the autoimmune process leading to Hashimoto's thyroiditis, but hypothyroidism, the end result of the thyroid gland destruction, can be treated by lifelong thyroid hormone replacement. (1)

In humans, laboratory tests for both serum thyroid hormone levels and anti-thyroid autoantibodies are routinely performed to assist in the diagnosis of the hypothyroidism induced by Hashimoto's thyroiditis. Hypothyroidism is indicated by normal to low concentrations of circulating thyroid hormones (T3/T4) in the presence of elevated levels of thyroid stimulating hormone (TSH). In addition to changes in hormone levels, autoantibodies against thyroid antigens such as thyroid peroxidase (TPO) and thyroglobulin are frequently seen in patients with autoimmune thyroiditis (1). TPO is a membrane-bound enzyme located on the surface of and in the cytoplasm of thyroid follicles; it catalyzes the production of the thyroid hormones T3 and T4 (1). In humans, anti-TPO autoantibodies have been detected using a variety of assays including hemagglutination and, more recently, radio- or enzyme-linked- immunoassays.

The development of animal models has enhanced our understanding of autoimmune thyroiditis. However, until recently, none of the known mouse

models of autoimmune thyroiditis had shown all the findings of the human disease and, specifically, none had shown spontaneous development of anti-TPO autoantibodies. In fact, one group has questioned whether non-primates are capable of spontaneously developing autoantibodies to thyroid peroxidase (2), even though such antibodies readily appear if mice are immunized with TPO in adjuvant (3) or with plasmid or adenoviral vectors (4, 5).

Currently, detection of circulating anti-TPO autoantibodies in mouse sera is accomplished by using an indirect immunofluorescence assay (iIFA) on histological sections of mouse thyroid gland; the assay is positive if a specific pattern of thyroid follicle membrane staining is observed. Although this approach is logical based on the abundance of TPO at this specific anatomical location, the assay is qualitative rather than a quantitative assay (although serial dilutions can give some indication of titre) and it does not specifically define the thyroid antigen(s) to which the autoantibodies are binding.

We discovered that a spontaneous autoimmune thyroiditis mouse model (NOD.DQ6/Ab^0; Chapter 3), on iIFA, clearly develops anti-thyroid follicle membrane autoantibodies and here we establish a complementary radioligand binding assay (RBA) for the direct quantification of anti-mouse TPO. Although designed for mouse thyroid peroxidase, this type of assay also has the potential to be applied to human thyroid peroxidase as an alternative highly sensitive method for diagnosis of anti-thyroid autoimmunity.

4.2 Materials and Methods

4.2.1 cDNA templates and other reagents

The full length cDNA encoding murine thyroid peroxidase (6), as well as an affinity-purified rabbit anti-human TPO polyclonal antibody known to be cross-reactive with mouse TPO were kindly provided by Dr. K. Umeki (Miyazaki Univeristy, Japan). The portion of the cDNA encoding the extracellular domain (i.e. lacking the predicted N-terminal signal sequence, transmembrane domain, and cytoplasmic segment) was amplified by PCR using Pfu DNA polymerase (Stratagene, La Jolla, CA) and primers CTCTCTATGCATATGAGAAGCAGAGAC ATCTTGTGT (MuTPO-Excell-NsiI-5') and CTCTCTCTAGACTAGGATGCCCGA GGTAGCCTG (MuTPO-Excell-XbaI-3'). The resulting ~2450 bp fragment was digested with Nsi I / Xba I and ligated into the vector pcDNAII (Invitrogen, Carlsbad, CA) cut with the same enzymes. I acknowledge K. Suzuki (University of Alberta, Edmonton, AB) for the cloning of this TPO-vector. The control vectors contained the full-length human GAD65 cDNA in vector pcDNAII and the cytoplasmic segment of human IA-2 (also called 'ICA512bdc') in vector pCRII (Invitrogen); both control vectors were obtained from G. Eisenbarth (University of Colorado Health Sciences Center, Denver, CO). All three vectors contain an upstream SP6 promoter and yield sense strand mRNA in the presence of SP6 RNA polymerasae and ribonucleotide triphosphates.

Wash Buffer consisted of 150mM NaCl, 20mM Tris-HCl pH 7.4, 0.15% (v/v) Tween-20, 0.1% (w/v) BSA, and 0.1% (w/v) sodium azide. The solution was passed through a 0.22 micron filter and stored at 4°C. Protein G-Sepharose 4B

Fast Flow (Sigma, St.Louis, MO) was washed once with DEPC treated/autoclaved H_2O, twice with wash buffer, then resuspended in wash buffer (50% v/v) and stored at 4˚C.

The mouse B cell hybridoma line GAD6 (produces an IgG2a against human GAD65) was obtained from the Developmental Studies Hybridoma Bank, University of Iowa, Iowa City, IA; GAD6 monoclonal antibody was affinity purified from hybrdioma supernatants using protein G-Sepharose. Rhodamine-conjugated goat anti-mouse IgG antibody was purchased from Jackson ImmunoResearch (West Grove, PA).

4.2.2 Mouse serum

Sera were collected from anaesthetized/euthanized mice via terminal cardiac bleed. The following strains were used: 1) Balb/c, 2) Nonobese Diabetic (NOD), and 3) NOD.DQ6/Ab^0. The latter line develops spontaneous autoimmune thyroiditis (Chapter 3). All mice were housed in conventional SPF facilities and all experimental protocols were approved by our institutional Health Sciences Animal Policy and Welfare Committee, according to Canadian Council on Animal Care guidelines.

4.2.3 Preparation and analysis of radiolabeled antigens.

Radiolabeled antigens were generated using the three different plasmid cDNAs described above, each placed in an *in vitro* transcription/translation system (TnT®SP6 coupled wheat germ extract) supplied by Promega Inc.

(Madison, WI). Transcription/translation reactions (Vt 50µl) contained DEPC treated/autoclaved water, reaction buffer, amino acids including ^{3}H leucine (PerkinElmer Life Sciences, Woodbridge, ON) [or for SDS-PAGE analysis ^{35}S Methionine (Amersham Biosciences, Baie D'Urfé, PQ)], RNasin (Promega), DNA template (1µg supercoiled plasmid DNA), SP6 RNA polymerase and wheat germ extract; reagents were combined according to the protocol supplied by Promega and incubated at 30˚C for 90 minutes. After incubation, transcription/translation reactions were stored at -70˚C until use.

To determine how much ^{3}H had been incorporated into protein in each transcription/translation reaction, a TCA precipitation assay was used. At the end of the 90 minute incubation, 2µl from each 50µl reaction was transferred to a fresh eppendorf tube already containing 98µl 1M NaOH. Tubes were vortexed briefly, incubated at 37˚C for 10 minutes and then 900µl ice-cold 25% trichloroacetic acid (TCA) was added to all tubes. They were re-vortexed, incubated on ice for a further 30 minutes and then TCA precipitated proteins were collected by transferring the contents of each tube to a vacuum filtration device containing a Whatman glass fiber filter. Filters were washed 5 times with ice-cold 5% TCA (evacuating between each wash), removed from the vacuum manifold, dried under a heat lamp (15 minutes) and, after addition of scintillation fluid, counted in a beta-counter; values obtained were designated 'cpm of protein'. To control for endogenous extract activity, 2µl of a reaction mix that did not include a DNA template was TCA precipitated, collected onto a glass fiber filter, washed, dried and counted as above; this constituted 'cpm of endogenous

activity'. Total cpm in each reaction tube was also determined by spotting 2µl of the reaction mix directly on a glass fibre filter, drying and counting (i.e. without TCA precipitation or washing steps). Percent ^{3}H incorporation into protein was calculated using the formula: [(cpm of protein - cpm of endogenous activity) / total cpm] x 100.

SDS-PAGE analysis of ^{35}S-methionine labeled *in vitro* translation products was performed using 8% SDS-polyacrylamide gels. Gels were stained with Coomassie R250, destained, dried for one hour on a gel drier and analyzed by autoradiography using Kodak Biomax MR film.

4.2.4 Detection of anti-thyroid peroxidase autoantibodies

This approach is based on methods developed by L. Yu and G. Eisenbarth for the detection of anti-huGAD65 autoantibodies (7). Transcription/Translation reactions were diluted in wash buffer to 800,000 cpm 'protein' per ml, and the resulting antigen solution aliquoted into pre-labeled ependorf tubes (25 µl/tube). Sera or antibodies to be tested were diluted in PBS and 25 µl/tube of the appropriate dilution added to triplicate tubes containing radiolabeled antigen. Tubes were vortexed, centrifuged briefly and incubated stationary at 4˚C overnight. Once these incubations were set up, the appropriate number of 96 well Vacuum Filter Plates (Millipore Inc., Bedford, MA) were charged with wash buffer (200µl/well) and incubated overnight at room temperature. The following morning the wash buffer was aspirated through the plate filters using a 96 well plate suction apparatus (i.e. vacuum is below each

well). The plate was transferred to the bench and 25µl of a protein G-sepharose slurry (50%v/v in wash buffer) added to all wells for antigen-antibody capture, followed by the antigen-serum mixtures (50µl/well) which had completed their overnight incubations (note that filter bottom in each well does not allow transfer of aqueous liquids unless placed under suction). The plate was placed on a shaker platform for 90 minutes at 4°C to maximize interactions between serum antibodies and protein G-sepharose, re-installed on the plate suction apparatus and all wells drained and then washed 3 times with 200µl wash buffer/well each time. The plate was returned to the bench, 150µl wash buffer added to each well and agitation continued on the shaker platform for a further 1 hour at 4°C. The filter plate was placed back on the suction apparatus, drained, washed 3 times as before and dried under a heat lamp (30 minutes). The bottom of the plate was sealed using backing tape (Perkin Elmer), 40µl of scintillant was added to each well and all wells were counted in a beta-counter.

4.2.5 Competitive RBA

Anti-thyroid peroxidase antibody reactivity was assessed for potential cross-reactivity with mouse thyroglobulin since it had been suggested that these two autoantigens share at least some epitopes (8, 9). The same procedure was followed as for the radioligand binding assay with the difference that the serum was preincubated with soluble antigen, Tg (or BSA as a control), in concentrations varying from 10^3 to 1 x 10^{-4} pmol/ml) for 90 minutes at 37°C, prior to incubation with ^{3}H-TPO. The results were expressed as percent inhibition

plotted versus concentration of inhibitor (pmol/ml).

4.2.6 Competitive ELISA

Falcon 353911 microtitre plates (Becton Dickinson Labware, Franklin Lakes, NJ) were coated overnight at 4°C with 50µl per well of 15µg/ml mouse thyroglobulin in PBS. The plates were washed with PBS-T, blocked for 1h at room temperature with 1% w/v BSA in PBS-T and incubated with mouse sera (various dilutions in PBS-T) for 90 minutes at 37°C. The serum was preincubated with soluble inhibitor (Tg or BSA, in concentrations varying from 10^{3} to 10^{-4} pmol/ml) for 90 minutes at 37°C, prior to addition to the plate. The plates were then washed with PBS-T and incubated with horseradish peroxidase (HRP) conjugated goat anti-mouse IgG (H+L; 1:5,000; Jackson ImmunoResearch, West Grove, PA) and developed by using TMB (Sigma, St.Louis, MO) as a substrate. OD 450nm was measured on a plate reader and expressed as the mean of triplicate wells. The results were expressed as inhibition percent (%) plotted versus concentration of inhibitor (pmol/ml).

4.2.7 Indirect immunofluorescence assay (iIFA)

To minimize the possibility of endogenous IgG contributing to background iIFA staining, thyroid glands were dissected from euthanized NOD Rag1 knockout (NOD.129S7(B6)-*Rag1*^{tm1Mom}/J) mice obtained from The Jackson Laboratory (Bar Harbor, ME). The glands were embedded in Tissue-Tek O.C.T. compound (Fisher Scientific, Nepean, ON), snap frozen in a isopropanol/dry ice

bath, cryostat sections cut, mounted on microscope slides and stored at –20°C. Slides were warmed at room temperature (RT) for 5 minutes, fixed with ice cold acetone for 5 minutes and then dried at RT for 3 minutes. The area of each slide containing the tissue section was circled with a pap pen, phosphate buffered saline (PBS) at RT was gently applied to this area for 5 minutes, removed and an antigen retrieval incubation step was performed (1% SDS/PBS applied for 15 minutes at 37°C). The SDS/PBS was removed, the slide washed with PBS (3 x 5min at RT), then blocked by applying 1% BSA/PBS for 30 minutes at 37°C followed by washing in PBS (3 x 5min at RT). To accomplish iIFA staining, mouse serum (100µl total volume at various dilutions in PBS) was added to the tissue section and the slide incubated for 1 hour at 37°C. After further washing with PBS (3 x 5min at RT), the secondary antibody (rhodamine conjugated goat anti-mouse IgG diluted 1:200 in PBS) was added and the slide incubated for a further 1 hour at 37°C. The slide was finally washed (3 x 5min with PBS), mounted with Immunomount (Thermo-Shandon, Pittsburgh, PA) and a coverslip and observed under a fluorescence microscope.

For those sera that were positive by iIFA, a semi-quantitative determination of iIFA titre was accomplished by preparing dilutions in PBS (1:100, 1:200, 1:400, 1:600, 1:800, and 1:1000) and incubating each of these on thyroid tissue sections as above. Microscope and camera settings were adjusted such that the fluorescence staining was bright and crisp for the 1:100 dilution. The microscope and camera settings were then kept constant while photographs were taken of 3 representative fields from each of the remaining slides (i.e. slides

stained at all of the other serum dilutions). Photographs were read by two different blinded observers to determine the presence or absence of fluorescent staining; the highest dilution at which fluorescence staining was still seen in the photograph was designated as the iIFA titre of that particular serum. Because there was 100% concurrence in the readings done by the two different observers, no averaging of titres was required.

4.3 Results

4.3.1 *In vitro* transcription/translation of muTPO, huGAD65, and huIA-2

The size and quality of *in vitro* translated, ^{35}S labeled muTPO, huGAD65 and huIA-2 was evaluated by SDS-PAGE and autoradiography (Figure 4-1). Lane 2 contains an aliquot from a transcription/translation mixture that did not include a DNA template, indicating that endogenous translation is very low in these extracts. The predicted molecular weight of the truncated muTPO is 91kDa, which correlates well with the approximately 89kDa band observed in Lane 1. Similarly, observed bands for huGAD65 (migrates at about 59kDa; predicted molecular weight 65kDa) and huIA-2 (migrates at about 72kDa; predicted molecular weight 71kDa) are within the range of experimental error for this type of gel. The presence of single distinct bands of appropriate sizes suggests that the majority of translated products are full length for each of the three coupled transcription/translation reactions. The weaker signal obtained for the huIA-2 product may relate in part to the lower number of methionine residues present (13 for huIA-2, 25 for huGAD65 and 15 for muTPO), but the result is also

consistent with our finding that the percentage of ^{3}H leucine converted to TCA precipitable counts was consistently lower for reactions containing the huIA-2 cDNA template (e.g. percent incorporation ranged from 1-2% for huIA-2, 5-6% for huGAD65 and 20-30% for muTPO). Thus despite its greater length, the truncated muTPO appeared to be the most efficiently translated template of the three tested in these experiments.

4.3.2 Assessment of optimal serum-antigen ratios in RBA assay

To determine the optimal conditions for using a radioligand binding assay to specifically detect TPO autoantibodies, a variety of serum to antigen ratios were assayed (1/100, 1/50, 1/25, 1/8, and 1/4 v/v). As expected, captured ^{3}H TPO increased as more serum was added; although, too much serum actually inhibited capture of antigen (Figure 4-2). Similar optimal serum to antigen ratios (1/25 v/v) were found irrespective of the actual quantity of thyroid peroxidase autoantibodies within a particular mouse's serum (Figure 4-2). This optimal ratio (1/25 v/v) was utilized in all subsequent experiments.

4.3.3 Detection and quantification of anti-TPO autoantibodies in NOD.DQ6/Ab^{0} mice

With the optimal ratio of serum to ^{3}H protein determined we next determined relatively how much serum antibody is present in different animals. Not all NOD.DQ6/Ab^{0} mice have the same titre of TPO autoantibodies, but they are consistently detected in these mice and not in controls (Table 4-1). This result is specific to ^{3}H protein being used. NOD.DQ6/Ab^{0} serum detects ^{3}H

muTPO, but shows no significant capturing of ^{3}H huGAD65 or ^{3}H huIA-2 (Table 4-1).

4.3.4 The anti-TPO autoantibodies in NOD.DQ6/Ab^{0} mice do not cross-react with thyroglobulin

Neither BSA nor soluble thyroglobulin was able to inhibit the binding of NOD.DQ6/Ab^{0} sera to ^{3}H-TPO when unlabeled antigen concentrations were varied from 10^{3}–10^{-4} pmol/ml (Figure 4-3A). In contrast, the same concentrations of soluble Tg were able to completely inhibit anti-Tg reactivity of NOD.DQ6/Ab^{0} sera in our anti-Tg Elisa (Figure 4-3B).

4.3.5 Anti-thyroid autoantibody titres can be semi-quantified by iIFA

Dilutions of NOD.DQ6/Ab^{0} serum were made in PBS (1:100, 1:200, 1:400, 1:600, 1:800, and 1:1000) and incubated with histological sections of NOD.Rag1^{0} thyroid tissue. Bound autoantibodies were detected using a rhodamine-conjugated anti-mouse IgG antibody. Microscope and camera settings were adjusted such that the fluorescence staining was bright and crisp for the 1:100 dilution; the settings were then kept constant while photographs were taken of the other serum dilutions. The highest dilution at which fluorescence staining was still seen in the photograph was designated as the iIFA titre of that particular serum. Shown in Figure 4-4 is a representative experiment in which the NOD.DQ6/Ab^{0} anti-thyroid autoantibody serum titre was determined to be 1:800. Fluorescence can be seen up to and including the 1:800 dilution, but cannot be seen at 1:1000.

4.3.6 Correlation of anti-TPO autoantibody titres determined by iIFA and RBA

The quantification of thyroid peroxidase autoantibody levels by the RBA correlates (R^2=0.88) to the semi-quantitative titre analysis by indirect immunofluorescence. That is, a NOD.DQ6/Ab^0 mouse with a titre of 1:800 by iIFA has a higher cpm count in the RBA method than a NOD.DQ6/Ab^0 mouse with a titre of 1:400 by iIFA (Figure 4-5). Thus, the two methods correlate.

4.4 Discussion

Researchers use indirect immunofluorescence (iIFA) as an indicator of what tissue type(s) is/are being targeted by autoantibodies and for an initial indication, for example, of whether the antigen is membrane bound or not, but in most cases use of this assay is followed by a more comprehensive look at specific autoantibodies. In mice, thyroid peroxidase (TPO) autoantibodies are often assessed by this technique; however, to our knowledge, all mouse models of autoimmune thyroiditis investigated, thus far, do not have anti-TPO autoantibodies (e.g. (2)). That is, iIFA staining with serum from these mice does not show membrane staining of the thyroid gland. This contrasts with the human disease where TPO is known to be the key membrane-bound thyroid autoantigen (1).

The NOD.DQ6/Ab^0 strain develops spontaneous autoimmune thyroiditis (Chapter 3) and, we believe, it is the first mouse model to show thyroid follicle membrane staining by iIFA. Since methods for identifying the autoantigen targeted and directly quantifying the titres of these autoantibodies have not been

developed, we here do so by developing a novel radioligand binding assay that is specific, highly reproducible and sensitive for thyroid peroxidase.

Radioligand binding assays (RBAs) are not a recently established technique. Historically, they have been used as an extremely powerful tool for studying receptors. A preparation containing a receptor of interest is incubated with a radioligand and, after a period of time, the amount of radioactivity bound to the receptor is quantified. Such radioligand binding assays are utilized for saturation, kinetic and inhibitory experiments (10).

The field of diabetes has harnessed radioligand binding assays for an alternative use: autoantibody detection. Autoantibodies are a key characteristic of autoimmune disease (11) and the detection and quantification of autoantibodies in both humans and animal models has significantly advanced our understanding of most autoimmune disease. Identification of autoantigens, disease diagnosis, preclinical diagnosis and susceptibility monitoring would all be severely hindered in the absence of autoantibody assays (12).

Insulin autoantibodies (IAA) are markers of the preclinical phase of diabetes and their measurement, in addition to other autoantibodies against antigens such as GAD, ICA (islet cell antigen) and IA-2, forms the foundation of the current strategies for predicting future onset of type 1 diabetes (13-15). The original IAA radioligand binding assay was developed in 1980 (16) and since then diabetes autoantibody RBAs have been routinely used and are consistently shown to be more sensitive than ELISA methods (17, 18). These autoantibody RBAs are continually improved (19, 20) and modified for different antigens (17,

21), but in essence are similar to the RBA we have described here: a radio-labeled antigen is combined with serum and then the antibodies, and bound antigen, are captured by protein A/G-sepharose and quantified (18).

Radioligand binding assays for autoantibodies have been applied to other autoimmune disorders, including Celiac Disease (22, 23), Addison's Disease (24), and Vitiligo (25), but, to our knowledge, they have not yet been applied to autoimmune thyroiditis.

Unlike indirect immunofluorescence, in this radioligand binding assay a specific antigen is assayed and a clear comparison of "titres" can be addressed. Utilization of indirect immunofluorescence as an indication of anti-TPO autoantibodies is inherently assumptive as no specific antigen is assayed. We have shown support for this assumption— NOD.DQ6/Ab^0 mice which are positive for thyroid follicle membrane staining are positive for TPO autoantibodies. The correlation (R^2=0.88) between the quantity of autoantibodies determined by RBA and the titre estimates determined by inIFA further substantiates the method.

It has been shown in other animal models of thyroiditis that when the anti-thyroid peroxidase autoantibodies are detected, they are actually a reflection of shared epitopes between thyroglobulin and thyroid peroxidase, and that the apparent anti-TPO antibodies are actually against thyroglobulin (8, 9). Unlike these models, however, the anti-TPO reactivity of NOD.DQ6/Ab^0 sera cannot be blocked with soluble thyroglobulin indicating that the shared epitopes of Tg and TPO are not the epitopes targeted by the NOD.DQ6/Ab^0 autoantibodies.

A sensitive, highly reproducible assay for thyroid peroxidase autoantibodies in mice is warranted and will likely become an essential assay to the field of autoimmune thyroiditis. Recent evidence (26, 27) has marked the importance of TPO autoantibodies. They have shown that transgenic mice, generated to express a human TPO epitope-specific T cell-receptor (derived from a thyroid-infiltrating T cell of a patient with thyroiditis) are able to develop spontaneous autoimmune thyroiditis—stressing the importance of an anti-thyroid peroxidase attack to disease progression.

We anticipate that this sensitive quantitative anti-thyroid peroxidase assay will be an effective tool to detect anti-TPO autoantibodies not only in mouse models, but perhaps even in Hashimoto's disease in humans—it has a high throughput potential that can be applied both in patient diagnosis and in susceptibility predictions.

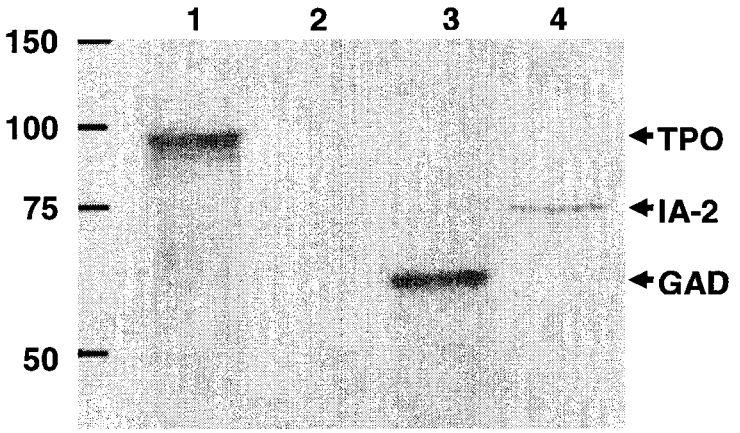

Figure 4-1: *In vitro* transcription/translation of muTPO, huGAD65, and hulA-2. 5µl of the *in vitro* transcription/translation reaction mixture was added to 25µl of SDS sample buffer and 10µl of this was then analyzed by SDS-PAGE and radiography as described in the methods. Lane 1: ^{35}S muTPO-extracellular domain. Lane 2: no DNA template. Lane 3: ^{35}S huGAD65. Lane 4: ^{35}S hulA-2.

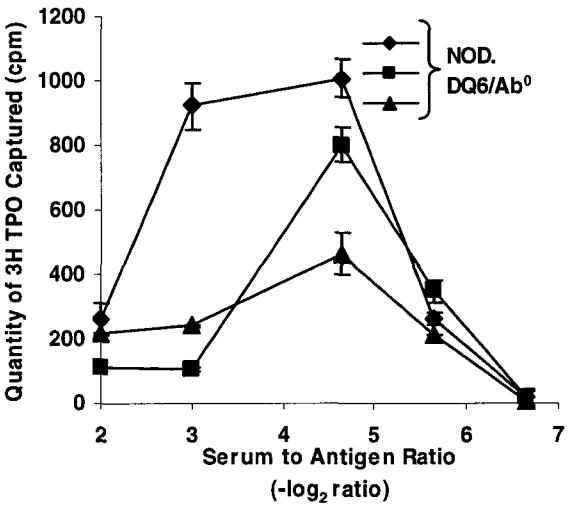

Figure 4-2: The optimal serum dilution in a thyroid peroxidase RBA is 1/25. Various ratios of serum to antigen combinations were made (1/100, 1/50, 1/25, 1/8, 1/4 v/v), antibodies were captured on protein G sepharose, and any antibody bound thyroid peroxidase was captured and detected. The quantity of thyroid peroxidase captured was compared to the serum-antigen ratio. Combinations were tested in triplicate and this is a representative experiment. Three separate experiments (n=3/expt) were completed. Each line represents serum from an individual mouse and error bars represent standard deviation.

	NOD.DQ6/Ab^0 serum	NOD Serum	Balb/c serum	GAD mAb	TPO pAb
muTPO	792 ± 95	157 ± 6	0 ± 2	37 ± 4	1000 ± 15
huGAD65	20 ± 3	195 ± 39	139 ± 17	721 ± 16	69 ± 7
hulA-2	53 ± 62	165 ± 22	10 ± 2	32 ± 4	72 ± 8

Table 4-1: The RBA assay detects and quantifies anti-TPO autoantibodies in NOD.DQ6/Ab^0 mice. Pooled NOD, Balb/c and NOD.DQ6/Ab^0 sera were each combined with ^{3}H muTPO, ^{3}H huGAD65, or ^{3}H hulA-2 at the optimized ratio of 1/25. The ^{3}H protein was captured on protein G sepharose and detected. The GAD-6 mAb was used at 5µg / 20000 cpm of protein. The TPO pAb is an affinity purified rabbit anti-human TPO polyclonal antibody and was used at 0.1µg/ 20000 cpm of protein. Combinations were tested in triplicate. The values listed represent cpm of captured ^{3}H protein ± standard deviation of a representative experiment.

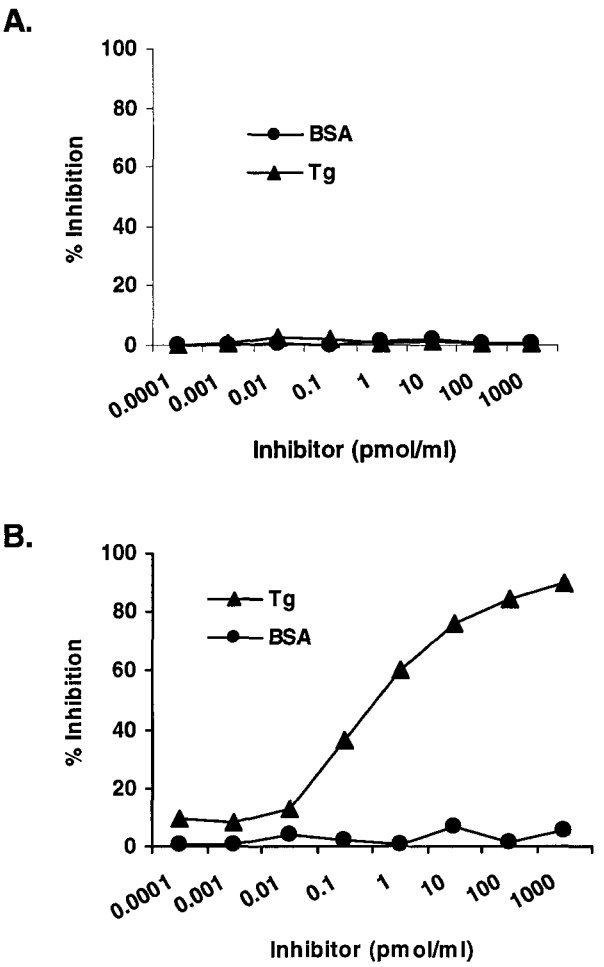

Figure 4-3: Thyroglobulin cannot inhibit the binding of NOD.DQ6/Ab^0 serum autoantibodies to thyroid peroxidase. Various concentrations of thyroglobulin or BSA were pre-incubated with sera from NOD.DQ6/Ab^0 animals before the sera was analyzed (A) for the presence of anti-TPO autoantibodies in the radioligand binding assay and % inhibition of anti-TPO binding was detected or (B) for the presence of anti-thyroglobulin autoantibodies by ELISA and % inhibition of anti-Tg binding was detected.

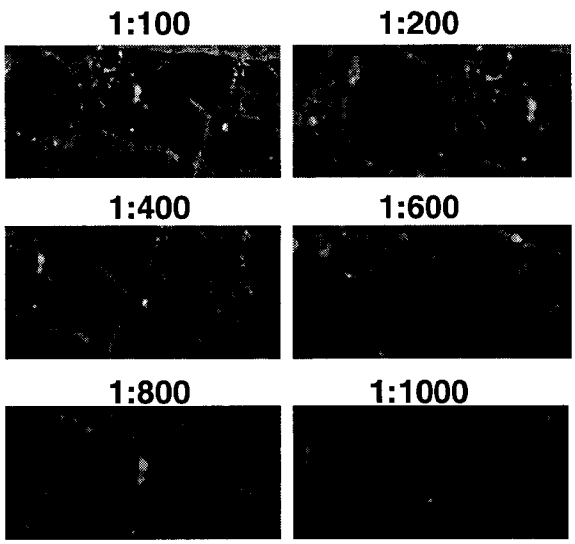

Figure 4-4: Example iIFA results demonstrating that iIFA can be used to semi-quantitatively measure titres of circulating anti-thyroid membrane autoantibodies in NOD.DQ6/Ab^0 mice. Dilutions of NOD.DQ6/Ab^0 serum were made in PBS (1:100, 1:200, 1:400, 1:600, 1:800, and 1:1000) and incubated with histological sections of thyroid tissue. Bound autoantibodies were detected using a rhodamine-conjugated anti-mouse IgG antibody. Titres were determined by two different blinded observers. In this example, a titre of 1:800 was obtained by both observers.

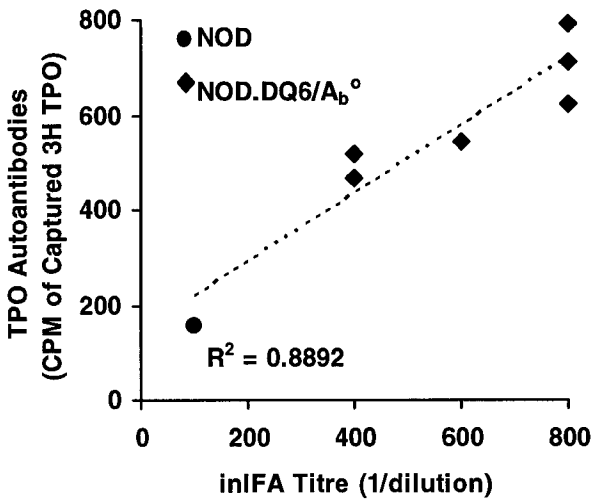

Figure 4-5: Indirect IFA titres of anti-thyroid membrane autoantibodies correlate with anti-thyroid peroxidase autoantibody levels determined by RBA. The same serum pools were used to detect anti-thyroid membrane autoantibodies by indirect immunofluorescence and anti-TPO autoantibodies by RBA. The largest serum dilution that could be detected by iIFA was designated that serum's titre and was compared to the cpm quantification by RBA. Control (NOD) and experimental (NOD.DQ6/Ab^0; n=6) serum was analyzed.

4.5 References

1. Mariotti, S., and G. Pinna. 2003. Autoimmune Thyroid Diseases. In *Contemporary Endocrnology: Disease of the Thyroid.* L. E. Braverman ed. Humana Press Inc., Totowa, p. 107.

2. Rasooly, L., C. L. Burek, and N. R. Rose. 1996. Iodine-induced autoimmune thyroiditis in NOD-H-2h4 mice. *Clin Immunol Immunopathol 81:287.*

3. Ng, H. P., J. P. Banga, and A. W. Kung. 2004. Development of a murine model of autoimmune thyroiditis induced with homologous mouse thyroid peroxidase. *Endocrinology 145:809.*

4. Guo, J., P. Pichurin, Y. Nagayama, B. Rapoport, and S. M. McLachlan. 2003. Insight into antibody responses induced by plasmid or adenoviral vectors encoding thyroid peroxidase, a major thyroid autoantigen. *Clin Exp Immunol 132:408.*

5. Flynn, J. C., A. Gardas, Q. Wan, M. Gora, G. Alsharabi, W. Z. Wei, A. A. Giraldo, C. S. David, Y. M. Kong, and J. P. Banga. 2004. Superiority of thyroid peroxidase DNA over protein immunization in replicating human thyroid autoimmunity in HLA-DRB1*0301 (DR3) transgenic mice. *Clin Exp Immunol 137:503.*

6. Kotani, T., K. Umeki, I. Yamamoto, M. Takeuchi, S. Takechi, T. Nakayama, and S. Ohtaki. 1993. Nucleotide sequence of the cDNA encoding mouse thyroid peroxidase. *Gene 123:289.*

7. Yu, L., M. Rewers, R. Gianani, E. Kawasaki, Y. Zhang, C. Verge, P. Chase, G. Klingensmith, H. Erlich, J. Norris, and G. S. Eisenbarth. 1996. Antiislet autoantibodies usually develop sequentially rather than simultaneously. *J Clin Endocrinol Metab 81:4264.*

8. Thrasyvoulides, A., and P. Lymberi. 2004. Antibodies cross-reacting with thyroglobulin and thyroid peroxidase are induced by immunization of rabbits with an immunogenic thyroglobulin 20mer peptide. *Clin Exp Immunol 138:423.*

9. Hoshioka, A., Y. Kohno, T. Katsuki, N. Shimojo, N. Maruyama, Y. Inagaki, T. Yokochi, O. Tarutani, T. Hosoya, and H. Niimi. 1993. A common T-cell

epitope between human thyroglobulin and human thyroid peroxidase is related to murine experimental autoimmune thyroiditis. *Immunol Lett 37:235.*

10. Bylund, D. B., and M. L. Toews. 1993. Radioligand binding methods: practical guide and tips. *Am J Physiol 265:L421.*

11. Dighiero, G., and N. R. Rose. 1999. Critical self-epitopes are key to the understanding of self-tolerance and autoimmunity. *Immunol Today 20:423.*

12. Gottlieb, P. A., and G. S. Eisenbarth. 1998. Diagnosis and treatment of pre-insulin dependent diabetes. *Annu Rev Med 49:391.*

13. Soeldner, J. S., M. Tuttleman, S. Srikanta, O. P. Ganda, and G. S. Eisenbarth. 1985. Insulin-dependent diabetes mellitus and autoimmunity: islet-cell autoantibodies, insulin autoantibodies, and beta-cell failure. *N Engl J Med 313:893.*

14. Verge, C. F., R. Gianani, E. Kawasaki, L. Yu, M. Pietropaolo, R. A. Jackson, H. P. Chase, and G. S. Eisenbarth. 1996. Prediction of type I diabetes in first-degree relatives using a combination of insulin, GAD, and ICA512bdc/IA-2 autoantibodies. *Diabetes 45:926.*

15. Ziegler, A. G., R. D. Herskowitz, R. A. Jackson, J. S. Soeldner, and G. S. Eisenbarth. 1990. Predicting type I diabetes. *Diabetes Care 13:762.*

16. Kurtz, A. B., J. A. Matthews, B. E. Mustaffa, P. R. Daggett, and J. D. Nabarro. 1980. Decrease of antibodies to insulin, proinsulin and contaminating hormones after changing treatment from conventional beef to purified pork insulin. *Diabetologia 18:147.*

17. Gianani, R., D. U. Rabin, C. F. Verge, L. Yu, S. R. Babu, M. Pietropaolo, and G. S. Eisenbarth. 1995. ICA512 autoantibody radioassay. *Diabetes 44:1340.*

18. Bonifacio, E., M. Atkinson, G. Eisenbarth, D. Serreze, T. W. Kay, E. Lee-Chan, and B. Singh. 2001. International Workshop on Lessons From Animal Models for Human Type 1 Diabetes: identification of insulin but not glutamic acid decarboxylase or IA-2 as specific autoantigens of humoral autoimmunity in nonobese diabetic mice. *Diabetes 50:2451.*

19. Naserke, H. E., N. Dozio, A. G. Ziegler, and E. Bonifacio. 1998. Comparison of a novel micro-assay for insulin autoantibodies with the conventional radiobinding assay. *Diabetologia 41:681.*

20. Williams, A. J., P. J. Bingley, E. Bonifacio, J. P. Palmer, and E. A. Gale. 1997. A novel micro-assay for insulin autoantibodies. *J Autoimmun 10:473.*

21. Yu, L., R. Gianani, and G. S. Eisenbarth. 1994. Quantitation of glutamic acid decarboxylase autoantibody levels in prospectively evaluated relatives of patients with type I diabetes. *Diabetes 43:1229.*

22. Williams, A. J., P. Annis, R. J. Lock, D. J. Unsworth, E. A. Gale, and P. J. Bingley. 1999. Evaluation of a high-throughput second antibody radiobinding assay for measuring IgA antibodies to human tissue transglutaminase. *J Immunol Methods 228:81.*

23. Bazzigaluppi, E., V. Lampasona, G. Barera, A. Venerando, C. Bianchi, G. Chiumello, E. Bonifacio, and E. Bosi. 1999. Comparison of tissue transglutaminase-specific antibody assays with established antibody measurements for coeliac disease. *J Autoimmun 12:51.*

24. Falorni, A., A. Nikoshkov, S. Laureti, E. Grenback, A. L. Hulting, G. Casucci, F. Santeusanio, P. Brunetti, H. Luthman, and A. Lernmark. 1995. High diagnostic accuracy for idiopathic Addison's disease with a sensitive radiobinding assay for autoantibodies against recombinant human 21-hydroxylase. *J Clin Endocrinol Metab 80:2752.*

25. Kemp, E. H., E. A. Waterman, D. J. Gawkrodger, P. F. Watson, and A. P. Weetman. 1998. Autoantibodies to tyrosinase-related protein-1 detected in the sera of vitiligo patients using a quantitative radiobinding assay. *Br J Dermatol 139:798.*

26. Badami, E., L. Maiuri, and S. Quaratino. 2005. High incidence of spontaneous autoimmune thyroiditis in immunocompetent self-reactive human T cell receptor transgenic mice. *J Autoimmun 24:85.*

27. Quaratino, S., E. Badami, Y. Y. Pang, I. Bartok, J. Dyson, D. Kioussis, M. Londei, and L. Maiuri. 2004. Degenerate self-reactive human T-cell receptor causes spontaneous autoimmune disease in mice. *Nat Med 10:920.*

CHAPTER 5

GENERAL DISCUSSION AND FUTURE DIRECTIONS

5.1 General Discussion and Future Directions

Over 80 autoimmune diseases have been identified, and collectively autoimmune diseases are thought to affect more than 5% of the North American population (1). Autoimmune diseases are chronic disabling disorders in which underlying defects in the immune response lead the body to attack its own organs and tissues. Although the initial trigger of autoimmunity still escapes us, it is critical to obtain an understanding of which individuals are susceptible to a particular autoimmune disease. In addition, a clear understanding of the self destructive mechanism is necessary. It may not be possible to prevent the initial trigger, but it might be possible to prevent the disease from progressing.

Researchers are only just beginning to comprehend the complexity of control in an autoimmune response. Autoimmune diseases develop in genetically susceptible individuals and can be triggered by environmental exposures. Understanding the interactions of genetic and environmental factors that are necessary for disease development offers the promise of preventing or treating autoimmune diseases via novel methods. Evidence for the importance of genes in the etiology of autoimmune diseases has been provided by studies showing that 1) identical twins are more likely to suffer from the same autoimmune disease than fraternal twins (2, 3); 2) relatives of patients with autoimmune diseases are at higher risk for development of the same or another autoimmune disease (4-7); and 3) certain races or ethnic groups are disproportionately affected by particular autoimmune diseases (8).

Particular genes within the major histocompatibility complex, a family of genes that regulate immune responses, contribute to susceptibility in multiple autoimmune diseases. Studies of these MHC genes in animal models are as important as studies of humans. The etiology and pathogenesis of autoimmune diseases often escapes our understanding and many animal models have been developed to assist our understanding of these breakdowns in self tolerance. No individual model perfectly mimics a human disease, but the constant reality is that humans are an extremely complex and dynamic system and models provide us with the opportunity to study the role of individual genes in order to investigate the genetic, environmental and pathogenic aspects of an autoimmune disease. Each animal model has its own unique attributes. For example, both spontaneous models and induced models have benefits; a spontaneous model often more closely resembles the natural condition in humans (e.g. NOD.DQ6/Ab^0 develop goiter and anti-TPO autoantibodies and the autoimmune thyroiditis is severe enough to induce hypothyroidism); however, in experimentally-induced models the onset and progression of the disease can be controlled (e.g. not all NOD.DQ6/Ab^0 animals develop thyroiditis at the same time and not all develop all aspects of the disease phenotype).

The objective of this thesis was to investigate the autoimmunity and immune pathogenesis of two humanized mouse models of autoimmunity, specifically the autoimmune myocarditis of NOD.DQ8/Ab^0 animals and the autoimmune thyroiditis of NOD.DQ6/Ab^0 animals. The purpose of our HLA transgenic mice was to provide valuable tools to mimic and understand the

molecular interactions that give rise to the human disease and to identify potential areas of disease pathogenesis that could be targeted to treat and/or prevent the human disease. Although HLA genes are associated with an increased risk for developing autoimmune diseases, these genes are forced to act in concert with unknown environmental factors, rather than acting directly such as with Mendelian genes. As a reflection of this complexity, HLA transgenic mice have not been predicted to spontaneously develop autoimmune diseases in the absence of additional disease factors (e.g. viral infection) due to the complex etiology and polygenic nature of the disease. It seems apparent that the genes of the NOD background provide what is necessary to spontaneously develop autoimmunity. For example, HLA-DQ8 transgenic mice generated by Lipes and colleagues were refractive to spontaneous autoimmunity when developed in the B6 background, but developed spontaneous myocarditis when they were backcrossed onto the NOD background (9). As discussed earlier, NOD mice show evidence of defective tolerance, both central and peripheral, and it is likely this contributes to the susceptibility. Specific defects have also been noted even within the various leukocyte subsets of the NOD immune system. These include reduced NK cell activity (10, 11), defects in NKT populations (11, 12), defective macrophage maturation and function (13), deficiencies in regulatory CD4+CD25+ T cell population (14), and the absence of CD5a and hemolytic complement (15). It would be of interest to determine if these same defects in tolerance and leukocyte subsets occur in our HLA-DQ transgenic mice; although it seems very likely.

Therapeutic approaches to autoimmune disease can be broadly divided into three general areas: 1) therapies to improve signs and symptoms; 2) therapies to modify the natural course of the disease; and 3) therapies directed at complications resulting from organ damage brought about the disease. In many instances, therapies are anticipated to have activities that will span these broad categories. Therapies include drugs, gene-based delivery systems, immunomodulation and cell-based treatments to name a few. Success in developing new therapies will rely increasingly on a comprehensive understanding of the etiology and pathogenesis of individual autoimmune diseases.

Characterization of the pathology of NOD.DQ8/Ab^0 mice, the majority of which was done prior to this thesis (9, 16), revealed that these HLA transgenic animals are a mouse model of autoimmune myocarditis and dilated cardiomyopathy. Prior analyses of the mononuclear cell infiltrate invading the hearts of NOD.DQ8/Ab^0 mice revealed the presence of B lymphocytes, CD4 T cells and CD8 T cells (9, 16), but the mechanism by which these immune cells attack and destroy the heart tissue had not been determined.

CD4 T cells recognize antigen in the context of MHC class II molecules; the fact that one particular MHC class II molecule (DQ8) promotes autoimmune myocarditis and another, DQ6, promotes autoimmune thyroiditis suggests that CD4 T cells play a role in the autoimmune process. In this thesis it has been shown that primed CD4 T cells alone can adoptively transfer the autoimmune myocarditis of NOD.DQ8/Ab^0 animals (and the autoimmune thyroiditis of

NOD.DQ6/Ab^0 animals). However, analysis of the mononuclear cell infiltrate invading the hearts of the adoptive transfer recipients revealed the presence of scattered CD4 T cells and occasional neutrophils and the predominate cell type was shown to be macrophage. We hypothesize that in autoimmune myocarditis the destruction of the heart tissue is likely accomplished through a pro-inflammatory mechanism (see Figure 2-17). We propose that pathogenic CD4 T cells enter the myocardium and secrete a number of cytokines including perhaps IL-17, which then induces the recruitment and activation of macrophages. These macrophages then produce inflammatory cytokines (e.g. TNF-α) and release proteolyic enzyme and reactive oxygen species which inflame and destroy the heart tissue. Similar inflammatory mechanisms are implied in other models such as transgenic mice with myocardial overexpression of TNF-α (17), coxsackie virus-induced autoimmune myocarditis (18) and in experimental autoimmune thyroiditis (19, 20).

Conceptually, except perhaps for delayed-type hypersensitivity, it is difficult to think of CD4 T cells as effector cells, at least within the classical dogma of immunology (21), which identifies them as helpers rather than cytotoxic cells. However, recently a new lineage of CD4 T cells has been proposed that is distinct from classic Th1 and Th2 cells (22, 23). These IL-17 producing CD4 effector T cells (Th-17) have already been implicated in other mouse models of autoimmune diseases including experimental autoimmune encephalitis (23, 24) and collagen-induced arthritis (25). It has been shown that adoptive transfer of Th-17 cells induces disease and that treatment with anti-IL-17 not only delays

onset of disease, but can also treat and reverse the disease after it has already been induced (23, 24). It would be interesting to determine if there is actually a predominance of Th-17 cells in NOD.DQ8/Ab^0 (and NOD.DQ6/Ab^0) mice and whether treatment with anti-IL-17 could in fact reverse (or prevent) the development of myocarditis (or thyroiditis).

The prevalence and importance of Th-17 cells in other autoimmune diseases, especially those shown to involve CD4 T cells as the final effectors, (such as in diabetes) must also be investigated. If in fact IL-17 is a key modulator of type 1 diabetes, for example, applications of anti-Th-17 therapy both in patients that have diabetes, and those undergoing islet transplantation could be investigated. Although the outcome of clinical islet transplantations has been seriously improved since the initiation of the Edmonton Protocol in 1999 (26), the protocol depends on potent immunosuppression to protect against rejection and recurrent autoimmunity (26). In addition, insulin independence rates were steady at 82% one year post-transplantation, but five years post transplant only 10% are insulin independent (27) and immunosuppressive side effects have been observed in some patients (28). Perhaps the immunosuppression therapy is sufficient to prevent rejection, but not block the recurring autoimmunity. It is possible that specific immunosuppressive targeting of the autoimmune mechanism (e.g. with anti-IL-17 treatment if that is indeed the mechanism) would revert the insulin independence rates at five years to those at 1 year post transplant. Although a greater understanding of this pathway is

needed first, gene therapy in which transplanted islets are modified so that they are protected from Th-17 recruitment of macrophages can also be envisaged.

The field of Th-17 cells is an important emerging area of research and evidence for the involvement of Th-17s in autoimmunity has certainly been found (22-24, 29, 30). IL-23 is the cytokine released from activated APCs that induces the production of IL-17 by CD4 T cells (31). In a recent study, IL-23 was shown to induce diabetes in mice that had received subdiabetogenic treatment with multiple doses of streptozotocin (a chemical inducer of diabetes) (30). IL-23 administration induced sustained hyperglycemia, weight loss, increase in infiltrating cells, lower insulin content and increased apoptosis (30). In addition, IL-17 expression was elevated (30).

When investigating and planning potential therapies such as these, the balance of CD4 helper subsets must be kept in perspective. Th1 and Th2 CD4 subsets have always been shown to be tightly linked to each other such that if one subset is blocked the other subset expands (e.g. anti-IL-4 treatment blocks Th2 cells and tips the balance towards a Th1 mechanism; (32)). The same is true of this new subset; Th-17 cells have been shown, in some models, to only really develop in the absence of IFN-γ, a Th1 cytokine (22). It is important to keep these balancing acts in mind when devising therapies, as blocking one pathway may push the balance to an equally detrimental pathway.

IL-17 and IL-23 are not the only potential therapeutic targets within this CD4-macrophage mechanism. The immune system produces a number of soluble mediators and interaction with their receptors on immune or non-immune

cells allows these cytokines and chemokines to influence the type of immune response that develops. Treatments with a number of recombinant mediators or agents that block their actions are already entering treatment and prevention trials. For example, anti-TNF-α treatment has been licensed for both rheumatoid arthritis (33) and Crohn's disease (34, 35) and could be applicable for combating CD4-macrophage destruction by blocking destructive release of TNF-α by macrophages.

Once this final effector mechanism has been more clearly shown and understood in NOD.DQ8/Ab^0 myocarditis, therapies can be tested with ease in this model. Our ability to track disease progression non-invasively and repeatedly by ECG makes this myocarditis model a very powerful model for testing therapies. For most individuals who develop idiopathic dilated cardiomyopathy the only treatment is a heart transplant. One can anticipate and hope that therapies that are applicable to NOD.DQ8/Ab^0 autoimmune myocarditis will be applicable to the human disease and that perhaps individuals with IDCM would not need a transplant or, at the very least, the therapy could allow more time for a matched heart to be found.

A diverse set of HLA-DQ molecules is expressed across the human population and it is impossible to know *a priori* what effect any one of these might have when expressed transgenically in the autoimmune-prone NOD mouse background. The effects of DQ molecules in NOD mice can be considered in two situations: 1) in the presence of the diabetogenic mouse class II MHC molecule IAg7; and 2) in the absence of any mouse class II MHC (i.e. in the NOD/Ab^0). In

this thesis two DQ transgenic NOD lines were investigated, expressing either DQ8 (associated in humans with susceptibility to type 1 diabetes (3, 36, 37), rheumatoid arthritis (38), etc.) or DQ6 (associated in humans with susceptibility to narcolepsy (39, 40), multiple sclerosis (41, 42), etc., but also with resistance to type 1 diabetes (3, 37)).

Although not a major focus of the present thesis, it is worth noting that the NOD.DQ8 line (i.e. with IAg7 present) remains completely diabetes prone (incidence of diabetes 85-90%, and equal to that of our regular NOD colony; Appendix III and L. Wicker personal communication with J. Elliott), whereas NOD.DQ6 line (again with IAg7 present) are completely resistant to diabetes (incidence of diabetes 0%; Appendix III). Although these are only single transgenic lines for each DQ, and therefore it is impossible to rule out a founder effect (e.g. due to transgene insertion site, etc.), it is interesting that thus far the effects of the DQ8 and DQ6 molecules on diabetes in the regular NOD background parallels what is observed in humans. Since Lipes and colleagues report some of their DQ8 transgenic NOD lines (that are $DQ8^{+}$ $IAg7^{+/-}$) are susceptible to spontaneous diabetes (9), it is, in fact, only in the NOD.DQ6 line where a possible founder effect (vis-a-vis conferring diabetes resistance) needs to be ruled out. Should a second independent NOD.DQ6 line also prove to be diabetes resistant, the phenomenon would warrant further investigation. In this case, comparison of CD4 T cell repertoires between the NOD.DQ8 and NOD.DQ6 lines could potentially further our understanding of the molecular and cellular mechanisms behind human diabetes susceptibility and resistance alleles.

We are further constrained in our ability to extrapolate from the human situation to our NOD.DQ8/Ab^0 animals, because in humans other class II MHC molecules (DP and DR) are always expressed alongside of the DQ8 (i.e. on the surface of APCs), whereas in our DQ8 transgenic animals there is only the one MHC class II molecule expressed. It would be interesting to investigate the phenotype of mice expressing more than one MHC class II. These double transgenics may reflect the variations in the natural condition of human disease. From this thesis one might imagine a DQ6 DQ8 transgenic NOD line. In type 1 diabetes in humans, DQ6 (DQA1*0102, DQB1*602) is dominantly protective over DQ8 (DQA1*0301, DQB1*0302); an individual who is DQ8 positive is completely protected from diabetes if they are also DQ6 positive (3, 36, 37). Is the same true in NOD mice? NOD.DQ8 mice are susceptible to diabetes, NOD.DQ6 mice are not—would NOD.DQ6/DQ8 mice also be resistant to diabetes? NOD.DQ8/Ab^0 mice develop autoimmune myocarditis and NOD.DQ6/Ab^0 mice develop autoimmune thyroiditis—what phenotype would dominate in double HLA transgenic NOD.DQ8.DQ6/Ab^0 mice? Or would both phenotypes be present? Or neither? Preliminary investigations with F1 mice (NOD.DQ6$^{+/-}$DQ8$^{+/-}$/Ab^0) would suggest that both phenotypes would be present (Appendix II). DQ6$^{+/-}$DQ8$^{+/-}$/Ab^0 animals develop both autoimmune myocarditis and autoimmune thyroiditis; however, the kinetics of autoimmune myocarditis is slowed (Appendix II)—perhaps in doubly homozygous mice, the autoimmune myocarditis would be completely blocked.

What makes a certain DQ transgenic mouse develop a certain phenotype? Why would one DQ molecule be dominant over another DQ? It seems apparent, and is intuitive, that MHC class II molecules have favorite self antigens, antigens that they bind better than any other, but why is a particular DQ molecule permitted to induce its favorite autoimmunity? Many have proposed that autoimmunity is triggered by molecular mimicry (43). In this proposed mechanism the immune system mounts a response against a viral protein and then these anti-viral cytotoxic CD8 lymphocytes go on to react with a self protein that shares sequence homology to the viral protein. For example, one of the epitopes of GAD65 has apparent structural homology to an epitope of a protein from the Coxsackie B4 virus (43). So perhaps the favorite DQ8 antigen is very similar to a viral antigen, but how can the presence of DQ6 completely ablate the effects of this similarity? Our DQ transgenic strains may aid in the deciphering of some of these questions.

So often the focus of susceptibility to autoimmune diseases is on MHC class II molecules, but MHC class I molecules are also linked to susceptibility (e.g. MHC class I, A-2, in diabetes (44, 45)). The role of CD8 T cells in the induction of autoimmune myocarditis (NOD.DQ8/Ab^0 $\beta 2m^0$ animals do not develop myocarditis) and in the pathogenesis of the autoimmune thyroiditis (CD8 T cells predominate the infiltrate of NOD.DQ6/Ab^0 goiters) in DQ transgenic mice suggests these diseases are also dependent on class I MHC. Wild-type NOD animals are Kd, Db, whereas both of our DQ transgenic NOD models are Kb, Db, and it is possible that the Kb molecule is contributing to the myocarditis and

thyroiditis phenotypes. It would be interesting to investigate whether the same phenotypes would be seen in our transgenic animals if they were Kd instead of Kb. Kb is believed to be protective against diabetes in NOD mice (46), do our DQ transgenic NOD lines develop autoimmune myocarditis and thyroiditis solely because of the transgenic DQ or because first the diabetes is blocked with the Kb?

Unlike CD4 and CD8 T lymphocytes, B lymphocytes are not necessary for the progression of autoimmune myocarditis in NOD.DQ8/Ab^0 animals despite the strong B cell presence in the heart tissue and the high autoantibody titres. Similar reports have been described for experimental autoimmune myocarditis (47), but they are in contrast to what is generally reported for NOD mice, where only a small percentage of Ig heavy chain knockout animals develop peri-insulitis and <5% of animals develop diabetes (48, 49). We hypothesize that NOD.DQ8/Ab^0 IgH^0 and NOD/IgH^0 animals have different requirements for B cells because NODs require their highly efficient APC function and NOD.DQ8/Ab^0 animals do not. This hypothesis is in agreement with reports that it is the APC activity of B lymphocytes rather than antibody production that is required to achieve the full diabetes phenotype in NOD mice (50-52). Similar arguments about near sub-threshold antigen presentation capacity in the NOD may partially explain why in NOD mice, injection of CFA significantly delays diabetes onset (53), whereas in our NOD.DQ8/Ab^0 animals CFA appeared to accelerate the onset of myocarditis (16). Since even minor non-specific immune stimulation appears to prevent (or at least significantly delay) diabetes onset in

NOD mice, it may be that these environmental factors also reduce the critical APC capacity. In this context it may be of interest to determine if housing Ig heavy chain knockout NOD mice in a germ-free environment might alter the non-diabetic phenotype. It would also be of interest to investigate whether B cells play an ancillary or critical role in the autoimmune thyroiditis of NOD.DQ6/Ab^0 mice. B cells can be detected within the thyroid infiltrate of NOD.DQ6/Ab^0 animals and both anti-thyroglobulin and anti-thyroid peroxidase autoantibodies are present; however, the phenotypic strength of NOD.DQ6/Ab^0 thyroiditis is more reminiscent of NOD diabetes than the autoimmune strength of NOD.DQ8/Ab^0 myocarditis and perhaps, like NODs, NOD.DQ6/Ab^0 mice will require the antigen presenting potential of B cells. Studies involving immunosuppressives such as cyclosporine and experiments with NOD.DQ6/Ab^0 IgH^0 animals would be very informative in this regard.

We must attack autoimmunity from all sides and, in addition to deciphering mechanisms and proposing therapies, we must establish definitive diagnostic markers for autoimmune diseases. Primary prevention requires the development of markers that not only determine the stage, activity and progression of disease, but also accurately identify individuals at high risk before the actual onset of clinical disease. Vast HLA haplotype analysis of general populations and individuals suffering from autoimmunity and their relatives has been and will continue to be performed, but direct, specific associations cannot always be made and as such non-HLA markers must also be investigated. Autoantibodies seem to be the most likely candidates and many multi-lab autoantibody (e.g. in

diabetes) studies are reported (54). Similar to the autoantibody detection techniques used in diabetes (54, 55), the anti-thyroid peroxidase radioligand binding method, described in this thesis, has the potential to be a specific and sensitive, high throughput method for detecting autoimmune thyroiditis susceptible individuals.

Recently a TCR transgenic model of spontaneous autoimmune thyroiditis has implied the importance of thyroid peroxidase to autoimmune thyroiditis (56). The transgenic TCR is from a human T cell clone isolated from the thyroid infiltrate of a patient with autoimmune thyroiditis (56) and it is specific to a cryptic epitope (an epitope not normally seen by the immune system) within thyroid peroxidase. Studies would suggest that the TCR sees this TPO peptide (TPO536-547) in the context of the HLA-DQ6 (DQA1*0102, DQB1*0602) (57) and the original autoimmune thyroiditis patient was in fact DQA1*0102, DQB1*0602 positive (58, 59). This HLA-DQ6 is the same HLA-DQ6 as our NOD.DQ6/Ab^0 line. It would be of great interest to see if our DQ6 animals show a response to this and other TPO epitopes.

In conclusion, our laboratory has developed two HLA-DQ transgenic IAb knockout lines utilizing HLA-DQ haplotypes associated with type 1 diabetes: NOD.DQ8 (DQA1*0301, DQB1*0302)/Ab^0 animals develop autoimmune myocarditis and NOD.DQ6 (DQA1*0102, DQB1*0602)/Ab^0 develop autoimmune thyroiditis. The spontaneous nature and the similarity to the human autoimmune disease phenotype in these transgenic lines makes them an invaluable resource for the autoimmune field. The genetic composition of these animals has the

potential to answer questions about favorite autoantigens, genetic susceptibility and autoimmune triggers; the utilization of these models to investigate the immune mechanisms of autoimmune diseases also is extremely informative as to the disease etiology. Further studies such as those investigating the disease important cytokines (ELISAs, flow cytometry, knockouts) and the T cell autoantigens (T cell lines and clones, T cell westerns) will only further our understanding of these extremely common autoimmune diseases allowing for the generation and testing of new immune therapies.

5.2 References

1. Collins, J., and S. Gough. 2002. Autoimmunity in thyroid disease. *Eur J Nucl Med Mol Imaging 29 Suppl 2:S417.*

2. Barnett, A. H., C. Eff, R. D. Leslie, and D. A. Pyke. 1981. Diabetes in identical twins. A study of 200 pairs. *Diabetologia 20:87.*

3. Thorsby, E., and K. S. Ronningen. 1993. Particular HLA-DQ molecules play a dominant role in determining susceptibility or resistance to type 1 (insulin-dependent) diabetes mellitus. *Diabetologia 36:371.*

4. Williams, A. J., P. J. Bingley, W. P. Moore, and E. A. Gale. 2002. Islet autoantibodies, nationality and gender: a multinational screening study in first-degree relatives of patients with Type I diabetes. *Diabetologia 45:217.*

5. Priori, R., E. Medda, F. Conti, E. A. Cassara, M. G. Danieli, R. Gerli, R. Giacomelli, F. Franceschini, A. Manfredi, M. Pietrogrande, M. A. Stazi, and G. Valesini. 2003. Familial autoimmunity as a risk factor for systemic lupus erythematosus and vice versa: a case-control study. *Lupus 12:735.*

6. Alarcon-Segovia, D., M. E. Alarcon-Riquelme, M. H. Cardiel, F. Caeiro, L. Massardo, A. R. Villa, and B. A. Pons-Estel. 2005. Familial aggregation of systemic lupus erythematosus, rheumatoid arthritis, and other autoimmune diseases in 1,177 lupus patients from the GLADEL cohort. *Arthritis Rheum 52:1138.*

7. Broadley, S. A., J. Deans, S. J. Sawcer, D. Clayton, and D. A. Compston. 2000. Autoimmune disease in first-degree relatives of patients with multiple sclerosis. A UK survey. *Brain 123 (Pt 6):1102.*

8. Cooper, G. S., and B. C. Stroehla. 2003. The epidemiology of autoimmune diseases. *Autoimmun Rev 2:119.*

9. Taylor, J. A., E. Havari, M. F. McInerney, R. Bronson, K. W. Wucherpfennig, and M. A. Lipes. 2004. A spontaneous model for autoimmune myocarditis using the human MHC molecule HLA-DQ8. *J Immunol 172:2651.*

10. Ogasawara, K., J. A. Hamerman, H. Hsin, S. Chikuma, H. Bour-Jordan, T. Chen, T. Pertel, C. Carnaud, J. A. Bluestone, and L. L. Lanier. 2003. Impairment of NK cell function by NKG2D modulation in NOD mice. *Immunity 18:41.*

11. Poulton, L. D., M. J. Smyth, C. G. Hawke, P. Silveira, D. Shepherd, O. V. Naidenko, D. I. Godfrey, and A. G. Baxter. 2001. Cytometric and functional analyses of NK and NKT cell deficiencies in NOD mice. *Int Immunol 13:887.*

12. Wang, B., Y. B. Geng, and C. R. Wang. 2001. CD1-restricted NK T cells protect nonobese diabetic mice from developing diabetes. *J Exp Med 194:313.*

13. Serreze, D. V., J. W. Gaedeke, and E. H. Leiter. 1993. Hematopoietic stem-cell defects underlying abnormal macrophage development and maturation in NOD/Lt mice: defective regulation of cytokine receptors and protein kinase C. *Proc Natl Acad Sci U S A 90:9625.*

14. Salomon, B., D. J. Lenschow, L. Rhee, N. Ashourian, B. Singh, A. Sharpe, and J. A. Bluestone. 2000. B7/CD28 costimulation is essential for the homeostasis of the CD4+CD25+ immunoregulatory T cells that control autoimmune diabetes. *Immunity 12:431.*

15. Baxter, A. G., and A. Cooke. 1993. Complement lytic activity has no role in the pathogenesis of autoimmune diabetes in NOD mice. *Diabetes 42:1574.*

16. Elliott, J. F., J. Liu, Z. N. Yuan, N. Bautista-Lopez, S. L. Wallbank, K. Suzuki, D. Rayner, P. Nation, M. A. Robertson, G. Liu, and K. M. Kavanagh. 2003. Autoimmune cardiomyopathy and heart block develop spontaneously in HLA-DQ8 transgenic IAbeta knockout NOD mice. *Proc Natl Acad Sci U S A 100:13447.*

17. Bryant, D., L. Becker, J. Richardson, J. Shelton, F. Franco, R. Peshock, M. Thompson, and B. Giroir. 1998. Cardiac failure in transgenic mice with myocardial expression of tumor necrosis factor-alpha. *Circulation 97:1375.*

18. Lane, J. R., D. A. Neumann, A. Lafond-Walker, A. Herskowitz, and N. R. Rose. 1993. Role of IL-1 and tumor necrosis factor in coxsackie virus-induced autoimmune myocarditis. *J Immunol 151:1682.*

19. Wang, S. H., J. D. Bretz, E. Phelps, E. Mezosi, P. L. Arscott, S. Utsugi, and J. R. Baker, Jr. 2002. A unique combination of inflammatory cytokines enhances apoptosis of thyroid follicular cells and transforms nondestructive to destructive thyroiditis in experimental autoimmune thyroiditis. *J Immunol 168:2470.*

20. Zaccone, P., Z. Fehervari, L. Blanchard, F. Nicoletti, C. K. Edwards, 3rd, and A. Cooke. 2002. Autoimmune thyroid disease induced by thyroglobulin and lipopolysaccharide is inhibited by soluble TNF receptor type I. *Eur J Immunol 32:1021.*

21. Goldsby, R. A., T. J. Kindt, and B. A. Osborne. 2000. *Kuby Immunology.* W.H. Freeman and Company, New York.

22. Harrington, L. E., R. D. Hatton, P. R. Mangan, H. Turner, T. L. Murphy, K. M. Murphy, and C. T. Weaver. 2005. Interleukin 17-producing CD4+ effector T cells develop via a lineage distinct from the T helper type 1 and 2 lineages. *Nat Immunol 6:1123.*

23. Park, H., Z. Li, X. O. Yang, S. H. Chang, R. Nurieva, Y. H. Wang, Y. Wang, L. Hood, Z. Zhu, Q. Tian, and C. Dong. 2005. A distinct lineage of CD4 T cells regulates tissue inflammation by producing interleukin 17. *Nat Immunol 6:1133.*

24. Langrish, C. L., Y. Chen, W. M. Blumenschein, J. Mattson, B. Basham, J. D. Sedgwick, T. McClanahan, R. A. Kastelein, and D. J. Cua. 2005. IL-23 drives a pathogenic T cell population that induces autoimmune inflammation. *J Exp Med 201:233.*

25. Murphy, C. A., C. L. Langrish, Y. Chen, W. Blumenschein, T. McClanahan, R. A. Kastelein, J. D. Sedgwick, and D. J. Cua. 2003. Divergent pro- and antiinflammatory roles for IL-23 and IL-12 in joint autoimmune inflammation. *J Exp Med 198:1951.*

26. Shapiro, A. M., J. R. Lakey, E. A. Ryan, G. S. Korbutt, E. Toth, G. L. Warnock, N. M. Kneteman, and R. V. Rajotte. 2000. Islet transplantation in seven patients with type 1 diabetes mellitus using a glucocorticoid-free immunosuppressive regimen. *N Engl J Med 343:230.*

27. Emamaullee, J. 2005. Apoptosis Inhibition in Islet Transplantation. In *Medical Microbiology and Immunology*. University of Alberta, Edmonton, p. 187.

28. Ryan, E. A., J. R. Lakey, B. W. Paty, S. Imes, G. S. Korbutt, N. M. Kneteman, D. Bigam, R. V. Rajotte, and A. M. Shapiro. 2002. Successful islet transplantation: continued insulin reserve provides long-term glycemic control. *Diabetes 51:2148.*

29. Hofstetter, H. H., S. M. Ibrahim, D. Koczan, N. Kruse, A. Weishaupt, K. V. Toyka, and R. Gold. 2005. Therapeutic efficacy of IL-17 neutralization in murine experimental autoimmune encephalomyelitis. *Cell Immunol.*

30. Mensah-Brown, E. P., A. Shahin, M. Al-Shamisi, X. Wei, and M. L. Lukic. 2006. IL-23 leads to diabetes induction after subdiabetogenic treatment with multiple low doses of streptozotocin. *Eur J Immunol 36:216.*

31. McKenzie, B. S., R. A. Kastelein, and D. J. Cua. 2005. Understanding the IL-23-IL-17 immune pathway. *Trends Immunol.*

32. Del Prete, G. 1998. The concept of type-1 and type-2 helper T cells and their cytokines in humans. *Int Rev Immunol 16:427.*

33. Hamilton, K., and E. W. Clair. 2000. Tumour necrosis factor-alpha blockade: a new era for effective management of rheumatoid arthritis. *Expert Opin Pharmacother 1:1041.*

34. Sandborn, W. J., and S. B. Hanauer. 1999. Antitumor necrosis factor therapy for inflammatory bowel disease: a review of agents, pharmacology, clinical results, and safety. *Inflamm Bowel Dis 5:119.*

35. Kam, L. Y., and S. R. Targan. 2000. TNF-alpha antagonists for the treatment of Crohn's disease. *Expert Opin Pharmacother 1:615.*

36. Thomson, G. 1983. Investigation of the mode of inheritance of the HLA associated diseases by the method of antigen genotype frequencies among diseased individuals. *Tissue Antigens 21:81.*

37. Baisch, J. M., T. Weeks, R. Giles, M. Hoover, P. Stastny, and J. D. Capra. 1990. Analysis of HLA-DQ genotypes and susceptibility in insulin-dependent diabetes mellitus. *N Engl J Med 322:1836.*

38. Nabozny, G. H., J. M. Baisch, S. Cheng, D. Cosgrove, M. M. Griffiths, H. S. Luthra, and C. S. David. 1996. HLA-DQ8 transgenic mice are highly susceptible to collagen-induced arthritis: a novel model for human polyarthritis. *J Exp Med 183:27.*

39. Mignot, E., X. Lin, J. Arrigoni, C. Macaubas, F. Olive, J. Hallmayer, P. Underhill, C. Guilleminault, W. C. Dement, and F. C. Grumet. 1994. DQB1*0602 and DQA1*0102 (DQ1) are better markers than DR2 for narcolepsy in Caucasian and black Americans. *Sleep 17:S60.*

40. Planelles, D., N. Puig, A. Beneto, E. Gomez, P. Rubio, V. Mirabet, S. Bonanad, I. Blasco, and J. A. Montoro. 1997. HLA-DQA, -DQB and -DRB allele contribution to narcolepsy susceptibility. *Eur J Immunogenet 24:409.*

41. Hillert, J. 1994. Human leukocyte antigen studies in multiple sclerosis. *Ann Neurol 36 Suppl:S15.*

42. Spurkland, A., E. G. Celius, I. Knutsen, A. Beiske, E. Thorsby, and F. Vartdal. 1997. The HLA-DQ(alpha 1*0102, beta 1*0602) heterodimer may confer susceptibility to multiple sclerosis in the absence of the HLA-DR(alpha 1*01, beta 1*1501) heterodimer. *Tissue Antigens 50:15.*

43. Atkinson, M. A., and N. K. Maclaren. 1994. The pathogenesis of insulin-dependent diabetes mellitus. *N Engl J Med 331:1428.*

44. Marron, M. P., R. T. Graser, H. D. Chapman, and D. V. Serreze. 2002. Functional evidence for the mediation of diabetogenic T cell responses by HLA-A2.1 MHC class I molecules through transgenic expression in NOD mice. *Proc Natl Acad Sci U S A 99:13753.*

45. Fennessy, M., K. Metcalfe, G. A. Hitman, M. Niven, P. A. Biro, J. Tuomilehto, and E. Tuomilehto-Wolf. 1994. A gene in the HLA class I region contributes to susceptibility to IDDM in the Finnish population. Childhood Diabetes in Finland (DiMe) Study Group. *Diabetologia 37:937.*

46. Serreze, D. V., T. M. Holl, M. P. Marron, R. T. Graser, E. A. Johnson, C. Choisy-Rossi, R. M. Slattery, S. M. Lieberman, and T. P. DiLorenzo. 2004. MHC class II molecules play a role in the selection of autoreactive class I-restricted CD8 T cells that are essential contributors to type 1 diabetes development in nonobese diabetic mice. *J Immunol 172:871.*

47. Malkiel, S., S. Factor, and B. Diamond. 1999. Autoimmune myocarditis does not require B cells for antigen presentation. *J Immunol 163:5265.*

48. Serreze, D. V., H. D. Chapman, D. S. Varnum, M. S. Hanson, P. C. Reifsnyder, S. D. Richard, S. A. Fleming, E. H. Leiter, and L. D. Shultz. 1996. B lymphocytes are essential for the initiation of T cell-mediated autoimmune diabetes: analysis of a new "speed congenic" stock of NOD.Ig mu null mice. *J Exp Med 184:2049.*

49. Akashi, T., S. Nagafuchi, K. Anzai, S. Kondo, D. Kitamura, S. Wakana, J. Ono, M. Kikuchi, Y. Niho, and T. Watanabe. 1997. Direct evidence for the contribution of B cells to the progression of insulitis and the development of diabetes in non-obese diabetic mice. *Int Immunol 9:1159.*

50. Serreze, D. V., S. A. Fleming, H. D. Chapman, S. D. Richard, E. H. Leiter, and R. M. Tisch. 1998. B lymphocytes are critical antigen-presenting cells for the initiation of T cell-mediated autoimmune diabetes in nonobese diabetic mice. *J Immunol 161:3912.*

51. Serreze, D. V., and P. A. Silveira. 2003. The role of B lymphocytes as key antigen-presenting cells in the development of T cell-mediated autoimmune type 1 diabetes. *Curr Dir Autoimmun 6:212.*

52. Wong, F. S., L. Wen, M. Tang, M. Ramanathan, I. Visintin, J. Daugherty, L. G. Hannum, C. A. Janeway, Jr., and M. J. Shlomchik. 2004. Investigation of the role of B-cells in type 1 diabetes in the NOD mouse. *Diabetes 53:2581.*

53. Sadelain, M. W., H. Y. Qin, J. Lauzon, and B. Singh. 1990. Prevention of type I diabetes in NOD mice by adjuvant immunotherapy. *Diabetes 39:583.*

54. Bonifacio, E., M. Atkinson, G. Eisenbarth, D. Serreze, T. W. Kay, E. Lee-Chan, and B. Singh. 2001. International Workshop on Lessons From Animal Models for Human Type 1 Diabetes: identification of insulin but not

glutamic acid decarboxylase or IA-2 as specific autoantigens of humoral autoimmunity in nonobese diabetic mice. *Diabetes 50:2451.*

55. Gianani, R., D. U. Rabin, C. F. Verge, L. Yu, S. R. Babu, M. Pietropaolo, and G. S. Eisenbarth. 1995. ICA512 autoantibody radioassay. *Diabetes 44:1340.*

56. Quaratino, S., E. Badami, Y. Y. Pang, I. Bartok, J. Dyson, D. Kioussis, M. Londei, and L. Maiuri. 2004. Degenerate self-reactive human T-cell receptor causes spontaneous autoimmune disease in mice. *Nat Med 10:920.*

57. Quaratino, S., M. Feldmann, C. M. Dayan, O. Acuto, and M. Londei. 1996. Human self-reactive T cell clones expressing identical T cell receptor beta chains differ in their ability to recognize a cryptic self-epitope. *J Exp Med 183:349.*

58. Quaratino, S., L. P. Duddy, and M. Londei. 2000. Fully competent dendritic cells as inducers of T cell anergy in autoimmunity. *Proc Natl Acad Sci U S A 97:10911.*

59. Badami, E., L. Maiuri, and S. Quaratino. 2005. High incidence of spontaneous autoimmune thyroiditis in immunocompetent self-reactive human T cell receptor transgenic mice. *J Autoimmun 24:85.*

APPENDIX I

SUPPLEMENTARY FIGURES AND TABLES

A.

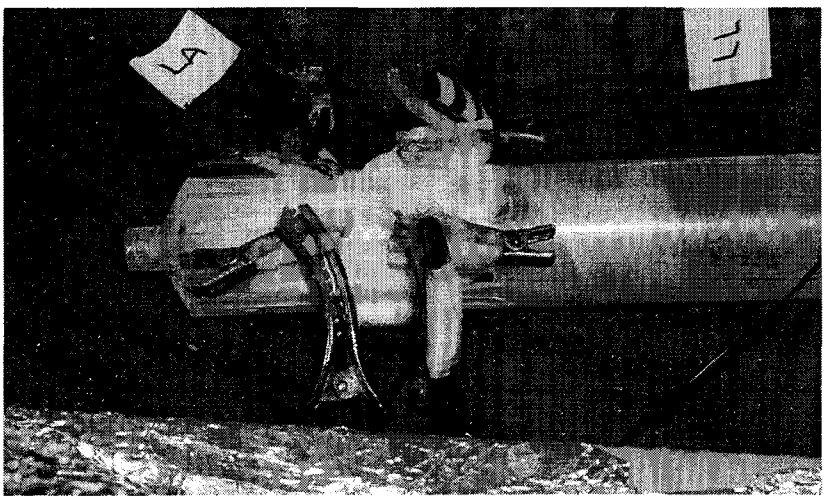

B.

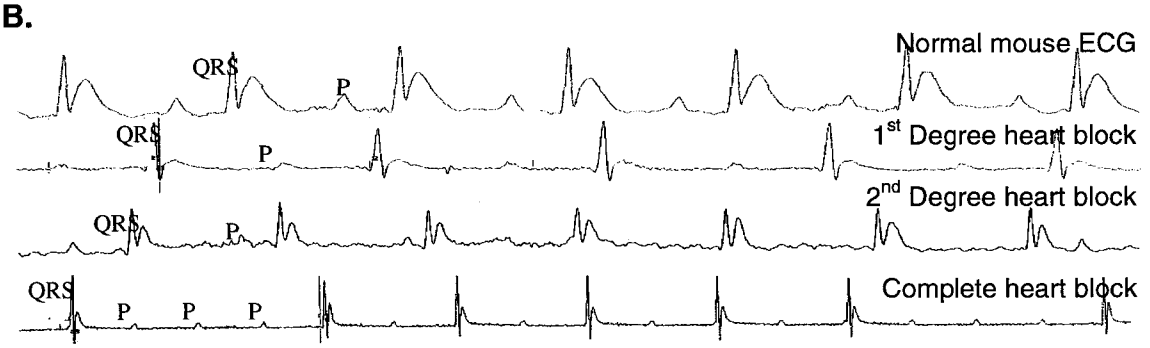

Supplementary Figure AI.1: ECG apparatus. (A) Mouse inside the modified syringe barrel with limb leads attached to each paw for ECG acquisition. (B) Representative ECG analyses, with the location of P waves and QRS complexes as indicated. A healthy mouse ECG, taken from a NOD.DQ6/Ab^0 mouse has a P wave value of ≤36msec. NOD.DQ8/Ab^0 mice with 1st degree A-V block have P wave values that are >36msec, while mice exhibiting 2nd degree A-V block have migrating P waves, and mice with complete A-V block have P waves that are completely dissociated from the QRS complex.

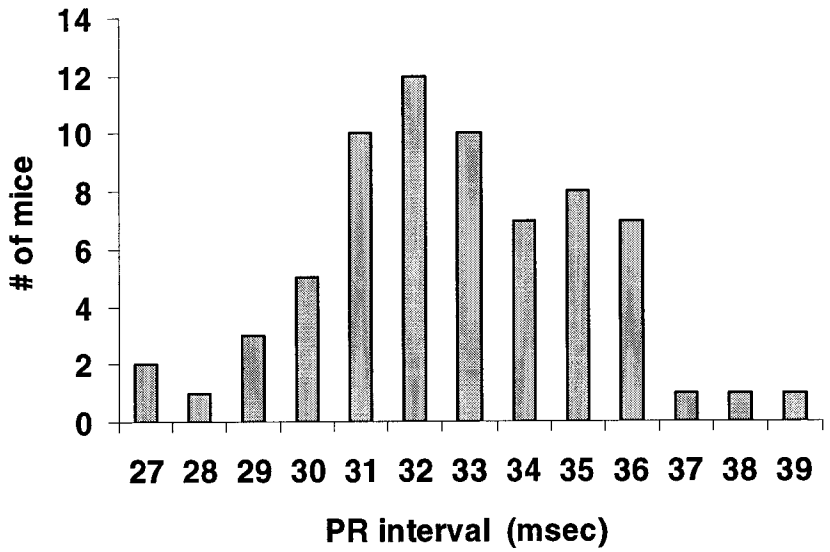

Supplementary Figure AI.2: Determination of normal PR interval. ECGs were collected on 68 normal mice of various backgrounds and the PR interval was calculated for each mouse and normal PR intervals were generally less than 37msec.

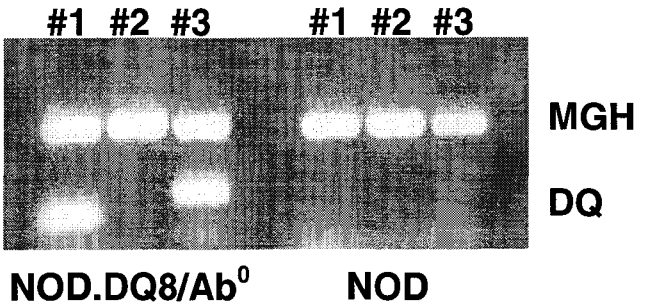

Supplementary Figure AI.3: PCR confirms that NOD.DQ8/Ab^0 mice are DQA1*0301, DQB1*0302. NOD and NOD.DQ8/Ab^0 mouse tail DNA, prepared with Qiagen DNeasy Kit, was PCRed with primer mixes containing primers for mouse growth hormone and primers for DQ halpotypes. A mouse that is DQA1*0301, DQB1*0302 will be positive for primer pairs #1 and #3, but negative for primer pair #2.

A. Digest

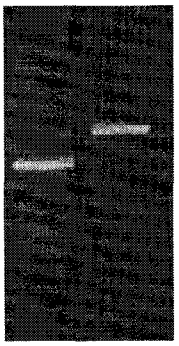

Plasmid / Linearized

B. PCR insert

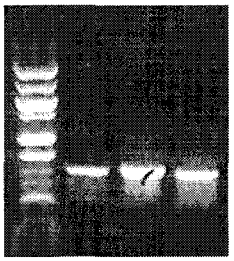

C. Gel Slices, Insert and vector

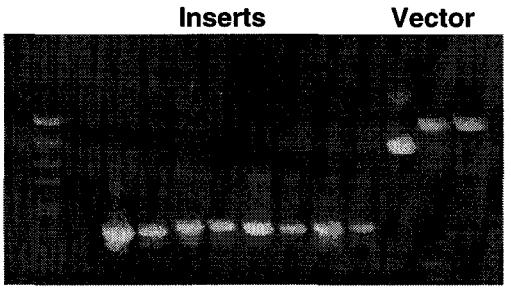

D. Digest of Wizards

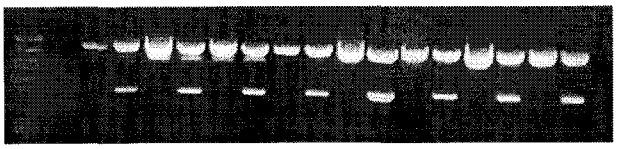

E. RNA

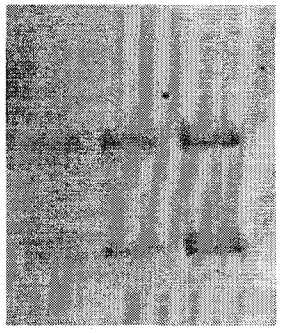

Supplementary Figure AI.4: Preparation of RNA and probes for RNAse protection assay—Representative results. A. Not I digest (right) to linearize DNA templates (left) containing the MHC class II chain. IAb^{g7} is shown. B. PCR of MHC class II chain insert using primers that also add Sfi I restriction sites to each end of the insert. $IA\alpha^{g7}$, $IA\beta^{g7}$, and DQ8α are shown. C. DNA run on a low melting point agarose gel to cut out gel slices for ligations. Inserts: Undigested and digested for $IA\alpha^{g7}$, $IA\beta^{g7}$, and DQ8α. Vector: circular, linearized in the absence and presence of CIP. D. After ligation and transformation DNA preparations were prepared (wizards). Digestion of the wizard preparations with Sfi I shows the presence of the MHC class II insert. E. RNA for RNAse protection assay was prepared using Qiagen RNeasy Kit.

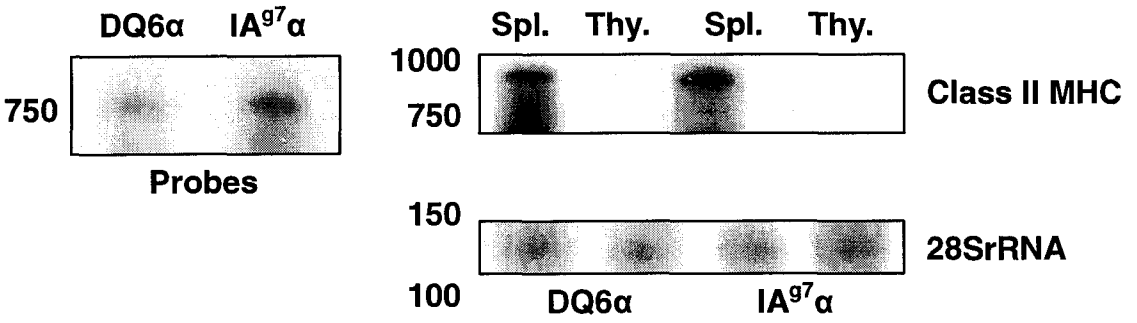

Supplementary Figure AI.5: DQ transgene mRNA levels are not abnormally elevated in thyroids of NOD.DQ6$^{+/-}$/Ab$^{+/-}$ mice. DQ6α, IAα and 28SrRNA RNA probes were made (see materials and methods in Chapter 2) and used to probe various NOD.DQ6$^{+/-}$/Ab$^{+/-}$ tissues, including the thyroid and spleen shown here, using a RNAse Protection Assay. Identical results were seen with probes for the β chains. (Note: the mice are a result of a F1 cross and do not develop autoimmune thyroiditis. The cross was made so that the levels of DQ and IA mRNA could be compared in the same RNA samples. These experiments disprove the hypothesis that thyroid disease in the NOD.DQ6/Ab^{0} mice might be due to abnormally high/aberrant expression of the DQ transgene specifically in the thyroid.

A. B.

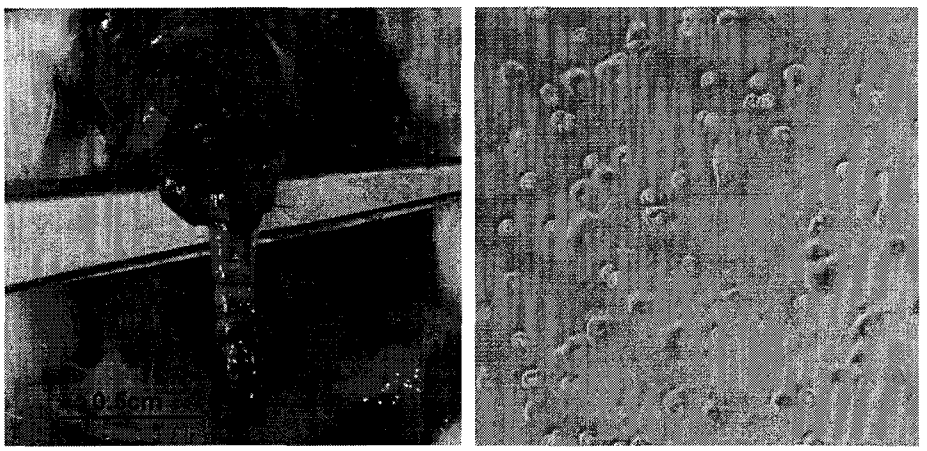

Supplementary Figure AI.6: Thyroid cell line and mouse thyroid glands used to prepare antigen lysates. A. IAb knockout NOD mice were maintained on 0.01% ATA water for 10 weeks and enlarged thyroids were then dissected to be used as a source of mouse thyroid antigen in Western blot and ELISA assays. B. FRTL-5, rat thyroid cell line, cells (ATCC#CRL-1468) were cultured in F12 COON's modification medium plus hormone cocktail (See Methods 3.2.6). Cells were harvested with CTC solution for a source of thyroid antigen in Western blot and ELISA assays.

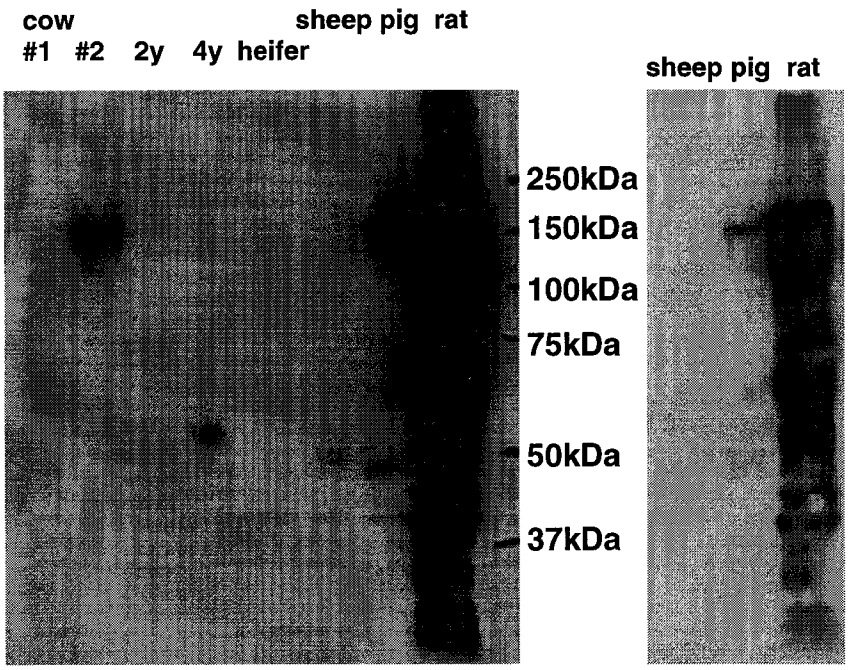

Supplementary Figure AI.7: Anti-thyroid autoantibodies in NOD.DQ6/Ab^0 serum appear to specifically recognize rodent thyroid antigens. Various sources of thyroids were homogenized with 1ml SDS-PAGE stacking buffer and then passed through a 18G needle ten times to shear the DNA and RNA. After spinning at 16,000 *x g* (10min) the protein concentration of the supernatants were analyzed by BCA protein assay. 50µg of protein was loaded on 7.5% polyacrylamide gels and run at constant current of 40mA. After separation, the proteins were transferred onto nitrocellulose membrane at constant current of 250mA. Blots were then blocked for 1 hour in soy milk, incubated for 2 hours with mouse serum at 1:100 in soy milk, washed with PBS-T (3 x 15min), incubated for 1 hour with HRP-conjugated goat anti-mouse IgG at 1:2500 in soy milk, washed with PBS-T (3 x 15min), developed with ECL for 2min, and exposed to film. All incubations were done at room temperature. A control blot with Balb/c serum did not show any staining.

	5' Primer	3' Primer
IAα-Sfi	CTCTCTGGCCGGAGA-GGCCACCATGCCGTG-CAGCAGAGCTCT	CTCTCTGGCCAAGAT-GGCCTCATAAAGGCC-CTGGGTGTC
IAβ-Sfi	CTCTCTGGCCGGAGA-GGCCACCATGGCTCT-GCAGATCCCCAG	CTCTCTGGCCAAGAT-GGCCTCACTGCAGGA-GCCCTGCT
DQα-Sfi	CTCTCTGGCCGGAGA-GGCCACCATGATCCT-AAACAAAGCTCT	CTCTCTGGCCAAGAT-GGCCTACAATGGCCC-TTGGTGTCTGGAAG
DQβa-Sfi	CTCTCTGGCCGGAGA-GGCCACCATGTCTTG-GAAGAAGGCTTT	CTCTCTGGCCAAGAT-GGCCTCAGTGCAGAA-GCCCTTTC
DQβb-Sfi	CTCTCTGGCCGGAGA-GGCCACCATGTCTTG-GAAAAAGGCTTT	CTCTCTGGCCAAGAT-GGCCTCAGTGCAGGA-GCCCTTTC
DQβc-Sfi	CTCTCTGGCCGGAGA-GGCCACCATGTCTTG-GAAGAAGGTCTTT	CTCTCTGGCCAAGAT-GGCCTCAGTGCAGAA-GCCCTGC

Table AI.1: MHC class II/Sfi I primers for cloning of RNA probes. Primers were designed to amplify the specific MHC class II chain as well as inserting Sfi I restriction sites so that the DNA could be inserted into the vector pJFE7sCMV which has T3 and T7 polymerase sites.

APPENDIX II

AUTOIMMUNITY OF NOD.DQ6$^{+/-}$DQ8$^{+/-}$/Ab^{0} MICE

AII.1 Introduction

Specific MHC class II haplotypes have been shown repeatedly to be linked to susceptibility to a number of autoimmunity diseases including type 1 diabetes, autoimmune myocarditis and autoimmune thyroiditis; DQ8 (DQA1*0301, DQB1*0302) and DQ6 (DQA1*0102, DQB1*0602) are no exception. HLA-transgenic animal models have helped us understand the importance of genetics to autoimmunity.

NOD.DQ8/Ab^0 animals develop spontaneous autoimmune myocarditis (1, 2). NOD.DQ8/Ab^0 mice show an organ and cell specific response against normal cardiomyocytes. Mononuclear cell infiltrate is seen, anti-heart autoantibodies are present and animals develop complete heart block which results in complete heart failure (1, 2). NOD.DQ8/Ab^0 mice are a mouse model of human idiopathic dilated cardiomyopathy.

NOD.DQ6/Ab^0 animals develop spontaneous autoimmune thyroiditis (Chapter 3). NOD.DQ6/Ab^0 mice show infiltrate within the thyroid which causes thyroid follicular destruction and fibrosis and they also develop anti-thyroid autoantibodies (Chapter 3). The autoimmune thyroiditis of NOD.DQ6/Ab^0 animals progresses to hypothyroidism and they show elevated TSH levels and decreased T4 levels (Chapter 3). NOD.DQ6/Ab^0 mice are a mouse model of human Hashimoto's thyroiditis.

DQ8 (DQA1*0301, DQB1*0302) is associated with susceptibility to type 1 diabetes while DQ6 (DQA1*0102, DQB1*0602) is associated with resistance (3, 4). 90% of type 1 diabetics are DQ8 positive, but if an individual is DQ6 and DQ8

positive then the individual is completely protected from diabetes (3, 4) suggesting that DQ6 is dominant over DQ8. We posed the question of whether in transgenic NOD mice the same dominance would be observed. The generation of transgenic mice (e.g. NOD.DQ6.DQ8/Ab^0 animals) is an expensive venture and so we decided to do some preliminary experiments with DQ6 x DQ8 F1 mice.

Here we report data showing that NOD.$DQ6^{+/-}DQ8^{+/-}/Ab^0$ mice develop both phenotypes: autoimmune thyroiditis and autoimmune myocarditis. NOD.$DQ6^{+/-}DQ8^{+/-}/Ab^0$ animals have enlarged hearts and develop complete heart block. They show mononuclear cell infiltrate of the heart and anti-heart autoantibodies. NOD.$DQ6^{+/-}DQ8^{+/-}/Ab^0$ animals also show infiltrate within the thyroid, anti-thyroid autoantibodies and elevated serum TSH levels.

AII.2 Materials and Methods

AII.2.1 Mice

The origins of NOD.DQ8/Ab^0 and NOD.DQ6/Ab^0 lines have been described previously ((1) and Chapter 2).

NOD.$DQ6^{+/-}DQ8^{+/-}/Ab^0$ animals were generated by crossing NOD.DQ8/Ab^0 mice with NOD.DQ6/Ab^0 mice.

All breeding colonies were housed in conventional SPF facilities. Care and handling was done in accordance with the guidelines of the Canadian Council on Animal Care, and all experimental protocols were approved by our institutional Health Sciences Animal Policy and Welfare Committee.

AII.2.2 Histology

Tissues from NOD.DQ8$^{+/-}$DQ6$^{+/-}$/Ab^{0} were removed and placed in 10% buffered formalin (Fisher, Fair Lawn, NJ). The tissues were then processed into paraffin blocks by standard methods and slides were cut. Slides were then stained with hematoxylin and eosin (H&E) using standard methods and analyzed for the presence of mononuclear cell infiltrate

AII.2.3 Monitoring Mice for Myocarditis by Electrocardiogram

These methods have been described previously (see Supporting Text for (1)). In brief, non-sedated mice were placed in a syringe barrel which had been modified to allow access to the feet. Electrodes, with limb leads attached, were clipped to each of the four foot pads and ECG leads I, II, III, AVR, and AVL were simultaneously recorded (Supplementary Figure AI.1.A). Parameters measured included sinus rate (P-P interval), PR interval (onset of P wave to onset of QRS complex), and ventricular rate (QRS-QRS interval). First degree heart block was defined as a PR interval greater than 36msec, a value that is >3SD above the mean for a large group of normal animals (Supplementary Figure A1.2). Complete heart block was diagnosed whenever the P waves (i.e. atrial depolarization events) were completely dissociated from the QRS complexes (i.e. ventricular depolarization events) (Supplementary Figure AI.1.B).

AII.2.4 TSH Elisa

Analysis of serum TSH levels was also done using a Rodent Thyroid

Stimulating Hormone (TSH) ELISA Test Kit purchased from Endocrine Technologies, California. In brief, the microtiter wells included with the kit are coated with affinity purified anti-TSH antibody and serum and a constant amount of anti-TSH antibody conjugated with HRP (provided with kit) was added to those pre-coated wells. During incubation, the serum TSH reacts simultaneously with the two antibodies, resulting in the TSH being sandwiched between the solid-phase and enzyme-linked antibodies. Any unbound HRP-labelled TSH antibodies were washed away, TMB solution was added and the reaction was stopped using 2N HCl and the absorbance was measured at 450nm. A series of TSH standards were also analyzed, a standard curve was made, and the concentration of TSH in the serum was calculated.

AII.2.5 Protein Lysates

Spleen and heart lysates from Balb/c mice and rat thyroids were prepared by snap freezing the tissue in liquid nitrogen, grinding the tissue with a mortar and pestle in the presence of protease inhibitors in PBS, and pushing the lysate through a 18 gauge needle. Samples were spun down and the supernatant was used.

For mouse thyroid lysates, 14 week old IAb knockout NOD mice were maintained on 0.1% 3-amino-1,2,4-triazole (ATA; Sigma, St.Louis, MO) in their drinking water for 10 weeks. ATA has been shown to chemically induce enlarged thyroids (5). After 10 weeks, mice were euthanized and their thyroids dissected.

A larger thyroid reduces the amount of contaminating non-thyroid tissue dissected along with the thyroid.

For the cow thyroid lysate, the tissue was homogenized with 1ml SDS-PAGE stacking buffer and then passed through a 18 gauge needle 10 times. The lysate was then centrifuged (16,000 *x g*, 10min) and the supernatant was used.

The FRTL-5 cell line (ATCC# CRL-1468) was a gift from the Ginsberg Lab (University of Alberta, Edmonton, AB). FRTL-5 cells are an epithelial-like adherent cell line isolated from rat thyroids and they are grown in F12 COON's modification medium (plus sodium carbonate and pH adjusted to 7.35 with HCl) containing insulin (10ug/ml), Gly-His-Lys peptide (10ng/ml), cortisol (10nM), transferrin (5ug/ml), TSH (10mU/ml), and somatostatin (10ng/ml), all purchased from Sigma, St. Louis, MO. 10% heat inactivated fetal calf serum and 1X penicillin/streptomycin (both from Invitrogen, Burlington, ON) were also added. For lysates, cells were released from the flask with CTC solution which is composed of collagenase (20U/ml), trypsin-EDTA (0.076%), and heat inactivated chicken serum (2%) in F12 COON's modification medium. Cells were then harvested, washed, and then freeze-thawed three times and homogenized by passing through a 18 gauge needle in the presence of EDTA-free protease inhibitors.

For the control cell line, we used βTC-tets, a cell line we were culturing at the time in the lab. βTC-Tet cells are an islet β-cell line derived from a C3H transgenic mouse insulinoma and they express a tetracycline-regulated SV40

Tag (6, 7). Cells were maintained in DMEM supplemented with 10% fetal calf serum, 450 mg/dL glucose, 1 mM sodium pyruvate, 2 mM L-glutamine, 100 U/mL penicillin and 100 µg/mL streptomycin (Invitrogen Canada, Burlington, ON) and incubated at 5% CO_2 at 37°C. The cells were allowed to continuously proliferate and were then harvested using trypsin, washed, freeze-thawed 3 times in the presence of protease inhibitors and passed through an 18 gauge needle.

The protein concentration of all lysates was quantified by standard methods using a BCA protein assay.

The porcine cardiac myosin and skeletal myosin were purchased from Sigma (St.Louis, MO).

AII.2.6 SDS-PAGE and Western Blots

Antigens were loaded at 10µg/well into 10% polyacrylamide gels and run at 100V. Proteins were then transferred onto a nitrocellulose membrane at 250mA constant for 1 hour. The membrane was blocked for 1 hour with 5% skim milk-PBS at room temperature. The membrane was then incubated with mouse serum diluted 1:200 in 5% skim milk-PBS overnight at 4°C, washed with PBS-T, incubated with goat anti-mouse IgG-HRP diluted 1:2000 in 5% skim milk-PBS for 1 hour at room temperature. After washing with PBS-T, the membrane was developed with ECL (Amersham Biosciences, Piscataway, NJ) and Kodak Biomax MR film.

AII.3 Results

NOD.DQ8/Ab^0 animals develop spontaneous myocarditis (1) and as was shown in Chapter 3 of this thesis NOD.DQ6/Ab^0 animals develop spontaneous thyroiditis and hypothyroidism. Here we investigate the autoimmune phenotype of NOD.DQ6$^{+/-}$DQ8$^{+/-}$/Ab^0 mice.

NOD.DQ6$^{+/-}$DQ8$^{+/-}$/Ab^0 animals of various ages from 6 weeks to 50 weeks were sacrificed and their spleens, kidneys, livers, hearts, lungs, salivary glands, thyroids, and thymuses were analyzed for mononuclear cell infiltrate after H&E staining. Mononuclear cell infiltrate was initially observed in some animals over 14 weeks of age in the thyroid, heart, and lungs. Salivary gland infiltrate was noted in some older mice after about 35 weeks of age. Shown in Figure AII.1 is infiltrate in both the heart (AII.1.A) and thyroid (AII.1.B) of a 32 week old NOD.DQ6$^{+/-}$DQ8$^{+/-}$/Ab^0 mouse.

NOD.DQ6$^{+/-}$DQ8$^{+/-}$/Ab^0 animals were monitored from 8 weeks of age to 40 weeks of age by serial ECG measurements. NOD.DQ6$^{+/-}$DQ8$^{+/-}$/Ab^0 animals begin to develop first degree heart block by 12 weeks of age, by 20 weeks of age they begin to develop complete heart block, and by 30 weeks they begin to die from complete heart failure (Figure AII.2).

From histology it was apparent that NOD.DQ6$^{+/-}$DQ8$^{+/-}$/Ab^0 mice develop autoimmune thyroiditis, but whether this thyroiditis progressed to hypothyroidism was yet to be investigated. Hypothyroidism in NOD.DQ6$^{+/-}$DQ8$^{+/-}$/Ab^0 was analyzed using a TSH ELISA. NOD.DQ6$^{+/-}$DQ8$^{+/-}$/Ab^0 animals are indeed

hypothyroid, the majority of mice over about 25 weeks of age show elevated serum TSH levels (Figure AII.3).

NOD.DQ6$^{+/-}$DQ8$^{+/-}$/Ab^{0} animals show histological and physiological characteristics of myocarditis and thyroiditis, but we next questioned whether they also have autoantibodies. First, via Western blot we analyzed for the presence of anti-heart autoantibodies. NOD.DQ6$^{+/-}$DQ8$^{+/-}$/Ab^{0} serum showed reactivity towards heart, but not spleen, proteins (Figure AII.4.A). Specific reactivity was also seen to cardiac myosin and to a slightly lesser extent skeletal myosin (Figure AII.4.A). NOD.DQ6$^{+/-}$DQ8$^{+/-}$/Ab^{0} serum was also analyzed via Western blot for anti-thyroid autoantibodies. NOD.DQ6$^{+/-}$DQ8$^{+/-}$/Ab^{0} serum showed reactivity to rodent thyroid sources (Figure AII.4.B).

AII.4 Discussion

These experiments were designed as preliminary experiments and it is the generation of double transgenic NOD.DQ6.DQ8/Ab^{0} animals that will truly provide insight into whether the genetic control of these mice models of autoimmune thyroiditis and autoimmune myocarditis work similarly to human diabetes. The NOD.DQ6$^{+/-}$DQ8$^{+/-}$/Ab^{0} animals investigated here suggest that DQ6 and DQ8 can co-exist, but it is not apparent as to whether the slowed kinetics of the autoimmune myocarditis in these F1 animals is the effect of having only half the amount of DQ8 or if the presence of DQ6 will make NOD.DQ6.DQ8/Ab^{0} animals resistant to autoimmune myocarditis. And if NOD.DQ6.DQ8/Ab^{0} animals are resistant to autoimmune myocarditis will they

still develop the autoimmune thyroiditis of NOD.DQ6/ Ab^0 animals? The answers to these questions will be very informative.

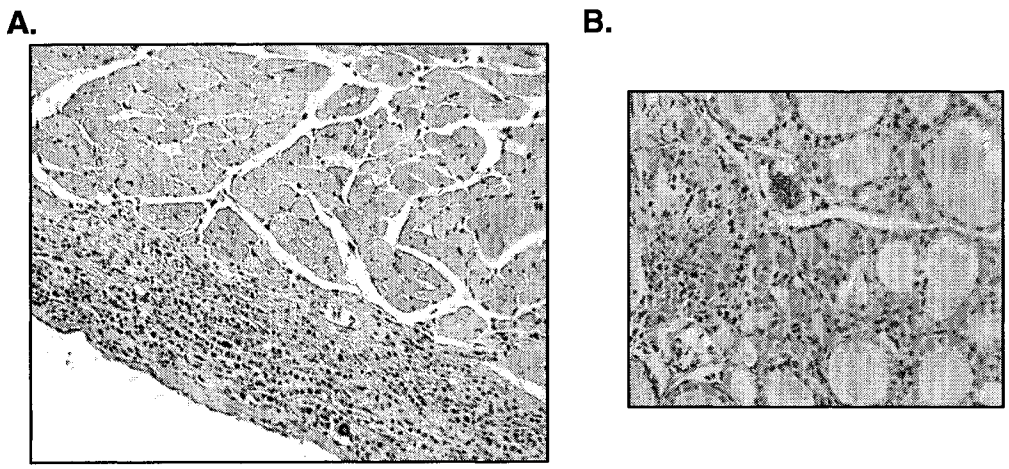

Figure AII.1: NOD.DQ6$^{+/-}$DQ8$^{+/-}$/Ab^{0} animals show both heart and thyroid pathology. A. Examination of NOD.DQ6$^{+/-}$DQ8$^{+/-}$/Ab^{0} hearts reveals the presence of mononuclear cell infiltrate. B. Examination of NOD.DQ6$^{+/-}$DQ8$^{+/-}$/Ab^{0} thyroids reveals the presence of mononuclear cell infiltrate. The mouse shown here is a 32 week old male.

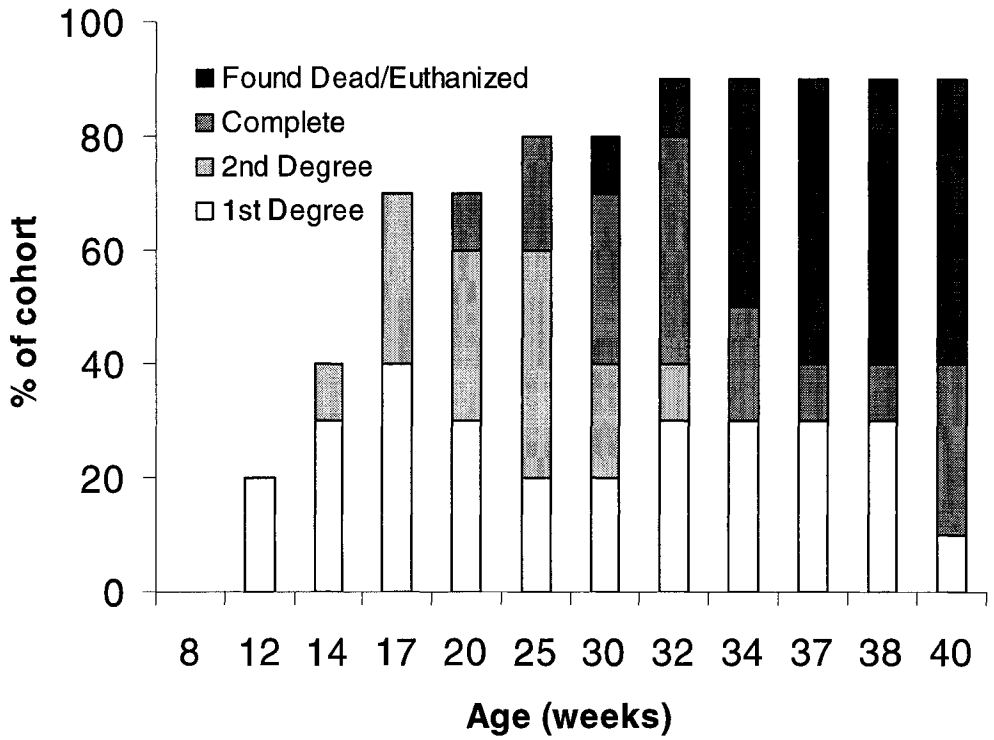

Figure AII.2: NOD.DQ6$^{+/-}$DQ8$^{+/-}$/Ab^{0} mice can progress to heart failure. NOD.DQ6/Ab^{0} mice were crossed with NOD.DQ8/Ab^{0} mice and the F1 mice were monitored for development of heart block by ECG (n=10). Once a mouse had complete heart block for two consecutive measurements it was euthanized.

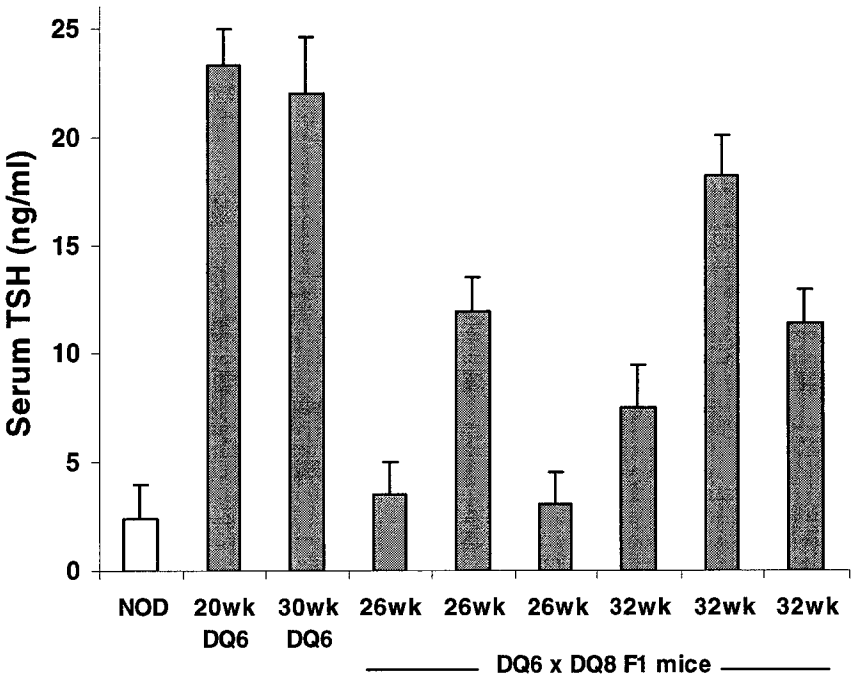

Figure AII.3: NOD.DQ6$^{+/-}$DQ8$^{+/-}$/Ab^{0} mice develop elevated serum TSH. Sera were prepared from NOD.DQ6$^{+/-}$DQ8$^{+/-}$/Ab^{0} mice of various ages and TSH levels were analyzed using a rodent TSH Elisa kit from Endocrine Technologies, California. Samples were run in triplicate and expressed as mean +/- standard deviation

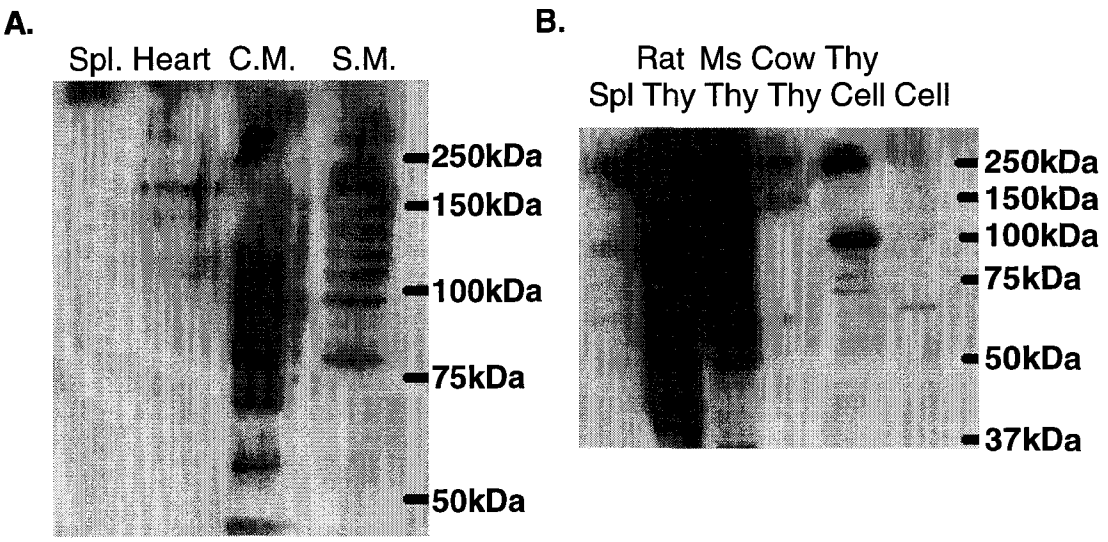

Figure AII.4: NOD.DQ6$^{+/-}$DQ8$^{+/-}$/Ab^{0} mice develop both anti-heart and anti-thyroid autoantibodies. A. 10μg of mouse spleen lysate (spl.), mouse heart lysate (heart), commercial porcine cardiac myosin (C.M.; Sigma), and commercial porcine skeletal myosin (S.M.; Sigma) were run on a 10% SDS-PAGE gel Proteins were transferred to nitrocellulose and probed with 28 week old NOD.DQ6$^{+/-}$DQ8$^{+/-}$/Ab^{0} serum B. 10μg of mouse spleen lysate (spl.), rat thyroid lysate (Rat Thy), mouse thyroid lysate (Ms Thy), bovine thyroid lysate (Cow Thy), rat thyroid cell line lysate (Thy Cell; FRTL-5), and βTC-Tet cell lysate (cell; this is a mouse pancreatic β-cell line) were run on a 10% SDS-PAGE gel. Proteins were transferred to nitrocellulose and probed with serum from a 28 week old NOD.DQ6$^{+/-}$DQ8$^{+/-}$/Ab^{0} mouse.

AII.5 References

1. Elliott, J. F., J. Liu, Z. N. Yuan, N. Bautista-Lopez, S. L. Wallbank, K. Suzuki, D. Rayner, P. Nation, M. A. Robertson, G. Liu, and K. M. Kavanagh. 2003. Autoimmune cardiomyopathy and heart block develop spontaneously in HLA-DQ8 transgenic IAbeta knockout NOD mice. *Proc Natl Acad Sci U S A 100:13447.*

2. Taylor, J. A., E. Havari, M. F. McInerney, R. Bronson, K. W. Wucherpfennig, and M. A. Lipes. 2004. A spontaneous model for autoimmune myocarditis using the human MHC molecule HLA-DQ8. *J Immunol 172:2651.*

3. Baisch, J. M., T. Weeks, R. Giles, M. Hoover, P. Stastny, and J. D. Capra. 1990. Analysis of HLA-DQ genotypes and susceptibility in insulin-dependent diabetes mellitus. *N Engl J Med 322:1836.*

4. Thorsby, E., and K. S. Ronningen. 1993. Particular HLA-DQ molecules play a dominant role in determining susceptibility or resistance to type 1 (insulin-dependent) diabetes mellitus. *Diabetologia 36:371.*

5. Champion, B. R., D. C. Rayner, P. G. Byfield, K. R. Page, C. T. Chan, and I. M. Roitt. 1987. Critical role of iodination for T cell recognition of thyroglobulin in experimental murine thyroid autoimmunity. *J Immunol 139:3665.*

6. Efrat, S., D. Fusco-DeMane, H. Lemberg, O. al Emran, and X. Wang. 1995. Conditional transformation of a pancreatic beta-cell line derived from transgenic mice expressing a tetracycline-regulated oncogene. *Proc Natl Acad Sci U S A 92:3576.*

7. Fleischer, N., C. Chen, M. Surana, M. Leiser, L. Rossetti, W. Pralong, and S. Efrat. 1998. Functional analysis of a conditionally transformed pancreatic beta-cell line. *Diabetes 47:1419.*

APPENDIX III

NOD.DQ6/Ab^0 MOUSE ISLETS

AIII.1 Introduction

Insulin dependent diabetes mellitus (IDDM) is an autoimmune disease mediated by T cells against the pancreatic β-cell and results in the dysfunctional regulation of the body's glucose metabolism (1). Many genes contribute to the heredity of the disease, with the genes within the HLA complex being the most important (1). Several human class II MHCs have been implicated as important in the development, or lack thereof, of type 1 diabetes, including DQ2 (DQA1*0501, DQB1*0201), DQ6 (DQA1*0102 and DQB1*0602), and DQ8 (DQA1*301 and DQB1*302), although the respective roles of these highly polymorphic MHCs have not yet been clearly defined (2-4).

DQ HLA cell-membrane molecules are glycoproteins composed of an α and a β chain heterodimer and it is believed that the selective binding of self peptides to these disease-associated MHC class II molecules, presented by professional antigen presenting cells (APCs), may potentially explain the observed T and B cell reactivity towards autoantigens. In humans, 90% of type 1 diabetes patients express the MHC class II DQ8 (*0301, *0302). However, if an individual expresses both DQ8 and DQ6 (*0102, *0602) then the individual will never develop type 1 diabetes (2-4). By an undetermined mechanism, DQ6 is dominantly protective over DQ8.

NOD.DQ8 mice develop diabetes, but upon removal of the mouse MHC class II, NOD.DQ8/Ab^{o} mice fail to develop diabetes and instead develop spontaneous autoimmune myocarditis (5, 6). It appears as though the dominant peptide for DQ8 in this context, i.e. in the absence of any other class II MHC, is a

cardiac antigen. There is also evidence that the class I MHC Kb, which is present in these mice, is, protective from diabetes (in contrast to the Kd normally in NOD mice). Serreze and colleagues have shown that when maturing in the presence of Kb class I MHC, the NOD derived diabetogenic CD8 T cell clonotype AI4 is functionally anergized (7). DQ8 (DQA1*0301, DQB1*0302) has been shown to correlate with cases of idiopathic dilated cardiomyopathy (8-11), but it has also been linked to other disease such as rheumatoid arthritis (12) and of course diabetes (4, 13).

We hypothesized that the reason NOD.DQ8 mice develop diabetes, therefore, is that in the presence of the endogenous mouse MHC class II, the mouse's immune system is unable to recognize antigen in the context of the human DQ8 MHC class II. In fact, it was shown that the CD4 T cell responses in NOD.DQ8 mice are dominated by the mouse MHC class II, IAg7. Of 87 hybridomas all made to OVA, 86 of them were restricted to IAg7 (L Wicker personal communication with J. Elliott). Therefore, initially we hypothesized that the DQ6 (DQA1*0102, DQB1*0602) in NOD.DQ6 mice would not be protective, due to "immune neglect", and that NOD.DQ6 mice would still develop diabetes. However NOD.DQ6 did not develop diabetes and the reason for this has yet to be determined. Like NOD.DQ8/Ab^0 mice, NOD.DQ6/Ab^0 mice did not develop diabetes, perhaps due to the human class II DQ or perhaps do to the presence of Kb rather than Kd. However, upon observation of NOD.DQ6/Ab^0 pancreases, it appeared that the islets were enlarged in these mice and so this observation was investigated further.

As you will see, NOD.DQ6/Ab^0 do generally have enlarged islets and they do have a rapid glucose tolerance, however the total insulin content of a NOD.DQ6/Ab^0 pancreas is no different than control mice.

AIII.2 Materials and Methods

AIII.2.1 Mice

NOD-Lt/J mice were purchased from The Jackson Laboratory (Bar Harbor, ME) and Balb/c mice were provided in-house by Health Sciences Laboratory Animals Services, (University of Alberta, Edmonton, AB).

The origins of NOD.DQ8, NOD.DQ8/Ab^0, NOD.DQ6, and NOD.DQ6/Ab^0 mice have all been described previously ((6) and Chapter 2)

All breeding colonies were housed in conventional SPF facilities. Care and handling was done in accordance with the guidelines of the Canadian Council on Animal Care, and all experimental protocols were approved by our institutional Health Sciences Animal Policy and Welfare Committee.

AIII.2.2 Diabetes Monitoring

Mice were monitored regularly for polyurea, polydipsia, glucosurea and general signs of malaise. Suspected cases of diabetes were confirmed using a One-Touch ® Ultra Blood Glucose Meter (LifeScan, Inc., Milpitas, CA).

AIII.2.3 Histology

Pancreases were removed and placed in 10% buffered formalin (Fisher, Fair Lawn, NJ). The pancreases were then processed into paraffin blocks by standard methods and slides were cut. Slides were then stained for insulin. In brief, the slides were de-paraffinized and endogenous peroxide activity was quenched with 10% hydrogen peroxide in methanol. The slides were then blocked with 20% normal goat serum (Sigma, St. Louis, MO), incubated with the primary antibody (polyclonal guinea pig anti-swine insulin; Dako Cytomation, Mississauga), followed by the secondary antibody (biotinylated goat anti-guinea pig IgG (H+L); Jackson Immunoresearch, West Grove, PA). Staining was then revealed using ABC kit (Vector Labs, Burlington, ON) and DAB (Sigma). The slides were then counterstained with hematoxylin, dehydrated and mounted.

AIII.2.4 Islet Measurement

A crude measurement of islet size was performed by measuring islet diameters in multiple fields of view from multiple mice at a set magnification.

AIII.2.5 Glucose Tolerance Test

Mice were fasted overnight and then injected I.P. with a pre-warmed (37°C) 15% glucose solution in PBS at 2 grams of glucose/kg. Blood glucose readings were then taken using the OneTouch® Ultra Blood Glucose Meter (LifeScan, Inc., Milpitas, CA) at various times from 1 minute after injection up to 3 hours post injection.

AIII.2.6 Whole Pancreas Insulin Extraction

A mouse was euthanized and weighed. The pancreas was then dissected and also weighed. The pancreas was added to 5ml AZOL (cold 2mM acetic acid with 0.25% BSA) and homogenized, and another 5ml AZOL was used to ensure all homogenized pancreas was collected. The homogenate was sonicated for 20 seconds and incubated at 4°C for two hours. The sample was then resonicated and spun (~1000 *x g*, 25min, 4°C, without a brake in a JA-20 rotor), 4ml of the clear supernatant was removed and the remaining supernatant was discarded. 5ml of AZOL was added to the pellet, sonicated for 20 seconds, incubated at 4°C for 25 minutes and spun as previously. An additional 2ml of clear supernatant was removed and added to the previous 4ml. A 50µl aliquot of each sample was neutralized using 2ml of 0.25% BSA in PBS, pH 11. Samples were then analyzed for its insulin content by the Department of Lab Medicine and Pathology, University of Alberta Hospital, Edmonton, Alberta. Back calculations were then performed to determine the mU insulin per gram of pancreas and per gram of mouse.

AIII.3 Results

Despite their similar construction, NOD.DQ6 mice, unlike NOD.DQ8 mice, fail to develop diabetes. The NOD.DQ8 incidence data is courtesy of L.Wicker, (but we saw a similar incidence rate in our colony) and the NOD.DQ6, NOD.DQ8/Ab^0, and NOD.DQ6/Ab^0 are from our conventional colonies at the University of Alberta. As shown in Figure AIII.1, NOD.DQ8 mice show 75%

diabetes by 25 weeks of age (100% by ~50 weeks of age) while NOD.DQ6, NOD.DQ6/Ab^0, and NOD.DQ8/Ab^0 animals show 0% incidence at any age.

Qualitative histological examination of pancreases from DQ6 and DQ8 transgenic NOD mice suggested the islets of NOD.DQ6/Ab^0 mice (Figure AIII.2.A) are larger than control mice such as Balb/c (Figure AIII.2.B). Crude quantitative measurement of the diameter of islets from NOD.DQ6/Ab^0 and from Balb/c revealed that DQ6 islets are statistically larger than Balb/c islets (Figure AIII.2.C; $p<0.04$).

Perhaps one of the methods through which NOD.DQ6/Ab^0 mice are protected from diabetes is because they have larger islets and thus are capable of producing more insulin. Glucose tolerance analysis of NOD.DQ6/Ab^0 mice reveals that not only do they have efficient glucose tolerance, but the kinetics of their tolerance are slightly faster than wild-type NOD or NOD.DQ8/Ab^0 animals (Figure AIII.3). However, whole pancreas insulin extraction revealed that despite having larger islets, the insulin content of NOD.DQ6/Ab^0 pancreases (is not different from control mice (Figure AIII.4).

AIII.4 Discussion

NOD.DQ6/Ab^0 animals do not develop diabetes, but it seems apparent that although NOD.DQ6/Ab^0 animals do have enlarged islets that work efficiently, the total insulin content of their pancreases is not abnormal. More than likely NOD.DQ6/Ab^0 animals do not develop diabetes instead because of the MHC class I molecule. NOD.DQ6/Ab^0 animals are MHC class I Kb, instead of the Kd

that NOD mice are, and Kb is believed to be protective against diabetes (7). This does not however explain why NOD.DQ6 mice do not develop diabetes as they are MHC class I Kd positive, DQ6 may be protective in addition to the Kb molecule. It would be of interest to determine if NOD.DQ6 islets are enlarged like those of NOD.DQ6/Ab^0 as an indication as to whether this might be part of the mechanism.

Perhaps the enlarged islets of NOD.DQ6/Ab^0 animals are related to the DQ6 association with thyroiditis (Chapter 3). Thyroid hormones assist cells and systems all over the body through their effects on metabolism and transcription factors (14). It is highly possible that the enlarged islets are a by-product of the changes in hormone production in NOD.DQ6/Ab^0 mice. There are many examples in the literature of thyroid related hormones having effects on various cell types within the pancreas. To list a few examples, the thyroid hormone receptor has been found localized in pancreatic alpha cells (15), thyroid hormone plays a role in rat pancreas development (16), T3 induces cell proliferation in the pancreas (17), thyroid hormones can induce cell cycle perturbations and play an important role in the process of transdifferentiation of a human pancreatic duct line (hPANC-1) into pancreatic β-cell-like cells that produce insulin (18), and TRH may affect gene expression and influence β-cell function (19).

Further investigation of the cellular composition as well as thyroid-related receptor expression in NOD.DQ6/Ab^0 islets is needed. Perhaps there is a thyroid-related factor generated in NOD.DQ6/Ab^0 animals (and maybe NOD.DQ6 mice) that enlarges the islets and helps protect them from diabetes.

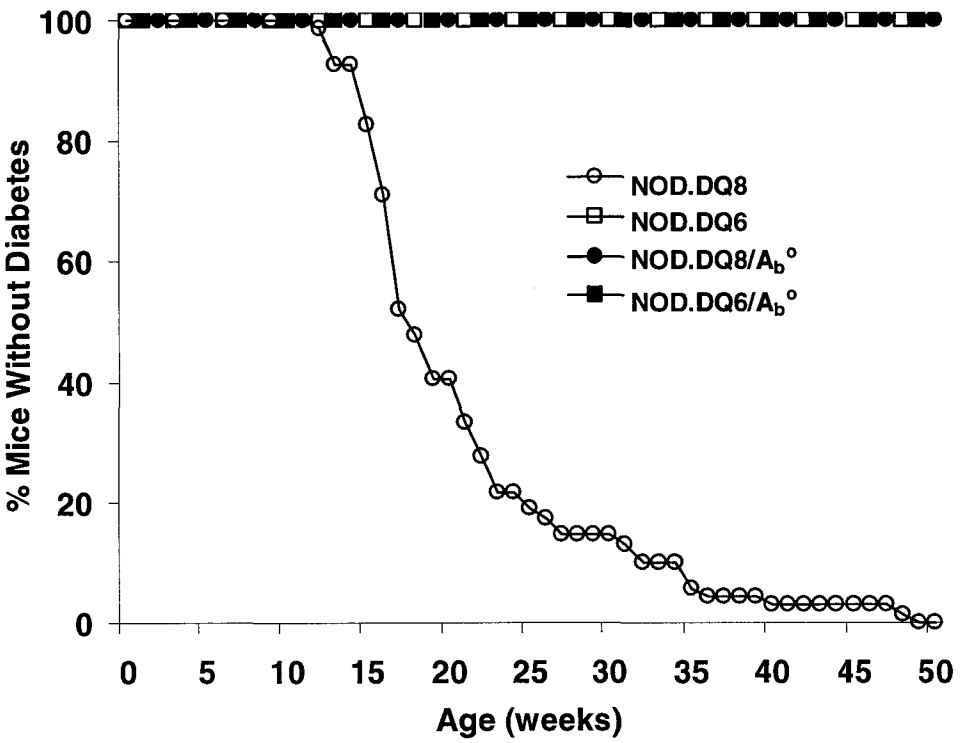

Figure AIII.1: Unlike NOD.DQ8 mice, NOD.DQ6 mice do not develop diabetes. Diabetes incidence was monitored by standard methods (see materials and methods) in these mouse lines over 50 weeks. NOD.DQ6, NOD.DQ6/Ab^0, and NOD.DQ8/Ab^0 mice are all resistant to diabetes. The NOD.DQ8 data is courtesy of Dr. Linda Wicker.

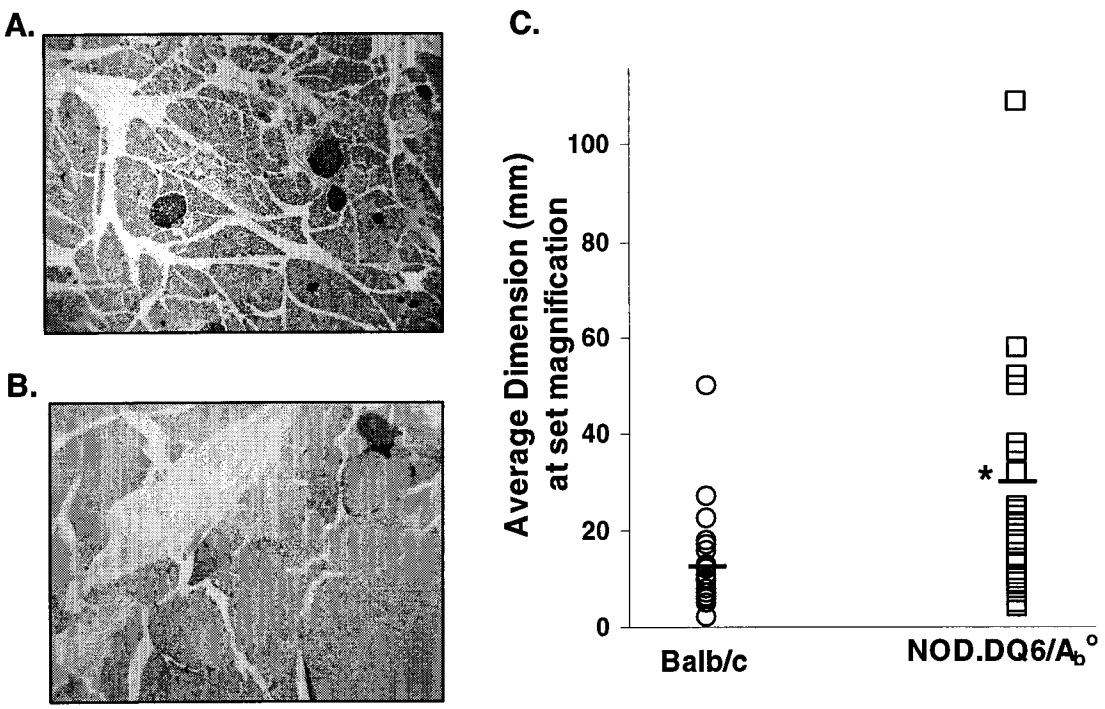

Figure AIII.2: NOD.DQ6/Ab^0 islets never show intra-islet mononuclear cell infiltrates and they appear to be larger than islets of other strains (e.g. Balb/c, NOD.DQ8/Ab^0). Insulin staining of a Balb/c pancreas (A) and a NOD.DQ6/Ab^0 pancreas (B). Magnification (including camera zoom) is 184X. C.The diameter of 30 islets was measured for each strain of mice at a set magnification of 184X. *p<0.04. (Only Balb/c is shown, but results are similar to NOD.DQ8/Ab^0.)

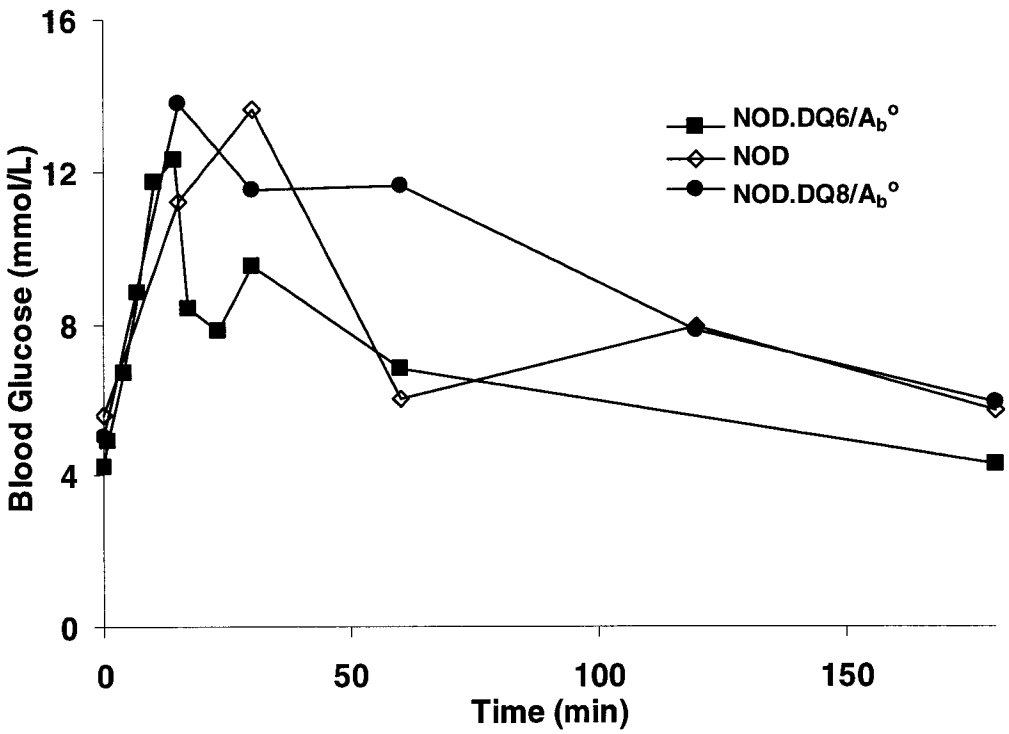

Figure AIII.3: NOD.DQ6/Ab^0 mice have efficient glucose tolerance. After an overnight fast, mice were given an I.P. injection of pre-warmed glucose and their blood glucose was measured at various times up to 3 hours post injection. Results for a representative experiment are shown; similar results were obtained on three occasions.

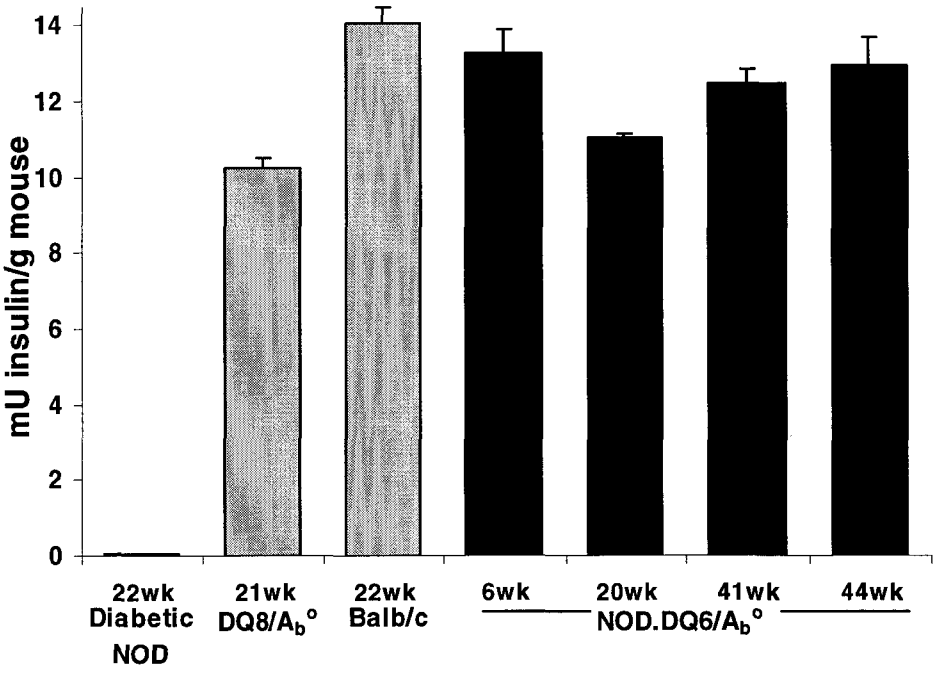

Figure AIII.4: NOD.DQ6/Ab^0 pancreases contain normal levels of insulin. Pancreases were removed from these mice and the insulin was extracted using standard methods (see materials and methods). Aliquots were sent for analysis at the University of Alberta Hospital and then back calculations were done to determine the mU insulin per gram of pancreas and per gram of mouse. This is a representative experiment. Error bars represent standard deviation.

AIII.5 References

1. Atkinson, M. A., and N. K. Maclaren. 1994. The pathogenesis of insulin-dependent diabetes mellitus. *N Engl J Med 331:1428.*

2. Thomson, G. 1983. Investigation of the mode of inheritance of the HLA associated diseases by the method of antigen genotype frequencies among diseased individuals. *Tissue Antigens 21:81.*

3. Thorsby, E., and K. S. Ronningen. 1993. Particular HLA-DQ molecules play a dominant role in determining susceptibility or resistance to type 1 (insulin-dependent) diabetes mellitus. *Diabetologia 36:371.*

4. Baisch, J. M., T. Weeks, R. Giles, M. Hoover, P. Stastny, and J. D. Capra. 1990. Analysis of HLA-DQ genotypes and susceptibility in insulin-dependent diabetes mellitus. *N Engl J Med 322:1836.*

5. Liu, J., L. E. Purdy, S. Rabinovitch, A. M. Jevnikar, and J. F. Elliott. 1999. Major DQ8-restricted T-cell epitopes for human GAD65 mapped using human CD4, DQA1*0301, DQB1*0302 transgenic IA(null) NOD mice. *Diabetes 48:469.*

6. Elliott, J. F., J. Liu, Z. N. Yuan, N. Bautista-Lopez, S. L. Wallbank, K. Suzuki, D. Rayner, P. Nation, M. A. Robertson, G. Liu, and K. M. Kavanagh. 2003. Autoimmune cardiomyopathy and heart block develop spontaneously in HLA-DQ8 transgenic IAbeta knockout NOD mice. *Proc Natl Acad Sci U S A 100:13447.*

7. Serreze, D. V., T. M. Holl, M. P. Marron, R. T. Graser, E. A. Johnson, C. Choisy-Rossi, R. M. Slattery, S. M. Lieberman, and T. P. DiLorenzo. 2004. MHC class II molecules play a role in the selection of autoreactive class I-restricted CD8 T cells that are essential contributors to type 1 diabetes development in nonobese diabetic mice. *J Immunol 172:871.*

8. Carlquist, J. F., R. L. Menlove, M. B. Murray, J. B. O'Connell, and J. L. Anderson. 1991. HLA class II (DR and DQ) antigen associations in idiopathic dilated cardiomyopathy. Validation study and meta-analysis of published HLA association studies. *Circulation 83:515.*

9. Carlquist, J. F., R. H. Ward, D. Husebye, M. Feolo, and J. L. Anderson. 1994. Major histocompatibility complex class II gene frequencies by

serologic and deoxyribonucleic acid genomic typing in idiopathic dilated cardiomyopathy. *Am J Cardiol 74:918.*

10. Limas, C. J. 1996. Autoimmunity in dilated cardiomyopathy and the major histocompatibility complex. *Int J Cardiol 54:113.*

11. McKenna, C. J., M. B. Codd, H. A. McCann, and D. D. Sugrue. 1997. Idiopathic dilated cardiomyopathy: familial prevalence and HLA distribution. *Heart 77:549.*

12. Nabozny, G. H., J. M. Baisch, S. Cheng, D. Cosgrove, M. M. Griffiths, H. S. Luthra, and C. S. David. 1996. HLA-DQ8 transgenic mice are highly susceptible to collagen-induced arthritis: a novel model for human polyarthritis. *J Exp Med 183:27.*

13. Todd, J. A., J. I. Bell, and H. O. McDevitt. 1987. HLA-DQ beta gene contributes to susceptibility and resistance to insulin-dependent diabetes mellitus. *Nature 329:599.*

14. Rayner, D. C., and B. R. Champion. 1995. *Thyroid Autoimmunity.* R.G. Landes Company, Austin.

15. Zinke, A., D. Schmoll, M. Zachmann, J. Schmoll, H. Junker, R. Grempler, G. Kirsch, and R. Walther. 2003. Expression of thyroid hormone receptor isoform alpha1 in pancreatic islets. *Exp Clin Endocrinol Diabetes 111:198.*

16. Lee, J. T., E. Lebenthal, and P. C. Lee. 1989. Rat pancreatic nuclear thyroid hormone receptor: characterization and postnatal development. *Gastroenterology 96:1151.*

17. Ledda-Columbano, G. M., A. Perra, M. Pibiri, F. Molotzu, and A. Columbano. 2005. Induction of pancreatic acinar cell proliferation by thyroid hormone. *J Endocrinol 185:393.*

18. Misiti, S., E. Anastasi, S. Sciacchitano, C. Verga Falzacappa, L. Panacchia, B. Bucci, D. Khouri, I. D'Acquarica, E. Brunetti, U. Di Mario, V. Toscano, and R. Perfetti. 2005. 3,5,3'-Triiodo-L-thyronine enhances the differentiation of a human pancreatic duct cell line (hPANC-1) towards a beta-cell-Like phenotype. *J Cell Physiol 204:286.*

19. Luo, L., and N. Yano. 2005. Thyrotropin releasing hormone (TRH) affects gene expression in pancreatic beta-cells. *Endocr Res 31:185.*